

Electronic Thesis and Dissertation Repository

---

1-18-2018 2:00 PM

## Development of Nanostructured Glucose Biosensor

Longyi Chen

*The University of Western Ontario*

Supervisor

Dr Zhang, Jin

*The University of Western Ontario*

Graduate Program in Chemical and Biochemical Engineering

A thesis submitted in partial fulfillment of the requirements for the degree in Doctor of  
Philosophy

© Longyi Chen 2018

Follow this and additional works at: <https://ir.lib.uwo.ca/etd>

---

### Recommended Citation

Chen, Longyi, "Development of Nanostructured Glucose Biosensor" (2018). *Electronic Thesis and  
Dissertation Repository*. 5178.

<https://ir.lib.uwo.ca/etd/5178>

This Dissertation/Thesis is brought to you for free and open access by Scholarship@Western. It has been accepted for inclusion in Electronic Thesis and Dissertation Repository by an authorized administrator of Scholarship@Western. For more information, please contact [wlsadmin@uwo.ca](mailto:wlsadmin@uwo.ca).

## Abstract

With the development of nanotechnology and nanomaterials, biosensors incorporated with novel nanomaterials and nanostructures have shown significant potential in point-of-care medical devices because of their rapid interaction with target analytes and their miniaturized systems. Nanomaterials and nanostructures with special chemical, physical and biological characteristics are able to enhance biosensors' performance in terms of sensitivity and selectivity. Therefore, my study focused on development of special nanostructures used for advanced glucose biosensor. Monitoring of blood glucose level is essential for diabetes management. However, current methods require people with diabetes to have blood test with 5–8 times per day. Compared to other methods, optical and magnetic techniques have a potential in developing minimally invasive or non-invasive, and continuous glucose monitoring nanostructured biosensors. Consequently, this thesis presented nanostructured optical and magnetic glucose biosensors by incorporating novel nanomaterials and fabricating nanostructures for the next generation of glucose biosensor in the tears. The glucose biorecognition biomolecule used in the biosensors was Concanavalin A (Con A). Con A is a lectin protein that has strong affinity to glucose.

Fluorescence resonance energy transfer (FRET) technique was applied to develop optical glucose biosensors. FRET biosensor is a distance-dependent biosensor. The fluorescence emission of a donor molecule could be used to excite acceptor when the distance between donor and acceptor is close enough ( $< 20$  nm). Three different types of nanostructures were developed and used as the donors of the glucose FRET biosensors. The first type of sensor is a ZnO/quantum dots-based glucose biosensors. Hybrid ZnO nanorod array with decoration of CdSe/ZnS quantum dots were prepared and coated on silicone hydrogel which is a common materials of contact lens. The patterned nanostructured FRET sensor could quickly measure rats' tear glucose in an extremely small amount ( $2 \mu\text{L}$ ) of diluted tear sample. The second type of biosensor is based on upconversion nanomaterials. Upconversion  $\text{NaGdF}_4: \text{Yb}, \text{Er}$  nanoparticles with diameter of about  $40 \pm 5$  nm have been prepared by polyol process and coated on silicone hydrogel to directly sense the tear glucose level on the rats' eye surface. The results show that the upconversion nanomaterials

based lens sensor is able to quickly measure glucose in rats' blood samples. The third type of sensor utilizes the unique optical properties of carbon nanomaterial, fluorescent carbon dots and graphene oxide nanosheets. The carbon dots with tunable fluorescence were developed by a microwave-assisted process. The carbon dots are used as a fluorescence donor in the biosensor, the chitosan coated graphene oxide acts as the fluorescence acceptor to quench the emission of carbon quantum dots. In the presence of glucose, the emission of carbon quantum dots could be restored as a function of the concentration of glucose. Two linear relationships of the restored emission of the sensor and the concentration of glucose were observed, in the range of 0.2 mM to 1 mM, and 1 mM to 10 mM, respectively.

On the other hand, a magnetoresistive (MR) nanostructured glucose biosensor has been developed by exploiting hybrid graphene nanosheets decorated with FeCo magnetic nanoparticles. The Fe<sub>3</sub>O<sub>4</sub>/silica core/shell nanoparticles are used as the magnetic label of glucose, which could bind onto the surface of FeCo/graphene nanocomposited sensor. The binding of magnetic label onto the hybrid graphene nanosheets can result in the change of the magnetoresistance. The MR signal as a function of the glucose level of diluted rat blood samples is measured in a range of 2 mM to 10 mM.

In summary, novel nanomaterials and nanostructures with special fluorescent and magnetoresistive properties are fabricated for developing nanostructured glucose biosensors, which could bring alternative approaches for convenient management diabetes.

### **Keywords**

Diabetes, glucose sensing, nanostructured glucose biosensor, ZnO nanorod, quantum dots, upconverting nanoparticles, silicone hydrogel, carbon dots, graphene oxide, FeCo nanoparticles, graphene, fluorescence, magnetoresistance.

## Co-Authorship Statement

Chapters 1 entitled “General Introduction and Motivation”, and chapter 2 entitled “Background and Literature Review” were written by Longyi Chen with suggestions from Dr. Jin Zhang. The cited figures’ copyrights are gathered in the Appendices in the end of the thesis.

Chapter 3, 4, 5 and 6 consist of research studies that have been published or are in preparation for publication. Individual contributions of the author of each article are stated below. All animal tests were cooperated with Dr James Melling lab (Kinesiology, UWO) and ethics approval was obtained through the University of Western Ontario Research Ethics Board, in accordance with Canadian Council on Animal Care guidelines.

Chapter 3: This chapter consists of one research study that has been published. This work is focused on ZnO/quantum dots nanostructured glucose biosensor. The experiment was carried out mainly by Longyi Chen (Chemical and Biochemical Engineering, UWO) and Wai Hei Tse (Medical Biophysics, UWO). Dr Yi Chen (Chemical and Biochemical Engineering, UWO) helped with ZnO nanorod array preparation. Matthew W. McDonald (Kinesiology, UWO) and James Melling (Kinesiology, UWO) provided animal tests. This work was supervised by Dr. Jin Zhang.

- ❖ Longyi Chen, Wai Hei Tse, Yi Chen, Matthew W. McDonald, James Melling and Jin Zhang. Nanostructured biosensor for detecting glucose in tear by applying fluorescence resonance energy transfer quenching mechanism. *Biosensors and Bioelectronics* 2017, 91, 393-399. (Longyi Chen and Wai Hei Tse contributed equally)

Chapter 4: This chapter consists of one research study that has been published and one study that has been submitted. This work is related to upconverting NaGdF<sub>4</sub>: Yb<sup>3+</sup>, Er<sup>3+</sup> nanomaterials for nanostructured glucose biosensor. In this paper (*RSC Advances* 2017, 7 (43), 26770-26775.), Longyi Chen (Chemical and Biochemical Engineering, UWO) carried out the major experiment. Wai Hei Tse (Medical Biophysics, UWO) helped with cytotoxicity analysis. Dr Alex Siemiarzuk (HORIBA Scientific Instruments & Systems -

HORIBA) assisted with the upconversion fluorescence measurement and discussed the upconversion fluorescence data with us. This work was supervised by Dr. Jin Zhang.

In the submitted paper, the experiment was carried out mainly by Longyi Chen (Chemical and Biochemical Engineering, UWO) and Wai Hei Tse (Medical Biophysics, UWO). Dr Yi Chen (Chemical and Biochemical Engineering, UWO) helped with NaGdF<sub>4</sub>: Yb<sup>3+</sup>, Er<sup>3+</sup> nanomaterials preparation. Matthew W. McDonald (Kinesiology, UWO) and James Melling (Kinesiology, UWO) provided animal tests. This work was supervised by Dr. Jin Zhang.

- ❖ Longyi Chen, Wai Hei Tse, Alex Siemiarczuk and Jin Zhang. Special properties of luminescent magnetic NaGdF<sub>4</sub>: Yb<sup>3+</sup>, Er<sup>3+</sup> upconversion nanocubes with surface modifications. RSC Advances 2017, 7 (43), 26770-26775.
- ❖ Wai Hei Tse, Longyi Chen, Yi Chen, Matthew W. McDonald, James Melling and Jin Zhang. Harnessing Protein-conjugated Upconversion Nanostructures to Build a Hydrogel-based Biosensor for Tear Glucose Measurement. Submitted. (Longyi Chen and Wai Hei Tse contributed equally)

Chapter 5: This chapter consists of one research study that has been submitted. This work is focused on nanocarbon materials, carbon dots/graphene oxide based glucose nanobiosensor. The experiment was carried out mainly by Longyi Chen (Chemical and Biochemical Engineering, UWO). Michelle Dotzert (Kinesiology, UWO) and James Melling (Kinesiology, UWO) provided animal tests. This work was supervised by Dr. Jin Zhang.

- ❖ Longyi Chen, Michelle Dotzert, James Melling and Jin Zhang. Tunable Photoluminescent Carbon Dots as Glucose Biosensor. Submitted.

Chapter 6: This chapter consists of one research study that is in preparation. This work is focused on nanocarbon materials, graphene nanosheets decorated with FeCo nanoparticles and iron oxide/silica core/shell magnetic label based magnetoresistance glucose nanostructured biosensor. The experiment was carried out mainly by Longyi Chen (Chemical and Biochemical Engineering, UWO). Michelle Dotzert (Kinesiology, UWO)

and James Melling (Kinesiology, UWO) provided animal tests. This work was supervised by Dr. Jin Zhang.

- ❖ Longyi Chen, Michelle Dotzert, James Melling and Jin Zhang. Graphene/FeCo nanocomposites for magnetoresistive glucose biosensing. In preparation.

Chapter 7 entitled “Summary and Recommendations” was written by Longyi Chen with suggestions from Dr. Jin Zhang.

## Acknowledgments

First and foremost I want to thank my supervisor Dr. Jin Zhang. She has been supportive since the days I began working in her Multifunctional Nanocomposites Lab (MNL) in April 2014. I deeply appreciate all her dedications of time, ideas, and funding to realize my productive and stimulating Ph.D. experience. The joyful and enthusiastic attitude she has for her research was contagious and inspirational for me, even during the hard times in my Ph.D. pursuit. What impressed me most during my PhD study is that Dr Zhang will and always can spare her time to meet us almost every week face to face, we could discuss about experiments and other issues. And Dr Zhang are always happy and willing to help and support me in work and life! I want to show my highest gratitude for her as a successful woman scientist and professor!

The members of Zhang's group have contributed greatly to my personal and professional time at Western. The group has offered happiness and friendship as well as good advice and collaborations. I am especially grateful for all previous and current colleagues at Multifunctional Nanocomposites Lab. Special thanks to Dr Yi Chen and Mr Guobang Huang, Dr Wai Hei Tse, Dr Longyan Chen. They have helped me tremendously in my work and life.

I would like to thank Dr. Richard Gardiner and Karen Nygard in Biotron for their assistance and help in TEM, SEM, EDX and confocal microscopy. I would like to thank Kim Law and Grace Yau in Department of Earth Sciences for their help in XRD analysis. I would like to thank Professor James Melling group in School of Kinesiology for their help in animal tests. I would like to thank Dr. Alex Siemiarzuk in Horiba for his help in fluorescence measurement and discussions.

I would like to thank my examination committee, Dr. Naomi Matsuura, Dr Lyudmila Goncharova, Dr Chunbao Xu and Dr Sohrab Rohani.

Finally I would like to thank my family for their support and encouragement.

This work has been supported by funding from Natural Science and Engineering Research Council of Canada (NSERC) through a Discovery Grant and Western Engineering Graduate Scholarship.



# Table of Contents

Abstract .....	i
Co-Authorship Statement.....	iii
Acknowledgments.....	vi
Table of Contents .....	viii
List of Tables .....	xiii
List of Figures .....	xiv
List of Abbreviations .....	xix
Chapter 1 .....	1
1 General Introduction and Motivation.....	1
1.1 Overview.....	1
1.1.1 Diabetes Mellitus .....	1
1.1.2 Nanostructured Glucose Biosensor.....	2
1.1.3 Fluorescence Resonance Energy Transfer .....	4
1.1.4 Upconversion Fluorescence .....	5
1.1.5 Magnetoresistance.....	6
1.2 Current Challenges in Glucose Sensor for Diabetics.....	8
1.2.1 Objectives and Outcomes .....	12
1.3 References.....	16
Chapter 2.....	25
2 Background and Literature Review .....	25
2.1 Nanomaterials for Glucose Biosensing.....	25
2.2 Detection Principles of Nanostructured Fluorescent Biosensor .....	26
2.3 Glucose Recognition Biomolecules .....	28
2.4 Fluorescent Exerting/Interacting Nanomaterials .....	29
2.4.1 Semiconductor Quantum Dots .....	31
2.4.2 Fluorescent Polymer/Silica Nanomaterials.....	34
2.4.3 Upconverting Nanomaterials .....	37
2.4.4 Gold/Silver Nanoparticles/Nanoclusters.....	39
2.4.5 Fluorescent Carbon Nanomaterials.....	41
2.4.6 Graphene Nanomaterials.....	44
2.5 Magnetoresistive Nanomaterials.....	44

2.6 Summary .....	45
2.7 References .....	47
Chapter 3 .....	59
3 Development of ZnO/QD Patterned Nanostructured Glucose Biosensor .....	59
3.1 Introduction .....	59
3.2 Experimental .....	63
3.2.1 Synthesis of CdSe/ZnS Core Shell QDs .....	63
3.2.2 Preparation of ZnO/Silicone Hydrogel .....	64
3.2.3 Fabrication Patterned QDs Decorated-ZnO NRs Array on Silicone Hydrogel .....	65
3.2.4 Synthesis of Malachite Green Dextran .....	66
3.2.5 Synthesis and Optimization of FRET Sensor .....	67
3.2.6 Sensor Measurement .....	68
3.2.7 Fluorescence Sensor Signal Converting to Image Pixel Intensity .....	68
3.2.8 Cellular Viability .....	69
3.2.9 Animal Tear Test .....	71
3.3 Results and Discussion .....	71
3.3.1 Characterization of Nanostructured FRET Sensor Deposited on Silicone Hydrogel .....	71
3.3.2 Fluorescence Intensity of the FRET Sensor as a Function of Glucose Level in Aqueous .....	74
3.3.3 Pixel Intensity Value of Fluorescence Image of FRET Sensor as a Function of Glucose Level in Aqueous .....	76
3.3.4 Response of Designed FRET Sensor to 2 $\mu$ L Rat Tears .....	77
3.3.5 Selectivity of Designed FRET Sensor .....	79
3.4 Conclusion .....	80
3.5 References .....	80
Chapter 4 .....	84
4 Development of Upconversion NaGdF <sub>4</sub> : Yb, Er Glucose Biosensor .....	84
4.1 Introduction .....	84
4.2 Experimental .....	88
4.2.1 Synthesis of Polyethylenimine (PEI) Modified Upconversion Nanostructures .....	88
4.2.2 Synthesis of Malachite Green Dextran .....	89

4.2.3	Conjugation of Glucose Sensor Components .....	89
4.2.4	Sensor Deposition onto Silicone Hydrogel.....	89
4.2.5	<i>In Vivo</i> Animal Model .....	89
4.3	Results and Discussion .....	90
4.3.1	TEM and XRD.....	90
4.3.2	FTIR Spectrum of PEI Modified Upconverting Nanoparticles .....	92
4.3.3	Upconverting Fluorescence .....	93
4.3.4	Magnetic Properties Analysis .....	93
4.3.5	Cytotoxicity Study .....	95
4.3.6	Sensitivity of Sensor Construct to Detect Glucose in Solution .....	95
4.3.7	<i>In Vivo</i> Sensing of Glucose in Murine Tears .....	96
4.3.8	Contact Lens-like Material Incorporation of Glucose Sensor .....	96
4.4	Conclusion .....	98
4.5	References.....	99
Chapter 5	.....	105
5	Development of Carbon Dots/Graphene Oxide Glucose Biosensor .....	105
5.1	Introduction.....	105
5.2	Experimental.....	108
5.2.1	Materials .....	108
5.2.2	Preparation of Carbon Dots .....	108
5.2.3	Preparation of CD-Con A Conjugates: .....	109
5.2.4	Preparation of Graphite Oxide.....	109
5.2.5	Preparation of Graphene Oxide Solution.....	110
5.2.6	Preparation of GO-CS Conjugates:.....	111
5.2.7	GO-CS Titration.....	111
5.2.8	Glucose Nanobiosensing.....	111
5.2.9	Rat Blood Samples.....	111
5.2.10	Characterizations.....	112
5.3	Results and Discussion .....	112
5.3.1	Photoluminescent Tunable Carbon Dots .....	112
5.3.2	TEM Images of Carbon dots.....	115
5.3.3	Fluorescence of Carbon Dots and Carbon Dots-Con A Bioconjugate .....	117

5.3.4	UV-vis Spectrum .....	119
5.3.5	FTIR Spectrum.....	119
5.3.6	GO-CS Titration of Con A-Carbon Dots .....	120
5.3.7	Glucose Nanobiosensing.....	121
5.4	Conclusion .....	123
5.5	References.....	124
Chapter 6	.....	129
6	Development of FeCo/graphene Magneto-resistive Nanostructured Glucose Biosensor.....	129
6.1	Introduction.....	129
6.2	Experimental.....	131
6.2.1	Synthesis of Graphene Nanosheets.....	131
6.2.2	Synthesis of Magnetic Fe <sub>50</sub> Co <sub>50</sub> Crystals.....	132
6.2.3	Synthesis of FeCo/graphene Magnetic Nanocomposites.....	132
6.2.4	APTES Modification of GMR Sensor Surface.....	133
6.2.5	Con A Modification of GMR Sensor Surface.....	133
6.2.6	Iron Oxide/Silica Surface Modification.....	134
6.2.7	Preparation of 3, 5-Dinitrosalicylic Acid (DNS) Solution.....	134
6.2.8	MR Measurement.....	136
6.2.9	Rat Blood Samples Sensing .....	137
6.3	Results and Discussion .....	138
6.3.1	Magnetic Nanoparticle Label Characterization .....	138
6.3.2	Magneto-resistance Chip Characterization .....	140
6.3.3	Glucose Biosensing of Diluted Rats Blood Samples.....	145
6.4	Conclusion .....	146
6.5	References.....	146
Chapter 7	.....	150
7	Summary and Recommendations.....	150
7.1	Summary and Conclusion.....	150
7.2	Contributions of the Research to the Current State of Knowledge.....	154
7.3	Future Studies .....	159
7.4	References.....	160
Appendices	.....	165

Appendix 1 .....	165
Appendix 2 .....	166
Appendix 3 .....	167
Appendix 4 .....	168
Appendix 5 .....	169
Appendix 6 .....	170
Appendix 7 .....	171
Appendix 8 .....	172
Appendix 9 .....	173
Appendix 10 .....	174
Appendix 11 .....	175
Appendix 12 .....	176
Appendix 13 .....	177
Appendix 14 .....	178
Curriculum Vitae .....	179

## List of Tables

Table 1.1 Summary of current glucose sensing methods. ....	8
Table 1.2 Tear glucose level. [95-96] .....	10
Table 3.1 Glucose level in rats' tear samples measured by the nanostructured FRET sensor as compared to the blood glucose level of the four rats.....	79
Table 5.1 Summary of carbon source and ethylene glycol quantity. ....	109
Table 6.1 Magnetic data of FeCo crystal and graphene/FeCo magnetic nanocomposites at room temperature. ....	143
Table 7.1 Summary of investigated fluorescent nanomaterials. ....	156

## List of Figures

Figure 1.1 Schematic of a biosensor. ....	2
Figure 1.2 Schematic of fluorescent resonance energy transfer (FRET) process, $r$ is the distance between the donor and acceptor.....	4
Figure 1.3 Schematic principle of (a) conventional photoluminescence (Stokes) process, and (b) upconversion photoluminescence (anti Stokes) process. ....	5
Figure 1.4 Schematic of multilayer magnetoresistive system. ....	7
Figure 1.5 Schematic of multicomponent magnetoresistive system.....	8
Figure 1.6 Schematic of current challenge of marketed electrochemical glucometer and possible solving method by development of fluorescent, magnetoresistive nanostructured glucose biosensor. ....	12
Figure 1.7 Schematic of my work on four nanostructured glucose biosensors. ....	13
Figure 2.1 General steps involved in the application of functional nanomaterials. Reprinted with permission from [45], Copyright (2010) American Chemical Society. (Permission in Appendix 1) .....	30
Figure 2.2 Examples of nanomaterials and their functional groups for biological applications. Reproduced from [46] with permission of the Royal Society of Chemistry. (Permission in Appendix 2) .....	30
Figure 2.3 Chemical structure of the QDs-Con A- $\beta$ -CDs-Au NPs nanobiosensor and schematic illustration of its FRET-based operating principles. Reproduced from [61] with permission of the John Wiley and Sons. (Permission in Appendix 3).....	32
Figure 2.4 The glucose dehydrogenase biocatalyzed generation of NADH by the oxidation of glucose enables the fluorescence detection of glucose by methylene-blue-functionalized CdSe/ZnS quantum dots. Reproduced from [62] with permission of the John Wiley and Sons. (Permission in Appendix 4) .....	33
Figure 2.5 Sensing assembly: (a) top 3 bilayers of PAH/GOD, (b) 3 bilayers of PAH/PSS, and (c) 12 bilayers of PAH/CdTe QDs. PAH=poly(allylamine hydrochloride), GOD=glucose oxidase, PSS=polystyrenesulfonate, QD=quantum dots. Reprinted with permission from [63], Copyright (2009) American Chemical Society. (Permission in Appendix 5) .....	34
Figure 2.6 Schematic illustration of the process for protein encapsulation in silica nanoparticles. After formation of a microemulsion, silica nanoparticles are formed by addition of ammonium hydroxide to increase the pH. In a last step, the inverse microemulsion is redispersed in water to give an aqueous silica dispersion with the FRET-based biosensor encapsulated in the silica nanomatrix. A specific interaction between the silica matrix and the biosensor is mediated by a silica-calcium-hexa-histidine-tag complex. Reproduced from [66] with permission of the Royal Society of Chemistry. (Permission in Appendix 6) .....	35

Figure 2.7 Ru(bipy) <sub>3</sub> <sup>2+</sup> loaded mesoporous silica capped with cyclodextrin-modified glucose oxidase (CD-GOx) for the detection of glucose. Reproduced from [35] with permission of the Royal Society of Chemistry. (Permission in Appendix 7).....	36
Figure 2.8 (a) Schematic diagram for the selective detection of H <sub>2</sub> O <sub>2</sub> and glucose and the specific recognition of H <sub>2</sub> O <sub>2</sub> by HRP and TMB. (b) The colorless TMB was oxidized into blue oxTMB by polymerization. (For interpretation of the references to color in this scheme legend, the reader is referred to the web version of this article.) Reprinted from [75], Copyright (2015), with permission from Elsevier. (Permission in Appendix 8).....	38
Figure 2.9 Design and principle for H <sub>2</sub> O <sub>2</sub> and glucose detection using a MnO <sub>2</sub> -nanosheet-modified UCNP nanocomposite. Reprinted with permission from [76], Copyright (2015) American Chemical Society. (Permission in Appendix 9).....	39
Figure 2.10 Schematic sensing mechanism of the sensor for urea and Glucose detection. Reproduced from [85] with permission of the Nature Publishing Group. (Permission in Appendix 10) .....	40
Figure 2.11 Glucose-binding protein (GBP) covalently conjugated to a fluorescent single-walled carbon nanotube (SWNT) is shown to act as an optical switch. Hinge-bending response to glucose causes a reversible exciton quenching of the SWNT fluorescence with high selectivity. Reproduced from [103] with permission of the John Wiley and Sons. (Permission in Appendix 11) .....	42
Figure 2.12 Fluorescence turn-on strategy for glucose detection based on combination of Carbon nanodots supported on silver nanoparticles and GOx-mediated oxidation of glucose. Reprinted with permission from [104], Copyright (2016) American Chemical Society. (Permission in Appendix 12) .....	43
Figure 3.1 (a) Illustration of the designed FRET transducer made of Con A-conjugating quantum dots (donor) and MG (acceptor) for detecting glucose. Competitive affinity for glucose displaces MG to restore the quenched fluorescence. (b) Immobilization of the nanostructured FRET transducers on ZnO nanorod array deposited on silicone hydrogel. ....	62
Figure 3.2 A lift-off process for fabricating the patterned ZnO nanorod array on silicone hydrogel. ....	65
Figure 3.3 Chromatography of the conjugation of MG to dextran. ....	66
Figure 3.4 FRET signal (fluorescence intensity) vs. the weight ratio of QDs to Con A loading with acceptor. ....	67
Figure 3.5 Relative cell viability vs. the amount of the patterned FRET sensors deposited on silicone hydrogel. ....	70
Figure 3.6 Characterization of nanomaterials by electron microscopes. (a) SEM micrographs of patterned ZnO NRs deposited on a silicone hydrogel. The small inset is the photomask. (b) The magnified SEM micrograph of ZnO nanorod array deposited on a silicone hydrogel. (c) SEM micrograph of ZnO nanorods. (d) SEM micrograph of QDs coated ZnO nanorods. (e) TEM micrograph of QDs coated ZnO nanorods. (f) HRTEM of CdSe/ZnS QDs.....	72



Figure 3.7 FTIR spectra of the cysteamine (Cys) modified QDs and ZnO nanorod (NR), and the hybrid ZnO NR coated with QDs (ZnO NR-QDs). .....	73
Figure 3.8 Photoluminescence of ZnO NR arrays on silicone hydrogel with/without QDs, and QDs-based fret sensors, and the UV-vis absorption of MG.....	74
Figure 3.9 A linear relationship between fluorescence intensity of the designed sensor and the concentration of glucose. ....	75
Figure 3.10 Fluorescence images of the patterned FRET sensor on silicone hydrogel and the relative pixel intensities of the sensors responding to the concentrations of glucose. (a) Fluorescence images of the patterned FRET sensor to aqueous glucose with 0.04 mmol/L and 0.4 mmol/L, respectively. (b) The relative pixel intensities of the sensors vs. the concentration of aqueous glucose. ....	77
Figure 3.11 Photoluminescence spectra of designed sensor responding to tear samples from rats with different glucose level in blood.....	78
Figure 3.12 Relative sensing signal ( $I_{\text{test sample}}/I_{\text{glucose}}$ ) to different biomolecules. ....	79
Figure 4.1 Schematic of LRET sensor sensing mechanism.....	88
Figure 4.2 (a) TEM micrograph of NaGdF <sub>4</sub> : Yb <sup>3+</sup> , Er <sup>3+</sup> UCNCs, the small inset is the size distribution histogram chart. (b) HRTEM image of as-synthesized NaGdF <sub>4</sub> : Yb <sup>3+</sup> , Er <sup>3+</sup> UCNCs.....	90
Figure 4.3 XRD profile of NaGdF <sub>4</sub> : Yb <sup>3+</sup> , Er <sup>3+</sup> upconverting nanoparticles and the line pattern of standard cubic phase of NaGdF <sub>4</sub> (JCPDS 27-0697) and hexagonal phase of NaGdF <sub>4</sub> (JCPDS 27-0699).....	91
Figure 4.4 FTIR spectrum of PEI capped NaGdF <sub>4</sub> : Yb, Er upconversion nanocubes.....	92
Figure 4.5 Photoluminescent spectrum of NaGdF <sub>4</sub> : Er, Yb solution (1 mg/mL). (a) Photoluminescence as a function of laser light powered in the range of 0.5 W to 1.5 W. (b) Power dependence of red and green emissions.....	93
Figure 4.6 (a) Magnetic hysteresis curves of PEI capped NaGdF <sub>4</sub> :Yb <sup>3+</sup> , Er <sup>3+</sup> nanocubes with temperatures. (b) Magnetic susceptibility of NaGdF <sub>4</sub> :Yb <sup>3+</sup> , Er <sup>3+</sup> nanocubes at various temperatures.....	94
Figure 4.7 Relative cell viability as a function of the concentration of UCNCs with surface modification. ....	95
Figure 4.8 SEM image of contact lens nanostructured glucose biosensor surface. ....	97
Figure 4.9 Nanostructured upconverting glucose biosensor response to plasma glucose. ....	98
Figure 5.1 Schematic mechanism of carbon dots/graphene oxide glucose nanobiosensor. ....	107
Figure 5.2 UV-vis spectrum of graphene oxide solution.....	110
Figure 5.3 Photo image of carbon dots under room light and under 312 nm excitation from UV panel. ....	112

Figure 5.4 (a) Photoluminescence spectrum of color tunable carbon dots excited by 400 nm and UV-vis absorbance spectrum of graphene oxide solution; (b) Emission peaks of carbon dots samples versus carbon source/ethylene glycol ratio (%).....	113
Figure 5.5 UV-vis absorbance spectrum of carbon dots samples. ....	114
Figure 5.6 TEM image of sample 3 carbon dots.....	115
Figure 5.7 TEM images of carbon dots sample 1, 2, 4 and 5. ....	116
Figure 5.8 Fluorescent spectrum of carbon dots sample of 1, 2, 4 and 5 (all 0.1 mg/mL). .....	117
Figure 5.9 Fluorescence spectrum of sample 3 carbon dots, (a) Measured spectrum and (b) Normalized fluorescence intensity spectrum. ....	118
Figure 5.10 Fluorescence spectrum of bioconjugate Con A-carbon dots (sample 3), (a) Measured spectrum and (b) Normalized spectrum. ....	118
Figure 5.11 UV-Vis absorbance spectrum of carbon dots, Con A and carbon dots-Con A bioconjugate.....	119
Figure 5.12 FTIR spectrum of (a) graphene oxide, (b) graphene oxide-chitosan and (c) chitosan. ....	120
Figure 5.13 Fluorescence spectra of GO-CS titration of Con A-carbon dots.....	121
Figure 5.14 Glucose biosensing of two ranges of glucose level. (a) and (b) shows the sensing results of glucose level in 1 mM to 10 mM; (c) and (d) shows the sensing results of glucose in 0.2 mM to 1 mM. ....	122
Figure 5.15 Biosensing of diluted rat blood samples with glucose concentrations of 3 mM, 4.5 mM, 6 mM, 7.5 mM, 9 mM and 10.5 mM. ....	123
Figure 6.1 Schematic of nanostructured magnetoresistive glucose biosensor. (a) Facile polyol process of production of magnetic graphene/Fe <sub>50</sub> Co <sub>50</sub> hybrid nanosheets. (b) TEM image graphene nanosheet, scale bar 1000 nm. (c) TEM image of magnetic graphene (120 mg) /Fe <sub>50</sub> Co <sub>50</sub> hybrid nanosheets, scale bar 1000 nm. (d) Hydraulic press for making magnetic graphene/Fe <sub>50</sub> Co <sub>50</sub> hybrid nanosheets and magnetoresistance measurements. ....	131
Figure 6.2 Standard curve of Con A quantification by UV absorbance and quantity of Con A adsorbed on each MR film. ....	133
Figure 6.3 Standard curve of glucose concentration by DNS assay and quantity of glucose adsorbed on each magnetic nanoparticle. ....	134
Figure 6.4 Standard curve of glucose concentration by DNS assay and quantity of glucose adsorbed on each MR film. ....	135
Figure 6.5 Quantification of fluorescent magnetic label by doped dye (FITC) absorbance at 502 nm.....	136
Figure 6.6 Adsorbed fluorescent magnetic label on each MR sensor chip under different glucose concentrations. ....	137
Figure 6.7 (a) TEM image of iron oxide nanoparticle and inset of iron oxide/silica core/shell nanoparticle, scale bar 100 nm; (b) Fluorescence spectra of FITC doped iron	

oxide/silica core/shell nanoparticle; (c) FTIR spectrum of GA modified FITC-iron oxide/silica nanoparticle; .....	138
Figure 6.8 (a) Magnetic hysteresis loop of Fe <sub>3</sub> O <sub>4</sub> nanoparticles; (b) Magnetic hysteresis loop of FITC-iron oxide/silica core/shell nanoparticle.....	139
Figure 6.9 (a) TEM image of graphene (scale bar 2000 nm), (b) XRD pattern of graphite and graphene, (c) TEM image (scale bar 100 nm) of single Fe <sub>50</sub> Co <sub>50</sub> crystal, inset image is corresponding electron diffraction pattern of Fe <sub>50</sub> Co <sub>50</sub> crystal, and (d) Energy-dispersive X-ray analysis of Fe <sub>50</sub> Co <sub>50</sub> crystals.....	140
Figure 6.10 Magnetic hysteresis loop of graphene nanosheets.....	141
Figure 6.11 Samples morphology and magnetic properties of Fe <sub>50</sub> Co <sub>50</sub> crystals and magnetic graphene/Fe <sub>50</sub> Co <sub>50</sub> hybrid nanosheets samples: (a) Fe <sub>50</sub> Co <sub>50</sub> crystal (scale bar 500 nm), (b) FeCo magnetic hysteresis loop, inset showing the enlarged area near Field=0, (c) G <sub>30</sub> FeCo hybrids (graphene 30 mg) (scale bar 2000 nm), (d) G <sub>30</sub> FeCo, G <sub>60</sub> FeCo and G <sub>120</sub> FeCo magnetic nanocomposites magnetic hysteresis loop, inset showing the enlarged area near Field=0. ....	142
Figure 6.12 Actual FeCo weight ratio data from SEM-EDX spectra of a series of magnetic graphene/FeCo samples. ....	143
Figure 6.13 Magnetoresistance of a series of varied graphene mass graphene/FeCo samples.....	144
Figure 6.14 SEM image of nanostructured magnetoresistive glucose biosensor chip surface. ....	145
Figure 6.15 Nanostructured magnetoresistive biosensor sensing diluted rat blood glucose concentration.....	146
Figure 7.1 Schematic of my work on four nanostructured glucose biosensors. ....	150

## List of Abbreviations

A	Acceptor
APB	3-Aminophenylboronic acid monohydrate
APTES/APS	(3-Aminopropyl)triethoxysilane
BCA	Bicinchoninic acid assay
CD	Carbon Dot
CD-GOx	Cyclodextrins modified Glucose Oxidase
CD-CA	Carbon dots-Con A
CdSe	Cadmium Selenium
Con A	Concanavalin A
cPVA	Carboxylated Poly(vinyl alcohol)
Cys	Cysteamine
D	Donor
DI	Deionized
DNA	Deoxyribonucleic Acid
DNS	3, 5-dinitrosalicylic acid
DDSN	Dye-Doped Silica Nanoparticle
EDC	N-(3-Dimethylaminopropyl)-N'-ethylcarbodiimide hydrochloride
EDX	Energy-dispersive X-ray
EG	Ethylene Glycol
FITC	Fluorescein Isothiocyanate
FRET	Fluorescence Resonance Energy Transfer Forster Resonance Energy Transfer
BRET	Bioluminescence Resonance Energy Transfer
CRET	Chemiluminescence Resonance Energy Transfer
HAD	Hexadecylamine
HRP	Horseradish Peroxidase
LRET	Luminescence Resonance Energy Transfer
LOD	Limit of Detection
FTIR	Fourier Transform Infrared Spectroscopy

GA	GLYMO-APB Glycidyloxypropyltrimethoxysilane-3-Aminophenylboronic acid monohydrate
GBP	Glucose Binding Protein
GFP	Green Fluorescent Protein
GMR	Giant Magnetoresistance
GLYMO	Glycidyloxypropyltrimethoxysilane
GO	Graphene Oxide
GO-CS	Graphene Oxide-Chitosan
GOD or GOx	Glucose Oxidase
IR	Infrared
M	mol/L
mM	mmol/L
MR	Magnetoresistance Magnetoresistive
MG	Malachite Green
MGFC	Magnetic Graphene/FeCo
MW	Molecular Weight
NAD	Nicotinamide Adenine Dinucleotide
NHS	N-hydroxysuccinimide
NIR	Near-Infrared
NP	Nanoparticle
NR	Nano Rod
PAH	Poly(allylamine hydrochloride)
PBS	Phosphate Buffered Saline
PEI	Polyethylenimine
PL	Photoluminescence
PR	Photoresist
PSS	Polystyrenesulfonate
QD	Quantum Dot
RBG	Red Blue Green

RET	Resonance Energy Transfer
RGO	Reduced Graphene Oxide
RNA	Ribonucleic Acid
SDS-PAGE	Sodium Dodecyl Sulfate Polyacrylamide Gel Electrophoresis
SEM	Scanning Electron Microscope
SPR	Surface Plasmon Resonance
SWNT	Single-Walled Carbon Nanotube
TEM	Transmission Electron Microscope
TOP	Trioctylphosphine
TMB	3, 3', 5, 5'-tetramethylbenzidine
TOPO	Trioctylphosphine oxide
UCNP	Upconverting/Upconversion Nanoparticle
UCNC	Upconverting/Upconversion Nanocube
UV-vis	Ultraviolet–visible
VSM	Vibrating Sample Magnetometer
WHO	World Health Organization
XRD	X-ray Diffraction
ZnO	Zinc Oxide
ZnS	Zinc Sulfide

# Chapter 1

## 1 General Introduction and Motivation

### 1.1 Overview

#### 1.1.1 Diabetes Mellitus

Diabetes mellitus is recognized as a chronic disease that is characterized by impaired glucose metabolism which often contributes to long-term high blood levels of glucose (hyperglycemia) and is reflected by blood glucose concentrations higher or lower than the normal range of 80 mg/mL–120 mg/mL (4.4 mM–6.6 mM). [1-3]

According to the report of World Health Organization (WHO), over 400 million people in 2014 have to live with diabetes. The global prevalence of diabetes mellitus has caused significant economic burden on health care system in the world. Blood glucose levels in diabetes mellitus patients could fluctuate greatly throughout the day, causing serious complications including heart attacks, strokes, high blood pressure, kidney failure, blindness and limb amputation etc. [4-6] Therefore, the diagnosis and management of diabetes mellitus require a tight monitoring of patients' blood glucose level and the apply corresponding treatments. The importance of sensing blood glucose is reflected on the fact that glucose biosensors account for about 85% of the entire biosensor market. [7-8]

Nanotechnology is the term used to cover the design, construction and utilization of functional structures with at least one characteristic dimension measured in nanometers. [9] Such materials and systems could be designed to exhibit novel and significantly improved physical, chemical and biological properties, phenomena and processes as a result of the limited size of their constituent structures, particles or molecules. The reason for such interesting and very useful behavior is that when characteristic structural features are intermediate in extent between isolated atoms and bulk macroscopic materials; i.e., in the range of about  $10^9$  m to  $10^7$  m (1 nm to 100 nm), the objects may display special attributes substantially different from those displayed by either atoms or bulk materials.

Ultimately this could lead to new technological opportunities as well as new challenges. [10-12] The application of nanotechnology to glucose biosensor area are promising to develop highly sensitive and selective nanostructured glucose biosensor. The nanostructured glucose biosensors are promising to be minimally invasive or non-invasive and be more compliant and smart for management and therapy of diabetes. Current glucometers are designed to measure blood glucose levels of 3 mM to 25 mM. The sensing target could be other body fluids other than blood. For example, tear or saliva, their glucose concentration is much lower than blood glucose concentration. As the sensing analyte is in low concentration, the sensing error would be a concern. Especially in the nanostructured sensor, sensitivity and reproducibility are parameters that influence sensing results greatly. Therefore, we need highly sensitive nanostructured glucose biosensor to have correct results.

### 1.1.2 Nanostructured Glucose Biosensor

A biosensor is a device for the detection of an analyte that combines a biological sensing component (enzyme, antibody, protein, DNA (deoxyribonucleic acid), RNA (ribonucleic acid) etc.) with a physicochemical detector component, it consists of three parts: [13-17]

- ❖ The sensitive biological element, including biological material.
- ❖ The transducer in between.
- ❖ The detector element.

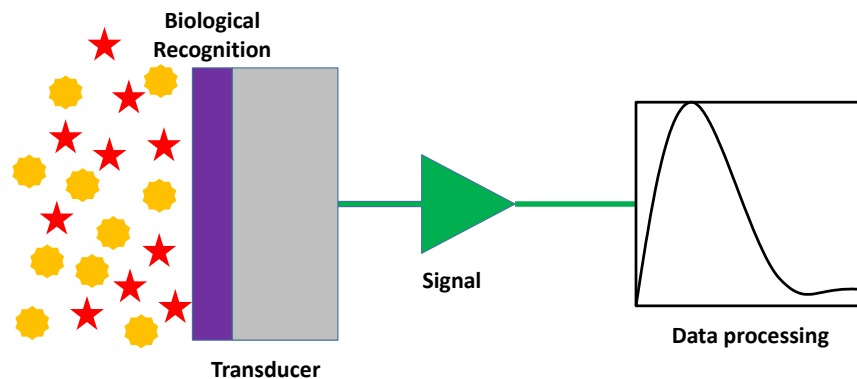


**Figure 1.1 Schematic of a biosensor.**



Nanomaterials and nanostructures have novel characteristics and special chemical, physical and biological properties. The unique size-dependent tunable electronic, optical, magnetic and mechanical properties of nanoscale materials (1–200 nm) offer excellent platform for developing novel bioelectronics and biosensing devices. Nanostructured biosensors are promising to enhance or supersede current analytical assays, and innovate research and clinical practice. So far the unique optical nanomaterials suit themselves ideal for biosensing application. Fluorescent exerting/interacting nanomaterials and nanostructures are especially intriguing as they yield strong optical responses to incident light and the response signal is linked with the target analyte, yielding extremely sensitive detection. [18-23] In past years, most of the researches have been focusing on the fluorescent quantum dots (QDs) and plasmonic gold nanoparticles (Au NPs). Recently, new nanoscale materials have been developed including carbon-based nanostructures, fluorescent polymer/silica nanoparticles, silicon dots, upconversion nanomaterials, alloyed plasmonic nanoparticles, and gold and silver nanoclusters etc. [24-30]

Magnetic nanoparticles have special magnetic properties like superparamagnetic, paramagnetic, ferrimagnetic and ferromagnetic etc. properties. These properties are attributed to different compositions, crystal structures and temperatures etc. Especially the superparamagnetic iron oxide ( $\text{Fe}_3\text{O}_4$ ) have been widely used in biomedical applications like thermal therapy, drug delivery etc. [31-32] Other magnetic nanomaterials are mostly composed of magnetic elements of Fe, Co and Ni and applied in biomedical, catalysis and energy areas. [33-34] Magnetic nanoscale materials are promising for developing magnetoresistive biosensors.

Nanoscale materials normally need a surface covering as a barrier between the nanomaterials and its ambient environment. This layer is usually composed of capping molecules that bind directly to the surface and ideally prevents nanoparticles aggregating or modifies nanostructures surface properties, so to disperse nanoparticles in water at a various range of pH values or biological surrounding, and facilitate the contact between modified nanostructures and external environment. The surface modification prevents nonspecific adsorption of surrounding molecules onto the nanomaterials and nanostructures surface, but also provides a conjugation place for functional biomolecules.

Functional nanomaterials could hold manifold perspectives e.g. miniaturization, novel materials properties and special functions, and complexity of technical device developments. Nanomaterials conjugation with biomolecules could offer excellent signal transduction of biological phenomena in the development of electronic, optical or magnetic biosensors. Optical sensing is more advantageous in biosensor design because it has high sensitivity, wide dynamic range, and multiplexing capabilities. [35-37] In contrast to organic dyes and fluorescent proteins, nanoscale probes e.g. fluorescence resonance energy transfer (FRET) nanomaterials and nanostructures provide enormous advantages in aspects like signal brightness, photo-stability, and emission of multicolored light. [38-40] Magnetic sensing uses magnetic nanoscale materials and nanostructures and is gaining interest over recent years. One reason is that magnetic sensing in biological systems could have almost zero noise due to the lack of magnetic elements in most biological components. [41]

### 1.1.3 Fluorescence Resonance Energy Transfer

Fluorescence resonance energy transfer (FRET) is a nonradioactive process. In this process, external excitation light excites the donor. The excited state fluorophore (donor) could transfer energy to a nearby ground state fluorophore (acceptor), normally the distance between donor and acceptor is 1 nm to 20 nm. FRET process is shown in the figure 1.2 below. The energy transfer efficiency is dependent on the distance between the donor and acceptor, the closer they are, the higher efficient the FRET process is. [42-45]

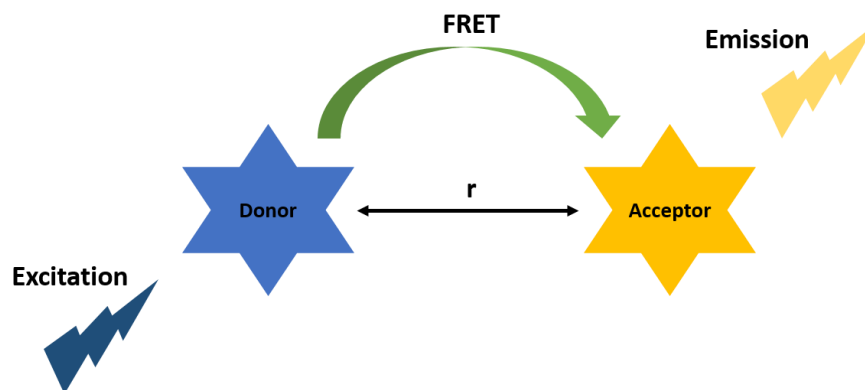


**Figure 1.2 Schematic of fluorescent resonance energy transfer (FRET) process,  $r$  is the distance between the donor and acceptor.**

Fluorescent nanoscale materials and nanostructures are suitable as either donor or acceptor for construction of FRET sensor. Some fluorescence quenching molecules or nanomaterials are also used as fluorescence acceptor to quench the fluorescence. Quantum dots, carbon dots, upconversion nanomaterials are usually used as either donor or acceptor. [46-48] Noble plasmonic nanoparticles like gold or silver nanoparticles are often used as fluorescence quencher, graphene oxide [49] are also used as fluorescence quenchers due to their  $\pi$  electrons which could quench fluorescence. [50]

### 1.1.4 Upconversion Fluorescence

Upconversion is an optical anti-Stokes process. In the upconverting process, the upconverting nanomaterials are excited by an excitation of near-infrared light (normally 980 nm) and then emits visible light of blue light, green light or yellow light. The emission are adjustable by choosing different element dopants. [51-53] One advantage of using upconversion nanostructured glucose biosensor is that near-infrared excitation are much less harmful to human tissue than UV light. [54-58]

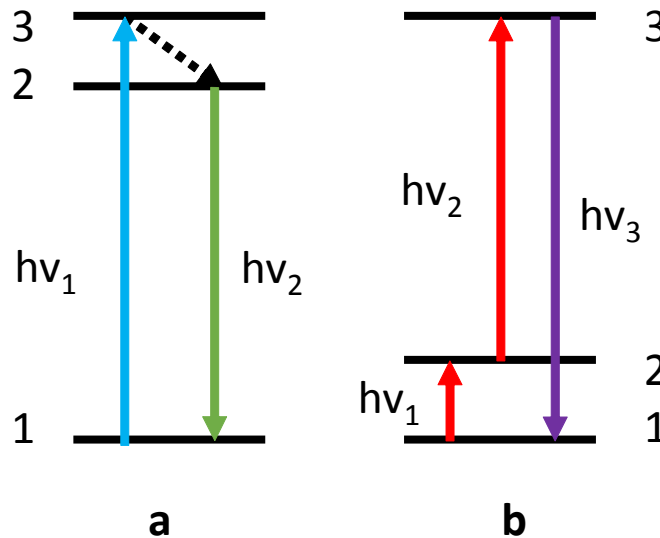


**Figure 1.3 Schematic principle of (a) conventional photoluminescence (Stokes) process, and (b) upconversion photoluminescence (anti Stokes) process.**

Figure 1.3 presents the schematic of convention (Stokes shift) and upconverting (anti Stokes shift) fluorescence process. The upconverting photoluminescence could be induced by low-power and incoherent excitation sources, such as continuous-wave lasers, standard xenon or halogen lamps, or even focused sunlight. [59] The primary theory of the upconversion luminescence process (figure 1.3 (b)) is that a luminescent center at the ground state 1 could absorb energy from either an excitation photon or a corresponding energy transfer process to reach the excited state 2. Subsequently, another excitation photon or a corresponding energy transfer process would promote the luminescent center from excited state 2 to the excited state 3. Then, a radiative transition from this excited state 3 back to the ground state or some other lower-energy state, results in a higher-energy photon emission. In the upconversion luminescence process, the metastable intermediate excited state is attained. This metastable intermediate excited state is expected to have a relatively long lifetime so as to maintain a high population in the intermediate excited state ahead of the second excitation energy. [60-62]

### 1.1.5 Magnetoresistance

Magnetic immunoassay is a novel immunoassay for early disease diagnosis compared to traditional radioimmunoassay or fluoroimmunoassay. This assay utilizes magnetic nanoparticle as biolabel and magnetoresistive sensor chip as detector. Most of the biological components do not have magnetic background, therefore the magnetoresistive sensor could have very high sensitivity. With careful design, MR sensor can even measure the presence of single glucose molecules. As the ultra-high sensitivity of MR sensor, we can use MR sensor to sense glucose in other body fluids like urine, saliva etc. For electrochemical and optical sensing of urine, the urine is a complicated mixture and would cause great errors for the detection. But MR sensor does not affected by the complicated urine compositions. Magnetoresistance is an electron spin effect phenomenon. The magnetoresistance effect was discovered early in the 1850s. At the early days, this effect was smaller than 5%. Until the discovery of Giant Magnetoresistance (GMR) in the late 1980s, which has boosted the hard disk development in computer industry. The magnetoresistance value is commonly calculated by the following equation: [63-66]

$$\text{MR}\% = \frac{R(H) - R(0)}{R(0)} \times 100\%$$

Where  $R(H)$  is the resistance under magnetic field  $H$ ,  $R(0)$  is the resistance without external magnetic field.

Normally a magnetic multilayer structure or magnetic multicomponent structure chip are the format of a magnetoresistive chip. Under the external applied magnetic field, the resistance of the MR chip is influenced, a magnetic nanoparticle label binding to the chip surface would cause a minute magnetic field influence. This minute magnetic field could be detected by the magnetoresistive sensor chip into resistance signal. [67-71] The schematics of multilayer and multicomponent magnetoresistive chip is shown below.

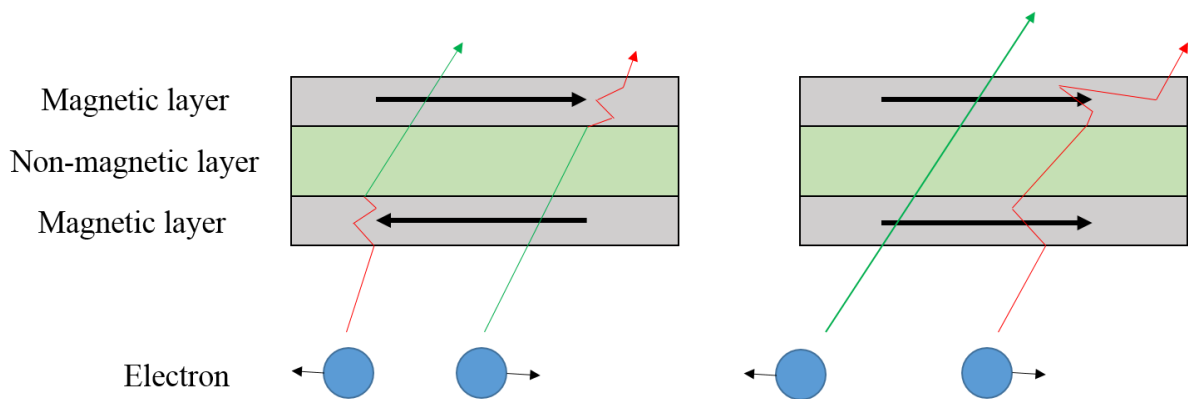


**Figure 1.4 Schematic of multilayer magnetoresistive system.**

In the multilayer system, ferromagnetic layers and non-magnetic conductive layers are sandwiched, the layer thickness is in the values of several or tens of nanometers. When the two magnetic layers are magnetized parallel, the electrons antiparallel to magnetization could travel through the magnetic layer smoothly. In condition without external applied field, the magnetization direction in the system are antiparallel, either spin up electron or spin down electron would scatter when passing the layers. As a result, this condition would have a higher resistance. When the multilayer magnetization are paralleled by external field, one spin direction of the electron could move smoothly through the layers, thus having a smaller resistance. [72-77]

In the multicomponent system, the magnetoresistance principle is similar. The more scattering of electrons, the larger resistance it has. Some multicomponent systems are based on graphene nanocomposites, doping magnetic nanoparticles like  $\text{Fe}_3\text{O}_4$ ,  $\text{FeNi}_3$  [78-83] onto graphene nanosheet could have magnetoresistive effects.

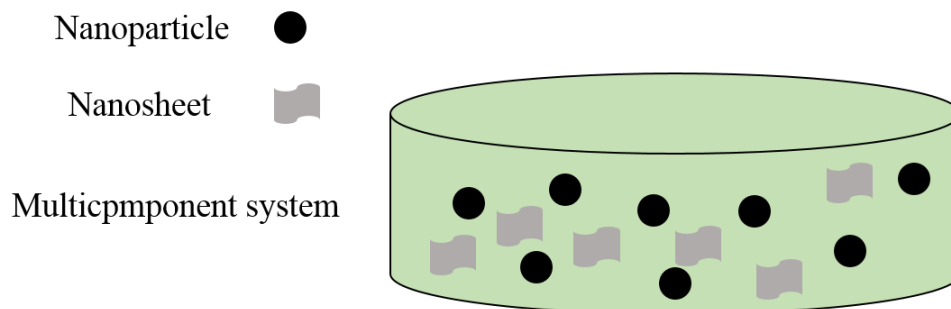


**Figure 1.5 Schematic of multicomponent magnetoresistive system.**

## 1.2 Current Challenges in Glucose Sensor for Diabetics

Currently, diabetes mellitus is a worldwide public health problem and the diagnosis and management of diabetes mellitus requires a tight monitoring of blood glucose levels. [3] Blood glucose levels in diabetics fluctuate significantly throughout the day, causing great challenge of reliable and convenient glucose sensing. [7] The electrochemical glucometer is the most widely used glucose sensor in daily use. However, the marketed glucometers have certain level of invasiveness (blood required, often by finger prick to obtain a small drop of blood) to patients. And the diabetics may need several times of finger pricks per day. And this invasive sensing are often characterized by infection risks and discomfort to diabetics.

**Table 1.1 Summary of current glucose sensing methods.**

Glucose sensing methods	Electrochemical	Optical	Impedance and electromagnetic spectroscopies
-------------------------	-----------------	---------	--

Advantage	Most developed, commercial product available	Room for potential boost Non-invasiveness, externally accessible (skin, saliva, tears), high sensitivity	Do not need patient blood samples, minimally or noninvasive
Disadvantage	Invasive, finger prick several, times per day, infection risk, discomfort, inconvenient	Less developed, not much commercial product	Poor accuracy, temperature and disease state impact <a href="#">[84-86]</a>

Table 1.1 summarizes the current glucose sensing profiles, electrochemical and optical are the major two sensing mechanisms. Other noninvasive optical techniques include optical coherence tomography, polarimetry, thermal infrared spectroscopy, photo acoustic spectroscopy, and Raman spectroscopy etc. [\[87-90\]](#) However, these methods required big machines in hospital and are not convenient for patients' home care of measuring glucose.

The challenge in the glucose sensing lies in the development of minimally invasive or non-invasive glucose sensors with high selectivity and sensitivity. Optical sensing approach is a sensitive and much minimally invasive path for glucose sensing. Magnetoresistive (MR) sensing is a highly sensitive sensing technique. Because most of the biological components are free of magnetic noise, therefore, MR sensing has very low or zero background noise and very sensitive to target analyte with magnetic labelling. The highly sensitive MR sensor could be designed to measure tear glucose or other body fluid glucose.

Other body fluids of skin sweat, urine, saliva, tears etc. have been studied and used as glucose sensing target. Certain accuracy of sensing glucose has been attained. However, each body fluid has its pros and cons. For example, sweat from different position may have different components and causing measure errors. Urine is a colored mixture of various

different compositions like protein, ions, impurities etc. and urine is varied from person to person that have different diets. Saliva and tear are more adequate for accurate continuous glucose sensing target. [91-94] Comparatively speaking, tear is more stable and continuous than saliva. And tear glucose level has certain relationship to blood glucose. Other affecting factors could be eye diseases which could affect the tear composition. This could be solved by survey enough patients' tear to get more understanding of tear glucose levels.

Table 1.2 shows the tear glucose level and blood glucose level for diabetics and healthy person. Statistic results shows that blood glucose is approximately two times higher in diabetics (*circa* 11 mM) compared with non-diabetes (*circa* 5 mM). Also, the average concentrations of tear glucose for diabetes patients and non-diabetes are  $0.35\pm 0.04$  mM and  $0.16\pm 0.03$  mM. [95-96] There is clearly enough evidence of a correlation between tear glucose and blood glucose to justify continued efforts on developing tear glucose sensing approach, although this correlation is not yet fully characterized. [95-97]

**Table 1.2 Tear glucose level. [95-96]**

Minimally invasive or non-invasive optical/magnetic approaches	Glucose level		
		Diabetes	Non-diabetes
	Tear		
Better accessible, continuously obtainable, stable, less susceptible than urine, saliva, sweat etc.	Blood	11 mM	5 mM
	Tear	$0.35\pm 0.04$ mM	$0.16\pm 0.03$ mM

However, the tear glucose level is very low, for diabetes patients and non-diabetes tear glucose concentrations are  $0.35\pm 0.04$  mM and  $0.16\pm 0.03$  mM. And the other considering factor is the acquisition of enough tear. Tear is not like urine, saliva or blood, average tear flow rate is at about 1.2  $\mu\text{L}/\text{min}$  with a range of 0.5 to 2.2  $\mu\text{L}/\text{min}$  and the average normal tear volume is about  $6.2\pm 2$   $\mu\text{L}$ . [98] Therefore, highly sensitive sensors are necessary for



development of tear glucose sensors. Nanoscale materials and nanostructures are promising to develop such highly sensitive and selective glucose sensors.

In order to measure the minute tear glucose concentration, sensitive sensor are required. The tear glucose concentration is in the range of 0.1 mM to 0.5 mM. The tear amounts needed are dependent on the sensitivity and design of the sensor. The marketed glucometer could be designed to measure glucose concentrations in the range of 0.1 mM to 0.5 mM. However, it required electrochemical reader, which would limit the glucometer incorporated into contact lens. Another concern is that as the glucometer sensing range decreases to 0.1 mM to 0.5 mM, the sensing errors are needed to be considered. For example if the sample collecting sensing cell is designed to be 100 nm cubic which absorbs sample by capillary effects or microfluidic control, the amounts of samples would be 0.001  $\mu\text{L}$ . Therefore, highly sensitive sensors are necessary to construct such glucometer. Magnetoresistive (MR) sensors are highly sensitive and able to measure up to several glucose molecules. The development of MR glucose sensors are promising to sensing glucose in tears and other body fluids.

The unique fluorescent, magnetoresistive nanomaterials and nanostructures have special chemophysical properties which make them ideal for biosensing with high sensitivity and selectivity. [99-101] First of all, nanomaterials and nanostructures have large surface area, which could greatly increase the sensor contact with target analyte. Thus nanostructures sensor could sense very minute samples of tens of  $\mu\text{L}$  volume sample with nanofabricated sensing cells in the nanoliter range. Secondly, nanoscale materials have special size-dependent properties, novel chemical, physical and biological properties, these properties enhance nanostructured sensor sensitivity as well. Moreover, the size-dependent properties provide practical approach to control nanomaterials and nanostructures properties. Various chemical methods, physical methods, top-down, bottom-up approaches have been developed to synthesize and fabricate different nanoscale materials and nanostructures with controlled surface fluorescent and magnetoresistive properties.

The fluorescent based nanostructures are promising for developing contact lens based tear glucose sensor. This contact lens based glucose sensor is a minimally invasive or non-

invasive approach. On the other hand, the magnetoresistive method provide high sensitivity sensing technique. Although the MR sensor is currently quite difficult to be incorporated into contact lens sensor to sense tear glucose, it is worthy to develop MR glucose sensor to sense blood glucose, urine glucose, sweat glucose, saliva glucose or other body fluids glucose. These body fluids are clear of magnetic interference and MR glucose sensor could provide highly sensitive results.

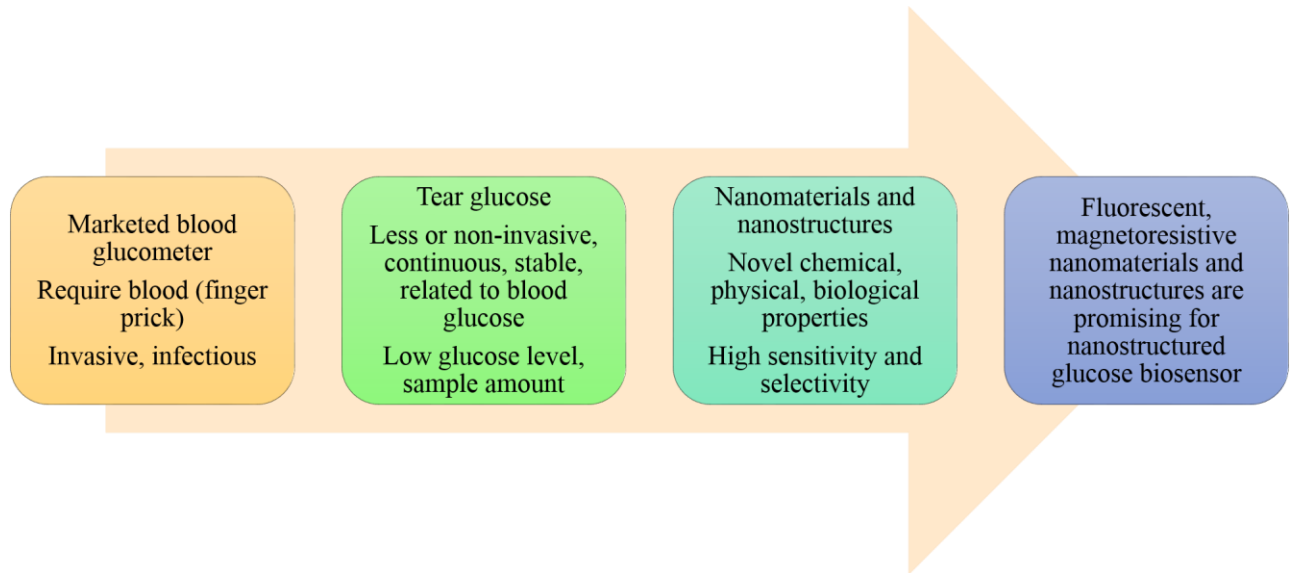


**Figure 1.6 Schematic of current challenge of marketed electrochemical glucometer and possible solving method by development of fluorescent, magnetoresistive nanostructured glucose biosensor.**

In summary (figure 1.6), the design and fabrication of fluorescent, magnetoresistive nanostructured glucose biosensors are promising to solve the current electrochemical glucometer problem of invasiveness, finger pricks, possible infections etc. while providing diabetics with much compliant glucose sensing alternatives and better management of diabetes diseases.

### 1.2.1 Objectives and Outcomes

The major motivation of my work is that the development of minimally invasive or non-invasive sensitive and selective glucose measurement method is urgent for diabetes patients. Optical approaches are less developed and have potential development. The

optical approaches meet the requirement of minimal invasiveness or non-invasiveness, highly sensitivity and highly selectivity. Magneto-resistive technique also has high sensitivity and selectivity due to lack of magnetic interference in most biological components. Therefore, fluorescent, magneto-resistive nanostructured glucose biosensor are promising in replacing current marketed electrochemical glucometer.

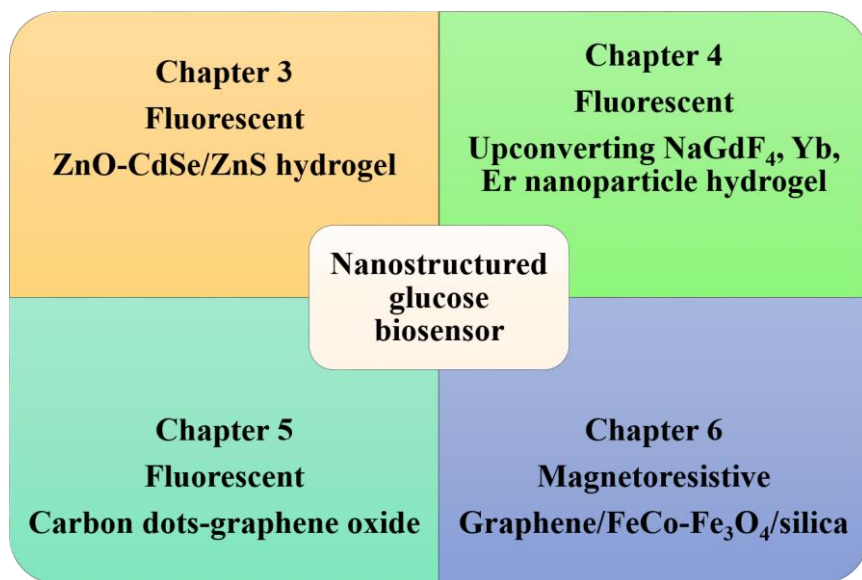


**Figure 1.7 Schematic of my work on four nanostructured glucose biosensors.**

The overall outcome of my work (figure 1.7) is to utilize various nanoscale materials and fabricated nanostructures to construct nanostructured glucose biosensors for tear glucose sensing and blood glucose sensing. The fluorescent and magneto-resistive approaches are studied. Several goals are set up to fulfill the objective as stated below.

- [1] To synthesize a variety of fluorescent, magnetic nanomaterials and fabrication of nanostructures.
- [2] To develop efficient methods for surface functionalization and bioconjugation of nanomaterials' and nanostructures' surface.
- [3] To fabricate nanostructured glucose biosensors using the synthesized fluorescent, magnetic nanomaterials.

- [4] To explore the nanostructured glucose biosensors (based on the synthesized fluorescent, magnetic nanomaterials) for tear glucose sensing, blood glucose sensing applications.

To achieve these goals, the following specific objectives are sought in various chapters of the thesis.

❖ Chapter 1 General Introduction and Motivation

This chapter provides an overview of diabetes mellitus, biosensors, nanostructured glucose biosensors, sensing techniques/mechanisms, current challenge in glucose sensing area and the outline of objectives and layout of the thesis.

❖ Chapter 2 Background and Literature Review

This chapter presents a general review of fluorescent exerting/interacting nanoscale materials (quantum dots, upconversion nanoparticles, nanocarbon materials of carbon dots, graphene oxide and graphene) and magnetoresistive nanomaterials for nanostructured glucose biosensors.

❖ Chapter 3 Development of ZnO/QD Patterned Nanostructured Glucose Biosensor

The objective of this chapter was to develop a fluorescence resonance energy transfer nanostructured glucose biosensor. This chapter presents the preparation of patterned ZnO nanorod array decorated with CdSe/ZnS quantum dots on hydrogel film. The surface of the patterned nanostructured was modified with Con A protein and binding with malachite green dextran. This nanostructured glucose biosensor was used to measure rats tear glucose.

❖ Chapter 4 Development of Upconversion NaGdF<sub>4</sub>: Yb, Er Glucose Biosensor

The objective of this chapter was to develop upconversion NaGdF<sub>4</sub>: Yb, Er nanomaterials based fluorescence resonance energy transfer nanostructured glucose biosensor. This chapter presents the preparation of upconversion NaGdF<sub>4</sub>: Yb, Er nanomaterials by a polyol process. The surface of the upconversion

nanomaterials was as-synthesized modified by amine groups ( $-NH_2$ ). The nanoparticles were further surface modified with Con A and deposited onto hydrogel film surface to construct nanostructured glucose biosensor to measure rats' blood glucose.

❖ Chapter 5 Development of Carbon Dots/Graphene Oxide Glucose Biosensor

The objective of this chapter was to develop nanocarbon materials based fluorescence resonance energy transfer glucose nanobiosensor using carbon dots/graphene oxide. This chapter presents the preparation of fluorescent carbon dots by a microwave assisted process. Graphene oxide was prepared by a Hummers' method. Carbon dots work as fluorescence donor with surface modified with Con A, graphene oxide work as fluorescent acceptor (fluorescent quencher). This glucose nanobiosensor was explored to measure rats' blood glucose.

❖ Chapter 6 Development of FeCo/graphene Magnetoresistive Nanostructured Glucose Biosensor

The objective of this chapter was to develop FeCo/graphene magnetoresistive nanostructured glucose biosensor. This chapter presents the preparation of FeCo magnetic nanoparticle, graphene nanomaterials and FeCo/graphene nanocomposite by a polyol process.  $Fe_3O_4$ /silica core/shell nanoparticles were prepared and used as magnetic label. The FeCo/graphene nanocomposite film surface was modified with Con A, the magnetic label surface was modified with phenylboronic acid (can bind to glucose molecule). The magnetoresistive nanostructured glucose biosensor was used to measure diluted rats' blood glucose.

❖ Chapter 7 Summary and Recommendations

This chapter provides a general conclusion of the above studies and recommendations for future work on the nanostructured glucose biosensors.

## 1.3 References

- [1] Brooke E. Harcourt; Sally A. Penfold; Josephine M. Forbes, Coming full circle in diabetes mellitus: from complications to initiation. *Nature Reviews Endocrinology* **2013**, 9 (2), 113-123.
- [2] David D Cunningham; Julie A Stenken, *In vivo glucose sensing*. John Wiley & Sons: 2009; Vol. 174.
- [3] Joseph Wang, Electrochemical Glucose Biosensors. *Chemical Reviews* **2008**, 108 (2), 814-825.
- [4] Katsuhito Mori; Masaaki Inaba, Diabetes and Vascular Calcification. In *Diabetes and Aging-related Complications*, Sho-ichi Yamagishi, Ed. Springer Singapore: Singapore, 2018; pp 59-68.
- [5] Ippei Kanazawa; Toshitsugu Sugimoto, Diabetes and Osteoporosis. In *Diabetes and Aging-related Complications*, Sho-ichi Yamagishi, Ed. Springer Singapore: Singapore, 2018; pp 127-139.
- [6] P. Mason McClatchey; Timothy A. Bauer; Judith G. Regensteiner; Jane E. B. Reusch, Exercise, Blood Flow, and the Skeletal Muscle Microcirculation in Diabetes Mellitus. In *Diabetes and Exercise: From Pathophysiology to Clinical Implementation*, M. D. Jane E. B. Reusch; PhD M. A. B. A. Judith G. Regensteiner; Ed D. Faha Maacypr Facsm Kerry J. Stewart; M. D. DSc Aristidis Veves, Eds. Springer International Publishing: Cham, 2018; pp 165-172.
- [7] Scott P. Nichols; Ahyeon Koh; Wesley L. Storm; Jae Ho Shin; Mark H. Schoenfisch, Biocompatible Materials for Continuous Glucose Monitoring Devices. *Chemical Reviews* **2013**, 113 (4), 2528-2549.
- [8] Anthony P. F. Turner, Biosensors: sense and sensibility. *Chemical Society Reviews* **2013**, 42 (8), 3184-3196.
- [9] Fritz Allhoff; Patrick Lin; Daniel Moore, *What is nanotechnology and why does it matter?: from science to ethics*. Wiley Online Library: 2010.
- [10] Bharat Bhushan, Introduction to nanotechnology. In *Springer handbook of nanotechnology*, Springer: 2017; pp 1-19.
- [11] William S Bainbridge, Nanoscience and Nanotechnology Convergence. In *Springer Handbook of Nanotechnology*, Springer: 2017; pp 1587-1602.
- [12] Sulabha K Kulkarni, *Nanotechnology: principles and practices*. Springer: 2015.
- [13] I. Palchetti; M. Mascini, Biosensor Technology: A Brief History. In *Sensors and Microsystems*, Piero Malcovati; Andrea Baschiroto; Arnaldo d'Amico; Corrado Natale, Eds. Springer Netherlands: 2010; Vol. 54, pp 15-23.

- [14] BhavikA Patel; CostasA Anastassiou; Danny O'Hare, Biosensor Design and Interfacing. In *Body Sensor Networks*, Guang-Zhong Yang, Ed. Springer London: 2006; pp 41-87.
- [15] Joseph Wang, Glucose Biosensors: 40 Years of Advances and Challenges. *Electroanalysis* **2001**, *13* (12), 983-988.
- [16] Young Je Yoo; Yan Feng; Yong Hwan Kim; Camila Flor J. Yagonia, Enzymes for Biosensors. In *Fundamentals of Enzyme Engineering*, Springer Netherlands: Dordrecht, 2017; pp 181-188.
- [17] Minal Garg; Sudhir Mehrotra, Biosensors. In *Principles and Applications of Environmental Biotechnology for a Sustainable Future*, Ram Lakhan Singh, Ed. Springer Singapore: Singapore, 2017; pp 341-363.
- [18] Philip D. Howes; Rona Chandrawati; Molly M. Stevens, Colloidal nanoparticles as advanced biological sensors. *Science* **2014**, *346* (6205).
- [19] Ke Xu; Mohsen Purahmad; Kimber Brenneman; Xenia Meshik; Sidra Farid; Shripriya Poduri; Preeti Pratap; Justin Abell; Yiping Zhao; Barbara Nichols; Eugene Zakar; Michael Stroschio; Mitra Dutta, Design and Applications of Nanomaterial-Based and Biomolecule-Based Nanodevices and Nanosensors. In *Design and Applications of Nanomaterials for Sensors*, Jorge M. Seminario, Ed. Springer Netherlands: 2014; Vol. 16, pp 61-97.
- [20] Tennyson L. Doane; Clemens Burda, The unique role of nanoparticles in nanomedicine: imaging, drug delivery and therapy. *Chemical Society Reviews* **2012**, *41* (7), 2885-2911.
- [21] Omid Veisheh; Benjamin C. Tang; Kathryn A. Whitehead; Daniel G. Anderson; Robert Langer, Managing diabetes with nanomedicine: challenges and opportunities. *Nature Reviews Drug Discovery* **2015**, *14* (1), 45-57.
- [22] Sergey M. Borisov; Otto S. Wolfbeis, Optical Biosensors. *Chemical Reviews* **2008**, *108* (2), 423-461.
- [23] Alyssa B. Chinen; Chenxia M. Guan; Jennifer R. Ferrer; Stacey N. Barnaby; Timothy J. Merkel; Chad A. Mirkin, Nanoparticle Probes for the Detection of Cancer Biomarkers, Cells, and Tissues by Fluorescence. *Chemical Reviews* **2015**, *115* (19), 10530-10574.
- [24] Vasudevanpillai Biju, Chemical modifications and bioconjugate reactions of nanomaterials for sensing, imaging, drug delivery and therapy. *Chemical Society Reviews* **2014**, *43* (3), 744-764.
- [25] Akrema; Rahisuddin, Metal Nanoparticles as Glucose Sensor. In *Nanomaterials and Their Applications*, Zishan Husain Khan, Ed. Springer Singapore: Singapore, 2018; pp 143-168.

- [26] Ling Bing Kong; Wenxiu Que; Kun Zhou; Sean Li; Tianshu Zhang, Carbon Nanomaterials Derived from Graphene and Graphene Oxide Nanosheets. In *Recent Trends in Nanomaterials: Synthesis and Properties*, Zishan Husain Khan, Ed. Springer Singapore: Singapore, 2017; pp 177-243.
- [27] Roberto A. S. Luz; Rodrigo M. Iost; Frank N. Crespilho, Nanomaterials for Biosensors and Implantable Biodevices. In *Nanobioelectrochemistry: From Implantable Biosensors to Green Power Generation*, Frank N. Crespilho, Ed. Springer Berlin Heidelberg: Berlin, Heidelberg, 2013; pp 27-48.
- [28] Joshua A. Jackman; Abdul Rahim Ferhan; Nam-Joon Cho, Nanoplasmonic sensors for biointerfacial science. *Chemical Society Reviews* **2017**, *46* (12), 3615-3660.
- [29] M. Montalti; L. Prodi; E. Rampazzo; N. Zaccheroni, Dye-doped silica nanoparticles as luminescent organized systems for nanomedicine. *Chemical Society Reviews* **2014**, *43* (12), 4243-4268.
- [30] Lourdes Basabe-Desmonts; David N. Reinhoudt; Mercedes Crego-Calama, Design of fluorescent materials for chemical sensing. *Chemical Society Reviews* **2007**, *36* (6), 993-1017.
- [31] Sophie Laurent; Delphine Forge; Marc Port; Alain Roch; Caroline Robic; Luce Vander Elst; Robert N. Muller, Magnetic Iron Oxide Nanoparticles: Synthesis, Stabilization, Vectorization, Physicochemical Characterizations, and Biological Applications. *Chemical Reviews* **2008**, *108* (6), 2064-2110.
- [32] L. Harivardhan Reddy; Jos éL. Arias; Julien Nicolas; Patrick Couvreur, Magnetic Nanoparticles: Design and Characterization, Toxicity and Biocompatibility, Pharmaceutical and Biomedical Applications. *Chemical Reviews* **2012**, *112* (11), 5818-5878.
- [33] Wei Zhou; Lin Guo, Iron triad (Fe, Co, Ni) nanomaterials: structural design, functionalization and their applications. *Chemical Society Reviews* **2015**, *44* (19), 6697-6707.
- [34] Sergey P Gubin, *Magnetic nanoparticles*. John Wiley & Sons: 2009.
- [35] Ramaier Narayanaswamy; Otto S Wolfbeis, *Optical sensors: industrial environmental and diagnostic applications*. Springer Science & Business Media: 2003; Vol. 1.
- [36] Laura Rodriguez-Lorenzo; Laura Fabris; Ramon A. Alvarez-Puebla, Multiplex optical sensing with surface-enhanced Raman scattering: A critical review. *Analytica Chimica Acta* **2012**, *745* (Supplement C), 10-23.
- [37] Yun Wang; Timothy V. Duncan, Nanoscale sensors for assuring the safety of food products. *Current Opinion in Biotechnology* **2017**, *44* (Supplement C), 74-86.



- [38] Tetsuya Haruyama, *Molecules, Cells, Materials, and Systems Design Based on Nanobiotechnology Use in Bioanalytical Technology*. In *Nanobiotechnology*, Oded Shoseyov; Ilan Levy, Eds. Humana Press: 2008; pp 369-382.
- [39] Huangxian Ju; Xueji Zhang; Joseph Wang, *Biofunctionalization of Nanomaterials*. In *NanoBiosensing*, Springer New York: 2011; pp 1-38.
- [40] Shuaidi Zhang; Ren Geryak; Jeffrey Geldmeier; Sunghan Kim; Vladimir V. Tsukruk, *Synthesis, Assembly, and Applications of Hybrid Nanostructures for Biosensing*. *Chemical Reviews* **2017**, *117* (20), 12942-13038.
- [41] D. Issadore; Y. I. Park; H. Shao; C. Min; K. Lee; M. Liong; R. Weissleder; H. Lee, *Magnetic sensing technology for molecular analyses*. *Lab on a Chip* **2014**, *14* (14), 2385-2397.
- [42] Thomas M. Jovin; Diane S. Lidke; Elizabeth A. Jares-Erijman, *Fluorescence Resonance Energy Transfer (FRET) and Fluorescence Lifetime Imaging Microscopy (FLIM)*. In *From Cells to Proteins: Imaging Nature across Dimensions: Proceedings of the NATO Advanced Study Institute on From Cells to Proteins: Imaging Nature across Dimensions Pisa, Italy 12–23 September 2004*, Valtere Evangelista; Laura Barsanti; Vincenzo Passarelli; Paolo Gualtieri, Eds. Springer Netherlands: Dordrecht, 2005; pp 209-216.
- [43] Igor L Medintz; Niko Hildebrandt, *FRET-Förster resonance energy transfer: from theory to applications*. John Wiley & Sons: 2013.
- [44] Harekrushna Sahoo, *Förster resonance energy transfer – A spectroscopic nanoruler: Principle and applications*. *Journal of Photochemistry and Photobiology C: Photochemistry Reviews* **2011**, *12* (1), 20-30.
- [45] Alexander Govorov; Pedro Ludwig Hernández Martínez; Hilmi Volkan Demir, *Förster-Type Nonradiative Energy Transfer Models*. In *Understanding and Modeling Förster-type Resonance Energy Transfer (FRET): Introduction to FRET, Vol. 1*, Alexander Govorov; Pedro Ludwig Hernández Martínez; Hilmi Volkan Demir, Eds. Springer Singapore: Singapore, 2016; pp 19-27.
- [46] Aaron R. Clapp; Igor L. Medintz; J. Matthew Mauro; Brent R. Fisher; Mounqi G. Bawendi; Hedi Mattoussi, *Fluorescence Resonance Energy Transfer Between Quantum Dot Donors and Dye-Labeled Protein Acceptors*. *Journal of the American Chemical Society* **2004**, *126* (1), 301-310.
- [47] Ellen R. Goldman; Igor L. Medintz; Jessica L. Whitley; Andrew Hayhurst; Aaron R. Clapp; H. Tetsuo Uyeda; Jeffrey R. Deschamps; Michael E. Lassman; Hedi Mattoussi, *A Hybrid Quantum Dot–Antibody Fragment Fluorescence Resonance Energy Transfer-Based TNT Sensor*. *Journal of the American Chemical Society* **2005**, *127* (18), 6744-6751.
- [48] Murat Kuscu; Ozgur B. Akan, *Nanoscale Communications Based on Fluorescence Resonance Energy Transfer (FRET)*. In *Modeling, Methodologies and Tools for Molecular*

*and Nano-scale Communications: Modeling, Methodologies and Tools*, Junichi Suzuki; Tadashi Nakano; Michael John Moore, Eds. Springer International Publishing: Cham, 2017; pp 349-375.

[49] Haifeng Dong; Wenchao Gao; Feng Yan; Hanxu Ji; Huangxian Ju, Fluorescence Resonance Energy Transfer between Quantum Dots and Graphene Oxide for Sensing Biomolecules. *Analytical Chemistry* **2010**, 82 (13), 5511-5517.

[50] Kim E. Sapsford; Lorenzo Berti; Igor L. Medintz, Materials for Fluorescence Resonance Energy Transfer Analysis: Beyond Traditional Donor–Acceptor Combinations. *Angewandte Chemie International Edition* **2006**, 45 (28), 4562-4589.

[51] Jing Zhou; Qian Liu; Wei Feng; Yun Sun; Fuyou Li, Upconversion Luminescent Materials: Advances and Applications. *Chemical Reviews* **2014**, 115 (1), 395-465.

[52] Guanying Chen; Hailong Qiu; Paras N. Prasad; Xiaoyuan Chen, Upconversion Nanoparticles: Design, Nanochemistry, and Applications in Theranostics. *Chemical Reviews* **2014**, 114 (10), 5161-5214.

[53] François Auzel, Upconversion and Anti-Stokes Processes with f and d Ions in Solids. *Chemical Reviews* **2003**, 104 (1), 139-174.

[54] Shuqing He; Kristina Krippes; Sandra Ritz; Zhijun Chen; Andreas Best; Hans-Jurgen Butt; Volker Mailander; Si Wu, Ultralow-intensity near-infrared light induces drug delivery by upconverting nanoparticles. *Chemical Communications* **2015**, 51 (2), 431-434.

[55] Yuanzeng Min; Jinming Li; Fang Liu; Edwin K. L. Yeow; Bengang Xing, Near-Infrared Light-Mediated Photoactivation of a Platinum Antitumor Prodrug and Simultaneous Cellular Apoptosis Imaging by Upconversion-Luminescent Nanoparticles. *Angewandte Chemie* **2014**, 126 (4), 1030-1034.

[56] Chao Wang; Liang Cheng; Yumeng Liu; Xiaojing Wang; Xinxing Ma; Zhaoyi Deng; Yonggang Li; Zhuang Liu, Imaging-Guided pH-Sensitive Photodynamic Therapy Using Charge Reversible Upconversion Nanoparticles under Near-Infrared Light. *Advanced Functional Materials* **2013**, 23 (24), 3077-3086.

[57] Yunlu Dai; Haihua Xiao; Jianhua Liu; Qinghai Yuan; Ping'an Ma; Dongmei Yang; Chunxia Li; Ziyong Cheng; Zhiyao Hou; Piaoping Yang; Jun Lin, *In Vivo* Multimodality Imaging and Cancer Therapy by Near-Infrared Light-Triggered trans-Platinum Pro-Drug-Conjugated Upconversion Nanoparticles. *Journal of the American Chemical Society* **2013**, 135 (50), 18920-18929.

[58] Jyoti Yadav; Asha Rani; Vijander Singh; Bhaskar Mohan Murari, Prospects and limitations of non-invasive blood glucose monitoring using near-infrared spectroscopy. *Biomedical Signal Processing and Control* **2015**, 18 (Supplement C), 214-227.

- [59] Xiaowang Liu; Renren Deng; Yuhai Zhang; Yu Wang; Hongjin Chang; Ling Huang; Xiaogang Liu, Probing the nature of upconversion nanocrystals: instrumentation matters. *Chemical Society Reviews* **2015**, 44 (6), 1479-1508.
- [60] Yong Il Park; Kang Taek Lee; Yung Doug Suh; Taeghwan Hyeon, Upconverting nanoparticles: a versatile platform for wide-field two-photon microscopy and multi-modal *in vivo* imaging. *Chemical Society Reviews* **2015**, 44 (6), 1302-1317.
- [61] Yongsheng Liu; Datao Tu; Haomiao Zhu; Xueyuan Chen, Lanthanide-doped luminescent nanoprobe: controlled synthesis, optical spectroscopy, and bioapplications. *Chemical Society Reviews* **2013**, 42 (16), 6924-6958.
- [62] Song Wang; Hongjie Zhang, Foundations of Up-conversion Nanoparticles. In *Phosphors, Up Conversion Nano Particles, Quantum Dots and Their Applications: Volume 2*, Ru-Shi Liu, Ed. Springer Singapore: Singapore, 2016; pp 215-236.
- [63] Albert Fert, Nobel Lecture: Origin, development, and future of spintronics\*. *Reviews of Modern Physics* **2008**, 80 (4), 1517-1530.
- [64] Peter A. Grünberg, Nobel Lecture: From spin waves to giant magnetoresistance and beyond\*. *Reviews of Modern Physics* **2008**, 80 (4), 1531-1540.
- [65] Thomas F. Rosenbaum, Magnetoresistance: A new spin on magnets. *Nature* **2000**, 404 (6778), 556-557.
- [66] YuFeng Tian; ShiShen Yan, Giant magnetoresistance: history, development and beyond. *Science China Physics, Mechanics and Astronomy* **2012**, 56 (1), 2-14.
- [67] Yi Wang; Wei Wang; Lina Yu; Liang Tu; Yinglong Feng; Todd Klein; Jian-Ping Wang, Giant magnetoresistive-based biosensing probe station system for multiplex protein assays. *Biosensors and Bioelectronics* **2015**, 70, 61-68.
- [68] Wei Wang; Yi Wang; Liang Tu; Todd Klein; Yinglong Feng; Qin Li; Jian-Ping Wang, Magnetic Detection of Mercuric Ion Using Giant Magnetoresistance-Based Biosensing System. *Analytical Chemistry* **2014**, 86 (8), 3712-3716.
- [69] Candid Reig; S Cardoso; Subhas Chandra Mukhopadhyay, *Giant Magnetoresistance (GMR) Sensors*. Springer: 2013.
- [70] S. X. Wang; G. Li, Advances in Giant Magnetoresistance Biosensors With Magnetic Nanoparticle Tags: Review and Outlook. *IEEE Transactions on Magnetics* **2008**, 44 (7), 1687-1702.
- [71] Xingkun Ning, Microstructure of the Nanostructured Oxide Composite Thin Films and Its Functional Properties. In *Outlook and Challenges of Nano Devices, Sensors, and MEMS*, Ting Li; Ziv Liu, Eds. Springer International Publishing: Cham, 2017; pp 397-427.

- [72] Claude Chappert; Albert Fert; Frederic Nguyen Van Dau, The emergence of spin electronics in data storage. *Nature Materials* **2007**, 6 (11), 813-823.
- [73] John B Parkinson; Damian JJ Farnell, *An introduction to quantum spin systems*. Springer: 2010; Vol. 816.
- [74] C. Vouille; A. Barth ́ ény; F. Elokani Mpondo; A. Fert; P. A. Schroeder; S. Y. Hsu; A. Reilly; R. Loloee, Microscopic mechanisms of giant magnetoresistance. *Physical Review B* **1999**, 60 (9), 6710-6722.
- [75] G. Binasch; P. Gr ́ unberg; F. Saurenbach; W. Zinn, Enhanced magnetoresistance in layered magnetic structures with antiferromagnetic interlayer exchange. *Physical Review B* **1989**, 39 (7), 4828-4830.
- [76] B. L. Johnson; R. E. Camley, Theory of giant magnetoresistance effects in Fe/Cr multilayers: Spin-dependent scattering from impurities. *Physical Review B* **1991**, 44 (18), 9997-10002.
- [77] Charbel Tannous; Jacek Gieraltowski, Magnetic Properties: From Traditional to Spintronic. In *Springer Handbook of Electronic and Photonic Materials*, Safa Kasap; Peter Capper, Eds. Springer International Publishing: Cham, 2017; pp 1-1.
- [78] Jiahua Zhu; Zhiping Luo; Shijie Wu; Neel Haldolaarachchige; David P. Young; Suying Wei; Zhanhu Guo, Magnetic graphene nanocomposites: electron conduction, giant magnetoresistance and tunable negative permittivity. *Journal of Materials Chemistry* **2012**, 22 (3), 835-844.
- [79] G. Abellan; H. Prima-Garcia; E. Coronado, Graphene enhances the magnetoresistance of FeNi<sub>3</sub> nanoparticles in hierarchical FeNi<sub>3</sub>-graphene nanocomposites. *Journal of Materials Chemistry C* **2016**, 4 (11), 2252-2258.
- [80] Zhenzhao Jia; Rui Zhang; Qi Han; Qiaojing Yan; Rui Zhu; Dapeng Yu; Xiaosong Wu, Large tunable linear magnetoresistance in gold nanoparticle decorated graphene. *Applied Physics Letters* **2014**, 105 (14), 143103.
- [81] Aigu L. Lin; J. N. B. Rodrigues; Chenliang Su; M. Milletari; Kian Ping Loh; Tom Wu; Wei Chen; A. H. Castro Neto; Shaffique Adam; Andrew T. S. Wee, Tunable room-temperature ferromagnet using an iron-oxide and graphene oxide nanocomposite. *Scientific Reports* **2015**, 5, 11430.
- [82] Silke Behrens, Preparation of functional magnetic nanocomposites and hybrid materials: recent progress and future directions. *Nanoscale* **2011**, 3 (3), 877-892.
- [83] Leandro M. Socolovsky; Oscar Moscoso Londo ́ ño, Consequences of Magnetic Interaction Phenomena in Granular Systems. In *Complex Magnetic Nanostructures: Synthesis, Assembly and Applications*, Surender Kumar Sharma, Ed. Springer International Publishing: Cham, 2017; pp 1-38.

- [84] N. S. Oliver; C. Toumazou; A. E. G. Cass; D. G. Johnston, Glucose sensors: a review of current and emerging technology. *Diabetic Medicine* **2009**, *26* (3), 197-210.
- [85] Sandeep Kumar Vashist, Non-invasive glucose monitoring technology in diabetes management: A review. *Analytica Chimica Acta* **2012**, *750* (Supplement C), 16-27.
- [86] Paul L. Stiles; Jon A. Dieringer; Nilam C. Shah; Richard P. Van Duyne, Surface-Enhanced Raman Spectroscopy. *Annual Review of Analytical Chemistry* **2008**, *1* (1), 601-626.
- [87] Amir H. Kashani; Chieh-Li Chen; Jin K. Gahm; Fang Zheng; Grace M. Richter; Philip J. Rosenfeld; Yonggang Shi; Ruikang K. Wang, Optical coherence tomography angiography: A comprehensive review of current methods and clinical applications. *Progress in Retinal and Eye Research* **2017**, *60* (Supplement C), 66-100.
- [88] Pavel Matousek; Nicholas Stone, Development of deep subsurface Raman spectroscopy for medical diagnosis and disease monitoring. *Chemical Society Reviews* **2016**, *45* (7), 1794-1802.
- [89] Omar S. Khalil, Spectroscopic and Clinical Aspects of Noninvasive Glucose Measurements. *Clinical Chemistry* **1999**, *45* (2), 165.
- [90] David C. Klonoff, Noninvasive Blood Glucose Monitoring. *Diabetes Care* **1997**, *20* (3), 433.
- [91] Jin Zhang; William Hodge; Cindy Hutnick; Xianbin Wang, Noninvasive Diagnostic Devices for Diabetes through Measuring Tear Glucose. *Journal of Diabetes Science and Technology* **2011**, *5* (1), 166-172.
- [92] Carlos Eduardo Ferrante do Amaral; Benhard Wolf, Current development in non-invasive glucose monitoring. *Medical Engineering and Physics* **2007**, *30* (5), 541-549.
- [93] Colette McDonagh; Conor S. Burke; Brian D. MacCraith, Optical Chemical Sensors. *Chemical Reviews* **2008**, *108* (2), 400-422.
- [94] Amay J. Bandodkar; Joseph Wang, Non-invasive wearable electrochemical sensors: a review. *Trends in Biotechnology* **2014**, *32* (7), 363-371.
- [95] Justin T. Baca; David N. Finegold; Sanford A. Asher, Tear Glucose Analysis for the Noninvasive Detection and Monitoring of Diabetes Mellitus. *The Ocular Surface* **2007**, *5* (4), 280-293.
- [96] Jennifer D. Lane; David M. Krumholz; Robert A. Sack; Carol Morris, Tear Glucose Dynamics in Diabetes Mellitus. *Current Eye Research* **2006**, *31* (11), 895-901.
- [97] J. G. Lewis; P. J. Stephens, Tear Glucose in Diabetics. *British Journal of Ophthalmology* **1958**, *42* (12), 754-758.

[98] S. Mishima; A. Gasset; Jr S. D. Klyce; J. L. Baum, Determination of Tear Volume and Tear Flow. *Investigative Ophthalmology and Visual Science* **1966**, 5 (3), 264-276.

[99] Michael Sch äferling; Ute Resch-Genger, Luminescent Nanoparticles for Chemical Sensing and Imaging. In *Reviews in Fluorescence 2016*, Chris D. Geddes, Ed. Springer International Publishing: Cham, 2017; pp 71-109.

[100] Zsolt K ása; Tam ás Gyulav ári; G ábor Ver éb; G ábor Kov ács; Lucian Baia; Zsolt Pap; Kl ára Hern ádi, Novel Applications and Future Perspectives of Nanocomposites. In *Nanocomposites for Visible Light-induced Photocatalysis*, Mohammad Mansoob Khan; Debabrata Pradhan; Youngku Sohn, Eds. Springer International Publishing: Cham, 2017; pp 333-398.

[101] P. P. Freitas; R. Ferreira; S. Cardoso; F. Cardoso, Magnetoresistive sensors. *Journal of Physics: Condensed Matter* **2007**, 19 (16), 165221.

## Chapter 2

### 2 Background and Literature Review

#### 2.1 Nanomaterials for Glucose Biosensing

Historically, the glucose was analyzed by colorimetric reaction methods. The most widely used method is Miller's colorimetric method. [1] Because glucose solution has no absorbance, no fluorescence in visible range, most of the analysis method in early days was dependent on the glucose chromogenic reaction. Take Miller method as demonstration, the glucose carbonyl group (C=O) is oxidized and at the same time, 3, 5-dinitrosalicylic acid (DNS) is reduced to 3-amino, 5-nitrosalicylic acid under alkaline conditions with colored products. The glucose content is related to the colorimetric products which could be quantified by UV-vis spectroscopy.

Sensing glucose is very important in food industry, pharmaceutical industry and specially, glucose monitoring is critical for diabetes management. Diabetes symptom is characterized with long term hyperglycemia and the monitoring of patients glucose state is required for the disease therapy. Although the electrochemical method for sensing glucose is marketed and widely used among diabetes patients, the multiple times of finger pricks daily to get minute blood for glucose sensing may cause patients with weak immune systems with infections and uncomfortable feelings. Therefore, more patient friendly, minimally invasive or non-invasive fluorescent detection methods has gained focus recently. [2-5] Fluorescent sensing has the following advantages: [6-9] (a) extremely sensitive, (b) minimally invasive or non-invasive, (c) fluorescence intensity and fluorescence lifetime could be utilized, (d) could provide structure and micro-environment of molecules, (e) fluorescence resonance energy transfer (FRET) technique could be utilized. Another promising glucose sensing approach is magnetoresistive method which has high sensitivity due to absence of magnetic interference in most biological components.

Nanotechnology has brought profound influence in biosensors area, the most favorable advantage of nanostructured sensor is their high sensitivity and selectivity and the miniaturization of sensor device. The development of nanotechnology allows materials to be prepared and fabricated in reduced dimensions at the nanoscale, forming construction of nanoscale structures for high throughput assay with the integration of microfluidics devices, and strengthening the biological activity of the biological components by using novel nanoscale materials and nanostructures. Nanomaterials and nanostructures have special chemical, physical and biological properties compared to their bulk counterpart. [10-14] The fluorescent, magnetoresistive nanomaterials and nanostructures have distinct novel properties and provide extensive nanoplatform for developing new nanostructured biosensors for glucose sensing. [15-20] Biosensors are sensors composed of or involved with a biological component. [21-24] Because the biological components have high sensitivity and selectivity to specific molecules, thus the utilization of biological component create highly accurate sensing devices for a variety of molecules including glucose, urea, cholesterol etc.

Biosensors are widely applied in the areas of food industry, pharmaceutical industry, environment monitoring and medical diagnostics etc. The early biosensors were using biocomponents decorating on the electrode surface as target recognizing parts. As the nanotechnology flourished, the conjugation of biocomponents onto nanomaterials and nanostructures has formed nanostructured biosensors with prevalent applications. The conjugation may need further control to offer reproducibility. As the equivalent size of nanoscale materials and nanostructures to biological systems, the nanostructured biosensors are promising tools for sensing biological activity *in vivo* and *in vitro*. [25-28] Some common biological receptors have been used in detection of glucose in fluorescent nanostructured biosensors, like Concanavalin A (Con A), glucose oxidase, glucose dehydrogenase and hexokinase/glucokinase, glucose binding proteins etc.

## 2.2 Detection Principles of Nanostructured Fluorescent Biosensor

Fluorescent nanomaterials and nanostructures are suitable signal transducers for correlating the glucose signals into fluorescent signals, either in peak intensity, peak shift,



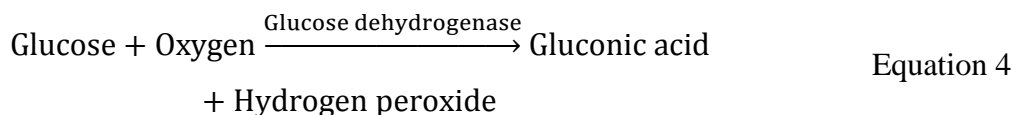
or fluorescent lifetime etc. Fluorescence resonance energy transfer (FRET) is acknowledged as a sensitive and reliable analytical technique and has been widely employed in the fluorescence biosensing systems. Fluorescent nanomaterials and nanostructures could work as a good platform for the bioconjugation of glucose recognized biomolecules. The bioconjugation methods include chemical bioconjugation or physical adsorption onto the nanomaterials and nanostructures. The biomolecules are greatly stabilized when bioconjugated or adsorbed onto the nanomaterials and nanostructures with higher biological activity and stability.

The primary sensing mechanisms include glucose direct binding, glucose competitive binding and fluorescent dye release etc., which would introduce corresponding fluorescence intensity changes, fluorescence turn-on or turn-off, fluorescent lifetime changes etc. Another type of sensing mechanisms employs the glucose catalysis oxidation reaction. The reaction products often contain hydrogen peroxide (H<sub>2</sub>O<sub>2</sub>) and/or gluconic acid (causing pH change). The oxidizing and acidic products then influence the fluorescence signal. Some of the glucose catalysis reactions are shown in the following equation 1–4.



In equation 1 and 2, the glucose binding reaction is dynamic and reversible, the \* mark represent the biomolecules binding with glucose. The fluorescence change could be induced by, (a) binding protein is labeled with fluorescent dye or fluorescent protein. The binding state would change the fluorescence of the fluorescent label. (b) binding protein is originally binding with other saccharide molecules, glucose competitively bind to the protein and replace the other saccharide molecules. The saccharide molecules could have optical properties, e.g. fluorescence, absorbance, etc. Therefore, the change of the optical signal could be correlated with glucose concentration; and the optimal parameters for improving sensor's performance include the types of the glucose binding proteins, and the

ratio of the glucose and glucose binding proteins. The Concanavalin A binds glucose and does not produce products.



Equation 3 and 4 represent the glucose catalysis reactions. The products contain gluconic acid and/or hydrogen peroxide. Provided the fluorescence of nanomaterials and nanostructures would be affected by the hydrogen peroxide and pH change. Thus the glucose content could be analyzed by correlating with the fluorescence change.

## 2.3 Glucose Recognition Biomolecules

Various glucose recognized biomolecules have been investigated and they include direct glucose binding by Concanavalin A, glucose binding proteins etc. Glucose catalytic oxidation reactions employ certain oxidase like glucose oxidase, glucokinase, hexokinase and glucose dehydrogenase. Concanavalin A (Con A) is a plant lectin protein extracted from Jack beans. Con A tetramer molecule has four binding sites for glucose molecules and has been widely used in glucose sensing assays.

Another type of glucose sensing biomolecules is the glucose binding proteins (GBP), which is one of the binding proteins found in bacteria like *Escherichia coli*. These glucose binding proteins have extremely high selectivity and sensitivity for glucose, of which the binding constants of the proteins to glucose are in the micromolar ( $\mu\text{M}$ ) range. The sensitivity and selectivity of glucose binding proteins render them ideal for GBP based glucose biosensor development for sensing tear glucose and other non-blood body fluids glucose. [29] The sensitivity and selectivity of GBP could be engineered by recombinant protein technique. [30-31]

## 2.4 Fluorescent Exerting/Interacting Nanomaterials

The mostly researched fluorescent exerting nanomaterials include fluorescent semiconductor quantum dots (QDs), dye-doped silica nanoparticles (DDSNs), lanthanide doped nanomaterials and upconversion nanoparticles (UCNPs), fluorescent gold/silver metal nanoclusters etc. [32-35] Some other nanomaterials are fluorescent interacting quenchers and have been investigated in the fluorescent assays as well. Plasmonic gold/silver nanoparticles are employed as fluorescent quenchers. [36]

Another big family of nanomaterials is the carbon nanomaterials, some carbon based nanomaterials are fluorescent and others are fluorescent quenchers. Graphene/graphene oxide, carbon dots, carbon nanotubes etc. carbon nanomaterials have been heavily studied in the fluorescent glucose biosensing. [37-39] Graphene/graphene oxide nanomaterials are fluorescent quenchers due to their large  $\pi$  electron plane on the nanosheet plane, which could quench fluorescence through fluorescence resonance energy transfer (FRET). On the contrary, carbon dots and carbon nanotubes are promising strong fluorescent nanomaterials for biosensing applications. Carbon dots could be prepared by many facile methods and the scale up production of carbon dots is not difficult. Carbon nanotubes emit fluorescence in the near-infrared range. This characteristic make carbon nanotubes very favorable for biomedical applications. However, currently the carbon nanotubes have not yet been able to be prepared facilely. [40]

Some other fluorescent nanomaterials include metal oxide nanostructured nanomaterials. As metal oxide nanostructures provide large effective surface areas for biomolecules immobilization, which could maintain better conformation, desired orientation and high biological activity of immobilized biomolecules. Thus a superior sensing characteristics was achieved. ZnO nanostructure film is a typical weak fluorescent nanomaterials, which is often used as substrate for nanobiosensing. For other metal oxide nanostructures, they are often used in electrochemical biosensing due to their good electrical properties. But still, these metal oxide nanostructures are potential candidates as device for fluorescent glucose biosensing, and they could be further incorporated into other devices. [41-44]

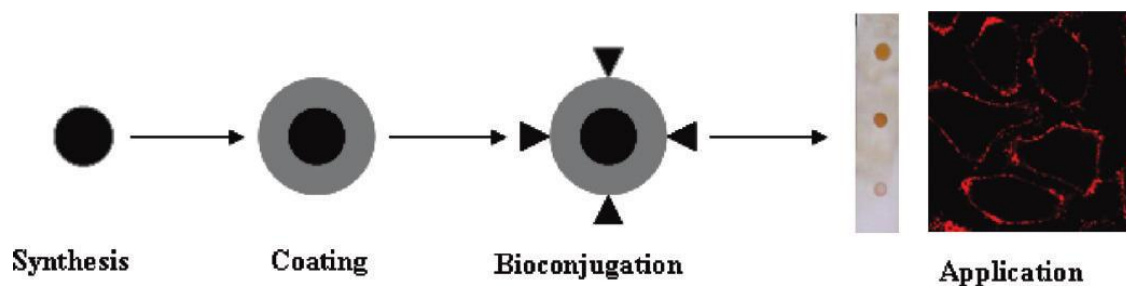


**Figure 2.1** General steps involved in the application of functional nanomaterials. Reprinted with permission from [45], Copyright (2010) American Chemical Society. (Permission in Appendix 1)

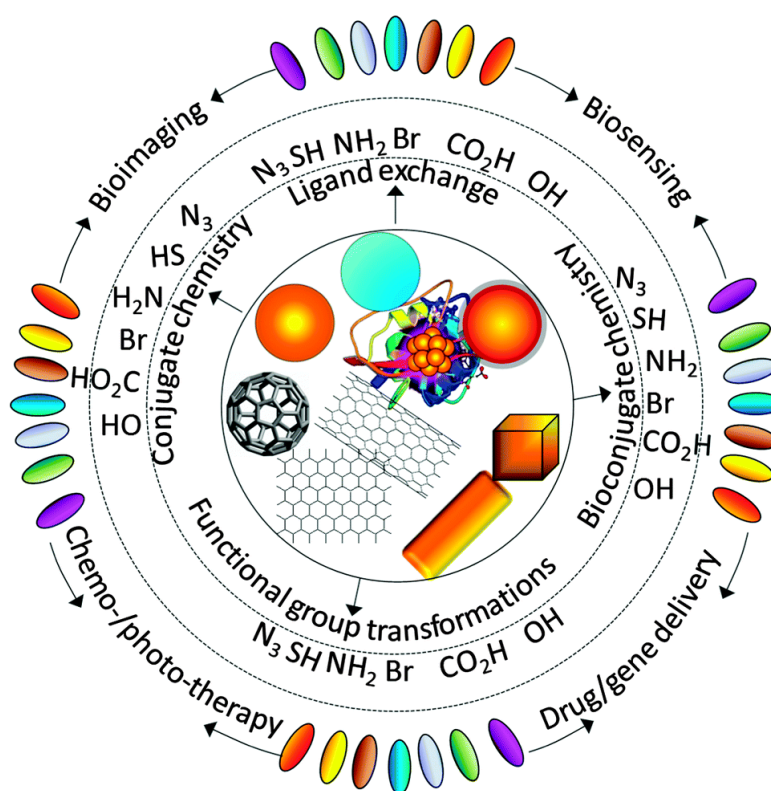


**Figure 2.2** Examples of nanomaterials and their functional groups for biological applications. Reproduced from [46] with permission of the Royal Society of Chemistry. (Permission in Appendix 2)

The nanomaterials and nanostructures normally need surface functionalization to obtain desirable physiochemical properties for various applications. As shown in figure 2.1, from the synthesis of a nanoparticle, then surface coating is applied to form core-shell

nanoparticle. Continuously, ligand exchange and functional groups are grafted or bioconjugated on the outer surface. The modification and functionalization of nanomaterials and nanostructures could make them more water soluble and biocompatible for further application in biosensing systems.

Nanomaterials and nanostructures surface functionalization aims to utilize them in catalysis, adsorption, drug delivery carrier, bioimaging, nanobiosensor and nanomedicine etc. applications. The surface properties have great influence on the nano-bio interface. Hydrophilic and hydrophobic surfaces can affect the interaction of nanomaterials with biomolecules and proteins adsorption. Related nanomaterials and nanostructures surface modification reviews [46-51] have demonstrated various chemical, physical modifications and bioconjugation methods. Various functional groups and applications of nanomaterials and nanostructures could be visualized with suitable surface modification and fabrications as shown in figure 2.2.

#### 2.4.1 Semiconductor Quantum Dots

Quantum dots are tiny semiconductor nanoparticles with diameters in the range of 2–10 nm, containing roughly 200 – 10,000 atoms and characterized by size-dependent fluorescent property, broad excitation range, narrow emission peak, large Stokes shift, ultrahigh brightness, high quantum yield and photo-stability. The synthesis method of the quantum dots are mature and abundant. The organic phase synthesis could yield high quality quantum dots, which are oil phase soluble, thus further surface modification is necessary to render their usage in biological sensing. [52-54] However due to the semiconductor elements' cytotoxicity (Cd element), the bio-application of quantum dots are hindered greatly. Normally a coating layer like silica shell, polymer shell or carbon shell would be coated on the surface of the semiconductor quantum dots to improve their water solubility and biocompatibility. [55-58] Compared to traditional fluorescent dye, Green Fluorescent Proteins (GFP) or enhanced GFP, quantum dots has superior luminescent properties like photo-stability to ambient environment, high quantum yield and bright size-dependent excitation photoluminescence. These luminescent properties of the semiconductor nanocrystals favor them as nanobiosensing probes. [59-60]

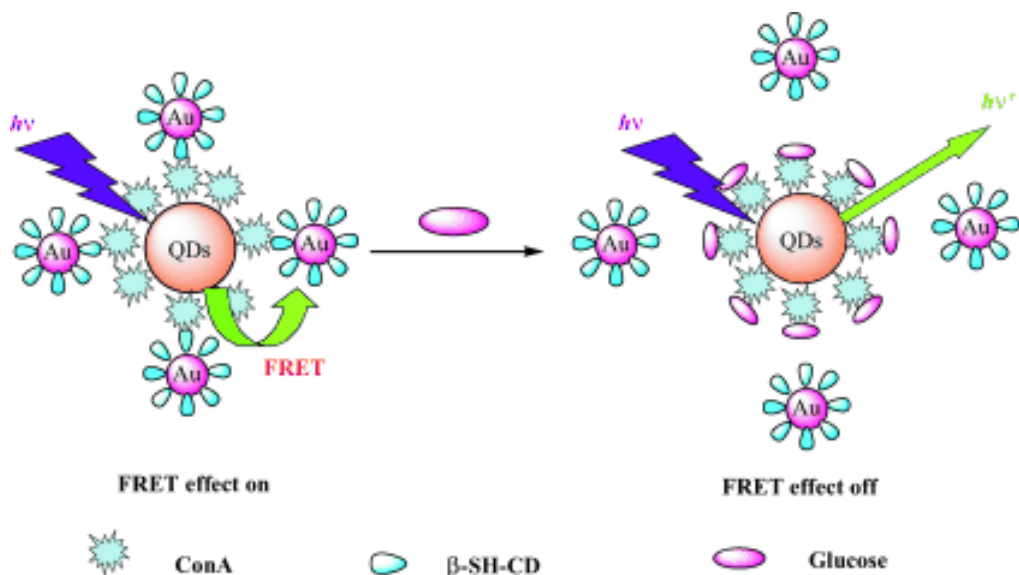


**Figure 2.3 Chemical structure of the QDs-Con A- $\beta$ -CDs-Au NPs nanobiosensor and schematic illustration of its FRET-based operating principles. Reproduced from [61] with permission of the John Wiley and Sons. (Permission in Appendix 3)**

An assembled competitive fluorescent glucose nanobiosensor was constructed (figure 2.3). [61] The designed nanobiosensor composed of modified quantum dots and plasmonic gold nanoparticles. As schematic shows in figure 2.3, the sensing mechanism is through the Fluorescence Resonance Energy Transfer (FRET) between quantum dots (energy donor) and gold nanoparticles (energy quenching acceptor). Concanavalin A were modified onto the quantum dots surface and  $\beta$ -SH-cyclodextrin were modified on the gold nanoparticle surface. Before glucose was introduced, the quantum dots and gold nanoparticles were connected by the Concanavalin A binding of the  $\beta$ -SH-cyclodextrin, and the fluorescence of the quantum dots was quenched by the plasmonic gold nanoparticles. After the glucose was introduced, the glucose competed for the binding to the Concanavalin A, then the plasmonic gold nanoparticles were separated from the quantum dots. As a result, the emission of quantum dots was recovered. Experimental results illustrated that the increase in fluorescence intensity was proportional to glucose concentration in the range of 0.1–50  $\mu$ M when optimized experimental conditions were reached. Also the serum test results showed that this fluorescent glucose nanobiosensor has excellent glucose selectivity over other sugars and most biological interferents.

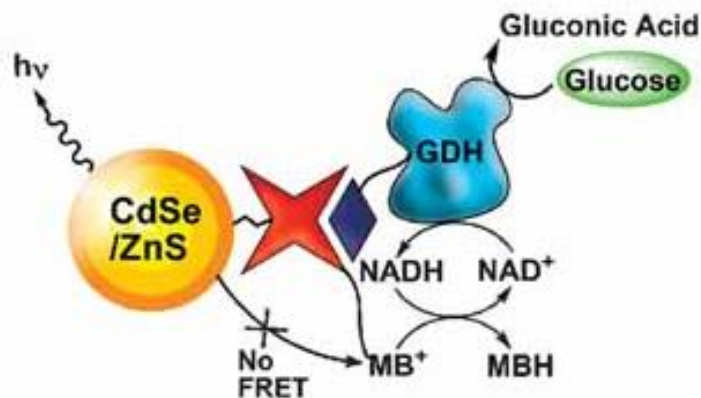


**Figure 2.4 The glucose dehydrogenase biocatalyzed generation of NADH by the oxidation of glucose enables the fluorescence detection of glucose by methylene-blue-functionalized CdSe/ZnS quantum dots. Reproduced from [62] with permission of the John Wiley and Sons. (Permission in Appendix 4)**

Another quantum dots based glucose nanobiosensor was developed utilizing glucose catalytic reaction (figure 2.4). [62] Glucose dehydrogenase modified CdSe/ZnS quantum dots were prepared to sense glucose. The sensing technique is fluorescence resonance energy transfer (FRET). The nanobiosensing mechanism is demonstrated in figure 2.4. Before adding glucose, the fluorescence of the quantum dots was quenched by the methylene blue. After adding glucose, the biocatalytic reactions took place and the fluorescence of quantum dots was recovered. In the biocatalytic reaction, glucose was converted to gluconic acid, the glucose dehydrogenase biocatalytic reaction was mediated by the NADH–NAD<sup>+</sup> (reduced-oxidized form of NAD) pair (NAD=Nicotinamide adenine dinucleotide), methylene blue was reduced by NADH to colorless MBH, then the fluorescence resonance energy transfer between quantum dots and methylene blue was terminated. The detection limit of this fluorescent glucose nanobiosensor was as low as 10<sup>-5</sup> M.

A fluorescent nanostructured glucose biosensor chip utilizing glucose oxidase was developed by Tang et al. (figure 2.5), [63] in which a layer-by-layer assembly technique was used to fabricate the thin film sensor. The facile step by step process is shown in figure 2.5, firstly polymer poly(allylamine hydrochloride) (PAH) and CdTe quantum dots were assembled on a substrate. Then three bilayers of polymer film of poly(allylamine

hydrochloride) (PAH) and polystyrenesulfonate (PSS) were assembled on top to avoid possible interference. Next, glucose oxidase (GOD or GOx) and PAH were deposited. The layer-by-layer thin film structure of  $(\text{PAH}/\text{CdTe})_x(\text{PAH}/\text{PSS})_3(\text{PAH}/\text{GOD})_y$  was constructed. The fluorescence of CdTe quantum dots was quenched by the  $\text{H}_2\text{O}_2$  produced by the glucose catalytic oxidization reaction. This glucose sensor has the advantage of adjustment of the quantum dots layer composition and the glucose oxidase layer compositions for adaptation to different sensing environment. Experimental results showed that the glucose responsive range for  $(\text{PAH}/\text{CdTe})_{12}(\text{PAH}/\text{PSS})_3(\text{PAH}/\text{GOD})_3$  was 0.5 mM–16 mM.

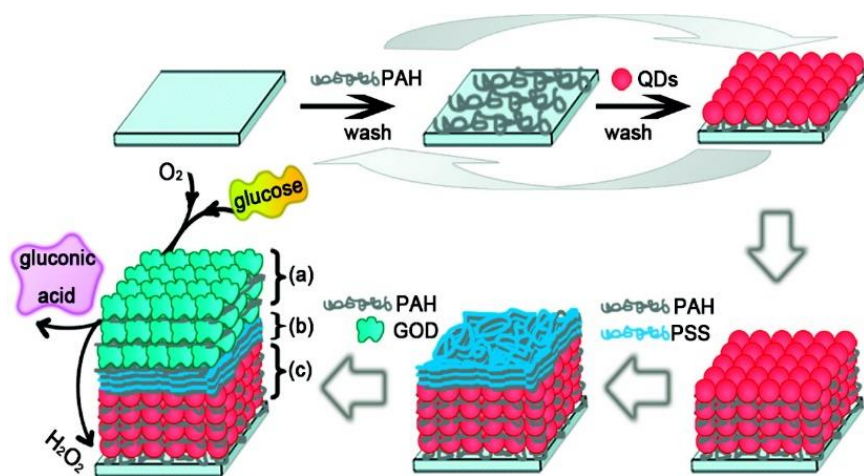


**Figure 2.5 Sensing assembly: (a) top 3 bilayers of PAH/GOD, (b) 3 bilayers of PAH/PSS, and (c) 12 bilayers of PAH/CdTe QDs. PAH=poly(allylamine hydrochloride), GOD=glucose oxidase, PSS=polystyrenesulfonate, QD=quantum dots. Reprinted with permission from [63], Copyright (2009) American Chemical Society. (Permission in Appendix 5)**

## 2.4.2 Fluorescent Polymer/Silica Nanomaterials

Another fluorescent nanomaterials are dye-doped silica nanoparticles or polymer nanoparticles. As polymers nanoparticles could employ many different monomers and thus they are varied from each other, but the idea is more or less the same with dye-doped silica nanoparticles by incorporating fluorescent elements inside polymerized matrix. Silica is a highly biocompatible material and the dye could be covalently conjugated or by physical



doping into the silica matrix. Due to the silica protection of doped dye, the photo-stability of doped dye is greatly improved. Moreover, the silica matrix provides a very good surface platform for surface functionalization and construction of various silica structures, including solid silica nanoparticles, mesoporous silica nanoparticles, hollow silica nanoparticles, core-shell silica nanoparticles and Janus silica nanoparticles etc. [64-65]

The universal silane chemistry could be well adapted to functionalize the silica matrix with various functional groups like amine group ( $-NH_2$ ), carboxylic group ( $-COOH$ ), thiol group ( $-SH$ ) and epoxy group ( $-CHOCH_2$ ) etc. The most common silane monomer is Tetraethyl Orthosilicate (TEOS), and the most used synthesis process is sol-gel process. The mesoporous silica nanomaterials have a large specific surface area and the mesopores are good container for loading fluorescent reporters. The mesopores could be gated by some target molecule. Silica or polymer nanoparticles represent useful tools for glucose sensing.

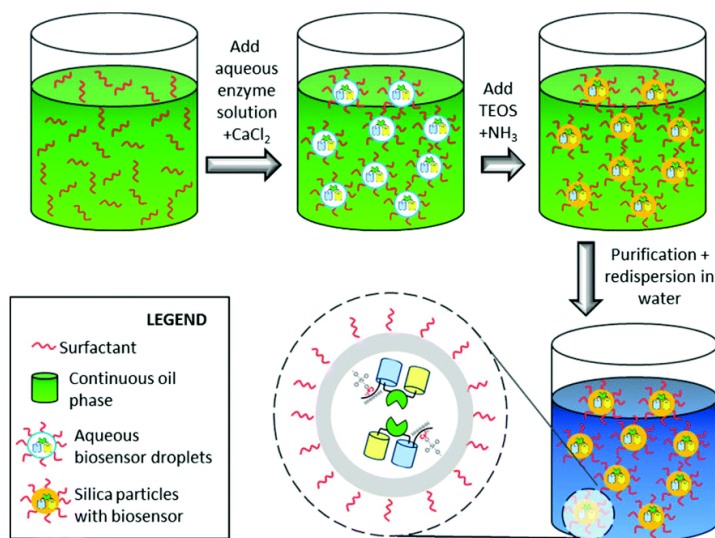


**Figure 2.6 Schematic illustration of the process for protein encapsulation in silica nanoparticles. After formation of a microemulsion, silica nanoparticles are formed by addition of ammonium hydroxide to increase the pH. In a last step, the inverse microemulsion is redispersed in water to give an aqueous silica dispersion with the FRET-based biosensor encapsulated in the silica nanomatrix. A specific interaction between the silica matrix and the biosensor is mediated by a silica–calcium–hexa-**

**histidine-tag complex. Reproduced from [66] with permission of the Royal Society of Chemistry. (Permission in Appendix 6)**

A fluorescence resonance energy transfer (FRET)-based glucose biosensor stabilized by incorporating into silica nanoparticle were prepared (figure 2.6). [66] The incorporation process is shown in figure 2.6, a microemulsion fabrication method is adopted in the synthesis. Silica matrix greatly stabilized the FRET biosensor from thermal and chemical denaturation. The specific interaction between hex-histidine-tag of the biosensor protein and a calcium silica complex was achieved, and the affinity to glucose was preserved. This study revealed that silica matrix has the stabilization effect of biomolecules compared to bare FRET-biosensor. This silica coated fluorescent glucose nanobiosensor was very promising for *in vitro* and *in vivo* sensing glucose.

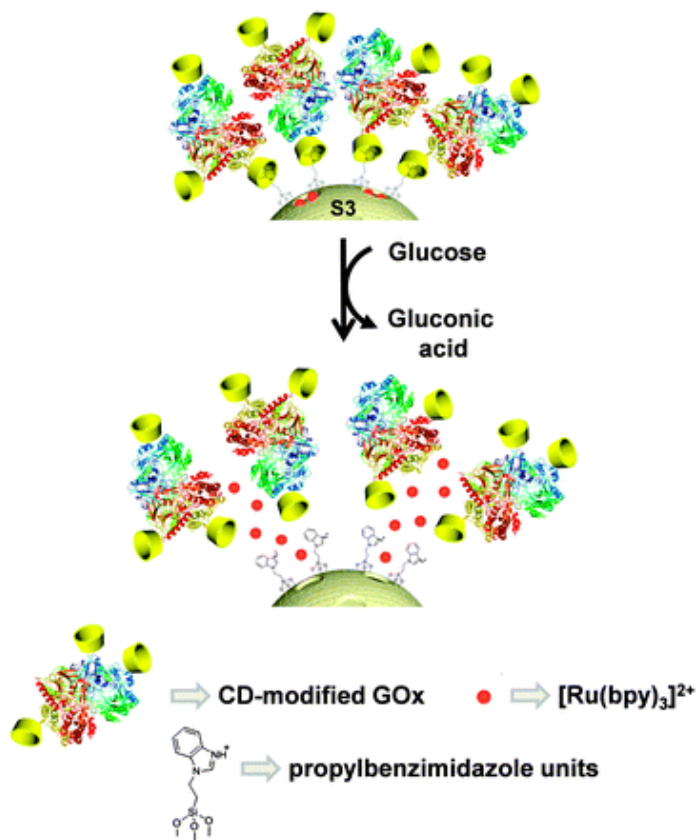


**Figure 2.7  $Ru(bipy)_3^{2+}$  loaded mesoporous silica capped with cyclodextrin-modified glucose oxidase (CD-GOx) for the detection of glucose. Reproduced from [35] with permission of the Royal Society of Chemistry. (Permission in Appendix 7)**

A gated mesoporous silica nanobiosensor for glucose sensing was prepared (figure 2.7). [35] This nanobiosensor was shown in figure 2.7, the fluorescent reporter (ruthenium bipyridine complexes) was loaded into the silica mesopores. The mesopores outlets were grafted with propylbenzimidazole moieties. Then the cyclodextrins modified glucose oxidase (CD-GOx) bioconjugates interacted with propylbenzimidazole groups by forming the inclusion complex, which blocked the loaded fluorescent reporters. After glucose was introduced, gluconic acid was produced and causing the protonation of benzimidazole group. Then the CD-GOx bioconjugates were detached from the silica nanoparticles, triggering the release of fluorescent ruthenium bipyridine complexes. A linear glucose responsive range of 0.1 mM to 10 mM was achieved by this nanobiosensor assays. Blood glucose levels of healthy and diabetics are 3 mM–8 mM and 9 mM–40 mM respectively. This gated mesoporous silica nanobiosensor were promising for the design of fluorescent nanobiosensor for glucose detection.

### 2.4.3 Upconverting Nanomaterials

Upconversion nanoparticles (UCNPs) is a large family of fluorescent nanomaterials. Upconverting nanomaterials have superior luminescent properties like long luminescent lifetime, large anti-Stokes shift, narrow emission bands and high photo-stability compared to quantum dots. Moreover upconverting nanomaterials could be modified with proper surface coatings and functional groups, thus having high biocompatibility and low toxicity that would favor them as a new generation of fluorescent nanoprobe for biomedical applications. [67-71] Normally, near-infrared 980 nm excitation is used to excite the upconverting nanomaterials to emit green, yellow or red light in the visible range (400–700 nm). The emission peaks are sharp and tunable by adjusting the doping lanthanide elements and corresponding ratios. Commonly used doping elements include Er, Tm, To etc., of which Er dopant enhances the green emission, Ho dopant enhances the yellow light while the Tm dopant enhances the red light, respectively. [72-74]

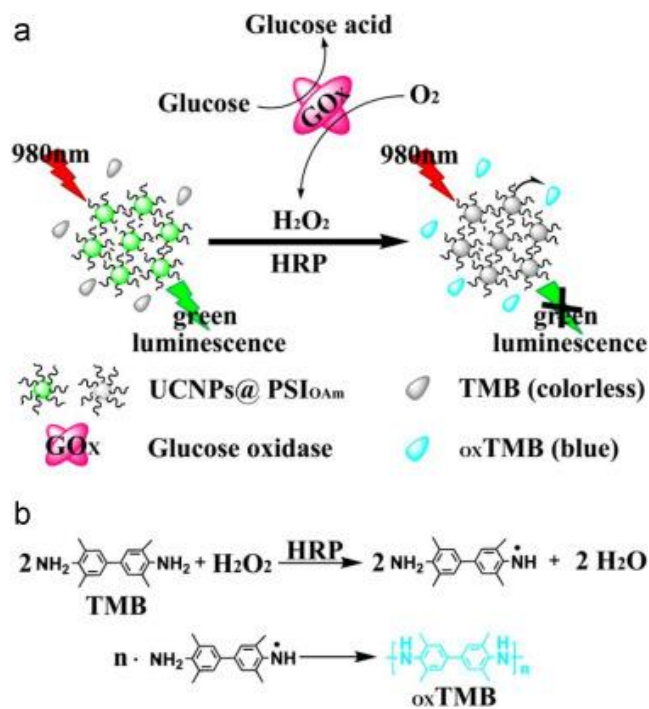


**Figure 2.8 (a) Schematic diagram for the selective detection of  $H_2O_2$  and glucose and the specific recognition of  $H_2O_2$  by HRP and TMB. (b) The colorless TMB was oxidized into blue oxTMB by polymerization. (For interpretation of the references to color in this scheme legend, the reader is referred to the web version of this article.) Reprinted from [75], Copyright (2015), with permission from Elsevier. (Permission in Appendix 8)**

An upconverting nanomaterials based fluorescent glucose nanobiosensor was studied as shown in figure 2.8. [75] In the sensing assay, glucose was first incubated with glucose oxidase at 37 °C. This reaction produced hydrogen peroxide. The produced  $H_2O_2$  mixed with green emitting  $NaYF_4: Yb^{3+}/Er^{3+}$  upconverting nanoparticles and colorless 3, 3', 5, 5'-tetramethylbenzidine (TMB) and horseradish peroxidase (HRP). The mixture was further incubated at room temperature for 10 minutes before measuring the fluorescence. The sensing mechanism was that the  $H_2O_2$  oxidized colorless TMB into blue oxidized TMB (oxTMB) by assistance of HRP. As a result, the upconverting green emission was quenched by the oxidized TMB. Their results showed that the glucose sensing linear range was 100 nM–4  $\mu$ M and the analysis results of serum glucose samples were in good accordance with hospital detecting results.

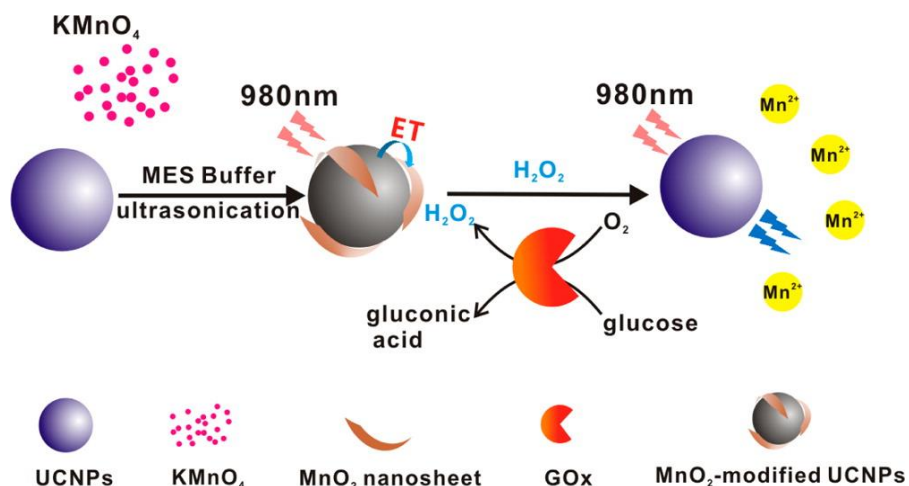


**Figure 2.9 Design and principle for  $\text{H}_2\text{O}_2$  and glucose detection using a  $\text{MnO}_2$ -nanosheet-modified UCNP nanocomposite. Reprinted with permission from [76], Copyright (2015) American Chemical Society. (Permission in Appendix 9)**

Another upconversion fluorescence turn-on nanosystem was developed (figure 2.9). [76] Manganese dioxide ( $\text{MnO}_2$ ) nanosheets were modified on upconverting nanoparticle surface and quenched the upconversion. Glucose oxidase catalyzed glucose and produced gluconic acid and  $\text{H}_2\text{O}_2$ . The  $\text{H}_2\text{O}_2$  reduced the  $\text{MnO}_2$  nanosheets to  $\text{Mn}^{2+}$ . Consequently the upconverting fluorescence was then turned on. By correlating the upconverting fluorescence at 450 nm, glucose concentrations range of 0  $\mu\text{M}$ –400  $\mu\text{M}$  could be detected.

#### 2.4.4 Gold/Silver Nanoparticles/Nanoclusters

Noble metal nanoparticles show distinct Surface Plasmon Resonance (SPR) phenomenon and noble metal nanoparticles are often utilized as fluorescence quenchers. Typical noble metal nanoparticles include gold nanoparticle, silver nanoparticle, platinum nanoparticles etc. These plasmonic nanoparticles are widely used in biosensing applications. Interestingly, as the size of the noble metal nanoparticles decrease to the extent of several to tens of atoms, roughly smaller than 1 nm. These noble metal nanoclusters would exhibit fluorescence properties and the fluorescence is tunable by controlling the nanoclusters size or atom numbers. [77-80]

Plasmonic gold metal nanoparticles are inert and stable in biological systems, representing a high biocompatibility. Also the gold atoms on the surface are especially prone to attach with thiol groups ( $-SH$ ), which facilitate the surface functionalization of gold nanoparticles. These properties make gold nanoparticles as a very useful as fluorescent quenching nanobiomaterials for biosensing. [81-82] In the synthesis of most metal quantum clusters, proteins are always used to assist formation and stabilization of the nanoclusters. Nanoclusters are size-equivalent to biological systems, have high biocompatibility and strong fluorescence. The size of noble nanoclusters are less than 1 nm. The compositions are gold or silver which is inert to biocomponents. The strong fluorescence comes from the discrete band gap due to their smaller size compared to gold/silver nanoparticles (2-50 nm). They have been widely investigated and applied in biosensing area. [83-84]

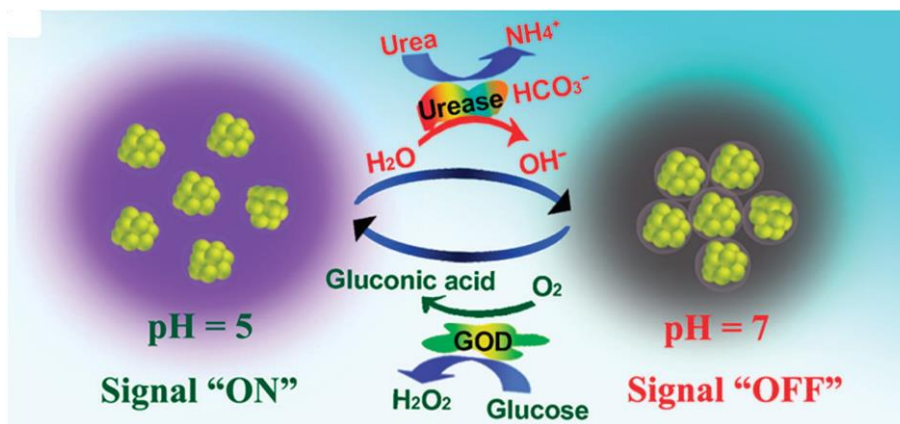


**Figure 2.10 Schematic sensing mechanism of the sensor for urea and Glucose detection. Reproduced from [85] with permission of the Nature Publishing Group. (Permission in Appendix 10)**

Fluorescent silver nanoclusters conjugate was developed as a nanobiosensor for glucose sensing (figure 2.10). [85] Silver nanoclusters were synthesized and its sensitivity to pH was used for sensing glucose as indicated in figure 2.10. The pH sensitivity originated from the carboxylic groups ( $-COOH$ ) on the silver nanoclusters surface. These carboxylic groups could create an easily formed molecular interaction (e.g. hydrogen bond) among silver nanoclusters. And the interaction is pH-switchable. This interaction consequently affected the fluorescence of silver quantum clusters. Therefore, the gluconic acid produced

by the glucose biocatalytic reaction could influence the fluorescence of the silver nanoclusters. The measured results indicated the glucose sensing range was 0.3 mM–13 mM and the silver quantum clusters could be regenerated by recovering the pH (urea sensing, urea catalyzed by urease to increase the pH).

#### 2.4.5 Fluorescent Carbon Nanomaterials

Fluorescent carbon nanomaterials are a broad family of carbon nanotube, graphene oxide, graphene quantum dots and carbon dots. Although the fluorescent mechanisms of some carbon nanomaterials are not yet fully understood, they have already been widely researched and applied in biosensing. [86-91] The main reason for their intense study is due to the benign nature of nanocarbon materials in biological systems and their special fluorescent characteristics. With proper surface coating of nanocarbon materials, their cytotoxicity are greatly lowered and benign to biological systems. Among these fluorescent carbon nanomaterials, graphene oxide also has weak fluorescence, graphene quantum dots and carbon dots, carbon nanotubes have good fluorescence. Multicolor graphene quantum dots and carbon dots have been widely studied. Graphene quantum dots (1–10 nm) sometimes are categorized into minimized sized graphene oxide (several hundred  $\mu\text{m}$ ). The graphene quantum dots are also categorized as one kind of single sheet carbon dots. Here, we would take carbon dots as a representative for fluorescent carbon nanomaterials and discuss their fluorescent properties. The most distinguished fluorescent characteristics of carbon dots is their excitation-dependent emission. For the majority carbon dots investigated so far, they possess this special character. As the excitation moves across from UV to even near-infrared, the carbon dots emission moves in correspondence with the excitation wavelength. [92-99] Some carbon dots have stabilized emission position even by shifting excitation wavelength, some carbon dots even possess upconversion fluorescence when excited by near-infrared light. [100-102]

Compared to other glucose recognized biomolecules, the glucose binding proteins are non-enzymatic glucose bioreceptors. And GBP could bind glucose with high sensitivity and selectivity. The binding event could naturally occur and no by-products are produced. After the GBP is binding with glucose. The conformation of binding proteins would change accompanied with hinge bending. This hinge bending behavior could be used to transduce

the binding event into fluorescent signal by using nanomaterials and nanostructures. Efficient glucose biosensing could be realized by using this kind of glucose binding protein. Taking advantage of recombinant protein engineering techniques, various glucose binding proteins could be design and produced as versatile nanobiotools for glucose sensing.

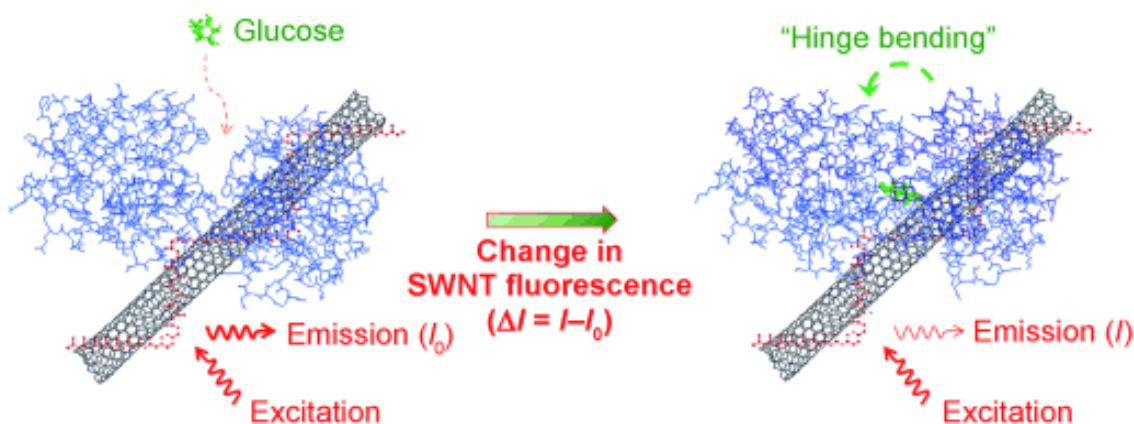


**Figure 2.11** Glucose-binding protein (GBP) covalently conjugated to a fluorescent single-walled carbon nanotube (SWNT) is shown to act as an optical switch. Hinge-bending response to glucose causes a reversible exciton quenching of the SWNT fluorescence with high selectivity. Reproduced from [103] with permission of the John Wiley and Sons. (Permission in Appendix 11)

A glucose binding protein-single carbon wall nanotube nanobiosensor was developed (figure 2.11). [103] The mechanism of this nanoscale glucose sensing device was shown in figure 2.11. First the carbon nanotube was wrapped and stabilized by carboxylated poly(vinyl alcohol) (cPVA). Then the glucose binding protein (GBP) was covalently bioconjugated with the cPVA. The emission of the single walled carbon nanotube was in the near-infrared area, which is the biological transparent windows. The adding of glucose led to the GBP hinge bending and conformation change. This allosterically change influenced the near-infrared fluorescence of carbon nanotube. Experimental data showed that the glucose sensing range was 2.5 mM–50 mM and the fluorescence change was reversible due to the reversible GBP binding behavior.



An important advantage of carbon dots over other fluorescent nanomaterials is their high water solubility and high biocompatibility after proper surface modification, which renders them very suitable for biomedical applications. Moreover, the surface of carbon dots often consist of carboxylic groups ( $-\text{COOH}$ ), amine groups ( $-\text{NH}_2$ ) and other groups for further functionalization.

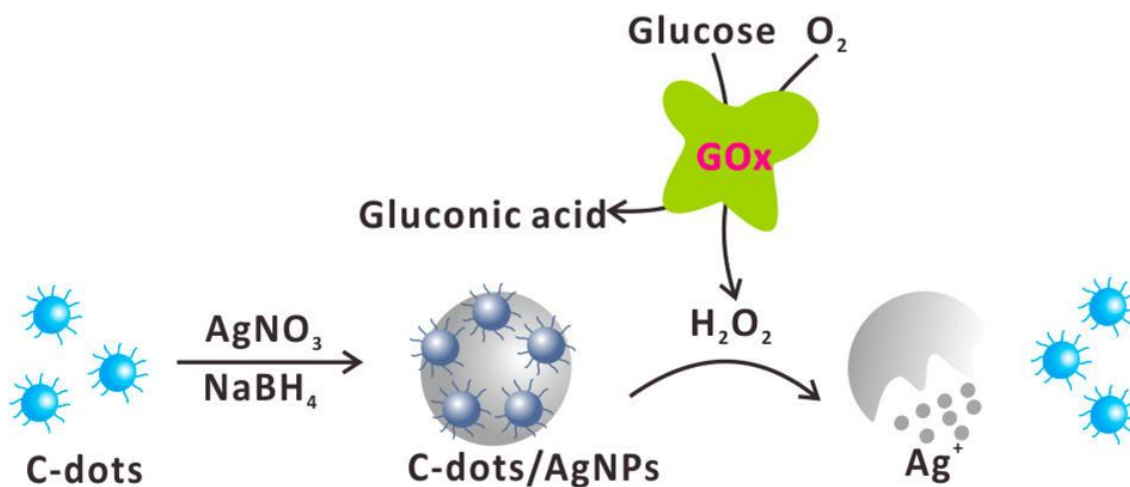


**Figure 2.12 Fluorescence turn-on strategy for glucose detection based on combination of Carbon nanodots supported on silver nanoparticles and GOx-mediated oxidation of glucose. Reprinted with permission from [104], Copyright (2016) American Chemical Society. (Permission in Appendix 12)**

A fluorescence turned-on strategy for glucose sensing was achieved by incorporating fluorescent carbon dots inside plasmonic silver nanoparticles shown in figure 2.12. [104] Fluorescent carbon dots were first incorporated inside the plasmonic silver nanoparticles during the synthesis silver nanoparticles. The glucose was oxidized by glucose oxidase and produced gluconic acid and  $\text{H}_2\text{O}_2$ . The hydrogen peroxide etched silver nanoparticles and consequently the inclusion of carbon dots were released. The advantage of this glucose nanobiosensor is the high biocompatibility of carbon dots and silver nanoparticles. Analytical results showed a linear response to glucose concentration at the range of  $2\ \mu\text{M}$ – $10\ \mu\text{M}$ .

## 2.4.6 Graphene Nanomaterials

Some nanomaterials were fluorescence quenchers, like noble plasmonic gold/silver metal nanoparticles and graphene/graphene oxide etc. In the glucose analysis process, these fluorescent interacting nanomaterials could quench the fluorescent component through the non-radiative transfer of electronic excitation energy to the  $\pi$  electron system of graphene. When glucose is introduced, the fluorescence would be either turned on or turned off depending on the sensor design. Reduced graphene oxide (RGO) or graphene oxide (GO) are widely used in the glucose sensing assay. Pure graphene is difficult to be stabilized and functionalized. Reduced graphene oxide or graphene oxide are more prevalently studied. RGO and GO have good water solubility and are also biocompatible, which favor their application in biosensing areas. [105-110] RGO/GO offer a large surface area and could be functionalized by various groups or decorated with various nanomaterials. The original existing carboxylic groups, epoxy groups and carbonyl groups on RGO/GO plane provide the anchoring place for further chemical modifications with molecule and biomolecule or other nanoscale materials. [111-113]

In summary, the above discussed fluorescent nanomaterials of semiconductor quantum dots, dye-doped silica nanoparticles and upconverting nanomaterials are mostly investigated and used in fluorescent glucose nanobiosensing. Besides that, fluorescent quenching nanomaterials like plasmonic gold/silver nanoparticle, graphene/graphene oxide nanomaterials are also heavily involved and used as fluorescence quenching components in the glucose nanobiosensing assays.

## 2.5 Magnetoresistive Nanomaterials

Magnetoresistance is a spin effect. Spin up electron and spin down electron scatter at the magnetic structures. The more scattering of the path, the larger resistance it has. Magnetic nanomaterials and non-magnetic conductive metals like Cr, Cu etc. are sandwiched or mixed as multilayer and/or multicomponent formats in nanoscale to form a magnetoresistive chip. Magnetoresistive biosensors has been developed by several research groups to sense proteins, antibody, antigen etc. [114-116] The Wang Group in Stanford [117] has contributed greatly to magnetoresistive biosensors. They have

developed a giant magnetoresistance (GMR) sensor arrays for quantification of protein interactions and solution transport. [118] This GMR sensor chip is a multilayer nanostructure, the target antibody were labeled with magnetic nanoparticle. They have also developed another GMR sensor for multiplex proteins assay. [119] Wang's group mainly focus on protein sensing and assays. Other groups like Wang group of nanospin research in University of Minnesota [120] has developed magnetoresistive biosensor for ion sensing, [121] influenza virus sensing etc. [122] The magnetoresistance biosensor are promising for future clinical applications. To our best knowledge, no glucose magnetoresistance biosensor has been developed yet. Therefore my work on the magnetoresistive nanostructured glucose biosensor is novel and important to MR biosensor development.

Graphene/magnetic nanoparticle composites are novel format for developing the magnetoresistive biosensor. Graphene or reduced graphene oxide are conductive and have no or very weak magnetic properties. The magnetic nanoparticle/graphene systems have been studied by several groups. [123-127] One study decorated magnetic  $\text{FeNi}_3$  nanoparticles onto graphene nanocomposites to obtain enhanced magnetoresistance of pressed pellets of graphene/ $\text{FeNi}_3$  nanoparticle composites. [128] An iron oxide/graphene oxide nanocomposite based magnetoresistive random access memory device was developed by Wee et al. [129] Therefore, magnetic carbon nanomaterials are promising for developing magnetoresistive biosensors.

## 2.6 Summary

In glucose nanobiosensing, biocompatibility and enhanced fluorescent properties are the major developing trends for highly sensitive and selective nanostructured biosensor. Most of the investigated fluorescent nanomaterials have mature synthesis and surface modification methods and superior fluorescent properties and they have been widely used in glucose nanobiosensing.

For semiconductor quantum dots, its high quantum yield and photo-stability boost its development. However the cytotoxicity of semiconductor quantum dots limits its clinical *in vivo* application. In order to improve the biocompatibility of QDs, a biocompatible coating layer is often applied to coat quantum dots before their further application *in vivo*

and *in vitro*. Dye-doped silica nanomaterials have high biocompatibility. Example like Cornell dots with high brightness and biocompatibility demonstrate the great potential for the *in vivo* and *in vitro* applications of silica nanomaterials. And the silica matrix structure and mesoporosity are facilely controllable. Moreover silica nanomaterials could be modified with various chemical group and functionalization under the universal silane chemistry. Encouragingly, the Cornell dots' clinical human trial [130] and clinical translation report [131] proved its biocompatibility and non-cytotoxicity effect for clinical application. The upconversion nanomaterials (UCNPs) are very suitable for *in vivo* applications in biosensing due to their high biocompatibility and superior upconverting fluorescence characteristics (line like emission, long fluorescence lifetime and photostability). Plasmonic gold/silver nanoparticles are often used as fluorescent quenching components, while fluorescent gold/silver nanoclusters are utilized as fluorescent components. These plasmonic noble metal nanoparticles and noble metal quantum clusters show high biocompatibility which have attracted intensive research in glucose nanobiosensing applications.

Carbon nanomaterials represent a broad nanotools for applications in glucose nanobiosensing. They have high biocompatibility, facile modification chemistry, facile preparation, multiple choice of different carbon nanomaterials. Nanocarbon family members have graphene/graphene oxide, graphene quantum dots, carbon dots, single-walled/multi-walled carbon nanotubes, carbon nanodiamonds and carbon nanohorns etc. They could be used as either fluorescent donor or fluorescence quenching acceptor in the glucose nanobiosensor design. Moreover, nanocomposites of graphene/magnetic nanomaterials are promising for constructing magnetoresistive nanostructures. Therefore, carbon nanomaterials have gained more and more attention in the development of nanostructured glucose biosensor.

Currently, the marketed electrochemical glucometer could provide accurate glucose measuring. But this measuring require certain amounts of blood, the blood is often obtained by finger prick. However the glucometer could only measure the blood glucose level at that time. Therefore, several finger pricks are applied to diabetics per day. The pricks are very uncomfortable for people and are susceptible to risks of infections. In a word, the

prevalent glucometer is invasive to people but in the market there is barely alternative available economic, minimally invasive or non-invasive glucose sensors for diabetics. Nanomaterials and nanostructures could have novel chemical, physical and biological properties. Nanostructured biosensors have high sensitivity and selectivity and are promising for developing minimally invasive or non-invasive glucose sensors. Especially the fluorescent and magnetoresistive nanomaterials and nanostructures are suitable for development of minimally invasive or non-invasive glucose biosensor with high sensitivity and selectivity.

In the long run, integrated nanostructured sensor chip device for continuous fluorescence/magnetoresistance glucose nanobiosensing should be the major developing strategy. Biocompatibility, stability, selectivity and sensitivity as well as economic benefit are the major progressing considering parameters. These chips are promising to integrate into *in vitro* nanostructured chips, microfluidics or semi *in vivo* contact lens and *in vivo* implanted device with convenient data acquisition models for long termed, human-friendly, real time, and dynamic measuring glucose levels in healthy people and diabetes people. For the glucose sensing in food, pharmaceutical industries etc., the stability and durability against all kinds of harsh environments like heat or cold, saline, acidic or basic etc. need to be taken into considerations for long-termed usage of nanostructured glucose biosensors.

## 2.7 References

- [1] G. L. Miller, Use of Dinitrosalicylic Acid Reagent for Determination of Reducing Sugar. *Analytical Chemistry* **1959**, *31* (3), 426-428.
- [2] Mark-Steven Steiner; Axel Duerkop; Otto S. Wolfbeis, Optical methods for sensing glucose. *Chemical Society Reviews* **2011**, *40* (9), 4805-4839.
- [3] N. S. Oliver; C. Toumazou; A. E. G. Cass; D. G. Johnston, Glucose sensors: a review of current and emerging technology. *Diabetic Medicine* **2009**, *26* (3), 197-210.
- [4] Sandeep Kumar Vashist, Non-invasive glucose monitoring technology in diabetes management: A review. *Analytica Chimica Acta* **2012**, *750* (Supplement C), 16-27.
- [5] Weijiang Guan; Wenjuan Zhou; Jun Lu; Chao Lu, Luminescent films for chemo- and biosensing. *Chemical Society Reviews* **2015**, *44* (19), 6981-7009.

- [6] John C. Pickup; Faeiza Hussain; Nicholas D. Evans; Olaf J. Rolinski; David J. S. Birch, Fluorescence-based glucose sensors. *Biosensors and Bioelectronics* **2005**, *20* (12), 2555-2565.
- [7] David C. Klonoff, Overview of Fluorescence Glucose Sensing: A Technology with a Bright Future. *Journal of Diabetes Science and Technology* **2012**, *6* (6), 1242-1250.
- [8] Sabato D'Auria; Giovanni Ghirlanda; Antonietta Parracino; Marcella de Champdor é Viviana Scognamiglio; Maria Staiano; Mos èRossi, Fluorescence Biosensors for Continuously Monitoring the Blood Glucose Level of Diabetic Patients. In *Glucose Sensing*, ChrisD Geddes; JosephR Lakowicz, Eds. Springer US: 2006; Vol. 11, pp 117-130.
- [9] Xiao-Peng He; Xi-Le Hu; Tony D. James; Juyoung Yoon; He Tian, Multiplexed photoluminescent sensors: towards improved disease diagnostics. *Chemical Society Reviews* **2017**, *46* (22), 6687-6696.
- [10] Mattias Björnmalm; Matthew Faria; Frank Caruso, Increasing the Impact of Materials in and beyond Bio-Nano Science. *Journal of the American Chemical Society* **2016**, *138* (41), 13449-13456.
- [11] Ran Tel-Vered; Omer Yehezkeli; Itamar Willner, Biomolecule/Nanomaterial Hybrid Systems for Nanobiotechnology. In *Nano-Biotechnology for Biomedical and Diagnostic Research*, Eran Zahavy; Arie Ordentlich; Shmuel Yitzhaki; Avigdor Shafferman, Eds. Springer Netherlands: Dordrecht, 2012; pp 1-16.
- [12] Nenad Petrovic; Mirjana Janicijevic Petrovic; Suncica Sreckovic; Svetlana Jovanovic; Dusan Todorovic; Tatjana Sarenac Vulovic, Nanotechnology in Ophthalmology. In *Commercialization of Nanotechnologies–A Case Study Approach*, Dermot Brabazon; Eva Pellicer; Fatima Zivic; Jordi Sort; Maria Dolors Bar ó Nenad Grujovic; Kwang-Leong Choy, Eds. Springer International Publishing: Cham, 2018; pp 275-297.
- [13] Claudio Parolo; Arben Merkoci, Paper-based nanobiosensors for diagnostics. *Chemical Society Reviews* **2013**, *42* (2), 450-457.
- [14] Anqi Zhang; Charles M. Lieber, Nano-Bioelectronics. *Chemical Reviews* **2016**, *116* (1), 215-257.
- [15] Andreas Thomas; Lutz Heinemann; Araceli Ramírez; Alfred Zehe, Options for the Development of Noninvasive Glucose Monitoring: Is Nanotechnology an Option to Break the Boundaries? *Journal of Diabetes Science and Technology* **2016**, *10* (3), 782-789.
- [16] Viviana Scognamiglio, Nanotechnology in glucose monitoring: Advances and challenges in the last 10 years. *Biosensors and Bioelectronics* **2013**, *47*, 12-25.

- [17] Masashige Taguchi; Andre Ptitsyn; Eric S. McLamore; Jonathan C. Claussen, Nanomaterial-mediated Biosensors for Monitoring Glucose. *Journal of Diabetes Science and Technology* **2014**, 8 (2), 403-411.
- [18] Kevin J. Cash; Heather A. Clark, Nanosensors and nanomaterials for monitoring glucose in diabetes. *Trends in Molecular Medicine* 16 (12), 584-593.
- [19] P. Demchenko Alexander, Nanoparticles and nanocomposites for fluorescence sensing and imaging. *Methods and Applications in Fluorescence* **2013**, 1 (2), 022001.
- [20] Sandeep Kumar; Wandit Ahlawat; Rajesh Kumar; Neeraj Dilbaghi, Graphene, carbon nanotubes, zinc oxide and gold as elite nanomaterials for fabrication of biosensors for healthcare. *Biosensors and Bioelectronics* **2015**, 70 (Supplement C), 498-503.
- [21] Anthony P. F. Turner, Biosensors: sense and sensibility. *Chemical Society Reviews* **2013**, 42 (8), 3184-3196.
- [22] Bhavika Patel; Costas Anastassiou; Danny O'Hare, Biosensor Design and Interfacing. In *Body Sensor Networks*, Guang-Zhong Yang, Ed. Springer London: 2006; pp 41-87.
- [23] Ke Xu; Mohsen Purahmad; Kimber Brenneman; Xenia Meshik; Sidra Farid; Shripriya Poduri; Preeti Pratap; Justin Abell; Yiping Zhao; Barbara Nichols; Eugene Zakar; Michael Stroschio; Mitra Dutta, Design and Applications of Nanomaterial-Based and Biomolecule-Based Nanodevices and Nanosensors. In *Design and Applications of Nanomaterials for Sensors*, Jorge M. Seminario, Ed. Springer Netherlands: 2014; Vol. 16, pp 61-97.
- [24] Kuldeep Mahato; Anupriya Baranwal; Ananya Srivastava; Pawan Kumar Maurya; Pranjal Chandra, Smart Materials for Biosensing Applications. In *Techno-Societal 2016: Proceedings of the International Conference on Advanced Technologies for Societal Applications*, Prashant M. Pawar; Babruvahan P. Ronge; R. Balasubramaniam; Sridevi Seshabhattar, Eds. Springer International Publishing: Cham, 2018; pp 421-431.
- [25] Philip D. Howes; Rona Chandrawati; Molly M. Stevens, Colloidal nanoparticles as advanced biological sensors. *Science* **2014**, 346 (6205).
- [26] Michael Holzinger; Alan Le Goff; Serge Cosnier, Nanomaterials for biosensing applications: a review. *Frontiers in Chemistry* **2014**, 2 (63).
- [27] Tetsuya Haruyama, Molecules, Cells, Materials, and Systems Design Based on Nanobiotechnology Use in Bioanalytical Technology. In *Nanobiotechnology*, Oded Shoseyov; Ilan Levy, Eds. Humana Press: 2008; pp 369-382.
- [28] C Vestergaard Mun'delanji; Kagan Kerman; I-Ming Hsing; Eiichi Tamiya, *Nanobiosensors and Nanobioanalyses*. Springer: 2015.

- [29] Leah Tolosa; Govind Rao, The Glucose Binding Protein as Glucose Sensor. In *Glucose Sensing*, ChrisD Geddes; JosephR Lakowicz, Eds. Springer US: 2006; Vol. 11, pp 323-331.
- [30] Jithesh V. Veetil; Sha Jin; Kaiming Ye, A glucose sensor protein for continuous glucose monitoring. *Biosensors and Bioelectronics* **2010**, 26 (4), 1650-1655.
- [31] ConstanceJ Jeffery, Engineering periplasmic ligand binding proteins as glucose nanosensors. *Nano Reviews* **2011**, 2 (1), 5743.
- [32] Libing Zhang; Erkang Wang, Metal nanoclusters: New fluorescent probes for sensors and bioimaging. *Nano Today* **2014**, 9 (1), 132-157.
- [33] Benjamin Hötzer; Igor L. Medintz; Niko Hildebrandt, Fluorescence in Nanobiotechnology: Sophisticated Fluorophores for Novel Applications. *Small* **2012**, 8 (15), 2297-2326.
- [34] Jun Yao; Mei Yang; Yixiang Duan, Chemistry, Biology, and Medicine of Fluorescent Nanomaterials and Related Systems: New Insights into Biosensing, Bioimaging, Genomics, Diagnostics, and Therapy. *Chemical Reviews* **2014**, 114 (12), 6130-6178.
- [35] Elena Aznar; Reynaldo Villalonga; Cristina Gimenez; Felix Sancenon; M. Dolores Marcos; Ramon Martinez-Manez; Paula Diez; Jose M. Pingarron; Pedro Amoros, Glucose-triggered release using enzyme-gated mesoporous silica nanoparticles. *Chemical Communications* **2013**, 49 (57), 6391-6393.
- [36] Krishnendu Saha; Sarit S. Agasti; Chaekyu Kim; Xiaoning Li; Vincent M. Rotello, Gold Nanoparticles in Chemical and Biological Sensing. *Chemical Reviews* **2012**, 112 (5), 2739-2779.
- [37] Shi Ying Lim; Wei Shen; Zhiqiang Gao, Carbon quantum dots and their applications. *Chemical Society Reviews* **2015**, 44 (1), 362-381.
- [38] Frederico R. Baptista; S. A. Belhout; S. Giordani; S. J. Quinn, Recent developments in carbon nanomaterial sensors. *Chemical Society Reviews* **2015**, 44 (13), 4433-4453.
- [39] Deep Jariwala; Vinod K. Sangwan; Lincoln J. Lauhon; Tobin J. Marks; Mark C. Hersam, Carbon nanomaterials for electronics, optoelectronics, photovoltaics, and sensing. *Chemical Society Reviews* **2013**, 42 (7), 2824-2860.
- [40] Michael F. L. De Volder; Sameh H. Tawfick; Ray H. Baughman; A. John Hart, Carbon Nanotubes: Present and Future Commercial Applications. *Science* **2013**, 339 (6119), 535.
- [41] Pratima R. Solanki; Ajeet Kaushik; Ved V. Agrawal; Bansi D. Malhotra, Nanostructured metal oxide-based biosensors. *NPG Asia Materials* **2011**, 3, 17-24.



- [42] Soumen Das; V. Jayaraman, SnO<sub>2</sub>: A comprehensive review on structures and gas sensors. *Progress in Materials Science* **2014**, *66* (Supplement C), 112-255.
- [43] Marco Righettoni; Anton Amann; Sotiris E. Pratsinis, Breath analysis by nanostructured metal oxides as chemo-resistive gas sensors. *Materials Today* **2015**, *18* (3), 163-171.
- [44] Thomas Fischer; Aadesh P. Singh; Trilok Singh; Francisco Hernández-Ramírez; Daniel Prades; Sanjay Mathur, Metal Oxide Nano-architectures and Heterostructures for Chemical Sensors. In *Metal Oxide Nanomaterials for Chemical Sensors*, Michael A. Carpenter; Sanjay Mathur; Andrei Kolmakov, Eds. Springer New York: New York, NY, 2013; pp 397-438.
- [45] Subramanian Tamil Selvan; Timothy Thatt Yang Tan; Dong Kee Yi; Nikhil R. Jana, Functional and Multifunctional Nanoparticles for Bioimaging and Biosensing. *Langmuir* **2010**, *26* (14), 11631-11641.
- [46] Vasudevanpillai Biju, Chemical modifications and bioconjugate reactions of nanomaterials for sensing, imaging, drug delivery and therapy. *Chemical Society Reviews* **2014**, *43* (3), 744-764.
- [47] Huangxian Ju; Xueji Zhang; Joseph Wang, Biofunctionalization of Nanomaterials. In *NanoBiosensing*, Springer New York: 2011; pp 1-38.
- [48] Meral Yuce; Hasan Kurt, How to make nanobiosensors: surface modification and characterisation of nanomaterials for biosensing applications. *RSC Advances* **2017**, *7* (78), 49386-49403.
- [49] Scott A. Walper; Kendrick B. Turner; Igor L. Medintz, Enzymatic bioconjugation of nanoparticles: developing specificity and control. *Current Opinion in Biotechnology* **2015**, *34* (Supplement C), 232-241.
- [50] Kim E. Sapsford; W. Russ Algar; Lorenzo Berti; Kelly Boeneman Gemmill; Brendan J. Casey; Eunkeu Oh; Michael H. Stewart; Igor L. Medintz, Functionalizing Nanoparticles with Biological Molecules: Developing Chemistries that Facilitate Nanotechnology. *Chemical Reviews* **2013**, *113* (3), 1904-2074.
- [51] Rajib Ghosh Chaudhuri; Santanu Paria, Core/Shell Nanoparticles: Classes, Properties, Synthesis Mechanisms, Characterization, and Applications. *Chemical Reviews* **2011**, *112* (4), 2373-2433.
- [52] Maja Stanisavljevic; Sona Krizkova; Marketa Vaculovicova; Rene Kizek; Vojtech Adam, Quantum dots-fluorescence resonance energy transfer-based nanosensors and their application. *Biosensors and Bioelectronics* **2015**, *74*, 562-574.
- [53] Andrew M. Smith; Hongwei Duan; Aaron M. Mohs; Shuming Nie, Bioconjugated quantum dots for *in vivo* molecular and cellular imaging. *Advanced Drug Delivery Reviews* **2008**, *60* (11), 1226-1240.

- [54] Juan B. Blanco-Canosa; Miao Wu; Kimihiro Susumu; Eleonora Petryayeva; Travis L. Jennings; Philip E. Dawson; W. Russ Algar; Igor L. Medintz, Recent progress in the bioconjugation of quantum dots. *Coordination Chemistry Reviews* **2014**, 263–264, 101-137.
- [55] Tingting Zhang; Jackie L. Stilwell; Daniele Gerion; Lianghao Ding; Omeed Elboudwarej; Patrick A. Cooke; Joe W. Gray; A. Paul Alivisatos; Fanqing Frank Chen, Cellular Effect of High Doses of Silica-Coated Quantum Dot Profiled with High Throughput Gene Expression Analysis and High Content Cellomics Measurements. *Nano Letters* **2006**, 6 (4), 800-808.
- [56] K. David Wegner; Niko Hildebrandt, Quantum dots: bright and versatile *in vitro* and *in vivo* fluorescence imaging biosensors. *Chemical Society Reviews* **2015**, 44 (14), 4792-4834.
- [57] Lihua Cao; Jian Ye; Lili Tong; Bo Tang, A New Route to the Considerable Enhancement of Glucose Oxidase (GOx) Activity: The Simple Assembly of a Complex from CdTe Quantum Dots and GOx, and Its Glucose Sensing. *Chemistry – A European Journal* **2008**, 14 (31), 9633-9640.
- [58] Robert Wilson; David G. Spiller; Alison Beckett; Ian A. Prior; Violaine S é, Highly Stable Dextran-Coated Quantum Dots for Biomolecular Detection and Cellular Imaging. *Chemistry of Materials* **2010**, 22 (23), 6361-6369.
- [59] Igor L. Medintz; H. Tetsuo Uyeda; Ellen R. Goldman; Hedi Mattoussi, Quantum dot bioconjugates for imaging, labelling and sensing. *Nature Materials* **2005**, 4 (6), 435-446.
- [60] Jingjing Li; Jun-Jie Zhu, Quantum dots for fluorescent biosensing and bio-imaging applications. *Analyst* **2013**, 138 (9), 2506-2515.
- [61] Bo Tang; Lihua Cao; Kehua Xu; Linhai Zhuo; Jiechao Ge; Qingling Li; Lijuan Yu, A New Nanobiosensor for Glucose with High Sensitivity and Selectivity in Serum Based on Fluorescence Resonance Energy Transfer (FRET) between CdTe Quantum Dots and Au Nanoparticles. *Chemistry – A European Journal* **2008**, 14 (12), 3637-3644.
- [62] Lily Bahshi; Ronit Freeman; Ron Gill; Itamar Willner, Optical Detection of Glucose by Means of Metal Nanoparticles or Semiconductor Quantum Dots. *Small* **2009**, 5 (6), 676-680.
- [63] Xinyu Li; Yunlong Zhou; Zhaozhu Zheng; Xiuli Yue; Zhifei Dai; Shaoqin Liu; Zhiyong Tang, Glucose Biosensor Based on Nanocomposite Films of CdTe Quantum Dots and Glucose Oxidase. *Langmuir* **2009**, 25 (11), 6580-6586.
- [64] Andrew Burns; Hooisweng Ow; Ulrich Wiesner, Fluorescent core-shell silica nanoparticles: towards "Lab on a Particle" architectures for nanobiotechnology. *Chemical Society Reviews* **2006**, 35 (11), 1028-1042.

- [65] Won Seok Han; Hye Young Lee; Sung Ho Jung; Soo Jin Lee; Jong Hwa Jung, Silica-based chromogenic and fluorogenic hybrid chemosensor materials. *Chemical Society Reviews* **2009**, 38 (7), 1904-1915.
- [66] G. Faccio; M. B. Bannwarth; C. Schulenburg; V. Steffen; D. Jankowska; M. Pohl; R. M. Rossi; K. Maniura-Weber; L. F. Boesel; M. Richter, Encapsulation of FRET-based glucose and maltose biosensors to develop functionalized silica nanoparticles. *Analyst* **2016**, 141 (13), 3982-3984.
- [67] Yongsheng Liu; Datao Tu; Haomiao Zhu; Xueyuan Chen, Lanthanide-doped luminescent nanoprobes: controlled synthesis, optical spectroscopy, and bioapplications. *Chemical Society Reviews* **2013**, 42 (16), 6924-6958.
- [68] Wei Kong; Tianying Sun; Bing Chen; Xian Chen; Fujin Ai; Xiaoyue Zhu; Mingyu Li; Wenjun Zhang; Guangyu Zhu; Feng Wang, A General Strategy for Ligand Exchange on Upconversion Nanoparticles. *Inorganic Chemistry* **2017**, 56 (2), 872-877.
- [69] Si Wu; Hans-Jürgen Butt, Near-Infrared-Sensitive Materials Based on Upconverting Nanoparticles. *Advanced Materials* **2016**, 28 (6), 1208-1226.
- [70] Fan Zhang, Upconversion Nanoparticles for Biosensing. In *Photon Upconversion Nanomaterials*, Springer Berlin Heidelberg: Berlin, Heidelberg, 2015; pp 255-284.
- [71] Wei Zheng; Ping Huang; Datao Tu; En Ma; Haomiao Zhu; Xueyuan Chen, Lanthanide-doped upconversion nano-bioprobes: electronic structures, optical properties, and biodetection. *Chemical Society Reviews* **2015**, 44 (6), 1379-1415.
- [72] Markus Haase; Helmut Sch äfer, Upconverting Nanoparticles. *Angewandte Chemie International Edition* **2011**, 50 (26), 5808-5829.
- [73] Feng Wang; Xiaogang Liu, Recent advances in the chemistry of lanthanide-doped upconversion nanocrystals. *Chemical Society Reviews* **2009**, 38 (4), 976-989.
- [74] Stefan Wilhelm, Perspectives for Upconverting Nanoparticles. *ACS Nano* **2017**, 11 (11), 10644-10653.
- [75] Jiali Liu; Lili Lu; Aiqin Li; Juan Tang; Shiguo Wang; Suying Xu; Leyu Wang, Simultaneous detection of hydrogen peroxide and glucose in human serum with upconversion luminescence. *Biosensors and Bioelectronics* **2015**, 68, 204-209.
- [76] Jing Yuan; Yao Cen; Xiang-Juan Kong; Shuang Wu; Chen-Liwei Liu; Ru-Qin Yu; Xia Chu, MnO<sub>2</sub>-Nanosheet-Modified Upconversion Nanosystem for Sensitive Turn-On Fluorescence Detection of H<sub>2</sub>O<sub>2</sub> and Glucose in Blood. *ACS Applied Materials & Interfaces* **2015**, 7 (19), 10548-10555.
- [77] Rongchao Jin; Chenjie Zeng; Meng Zhou; Yuxiang Chen, Atomically Precise Colloidal Metal Nanoclusters and Nanoparticles: Fundamentals and Opportunities. *Chemical Reviews* **2016**, 116 (18), 10346-10413.

- [78] Isabel Diez; Robin H. A. Ras, Fluorescent silver nanoclusters. *Nanoscale* **2011**, 3 (5), 1963-1970.
- [79] Yu Tao; Mingqiang Li; Jinsong Ren; Xiaogang Qu, Metal nanoclusters: novel probes for diagnostic and therapeutic applications. *Chemical Society Reviews* **2015**, 44 (23), 8636-8663.
- [80] Yizhong Lu; Wei Chen, Sub-nanometre sized metal clusters: from synthetic challenges to the unique property discoveries. *Chemical Society Reviews* **2012**, 41 (9), 3594-3623.
- [81] Jeffrey N. Anker; W. Paige Hall; Olga Lyandres; Nilam C. Shah; Jing Zhao; Richard P. Van Duyne, Biosensing with plasmonic nanosensors. *Nature Materials* **2008**, 7 (6), 442-453.
- [82] Borja Sepúlveda; Paula C. Angelomé; Laura M. Lechuga; Luis M. Liz-Marzán, LSPR-based nanobiosensors. *Nano Today* **2009**, 4 (3), 244-251.
- [83] Li-Yi Chen; Chia-Wei Wang; Zhiqin Yuan; Huan-Tsung Chang, Fluorescent Gold Nanoclusters: Recent Advances in Sensing and Imaging. *Analytical Chemistry* **2015**, 87 (1), 216-229.
- [84] Jingjing Li; Jun-Jie Zhu; Kai Xu, Fluorescent metal nanoclusters: From synthesis to applications. *TRAC Trends in Analytical Chemistry* **2014**, 58, 90-98.
- [85] Jiang Xue Dong; Zhong Feng Gao; Ying Zhang; Bang Lin Li; Wei Zhang; Jing Lei Lei; Nian Bing Li; Hong Qun Luo, The pH-switchable agglomeration and dispersion behavior of fluorescent Ag nanoclusters and its applications in urea and glucose biosensing. *NPG Asia Materials* **2016**, 8, e335.
- [86] Sebastian Kruss; Andrew J. Hilmer; Jingqing Zhang; Nigel F. Reuel; Bin Mu; Michael S. Strano, Carbon nanotubes as optical biomedical sensors. *Advanced Drug Delivery Reviews* **2013**, 65 (15), 1933-1950.
- [87] Xiangcheng Sun; Yu Lei, Fluorescent carbon dots and their sensing applications. *TRAC Trends in Analytical Chemistry* **2017**, 89, 163-180.
- [88] Hanjun Sun; Li Wu; Weili Wei; Xiaogang Qu, Recent advances in graphene quantum dots for sensing. *Materials Today* **2013**, 16 (11), 433-442.
- [89] Amal Rabti; Nouredine Raouafi; Arben Merkoçi, Bio(Sensing) devices based on ferrocene-functionalized graphene and carbon nanotubes. *Carbon* **2016**, 108 (Supplement C), 481-514.
- [90] Yan Du; Shaojun Guo, Chemically doped fluorescent carbon and graphene quantum dots for bioimaging, sensor, catalytic and photoelectronic applications. *Nanoscale* **2016**, 8 (5), 2532-2543.

- [91] Katsuhiko Ariga; Kosuke Minami; Lok Kumar Shrestha, Nanoarchitectonics for carbon-material-based sensors. *Analyst* **2016**, *141* (9), 2629-2638.
- [92] Vasilios Georgakilas; Jason A. Perman; Jiri Tucek; Radek Zboril, Broad Family of Carbon Nanoallotropes: Classification, Chemistry, and Applications of Fullerenes, Carbon Dots, Nanotubes, Graphene, Nanodiamonds, and Combined Superstructures. *Chemical Reviews* **2015**, *115* (11), 4744-4822.
- [93] Guosong Hong; Shuo Diao; Alexander L. Antaris; Hongjie Dai, Carbon Nanomaterials for Biological Imaging and Nanomedicinal Therapy. *Chemical Reviews* **2015**, *115* (19), 10816-10906.
- [94] Haitao Li; Zhenhui Kang; Yang Liu; Shuit-Tong Lee, Carbon nanodots: synthesis, properties and applications. *Journal of Materials Chemistry* **2012**, *22* (46), 24230-24253.
- [95] Youfu Wang; Aiguo Hu, Carbon quantum dots: synthesis, properties and applications. *Journal of Materials Chemistry C* **2014**, *2* (34), 6921-6939.
- [96] Sheila N Baker; Gary A Baker, Luminescent Carbon Nanodots: Emergent Nanolights. *Angewandte Chemie International Edition* **2010**, *49* (38), 6726-6744.
- [97] Bao-Ping Qi; Guo-Jun Zhang; Zhi-Ling Zhang; Dai-Wen Pang, Photoluminescent Properties of Carbon Nanodots. In *Carbon Nanoparticles and Nanostructures*, Nianjun Yang; Xin Jiang; Dai-Wen Pang, Eds. Springer International Publishing: Cham, 2016; pp 239-256.
- [98] Yongqiang Dong; Jianhua Cai; Yuwu Chi, Carbon Based Dots and Their Luminescent Properties and Analytical Applications. In *Carbon Nanoparticles and Nanostructures*, Nianjun Yang; Xin Jiang; Dai-Wen Pang, Eds. Springer International Publishing: Cham, 2016; pp 161-238.
- [99] Zhenhui Kang; Yang Liu; Shuit-Tong Lee, Carbon Dots for Bioimaging and Biosensing Applications. Springer Berlin Heidelberg: Berlin, Heidelberg, pp 1-31.
- [100] Hui Wang; Jinhui Yi; Yanyan Yu; Shuiqin Zhou, NIR upconversion fluorescence glucose sensing and glucose-responsive insulin release of carbon dot-immobilized hybrid microgels at physiological pH. *Nanoscale* **2017**, *9* (2), 509-516.
- [101] Jun Ke; Xinyong Li; Qidong Zhao; Baojun Liu; Shaomin Liu; Shaobin Wang, Upconversion carbon quantum dots as visible light responsive component for efficient enhancement of photocatalytic performance. *Journal of Colloid and Interface Science* **2017**, *496* (Supplement C), 425-433.
- [102] Jia-Yu Li; Yang Liu; Qun-Wei Shu; Jia-Man Liang; Fang Zhang; Xian-Ping Chen; Xiao-Yan Deng; Mark T. Swihart; Ke-Jun Tan, One-Pot Hydrothermal Synthesis of Carbon Dots with Efficient Up- and Down-Converted Photoluminescence for the Sensitive Detection of Morin in a Dual-Readout Assay. *Langmuir* **2017**, *33* (4), 1043-1050.

- [103] Hyeonseok Yoon; Jin-Ho Ahn; Paul W. Barone; Kyungsook Yum; Richa Sharma; Ardemis A. Boghossian; Jae-Hee Han; Michael S. Strano, Periplasmic Binding Proteins as Optical Modulators of Single-Walled Carbon Nanotube Fluorescence: Amplifying a Nanoscale Actuator. *Angewandte Chemie International Edition* **2011**, *50* (8), 1828-1831.
- [104] Jin-Liang Ma; Bin-Cheng Yin; Xin Wu; Bang-Ce Ye, Simple and Cost-Effective Glucose Detection Based on Carbon Nanodots Supported on Silver Nanoparticles. *Analytical Chemistry* **2016**, *89*, 1323–1328.
- [105] Martin Pumera, Graphene in biosensing. *Materials Today* **2011**, *14* (7–8), 308-315.
- [106] Yuxin Liu; Xiaochen Dong; Peng Chen, Biological and chemical sensors based on graphene materials. *Chemical Society Reviews* **2012**, *41* (6), 2283-2307.
- [107] Vasilios Georgakilas; Jitendra N. Tiwari; K. Christian Kemp; Jason A. Perman; Athanasios B. Bourlinos; Kwang S. Kim; Radek Zboril, Noncovalent Functionalization of Graphene and Graphene Oxide for Energy Materials, Biosensing, Catalytic, and Biomedical Applications. *Chemical Reviews* **2016**, *116* (9), 5464-5519.
- [108] Jieon Lee; Jung-ho Kim; Seongchan Kim; Dal-Hee Min, Biosensors based on graphene oxide and its biomedical application. *Advanced Drug Delivery Reviews* **2016**, *105* (Part B), 275-287.
- [109] Amedea B. Seabra; Amauri J. Paula; Renata de Lima; Oswaldo L. Alves; Nelson Durán, Nanotoxicity of Graphene and Graphene Oxide. *Chemical Research in Toxicology* **2014**, *27* (2), 159-168.
- [110] Sivaramapanicker Sreejith; Hrishikesh Joshi; Yanli Zhao, Graphene-Based Materials in Biosensing, Bioimaging, and Therapeutics. In *Graphene-based Materials in Health and Environment: New Paradigms*, Gil Gonçalves; Paula Marques; Mercedes Vila, Eds. Springer International Publishing: Cham, 2016; pp 35-61.
- [111] Siegfried Eigler; Andreas Hirsch, Chemistry with Graphene and Graphene Oxide—Challenges for Synthetic Chemists. *Angewandte Chemie International Edition* **2014**, *53* (30), 7720-7738.
- [112] Daniel R. Dreyer; Alexander D. Todd; Christopher W. Bielawski, Harnessing the chemistry of graphene oxide. *Chemical Society Reviews* **2014**, *43* (15), 5288-5301.
- [113] Rinky Sha; Sushmee Badhulika; Ashok Mulchandani, Graphene-Based Biosensors and Their Applications in Biomedical and Environmental Monitoring. Springer Berlin Heidelberg: Berlin, Heidelberg, pp 1-30.
- [114] P. P. Freitas; R. Ferreira; S. Cardoso; F. Cardoso, Magnetoresistive sensors. *Journal of Physics: Condensed Matter* **2007**, *19* (16), 165221.
- [115] Gungun Lin; Denys Makarov; Oliver G. Schmidt, Magnetic sensing platform technologies for biomedical applications. *Lab on a Chip* **2017**, *17* (11), 1884-1912.

- [116] Adarsh Sandhu, Biosensing: New probes offer much faster results. *Nature Nanotechnology* **2007**, 2 (12), 746-748.
- [117] <https://wanggroup.stanford.edu/>. (accessed November 2<sup>nd</sup> 2017).
- [118] Richard S. Gaster; Liang Xu; Shu-Jen Han; Robert J. Wilson; Drew A. Hall; Sebastian J. Osterfeld; Heng Yu; Shan X. Wang, Quantification of protein interactions and solution transport using high-density GMR sensor arrays. *Nature Nanotechnology* **2011**, 6, 314.
- [119] Sebastian J. Osterfeld; Heng Yu; Richard S. Gaster; Stefano Caramuta; Liang Xu; Shu-Jen Han; Drew A. Hall; Robert J. Wilson; Shouheng Sun; Robert L. White; Ronald W. Davis; Nader Pourmand; Shan X. Wang, Multiplex protein assays based on real-time magnetic nanotag sensing. *Proceedings of the National Academy of Sciences* **2008**, 105 (52), 20637-20640.
- [120] <http://www.nanospin.umn.edu/>. (accessed November 2<sup>nd</sup> 2017).
- [121] Wei Wang; Yi Wang; Liang Tu; Todd Klein; Yinglong Feng; Qin Li; Jian-Ping Wang, Magnetic Detection of Mercuric Ion Using Giant Magnetoresistance-Based Biosensing System. *Analytical Chemistry* **2014**, 86 (8), 3712-3716.
- [122] Venkatramana D. Krishna; Kai Wu; Andres M. Perez; Jian-Ping Wang, Giant Magnetoresistance-based Biosensor for Detection of Influenza A Virus. *Frontiers in Microbiology* **2016**, 7 (400).
- [123] Silke Behrens, Preparation of functional magnetic nanocomposites and hybrid materials: recent progress and future directions. *Nanoscale* **2011**, 3 (3), 877-892.
- [124] Y. C. Jiang; Z. P. Wu; W. Bao; S. J. Xu; J. Gao, Tunable positive magnetoresistance effect of Co-doped amorphous carbon films. *Journal of Applied Physics* **2012**, 111 (7), 07C510.
- [125] Vasilios Georgakilas; Michal Otyepka; Athanasios B. Bourlinos; Vimlesh Chandra; Namdong Kim; K. Christian Kemp; Pavel Hobza; Radek Zboril; Kwang S. Kim, Functionalization of Graphene: Covalent and Non-Covalent Approaches, Derivatives and Applications. *Chemical Reviews* **2012**, 112 (11), 6156-6214.
- [126] Perry T. Yin; Shreyas Shah; Manish Chhowalla; Ki-Bum Lee, Design, Synthesis, and Characterization of Graphene–Nanoparticle Hybrid Materials for Bioapplications. *Chemical Reviews* **2015**, 115 (7), 2483-2531.
- [127] Nan Gao; Xiaosheng Fang, Synthesis and Development of Graphene–Inorganic Semiconductor Nanocomposites. *Chemical Reviews* **2015**, 115 (16), 8294-8343.
- [128] G. Abellan; H. Prima-Garcia; E. Coronado, Graphene enhances the magnetoresistance of FeNi<sub>3</sub> nanoparticles in hierarchical FeNi<sub>3</sub>-graphene nanocomposites. *Journal of Materials Chemistry C* **2016**, 4 (11), 2252-2258.

[129] Aigu L. Lin; Haiyang Peng; Zhiqi Liu; Tom Wu; Chenliang Su; Kian Ping Loh; Ariando; Wei Chen; Andrew T. S. Wee, Room Temperature Magnetic Graphene Oxide-Iron Oxide Nanocomposite Based Magnetoresistive Random Access Memory Devices *via* Spin-Dependent Trapping of Electrons. *Small* **2014**, *10* (10), 1945-1952.

[130] Roberta Friedman, Nano Dot Technology Enters Clinical Trials. *Journal of the National Cancer Institute* **2011**, *103* (19), 1428-1429.

[131] Evan Phillips; Oula Penate-Medina; Pat B. Zanzonico; Richard D. Carvajal; Pauliah Mohan; Yunpeng Ye; John Humm; Mithat Gönen; Hovanes Kalaigian; Heiko Schöder; H. William Strauss; Steven M. Larson; Ulrich Wiesner; Michelle S. Bradbury, Clinical translation of an ultrasmall inorganic optical-PET imaging nanoparticle probe. *Science Translational Medicine* **2014**, *6* (260), 260ra149.



## Chapter 3

This chapter reuses the published journal paper (Biosensors and Bioelectronics 2017, 91, 393-399.). Permission is in Appendix 13.

### 3 Development of ZnO/QD Patterned Nanostructured Glucose Biosensor

#### 3.1 Introduction

In this chapter, a nanostructured glucose biosensor was developed to detect glucose in rats' tear by using fluorescence resonance energy transfer (FRET) quenching mechanism. The designed FRET pair, including the donor, CdSe/ZnS core/shell structured quantum dots (QDs), and the acceptor, dextran-binding malachite green (MG-dextran), was conjugated to concanavalin A (Con A), an enzyme with specific affinity to glucose. In the presence of glucose, the quenched emission of QDs through the FRET mechanism was restored by displacing the binding dextran from Con A. To have a dual-modulation sensor (one module is by fluorescence spectra and the other is by image pixel) for convenient and accurate detection, the nanostructured FRET sensors were assembled onto a patterned ZnO nanorod array deposited on the synthetic silicone hydrogel. Consequently, the concentration of glucose detected by the patterned sensor could be converted to fluorescence spectrum with high signal-to-noise ratio and calibrated image pixel value. The photoluminescence intensity of the patterned FRET sensor increased linearly with increasing concentration of glucose from 0.03 mmol/L to 3 mmol/L, which covered the range of tear glucose levels for both diabetics and healthy subjects. Meanwhile, the calibrated values of pixel intensities of the fluorescence images captured by a handheld fluorescence microscope increased with increasing glucose. Four male Sprague-Dawley rats with different blood glucose concentrations were utilized to demonstrate the quick response of the patterned FRET sensor to 2  $\mu\text{L}$  of diluted tear samples (2  $\mu\text{L}$  rats' tear mixed with 5  $\mu\text{L}$  PBS solution).

Tear fluid cleans and lubricates the eye while nourishing. Over 20 components have been found in tears, including salt water, proteins, glucose, and some small metallic ions, etc. [1] Diagnosis of biomolecules in tear fluid pertaining to ocular diseases such as ocular rosacea, have been performed primarily by clinicians to examine the high molecular-mass glycoproteins in tears. [2] The detection of ocular glucose dates back to 1930. [3] Following that, Michail and his collaborators first demonstrated the level of glucose in tears is often elevated in diabetic patients. [4] Sen and Sarin studied over 200 cases, their statistic results indicated the blood glucose is about 2 times higher in diabetic patients than that in non-diabetics, whereas tear glucose levels are about 5 times higher in diabetics than that in the general population. [5] In past decades, different research groups found a definite relationship between tear glucose and blood glucose, concluding hyperglycemia could be detected by measuring tear glucose levels. [6-8] Recent studies indicate tear glucose mean values were  $0.35 \pm 0.04$  mM and  $0.16 \pm 0.03$  mM, for patients with diabetes and healthy subjects, respectively. [9] It is also noted that time lag in measuring tear glucose is common to other glucose meters as it takes 5–15 minutes to allow the change of glucose in blood to eventually reflect in tear/interstitial fluids; [10] while it could be solved by a series of calibrations. [11-12]

However, it is very difficult to acquire enough tear samples in a short period. Furthermore, the concentration of glucose in tears is much lower than that in blood. Very few methods so far could measure such low concentration of glucose in a rapid fashion. [13-14] Compared to many other techniques, fluorescence resonance energy transfer (FRET), an inexpensive and very sensitive method, has been used in molecule imaging and glucose test. [14-16] It is a distance-dependent energy transfer from a fluorophore donor (D) to a fluorophore acceptor (A) in a nonradioactive process. When the distance of the two fluorophores is very close ( $<10$  nm), the excited D would transfer some of its energy to excite A that then emits light at a longer wavelength. [17] Using FRET technique for detecting the competitive reactions of glucose and other polysaccharide, such as dextran, to Concanavalin A (Con A), a protein, may result in accurate and convenient measures. [18-20] However, fluorophores/organic dyes used in FRET pair are subject to low fluorescent intensity, and poor signal responses influenced by the decay of chromophores and external environment. [21] Fluorescence nanostructures have been recognized as

excellent materials used in FRET sensor due to their photo-stability and narrow emission peaks. [22] We developed a nanostructured glucose biosensor by using fluorescence resonance energy transfer (FRET) technique which was able to be incorporated into hydrogel-based contact lens for measuring low concentration of glucose directly. [23-24] While, most reported FRET sensors have an inversely proportional relationship between the ratio of the fluorescence intensity of the donor to that of the acceptor ( $I_D/I_A$ ) and the amount of the targeted molecules because the rate constant of the energy transfer,  $k_{FRET}$ , decreases while the distance between the FRET pair increases. Consequently, most reported FRET sensors have significant measurement errors when detecting the increase of concentration of the targeted molecules because of the low fluorescence signal-to-noise ratio.

Quite recently, fluorescent quenching-based assay in which the donor fluorescence could be quenched by the acceptor without target analytes has shown significant advantages in biosensing, as it allows the restored fluorescence signal proportional response to the concentration of target analytes and lower background fluorescence. [16, 25] Consequently, a new nanostructured sensor by applying FRET quenching mechanism was developed here to detect small concentration of tear glucose from very small volume of tear samples in a fast and accurate fashion.

Fig. 3.1 (a) displayed a FRET pair-labeled Concanavalin A (Con A), an enzyme with specific affinity to glucose. [18-20] The donor in this designed FRET transducer was made of quantum dots with an emission ( $\lambda_{em}$ ) in the visible range; the acceptor was dextran-bound malachite green (MG) which has an absorption at the same wavelength of the emission of the quantum dots. The emitted fluorescence of the quantum dots could be quenched by malachite green through the FRET mechanism. In the presence of glucose, the binding between Con A and dextran was out competed by the affinity of Con A for glucose. As a result, dextran-bound MG would not quench the fluorescence of quantum dots, and therefore fluorescence intensity was restored. The change in fluorescence intensity was correlated to the amount of glucose reacting with Con A.

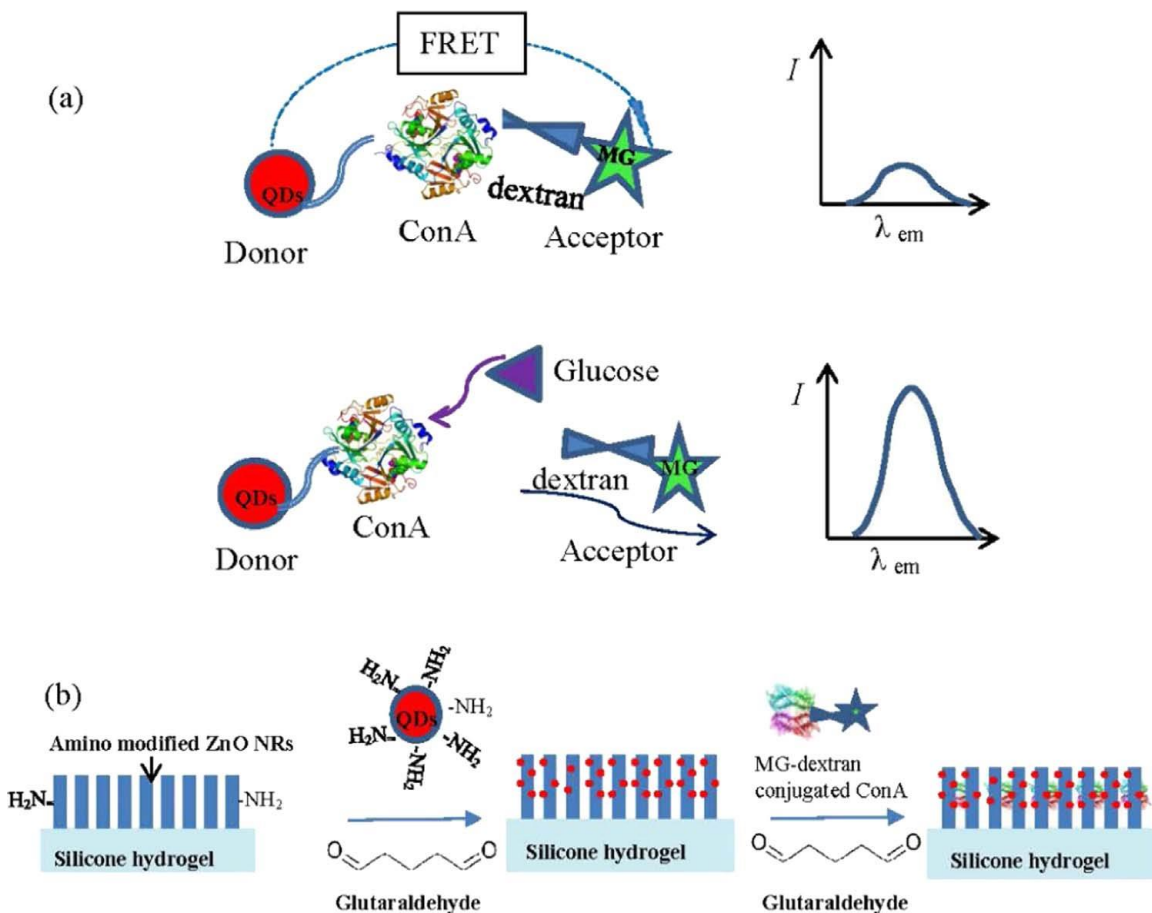


**Figure 3.1 (a) Illustration of the designed FRET transducer made of Con A-conjugating quantum dots (donor) and MG (acceptor) for detecting glucose. Competitive affinity for glucose displaces MG to restore the quenched fluorescence. (b) Immobilization of the nanostructured FRET transducers on ZnO nanorod array deposited on silicone hydrogel.**

In addition, we would like to further develop a dual-method for detecting glucose through both of fluorescence spectra and fluorescence images. To quickly and accurately detect the amount of glucose in a very small volume of tear sample by measuring the changes of fluorescence intensity of the sensor, the numerous nanostructured FRET sensors were immobilized on a single ZnO nanorod (NR) which have a high surface area to volume ratio as shown in Fig. 3.1 (b). This design allowed numerous FRET biosensors located at a nanoscale, and therefore, was able to amplify the resolution of the sensor. [26] Moreover, to quickly and accurately detect the amount of glucose in a very small volume of tear

sample by fluorescence images, the designed pattern made of ZnO NR array was utilized here which could be recognized easily through fluorescence image process. The pixel intensity values in a taken fluorescence image corresponding to the concentration of glucose could be calculated through an imaging process. Consequently, the patterned nanostructured FRET sensor on silicone hydrogel could realize the dual modulation for monitoring glucose level in tear samples through both of fluorescence spectrum and calibrated image pixel value.

## 3.2 Experimental

### 3.2.1 Synthesis of CdSe/ZnS Core Shell QDs

Cadmium selenium/zinc sulfide (CdSe/ZnS) core-shell quantum dots (QDs) were chosen as the donor of the FRET pair. The core-shell QDs were further functionalized with amine groups. [27] Selenium precursor prepared by dissolving 0.79g selenium powder in 10 mL trioctylphosphine (TOP). In one flask, 0.46g Cadmium Acetate dissolved in 10 mL TOP and heated to 100 °C under argon for 1 hour. Selenium precursor injected and allowed to stay at 80 °C. In another flask, a mixture of 20g TOPO, 10g hexadecylamine (HAD), and 5 mL TOP was heated 120 °C under vacuum for 2–3 hours. Mixture further heated to 340 °C under argon protection (slowly purge argon before heating). Once the mixture was heated to 340 °C, inject the precursor solution (20g TOPO, 10g hexadecylamine (HAD), and 5 mL TOP) inside the reaction. Temperature will decrease to 240 °C. Maintain the temperature for 5 min for 655 nm QDs. Remove heating mantle and cool reaction down to room temperature. Purify the CdSe QDs by adding excess methanol.

Mixture of hexadecylamine (HAD) (4g) and trioctylphosphine oxide (TOPO) (8g) were loaded into a 100 mL 3-neck flask and then degassed and heated to 180 °C. At 180 °C, the purified CdSe particles (50mg) was dispersed in 2 mL chloroform and added to solution. After the chloroform was completely pumped out, the flask was filled with argon gas. Temperature of reaction was then increased to 180–185 °C. Mixture of zinc acetate (54mg) and bis(trimethylsilyl)sulfide (0.05mL) was dissolved in 1.0 mL TOP and 1mL oleylamine. Then it was injected drop-wise for 5–10 min. After the injection, mixture was stirred for 1 hour at 180–185 °C. Solution was then cooled down to room temperature and the

particles were purified using chloroform and methanol. Collect and purify using 3 fold centrifugation and redispersion with methanol at 8000 rpm for 15 min.

Briefly, CdSe/ZnS (20 mg) dissolved in 3 mL of chloroform was mixed with a solution of cysteamine (Cys) hydrochloride (100 mg) dissolved in 5 mL of water. The solution was sonicated until the chloroform layer became clear. The remaining cysteamine was reacted with the addition in excess of 2-mercaptoethanol (20 mmol/L). CdSe/ZnS/Cys QDs were purified by threefold centrifugation (15 min at 10000 rpm) and rinsed with ethanol. Purified particles were re-dispersed in water.

### 3.2.2 Preparation of ZnO/Silicone Hydrogel

Silicone hydrogel with 150  $\mu\text{m}$  in thickness was produced using a photochemical process. [28] In a small 20mL glass bottle, add in sequence as N,N-dimethylacrylamide (0.86 mL), 3-[tris(trimethylsiloxy)silyl]propyl methacrylate (1.72 mL), macromer bis-alpha,omega-(methacryloxypropyl) polydimethylsiloxane (0.42 mL), 1-vinyl-2-pyrrolidinone (0.18 mL), ethylene glycol dimethacrylate (15  $\mu\text{L}$ ), and add 0.3 mL absolute ethanol for better dissolve the chemicals. Then introduce Nitrogen or Argon into the solution for about 10 min. Then add 8mg diphenyl(2,4,6-trimethylbenzoyl)phosphine oxide and add 0.1 mL absolute ethanol to dissolve the powder, add the solution into the Nitrogen degassed solution and keep on the Nitrogen for another 5 min. The solution is ready for ultraviolet to initiate the polymerization process. Set up the glass reactor by using a piece of glass and a piece of hard paper, exploit the transparent adhesive tape to rap the glass and the paper well, add 4 binder clips to hold the structure and add the solution into the gap, then put it into the ultraviolet oven for 50 min photo polymerization. The gel is washed with deionized water.

A well-aligned ZnO nanorod array was grown on hydrogel through modifying a previously reported method. [29] Briefly, zinc acetate dehydrate (0.01 M) was dissolved in 100 mL ethanol as a seed solution. The seed solution was dropped on a hydrogel substrate repeatedly followed by a heat treatment at 100  $^{\circ}\text{C}$  for 1 hour. The ZnO seed-coated hydrogel film was then immersed in a mixed solution of zinc nitrate hexahydrate (0.025 M) and hexamethylenetetramine (HMTA; 0.025 M) in 200 mL of distilled deionized water.

After heating at 90 °C for 3 h, the ZnO nanorod array was grown on the hydrogel. Samples were rinsed with distilled deionized water and dried at room temperature.

### 3.2.3 Fabrication Patterned QDs Decorated-ZnO NRs Array on Silicone Hydrogel

The patterned ZnO nanorod (NR) array was fabricated on the silicone hydrogel by a lift-off process (figure 3.2). The surface modification of the patterned ZnO NR array with amino groups was described as follows; the ZnO NR array on silicone hydrogel was immersed into 2 mL DMSO and 270  $\mu$ L 3-aminopropyltriethoxysilane (3-APS) suspension. After having reacted at 120 °C for 2 h, the ZnO hydrogel was taken out and washed with ethanol to remove unreacted compounds. [30-31] Please note that a small corner of the ZnO NR array on silicone hydrogel was not modified by 3-APS for further conjugation of FRET pair which would be used as a control area for imaging analysis.

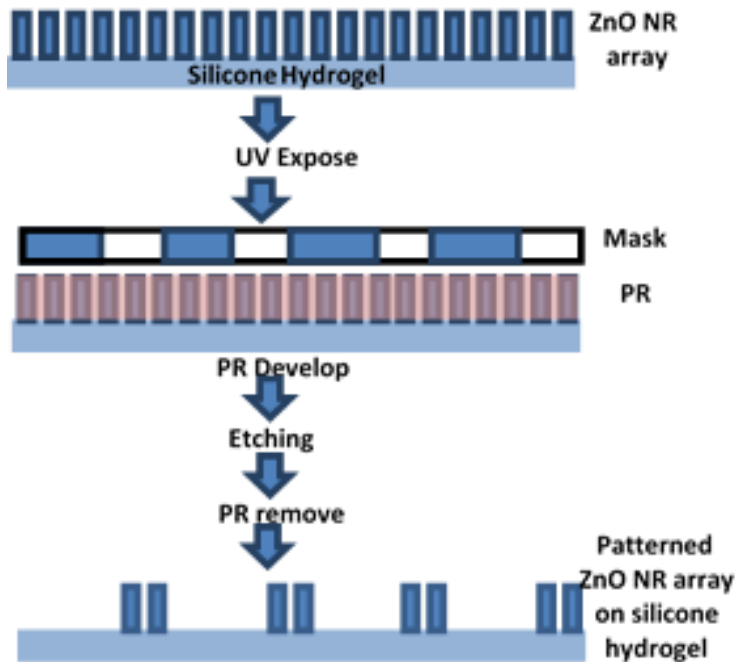


**Figure 3.2 A lift-off process for fabricating the patterned ZnO nanorod array on silicone hydrogel.**

The lift off process is described here. Photoresist (PR) (Shipley 1827) was deposited on the ZnO NR arrays by spin coating and the PR was UV (Karl Suss MJB3, Hg Arc Lamp)

irradiated over a patterned photomask for 30 seconds followed with post-baking. After the post-baking, the non-irradiated area was treated with a developer (Shipley Microposit MF-319) for 2 minutes treatment and rinsed with DI water. A wet chemical etching method was used to remove the ZnO area without PR by immersion in a diluted acetic acid solution. After washing with DI water, the remaining PR was washed away using ethanol. The final products were dried for further application.

Prior to coating QDs-based FRET sensor onto the surface of lithographically patterned ZnO NRs, glutaraldehyde first reacted with amino group modified ZnO NRs. Following that, ZnO NRs array on silicone hydrogel merged in a 20 mL CdSe/ZnS solution for 3 days at 4 °C, then washed with DI water to remove excess glutaraldehyde and CdSe/ZnS QDs. The obtained film was dried in the dark under vacuum to preserve sensing capabilities.

### 3.2.4 Synthesis of Malachite Green Dextran

Malachite green (MG) isothiocyanate and 70,000 MW amino-dextran purchased from Life Technologies (Burlington, Ontario, Canada) were mixed in a sodium bicarbonate buffer with 0.05 M at pH 9.6. [32] Successful conjugation of the isothiocyanate and dextran to form MG-dextran was verified by thin layer chromatography as shown in Fig. 3.3. Concentration of MG-dextran ( $\epsilon = 10^5 \text{ M}^{-1}\text{cm}^{-1}$  for malachite green at 621 nm) was determined by UV/Vis.

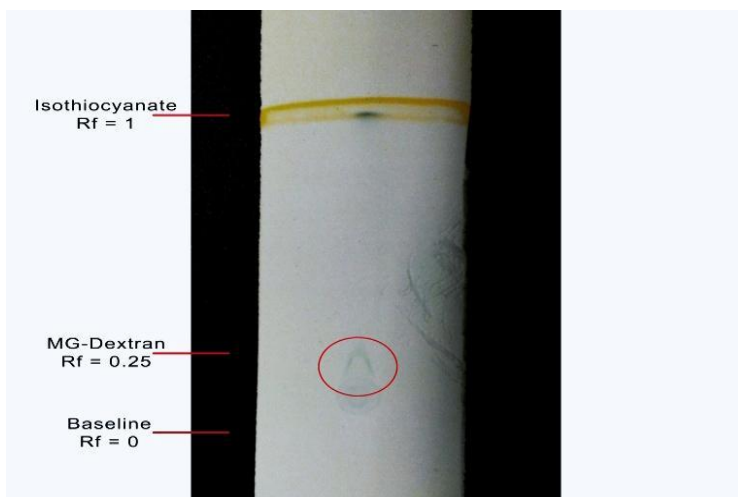


**Figure 3.3 Chromatography of the conjugation of MG to dextran.**



The isothiocyanate and MG-dextran had an  $R_f$  value of approximately 1.0 and less than 0.25, respectively. Concentration of MG-dextran ( $\epsilon=10^5 \text{ M}^{-1}\text{cm}^{-1}$  for malachite green at 621 nm) was determined by UV/Vis using the Beer-Lambert Law:

$$A = \epsilon lc$$

Where A is the absorbance,  $\epsilon$  the molar absorptivity, l the path length, and c the concentration (mol/L).

### 3.2.5 Synthesis and Optimization of FRET Sensor

Briefly, the dropwise application of Con A bonded with MG-dextran to the surface of QDs-decorated ZnO NRs with the aid of glutaraldehyde. The weight ratio of CdSe/ZnS/Cys QDs to Con A bonded with MG-dextran was 7:1. Non-conjugated Con A was rinsed off with DI water.

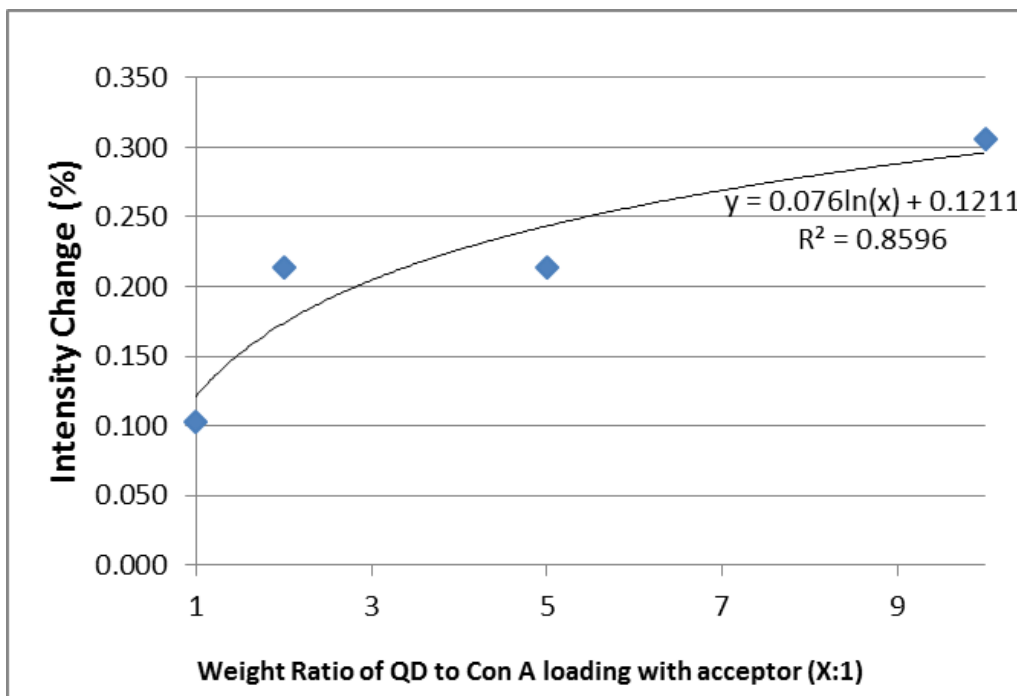


**Figure 3.4 FRET signal (fluorescence intensity) vs. the weight ratio of QDs to Con A loading with acceptor.**

The optimization ratio was described here. Con A protein was first loaded with MG-dextran at a molar ratio of 4:1 MG-dextran to Con A in water and agitated for 2 hours. Following that, glutaraldehyde was added to the above solution at 1:1 molar ratio and agitated for another 2 hours. The conjugation of MG-dextran to Con A was verified by the sodium dodecyl sulfate polyacrylamide gel electrophoresis (SDS-PAGE). To ensure maximum sensitivity in the presence of glucose, CdSe/ZnS quantum dots (QD) were conjugated to Con A bonded with MG-dextran at weight ratios of 10:1, 5:1, 3:1, 2:1, and 1:1, respectively, to determine the degree of quenching and when an increase in QD weight becomes negligible to the change in fluorescence. In this study, the weight ratio of the donor (QDs) to enzyme (Con A) bonded with the acceptor (MG-dextran) was maintained at 7:1. From the trend of the curve, it is going to reach a plateau after ratio of 9:1. After the ratio of 7:1, the FRET signal is not enhancing much. Considering the signal and economy, we chose the ratio of 7:1.

### 3.2.6 Sensor Measurement

10  $\mu\text{L}$  of glucose in different concentrations at pH=7.0, 0.03 mmol/L, 0.05 mmol/L, 0.2 mmol/L, 0.75 mmol/L, 1 mmol/L, 2 mmol/L, 3 mmol/L, were dropped on the patterned FRET sensors on silicone hydrogels with 30 seconds of interacting time. The fluorescence response of the patterned FRET sensors on silicone hydrogels to different concentrations of aqueous glucose were recorded by the fluorospectrometer at excitation wavelength ( $\lambda_{\text{ex}}$ ) =490 nm. At least five independent measures were conducted to measure the response of the sensor according to each glucose level. The standard deviation for each measured points was also calculated.

### 3.2.7 Fluorescence Sensor Signal Converting to Image Pixel Intensity

A USB powered portable digital microscope, MiScope, from Zarbeco (40X, pixels 640 $\times$ 480), was used to measure and digitally capture the fluorescence intensity of the 0.5 mg of glucose sensor conjugated onto ZnO NRs. 10  $\mu\text{L}$  of various concentrations of glucose was added; 0.03 mM, 0.05 mM, 0.2 mM, 0.75 mM, 1 mM, 2 mM, and 3 mM.

Glucose was allowed to react with the sensor for 5 min prior to fluorescent measurement. The donor molecule was excited with the UV light built into the MiScope.

The captured images were converted to RGB colors using Matlab as our previous reported results. [24] Both green and red channels were applied to record the pixel intensity pixel values. The values of pixel intensity of the patterned sensors responding to glucose amounts were calculated in comparison with that of the control areas where no FRET pair was conjugated. The recorded fluorescence images taken by the handheld fluorescence microscope could be converted to the value of pixel intensity through Matlab's imaging process. In this imaging conversion process, the image matrix of the control area were used to compare with that of sensing area of the FRET sensor to obtain the value of pixels intensity corresponding to the concentration of glucose. The captured FRET sensing image with pixels  $\sum XY$  is calibrated in comparison with the image of the control area (lowest fluorescence signal from substrate) with pixels  $\sum X'Y'$ . The calibrated pixel intensity ( $I_p$ ) generated from FRET sensors could be expressed as follow;

$$I_p = \sum I(X_i Y_i) - \sum I(X'_i Y'_i)$$

Where,  $i$  is the number of pixels in the chosen areas.

### 3.2.8 Cellular Viability

Cellular viability of the glucose biosensor was conducted in the Lab of Dr. David Litchfield in the Department of Biochemistry of the University of Western Ontario. UTA-06 human osteosarcoma cells were used in this work, which were derived from the human osteosarcoma cell line U2-OS. The cell line was a generous gift from Dr. Christoph Englert, Forschungszentrum Karlsruhe, Germany. This assay could provide a model to test the cytotoxicity of the sensor.

UTA-06 cells were cultured and grown under sterile conditions in Dulbecco's Modified Eagle Medium (DMEM) supplemented with 10% FBS and 100 units/mL penicillin and 100  $\mu\text{g}/\text{mL}$  streptomycin, kept at 37  $^{\circ}\text{C}$  with 5%  $\text{CO}_2$ . 250 000 cells were transferred into each well of a 24 well culture plate and incubated overnight to ensure adhesion to the plate.

Various amounts of patterned nanostructured FRET sensors (QDs-based FERT sensors assembled on ZnO NRs), i.e. 0.03 mg, 0.07 mg, 0.10 mg, 0.15 mg, deposited on the surface of silicone hydrogels with dimensions 1 cm × 1 cm. Samples were sterilized under UV for 10 minutes.

In quadruplicate, the UTA-06 cells were cultured with the above sensors deposited on hydrogel samples for 24 hours. After the incubation period the sensor samples were removed, and a MTT cell viability assay was performed. The absorbance of the plates was measured at  $\lambda_{em}=490$  nm, and the relative cellular viability was calculated.

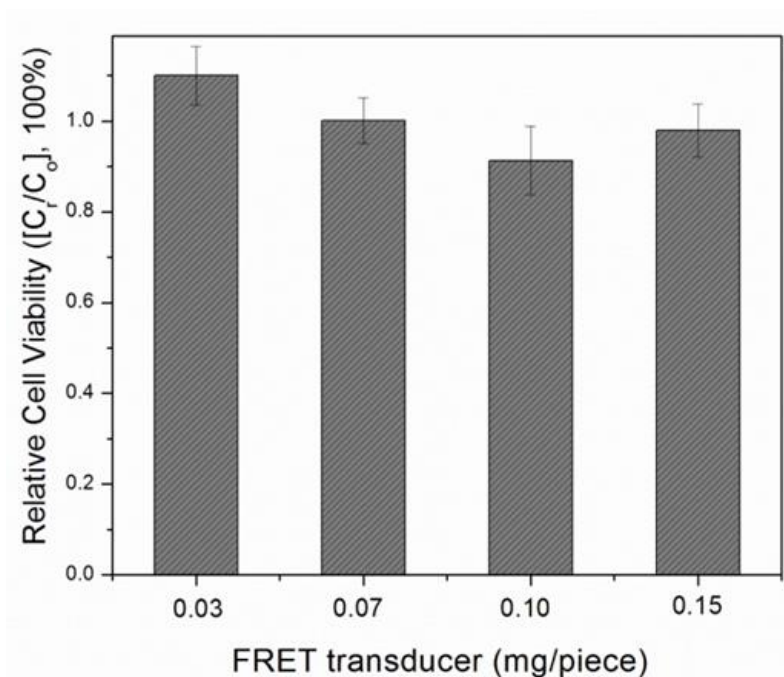


**Figure 3.5 Relative cell viability vs. the amount of the patterned FRET sensors deposited on silicone hydrogel.**

Figure 3.5 indicates relative cell viability ( $[C_r/C_0] 100\%$ ) vs. the amount of patterned FRET sensors on silicone hydrogel. The relative cell viabilities (%) of UTA-06 human osteosarcoma cells treated by patterned nanostructured FRET sensors are correspondingly normalized to the control sample. Here,  $C_0$  is the viable cell numbers of the control sample (bare silicone hydrogel), and  $C_r$  the viable cell numbers treated with the patterned FRET sensors. The error bars were the calculated standard deviation.

### 3.2.9 Animal Tear Test

This part was cooperated with Dr James Melling lab (Kinesiology, UWO). Following the positive results of cytotoxicity (figure 3.5), we conducted the animal test to evaluate the response of designed sensor to tear glucose. Four male Sprague-Dawley rats (Charles River Laboratories, St. Constant, QC, Canada) were housed in a 12-h light/dark cycle room with humidity (50%) and temperature (21.5 °C) kept constant. Rats were given water and chow ad libitum and made diabetic with streptozotocin (STZ; Sigma-Aldrich, Oakville, ON, Canada). Intraperitoneal injections of STZ (20 mg/kg) dissolved in a citrate buffer (0.1 M, pH 4.5) were given over five consecutive days. Following the confirmation of diabetes (two blood glucose readings larger than 18 mmol/L) subcutaneous insulin pellets were implanted in the abdominal region of rats. Rats were anesthetized with isoflurane for ease of application of the sensors to their eyes. Tear fluid was collected from the ocular surface with a 1 µL glass capillary tube (P1424 SIGMA). 2 µL of rat tear sample were collected from each male Sprague-Dawley rats. All samples were diluted by PBS (5 µL) with pH=7.0 into 7 µL total volume. Diluted tear samples (2 µL) were then dropped on the FRET sensors. The standard deviation for each measured points was also calculated. Fluorospectrometry was used to measure the fluorescence intensity of quantum dots (donor) after tear samples interact with FRET sensor for 30 seconds. A blood sample was taken from the saphenous vein concurrently with the application of the sensor for blood glucose concentration (Freestyle Lite Blood Glucose Monitoring System, Abbott Diabetes Care Inc., Mississauga, Ontario). Ethics approval was obtained through the University of Western Ontario Research Ethics Board, in accordance with Canadian Council on Animal Care guidelines.

## 3.3 Results and Discussion

### 3.3.1 Characterization of Nanostructured FRET Sensor Deposited on Silicone Hydrogel

The ZnO NR array pattern was fabricated on the silicone hydrogel using it as a substrate by a lift-off process shown in figure 3.2. SEM was used to study the patterned ZnO NR array deposited on the synthetic silicone hydrogel as shown in Fig. 3.6 (a) and (b). The

designed pattern is made for easy identification of the captured fluorescence images to calibrate the pixel intensity depending on the concentration of glucose.

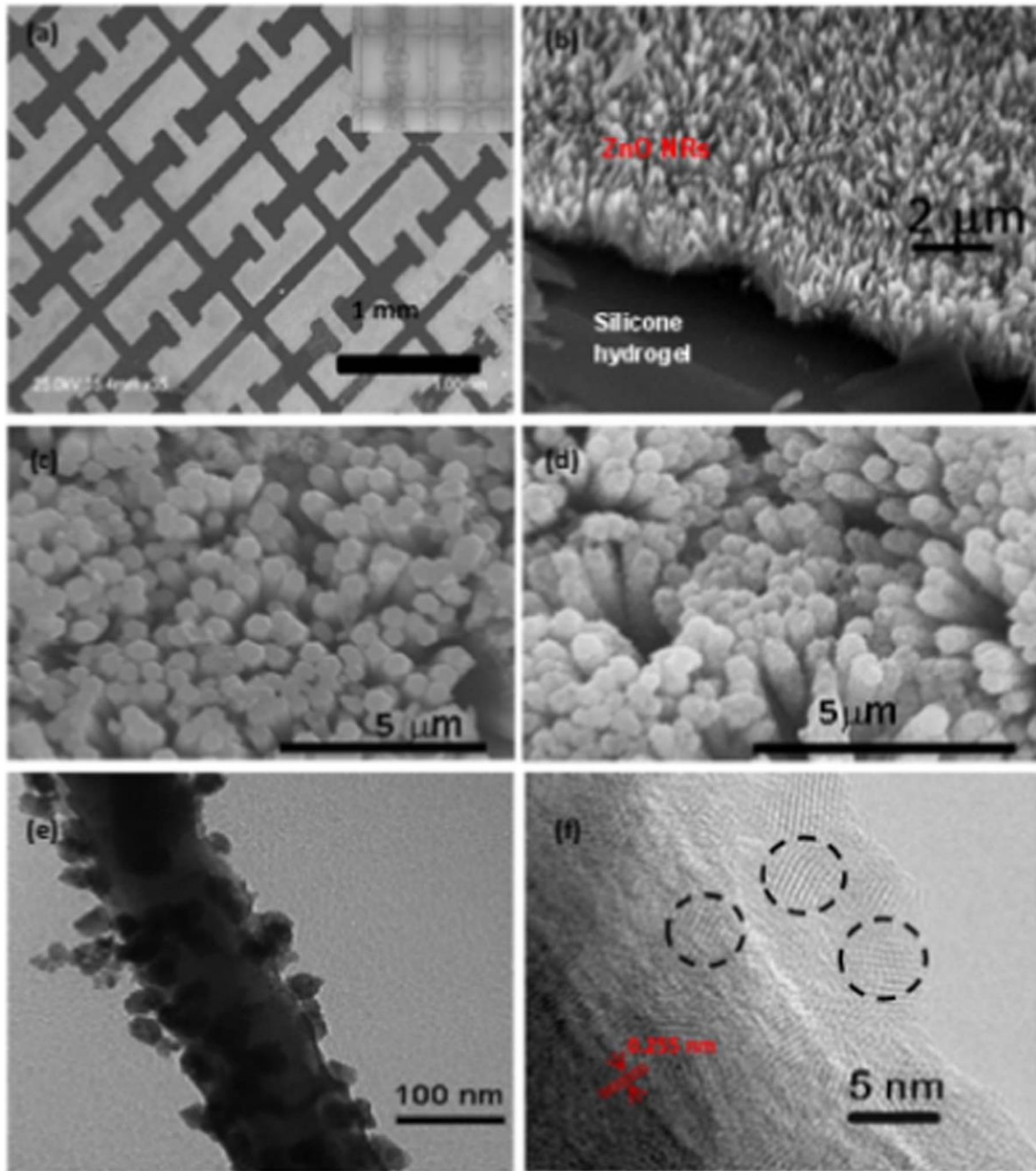


**Figure 3.6** Characterization of nanomaterials by electron microscopes. (a) SEM micrographs of patterned ZnO NRs deposited on a silicone hydrogel. The small inset is the photomask. (b) The magnified SEM micrograph of ZnO nanorod array deposited on a silicone hydrogel. (c) SEM micrograph of ZnO nanorods. (d) SEM

micrograph of QDs coated ZnO nanorods. (e) TEM micrograph of QDs coated ZnO nanorods. (f) HRTEM of CdSe/ZnS QDs.

The patterned ZnO NR arrays grown on the synthetic silicone hydrogel were modified with amino groups ( $-\text{NH}_2$ ) to immobilize CdSe/ZnS QDs onto the ZnO NRs. Glutaraldehyde first reacted with  $-\text{NH}_2$  functionalized ZnO NRs following the linkage formed by the reaction of glutaraldehyde with the amino group modified QDs. In Fig. 3.6 (c), the hexagonal rods with a smooth surface were grown on the silicone hydrogel. The average dimensions of the ZnO NRs are estimated at  $120 \pm 5$  nm in diameter and  $2.00 \pm 0.05$   $\mu\text{m}$  in length. The rough surface of the NRs could be observed when decorated with QDs, as shown in Fig. 3.6 (d). Furthermore, the TEM micrograph (Fig. 3.6 (e)) clearly shows the QDs are decorated on the ZnO NRs. The HRTEM micrograph (Fig. 3.6 (f)) further indicates the core-shell CdSe/ZnS QDs with  $5 \pm 2$  nm in diameter are decorated on the highly crystalline ZnO NRs with a lattice fringe of 0.255 nm, which corresponds to the (0002) lattice planes. [33]

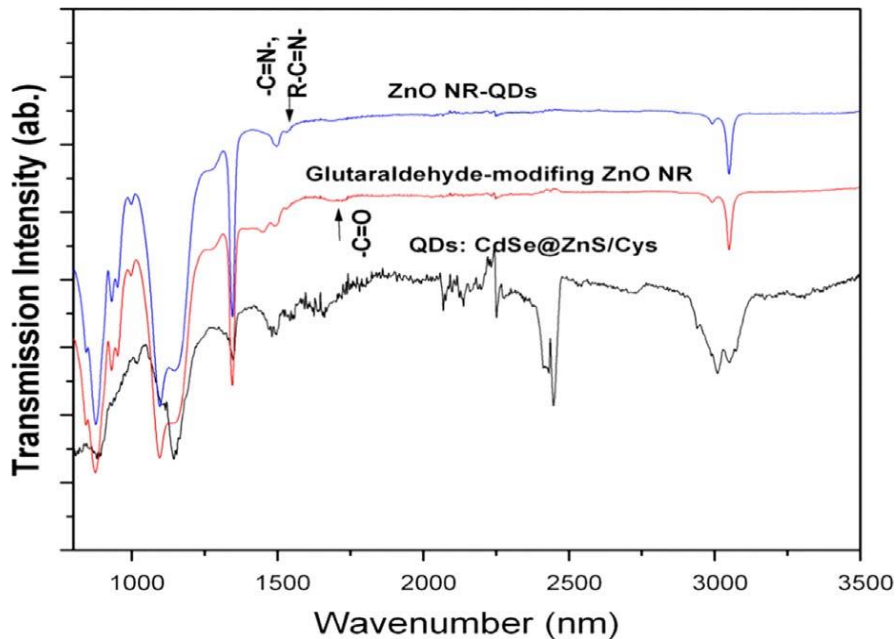


**Figure 3.7** FTIR spectra of the cysteamine (Cys) modified QDs and ZnO nanorod (NR), and the hybrid ZnO NR coated with QDs (ZnO NR-QDs).

Fig. 3.7 shows the FTIR spectra of the ZnO NRs with surface modification, amino modified QDs, and the hybrid ZnO NRs coated with QDs (ZnO NR-QDs). All samples demonstrate the typical  $-CH$  stretch, and  $-CH_2$  stretch in the FTIR spectra. The  $-C=O$  stretch at  $1750\text{ cm}^{-1}$  is observed when glutaraldehyde was modified onto ZnO NRs, while this stretch does not show up to sample of ZnO NR-QDs. The  $-C=N$  stretch of the imine group, and  $-C=N-R$  located around  $1620\text{ cm}^{-1}$  appears in the spectrum of ZnO NRs-QDs. Thus, two carbon-nitrogen double bonds ( $C=N$ ), i.e. Schiff bases, were formed to allow QDs to coat on the ZnO NRs through the linkage of glutaraldehyde.

### 3.3.2 Fluorescence Intensity of the FRET Sensor as a Function of Glucose Level in Aqueous

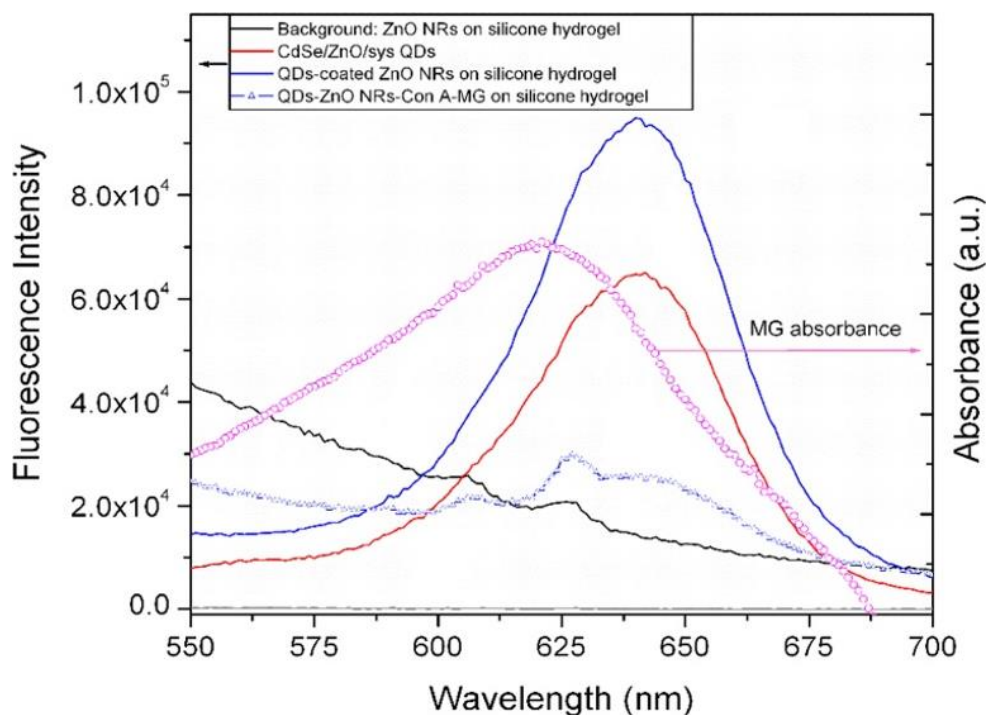


**Figure 3.8 Photoluminescence of ZnO NR arrays on silicone hydrogel with/without QDs, and QDs-based fret sensors, and the UV-vis absorption of MG.**

The optimization of the weight ratio of the donor (QDs) to enzyme (Con A) bonded with the acceptor (MG-dextran) was determined at 7:1 as shown in the figure 3.4. The photoluminescence (PL) properties of the nanostructured FRET transducer-coating ZnO NR array (i.e. the patterned FRET sensor), the nanostructured donor of the sensor (i.e.



CdSe/ZnS QDs) were studied by a fluorospectrometer in the range of 550–700 nm. In Fig. 3.8, the photoluminescence (PL) spectrum of ZnO in the visible range is observed with centering at 628 nm.

The maximum intensity of PL spectrum of CdSe/ZnS QDs is observed at 648 nm. The PL spectrum of ZnO NR-QDs is dominated by the decorated QDs because of the large amount of QDs on a single ZnO NR, centered at 648 nm. When the acceptor of FRET sensor, MG-dextran, bound to QDs through Con A, the PL peak of ZnO NRs could be observed with centering at 652 nm; whereas the PL peak at 652 nm attributed to the donor (QDs) of the patterned FRET sensor is significantly suppressed. The slight redshift of the emission of QDs may be caused by the surface conjugation of Con A and the acceptor of MG-dextran. MG quenches the fluorescence signal of QDs through the FRET mechanism because of its broad absorbance around 655 nm.

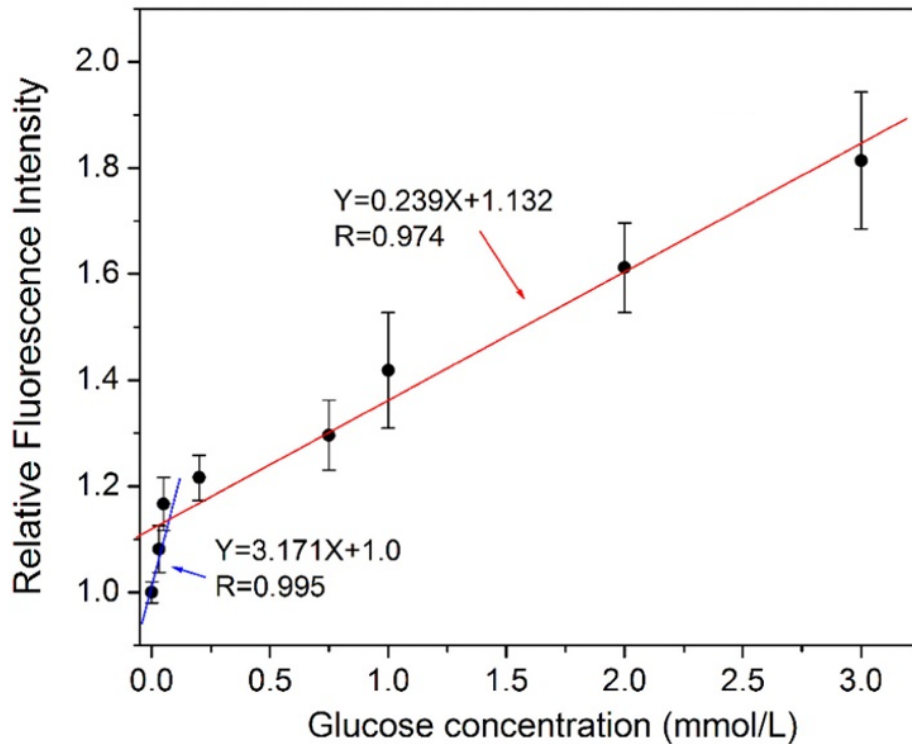


**Figure 3.9 A linear relationship between fluorescence intensity of the designed sensor and the concentration of glucose.**

10  $\mu\text{L}$  of aqueous glucose of various concentrations were dropped onto the patterned FRET sensors on silicone hydrogels with 30 seconds of interaction time. The fluorescence measurements were determined by fluorospectrometry. As shown in the illustration of Fig. 3.1, the fluorescence emission of the donor (CdSe/ZnS QDs) of the designed FRET sensor was quenched by the acceptor MG. In the presence of glucose, the quenched fluorescence of QDs is restored after the addition of glucose and the fluorescence emission of the patterned FRET sensors centered at 652 nm increases with increasing aqueous glucose. The FRET emission ( $\lambda_{\text{em}}=652$  nm) as a function of the concentration of aqueous glucose were measured. The relative fluorescence intensity ( $I_{\text{re}}$ ) is calculated by using the equation below;

$$I_{\text{re}} = \frac{I'}{I_0}$$

Where,  $I'$  is the restored intensity according to a glucose level,  $I_0$  is the intensity of the sensor without glucose. Fig. 3.9 shows that two linear regions; (1) from 0.03 mM to 3 mM; and (2) from 0 mM to 0.03 mM. It is noted that the concentration of glucose in the range of 0.03 mM–3 mM could cover the tear glucose level of both the diabetes and healthy subject. The linear relationship between relative fluorescence intensity and glucose concentration in the range of 0.03 mM–3 mM could be expressed as follows;

$$Y = 0.239X + 1.132$$

### 3.3.3 Pixel Intensity Value of Fluorescence Image of FRET Sensor as a Function of Glucose Level in Aqueous

The fluorescence images of the patterned FRET sensors on silicone hydrogel interacting 10  $\mu\text{L}$  of various concentrations of aqueous glucose were monitored by a handheld fluorescence microscope. Fig. 3.10 (a) shows two fluorescence images of the patterned FRET sensor interacting with two samples of aqueous glucose; 0.04 mmol/L (sample A) and 0.4 mmol/L (sample B). The recorded images by the handheld microscope were converted to the readable signal through Matlab's imaging process. The pixel intensity was calibrated using MatLab to plot the intensity as a function of aqueous glucose concentration. The calibrated pixel intensities of the patterned FRET sensor is clearly

increasing as glucose increases from 0.03 mmol/L to 0.6 mmol/L as shown in Fig. 3.10 (b). The difference in pixel intensity value does not change significantly when the concentration of glucose is beyond 0.6 mmol/L. It is expected that a more advanced fluorescence microscope would be able to overcome the limit.

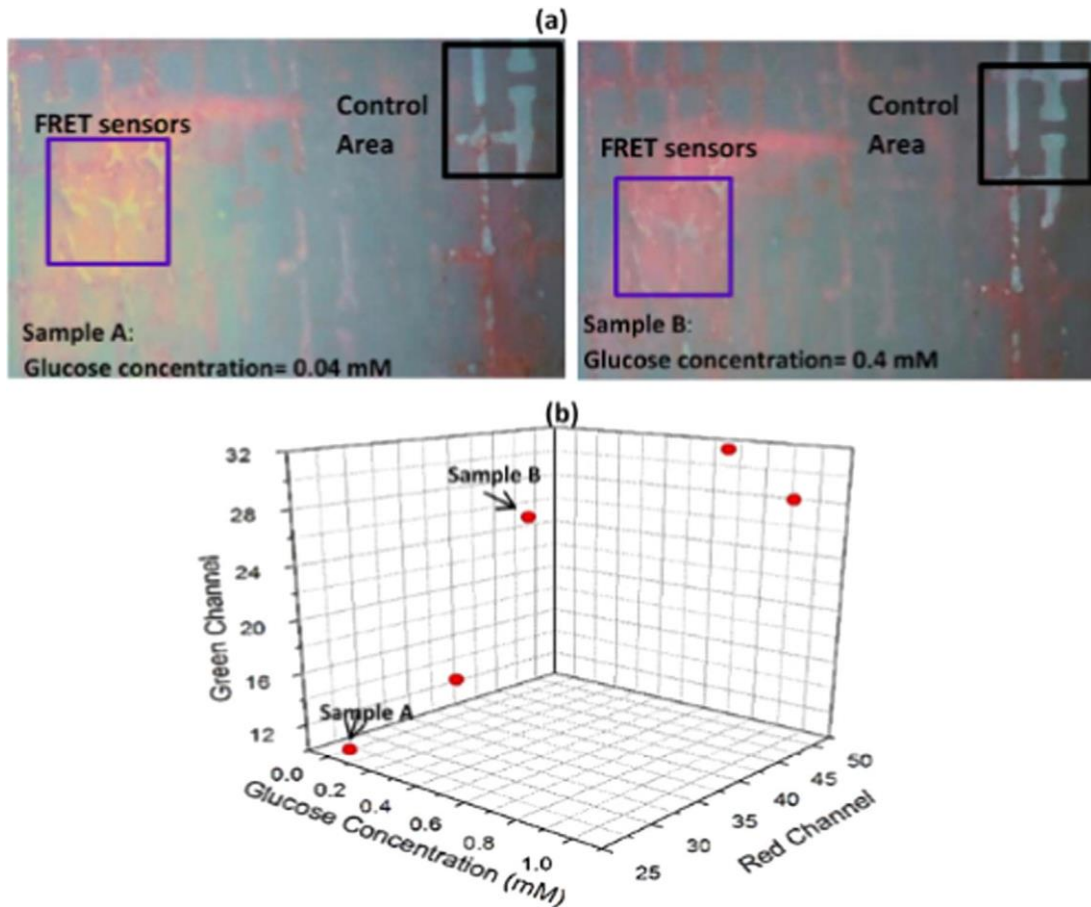


**Figure 3.10** Fluorescence images of the patterned FRET sensor on silicone hydrogel and the relative pixel intensities of the sensors responding to the concentrations of glucose. (a) Fluorescence images of the patterned FRET sensor to aqueous glucose with 0.04 mmol/L and 0.4 mmol/L, respectively. (b) The relative pixel intensities of the sensors vs. the concentration of aqueous glucose.

### 3.3.4 Response of Designed FRET Sensor to 2 $\mu$ L Rat Tears

The concentrations of blood glucose of the rats used in the current study were maintained in a range similar to patients with ‘poorly’ managed Type 1 diabetes. [34] Specifically, rats

were representative of low to moderate hyperglycemic patients with Type 1 diabetes mellitus under conventional insulin therapy. [35] Typically blood glucose concentrations in patient populations with type 1 diabetes fluctuate considerably; therefore, four rats with a range of blood glucose concentrations were utilized in the experiment to demonstrate.

The photoluminescence spectra of the patterned FRET sensor deposited on silicone hydrogels corresponding to the diluted rats' tear samples (2 $\mu$ L) could be seen in Figure 3.11 after interacting with rat tears.

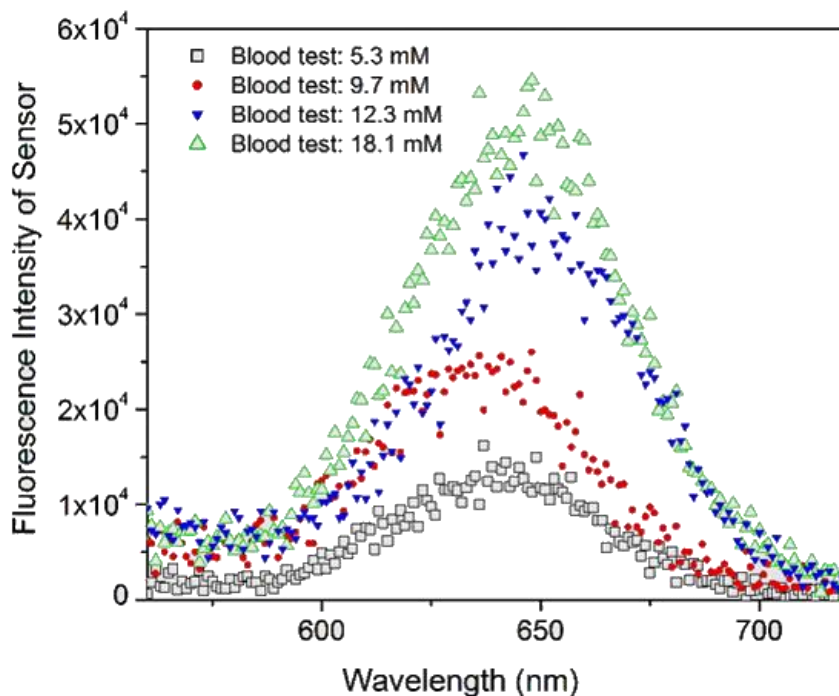


**Figure 3.11 Photoluminescence spectra of designed sensor responding to tear samples from rats with different glucose level in blood.**

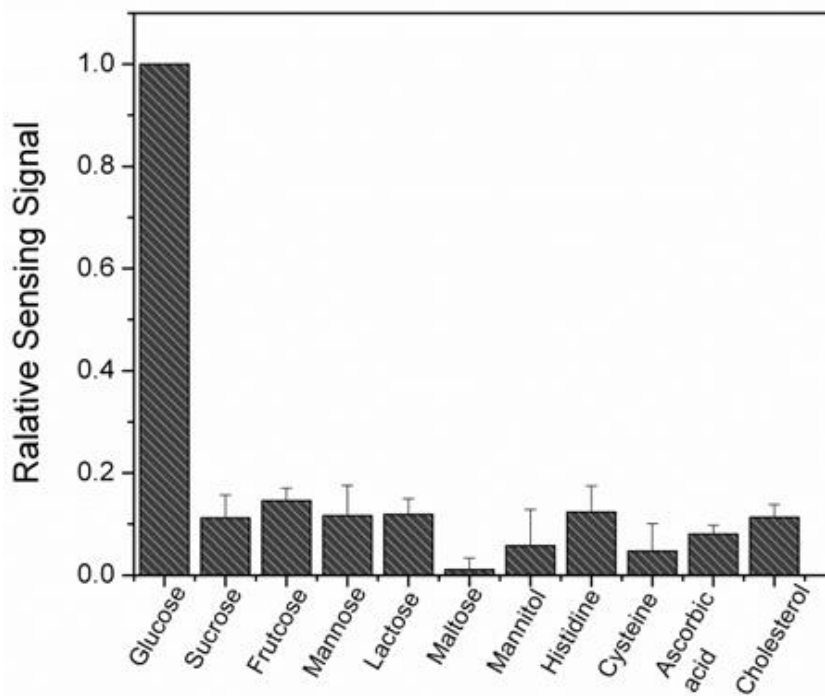
The rats' tear samples were diluted 3.5 times. The patterned FRET sensor deposited on silicone hydrogels were used to measure the 2  $\mu$ L diluted rats' tear samples. The PL spectra of the sensor corresponding to glucose in tears are shown in Fig. 3.11 after interacting with rat tears. The detected glucose level in rats' tear samples were calculated by using Eq.  $Y=0.239X+1.132$ . Meanwhile, the blood glucose levels to the four rats were measured by Freestyle Lite Blood Glucose Monitoring System, Abbott Diabetes Care Inc.

Table 3.1 shows the glucose level in rats' tear samples measured by the nanostructured FRET sensor as compared to the blood glucose level of the four rats. The small value of the calculated standard deviation of the measurement indicates the repeatability of the measure.

**Table 3.1 Glucose level in rats' tear samples measured by the nanostructured FRET sensor as compared to the blood glucose level of the four rats.**

Blood glucose (mmol/L)	Tear glucose (mmol/L)
5.3	0.14±0.03
9.7	0.42±0.04
12.3	0.95±0.05
18.2	1.28±0.05

### 3.3.5 Selectivity of Designed FRET Sensor



**Figure 3.12 Relative sensing signal ( $I_{\text{test sample}}/I_{\text{glucose}}$ ) to different biomolecules.**

The selectivity of the designed sensor towards glucose detection was further verified. 1 mM glucose in PBS solution and some possible interfering molecules, sucrose, fructose, mannose, lactose, maltose, mannitol, histidine, cysteine, ascorbic acid, and cholesterol at 1 mM, were tested by the designed sensor, respectively. The relative sensing signal is referring to the normalization of the fluorescence intensity of the designed sensor responding to 1mM test sample to the sensor's fluorescence intensity in the presence of 1 mM glucose ( $I_{\text{test sample}}/I_{\text{glucose}}$ ). Figure 3.12 suggests that the designed sensor has a high selectivity to glucose.

### 3.4 Conclusion

In summary, the patterned nanostructured FRET sensor deposited on the synthesized silicone hydrogel were designed for monitoring glucose in tears. The emission ( $\lambda_{\text{em}}$ )=655 nm of the CdSe/ZnS QDs could be quenched by the acceptor of dextran-bound malachite green (MG) which has an absorption at the same wavelength of the emission of the QDs. The dual modulation of detection is realized by depositing CdSe/ZnO QDs-based FRET sensors on the ZnO nanorod array. When the interaction time was maintained at 30 seconds, a linear relationship of the photoluminescence of the patterned nanostructured FRET sensor to the concentration of glucose from 0.03 mmol/L to 3 mmol/L is observed. It is noted that the tear glucose of diabetics is  $>0.35 \pm 0.04$  mmol/L, and the average value of tear glucose for healthy subjects is around  $0.16 \pm 0.03$  mmol/L. Meanwhile, the calibrated values of pixel intensities are increasing with increasing glucose from 0.03 mmol/L to 0.6 mmol/L. Four rats with a range of blood glucose concentrations were utilized in the experiment. The results clearly show that the patterned nanostructured FRET sensor is capable of quickly monitoring tear glucose in an extremely small drop (2  $\mu\text{L}$ ) of tear sample. Consequently, our designed nanostructured FRET glucose sensor is suitable for monitoring tear glucose in a non-invasive and quick manner.

### 3.5 References

- [1] Yoshiki Ohashi; Murat Dogru; Kazuo Tsubota, Laboratory findings in tear fluid analysis. *Clinica Chimica Acta* **2006**, 369 (1), 17-28.

- [2] Hyun Joo An; Milady Ninonuevo; Jennifer Aguilan; Hao Liu; Carlito B. Lebrilla; Lenio S. Alvarenga; Mark J. Mannis, Glycomics Analyses of Tear Fluid for the Diagnostic Detection of Ocular Rosacea. *Journal of Proteome Research* **2005**, 4 (6), 1981-1987.
- [3] Frederick Ridley, The Intraocular Pressure and Drainage of the Aqueous Humour. *British Journal of Experimental Pathology* **1930**, 11 (4), 217-240.
- [4] D Michail; P Vancea; N Zolog, Sur l'elimination lacrymale du glucose chez les diabetiques. *CR Soc. Biol., Paris* **1937**, 125, 1095.
- [5] D K Sen; G S Sarin, Tear glucose levels in normal people and in diabetic patients. *British Journal of Ophthalmology* **1980**, 64 (9), 693-695.
- [6] J. G. Lewis; P. J. Stephens, Tear Glucose in Diabetics. *British Journal of Ophthalmology* **1958**, 42 (12), 754-758.
- [7] Antonio R. Gasset; Lewis E. Braverman; Marie C. Fleming; Ronald A. Arky; Barry R. Alter, Tear Glucose Detection of Hyperglycemia. *American Journal of Ophthalmology* **1968**, 65 (3), 414-420.
- [8] K Motoji, The glucose content of tear fluid in normal and diabetic subjects. *Japanese Journal of Clinical Ophthalmology* **1971**, 25, 1945-50.
- [9] Jennifer D. Lane; David M. Krumholz; Robert A. Sack; Carol Morris, Tear Glucose Dynamics in Diabetes Mellitus. *Current Eye Research* **2006**, 31 (11), 895-901.
- [10] Michael S. Boyne; David M. Silver; Joy Kaplan; Christopher D. Saudek, Timing of Changes in Interstitial and Venous Blood Glucose Measured With a Continuous Subcutaneous Glucose Sensor. *Diabetes* **2003**, 52 (11), 2790-2794.
- [11] Volker Lodwig; Lutz Heinemann, Continuous Glucose Monitoring with Glucose Sensors: Calibration and Assessment Criteria. *Diabetes Technology & Therapeutics* **2003**, 5 (4), 572-586.
- [12] Peter H. Kvist; Henrik E. Jensen, Recent Advances in Continuous Glucose Monitoring: Biocompatibility of Glucose Sensors for Implantation in Subcutis. *Journal of Diabetes Science and Technology* **2007**, 1 (5), 746-752.
- [13] Clare O'Donnell; Nathan Efron; Andrew J. M. Boulton, A prospective study of contact lens wear in diabetes mellitus. *Ophthalmic and Physiological Optics* **2001**, 21 (2), 127-138.
- [14] Wayne March; Bill Long; Wolfgang Hofmann; Deborah Keys; Curt McKenney, Safety of Contact Lenses in Patients with Diabetes. *Diabetes Technology & Therapeutics* **2004**, 6 (1), 49-52.
- [15] Th Forster, 10th Spiers Memorial Lecture. Transfer mechanisms of electronic excitation. *Discussions of the Faraday Society* **1959**, 27 (0), 7-17.

- [16] Sanjay Tyagi; Salvatore A. E. Marras; Fred Russell Kramer, Wavelength-shifting molecular beacons. *Nature Biotechnology* **2000**, *18* (11), 1191-1196.
- [17] Elizabeth A. Moschou; Bethel V. Sharma; Sapna K. Deo; Sylvia Daunert, Fluorescence Glucose Detection: Advances Toward the Ideal *In Vivo* Biosensor. *Journal of Fluorescence* **2004**, *14* (5), 535-547.
- [18] Ryan J. Russell; Michael V. Pishko; Christopher C. Geffrides; Michael J. McShane; Gerard L. Coté A Fluorescence-Based Glucose Biosensor Using Concanavalin A and Dextran Encapsulated in a Poly(ethylene glycol) Hydrogel. *Analytical Chemistry* **1999**, *71* (15), 3126-3132.
- [19] John C. Pickup; Faeiza Hussain; Nicholas D. Evans; Olaf J. Rolinski; David J. S. Birch, Fluorescence-based glucose sensors. *Biosensors and Bioelectronics* **2005**, *20* (12), 2555-2565.
- [20] Ralph Ballerstadt; Colton Evans; Roger McNichols; Ashok Gowda, Concanavalin A for *in vivo* glucose sensing: A biotoxicity review. *Biosensors and Bioelectronics* **2006**, *22* (2), 275-284.
- [21] Ute Resch-Genger; Markus Grabolle; Sara Cavaliere-Jaricot; Roland Nitschke; Thomas Nann, Quantum dots versus organic dyes as fluorescent labels. *Nature Methods* **2008**, *5* (9), 763-775.
- [22] Timothy Jamieson; Raheleh Bakhshi; Daniela Petrova; Rachael Pocock; Mo Imani; Alexander M. Seifalian, Biological applications of quantum dots. *Biomaterials* **2007**, *28* (31), 4717-4732.
- [23] Jin Zhang; William Hodge; Cindy Hutnick; Xianbin Wang, Noninvasive Diagnostic Devices for Diabetes through Measuring Tear Glucose. *Journal of Diabetes Science and Technology* **2011**, *5* (1), 166-172.
- [24] Jin Zhang; Xianbin Wang; Longyan Chen; Jiaxin Li; Kevin Luzak, Harnessing a Nanostructured Fluorescence Energy Transfer Sensor for Quick Detection of Extremely Small Amounts of Glucose. *Journal of Diabetes Science and Technology* **2013**, *7* (1), 45-52.
- [25] Longyan Chen; Yige Bao; John Denstedt; Jin Zhang, Nanostructured bioluminescent sensor for rapidly detecting thrombin. *Biosensors and Bioelectronics* **2016**, *77*, 83-89.
- [26] Yi Chen; Wai Hei Tse; Longyan Chen; Jin Zhang, Ag nanoparticles-decorated ZnO nanorod array on a mechanical flexible substrate with enhanced optical and antimicrobial properties. *Nanoscale Research Letters* **2015**, *10* (1), 1-8.
- [27] Lee Chang-Moon; Jang DooRye; Cheong Su-Jin; Kim Eun-Mi; Jeong Min-Hee; Kim Sun-Hee; Kim Dong Wook; Lim Seok Tae; Sohn Myung-Hee; Jeong Hwan-Jeong,



Surface engineering of quantum dots for *in vivo* imaging. *Nanotechnology* **2010**, *21* (28), 285102.

[28] Jinah Kim; Anthony Conway; Anuj Chauhan, Extended delivery of ophthalmic drugs by silicone hydrogel contact lenses. *Biomaterials* **2008**, *29* (14), 2259-2269.

[29] Yi Chen; Xiaoxuan Guo; Wai Hei Tse; Tsun-Kong Sham; Jin Zhang, Magnetic anisotropy induced in NiCo granular nanostructures by ZnO nanorods deposited on a polymer substrate. *RSC Advances* **2014**, *4* (89), 47987-47991.

[30] Jin Young Kim; Frank E. Osterloh, ZnO–CdSe Nanoparticle Clusters as Directional Photoemitters with Tunable Wavelength. *Journal of the American Chemical Society* **2005**, *127* (29), 10152-10153.

[31] Daniele Costenaro; Fabio Carniato; Giorgio Gatti; Chiara Bisio; Leonardo Marchese, On the Physico-Chemical Properties of ZnO Nanosheets Modified with Luminescent CdTe Nanocrystals. *The Journal of Physical Chemistry C* **2011**, *115* (51), 25257-25265.

[32] Lydia J. McCartney; John C. Pickup; Olaf J. Rolinski; David J. S. Birch, Near-Infrared Fluorescence Lifetime Assay for Serum Glucose Based on Allophycocyanin-Labeled Concanavalin A. *Analytical Biochemistry* **2001**, *292* (2), 216-221.

[33] Chongqi Chen; Yuanhui Zheng; Yingying Zhan; Xingyi Lin; Qi Zheng; Kemei Wei, Enhanced Raman scattering and photocatalytic activity of Ag/ZnO heterojunction nanocrystals. *Dalton Transactions* **2011**, *40* (37), 9566-9570.

[34] David M. Nathan; for the DCCT/EDIC Research Group, The Diabetes Control and Complications Trial/Epidemiology of Diabetes Interventions and Complications Study at 30 Years: Overview. *Diabetes Care* **2014**, *37* (1), 9-16.

[35] C. W. J. Melling; K. N. Gris ę C. P. Hasilo; B. Fier; K. J. Milne; M. Karmazyn; E. G. Noble, A model of poorly controlled type 1 diabetes mellitus and its treatment with aerobic exercise training. *Diabetes and Metabolism* **2013**, *39* (3), 226-235.

## Chapter 4

Part of this chapter reuses part of the published journal paper (RSC Advances 2017, 7 (43), 26770-26775.). Permission is in Appendix 14.

### 4 Development of Upconversion NaGdF<sub>4</sub>: Yb, Er Glucose Biosensor

#### 4.1 Introduction

In this chapter, a one-pot process was developed to produce NaGdF<sub>4</sub>: Yb, Er upconversion nanocubes (UCNCs) with amine group surface modifications. The amine groups facilitated further surface conjugation of upconverting nanomaterials. After sufficient conjugation of the amine groups and suitable PEGylation, the adsorption of other proteins could be effectively avoided. The upconverting nanomaterials were used to fabricate an upconverting nanostructured glucose biosensor. The photoluminescence and magnetic properties of the amine modified upconversion nanocubes (UCNCs) were investigated. The emissions of green light at 541 nm and red light at 655 nm were observed under near-infrared excitation ( $\lambda_{\text{ex}}=980$  nm). In addition, the magnetic susceptibility of the nanocubes was  $1.049 \times 10^{-4}$  emu g<sup>-1</sup> Oe<sup>-1</sup> at room temperature, which was 29 % larger than the reported value. NIH/3T3 mouse fibroblast cell line was used to study the cytotoxicity of the UCNCs. The produced UCNCs with surface modification did not impose toxic effect on cells. Then, a nanostructured glucose biosensor was constructed based on this upconversion nanomaterials.

Upconversion nanoparticles could convert excited light with a lower energy into emission light with a higher energy because of the multiphoton excitation-involving nonlinear process, which could be applied in various areas, including luminescent display devices, optical devices, photo-therapy, and medicine, etc. [1-4] Most studies indicated that the dopants of lanthanide, such as Er, Tm, and Ho, could produce emission as the optically active centres due to the 4f-4f orbital electronic transitions. Fluoride materials, e.g. NaYF<sub>4</sub>

and NaGdF<sub>4</sub>, normally act as the excellent host lattices because of their high chemical stability and good optical transparency over a wide wavelength range. [5-6] Unique properties of lanthanide-doped upconversion nanomaterials have attracted extensive attention, e.g. optical-magnetic bi-functional properties of NaGdF<sub>4</sub>: Yb, Er. [7-8]

Various methods have been developed to produce upconversion nanocubes (UCNCs), including hydro(solvo)-thermal reaction, thermal decomposition of rare earth organic precursors, and ionic liquids methods etc. [9-11] Hydro(solvo)-thermal reaction and thermal decomposition could produce highly crystalline and monodispersed nanocubes, while the reactions need highly controlled reaction parameters, e.g. temperature, and toxic organic rare earth precursors which bring barriers to further modification for biomedical applications. Whereas, the ionic liquids-related methods yield less uniform nanocubes, but are relatively easy to control the process parameters. [12-13] Therefore, facile synthesis strategies for high-quality UCNCs with controlled composition, crystalline phase, particle size, are highly demanded. [14-15]

On the other hand, studies show that fluorescence properties of upconversion nanoparticles could be affected by energy levels of rare earth ions, the surface modification, etc. [16-17] Riman and his co-workers reported that the effects of three different surfactants; trioctylphosphine, polyethylene glycol monooleate, and polyvinylpyrrolidone on the emissions of NaYF<sub>4</sub>: Yb<sup>3+</sup>, Er<sup>3+</sup> nanomaterials. The emission intensity of NaYF<sub>4</sub>: Yb<sup>3+</sup>, Er<sup>3+</sup> dried powder decreased following the order, polyvinylpyrrolidone > polyethylene glycol monooleate > trioctylphosphine > unmodified nanoparticles because of the reduced reflectance loss at the boundary between upconversion nanoparticles with different surfactants and the air. Song et al. [18] reported that NaYF<sub>4</sub>: Yb<sup>3+</sup>, Er<sup>3+</sup> nanoparticles modified with thioglycolic acid could transfer hydrophobic upconversion nanoparticles into hydrophilic upconversion nanoparticles. And the results indicated that the blue emission (<sup>2</sup>H<sub>9/2</sub>→<sup>4</sup>I<sub>15/2</sub>) and red emission (<sup>4</sup>F<sub>9/2</sub>→<sup>4</sup>I<sub>15/2</sub>) with respect to the green emission (<sup>2</sup>H<sub>11/2</sub>, <sup>4</sup>S<sub>3/2</sub>→<sup>4</sup>I<sub>15/2</sub>) have been enhanced after surface modification.

In this chapter, we developed a modified solvothermal method to have a one-pot synthesis of NaGdF<sub>4</sub>: Yb<sup>3+</sup>, Er<sup>3+</sup> UCNCs with amine surface modification. It is noted that amine

functional group normally increases the hydrophilicity of nanomaterials, and is useful for further conjugating to different molecule. In order to avoid the amine groups interaction with other proteins. We deposited these upconversion nanoparticles onto silicone hydrogel surface and modified with a layer of PEGylation. As gadolinium-based upconversion nanomaterials could be used as a dual contrast agent and fluorescence imaging. The fluorescence and magnetic properties of the UCNCs with surface modification were investigated. The cytotoxicity of the produced UCNCs was also investigated for potential applications in bio-imaging.

With over decades' efforts, tear glucose is considered as a biomarker for diagnosis of diabetes. [19-20] The mean values of tear glucose were measured at  $0.35 \text{ mM} \pm 0.04 \text{ mM}$  and  $0.16 \text{ mM} \pm 0.03 \text{ mM}$ , for patients with diabetes and healthy subjects, respectively. [21] Most commercialized glucose meter is used for detecting glucose in blood with the testing range from 3 mM to 25 mM. The difficulties on using this tear glucose lies in quickly collecting enough tears for test, and accurately measuring such low concentration of glucose in tears. Here, we demonstrated that a nanostructured biosensor deposited on silicone hydrogel substrate could be used to detect rat's tear glucose *in vivo*. The designed biosensor was composed of protein (Con A) conjugated upconversion nanoparticles (UCNPs) incorporating with hydrogel, a contact lens materials.

Since Leonardo da Vinci introduced the concept of a contact lens in the year 1508, it has been one of the most commonly worn biomedical devices in the 21st century. [22] Future benefits of this wearable medical device from the developments of nanobiotechnology are not limited in vision correction, but also are promising for the topical eye treatment. [23-24] Quite recently, the engineered contact lenses for monitoring tear glucose was recognized as a means for non-invasive diagnosis and monitoring for diabetics. [25-26] Fluorescein eye stain test is common in eye exam. [27] Consequently, fluorescence sensors incorporating contact lens may be used for wearing on eyes and detecting components in tears directly. Small handheld fluorescent microscopy could be developed to measure the contact lens fluorescent signal. Though the discrepancy in the correlation between tear glucose and blood glucose were found caused by the collection methods and time lag in tear measurement. [28-29] detection of tear glucose could provide a non-invasive method

to be supplementary to the current blood glucose tests. Furthermore, glucose concentrations in diabetic individuals in comparison to healthy individuals were found to be 4 times and 2 times higher when assessed in ocular tears and blood respectively. [29]

Luminescence resonance energy transfer (LRET) is a distance-dependent nonradioactive process. When the distance of the two fluorophores is very close ( $< 10$  nm), the excited fluorophore donor (D) would transfer some of its energy to excite fluorophore acceptor (A). [30-31] LRET pair-labeled enzyme sensors have been used in studying protein-protein interactions. [32-35] Upconversion nanostructures are the emerging luminescent nanomaterials, which have the unique capability to convert the excited light with a lower energy to the emission light with a higher energy because of the multiphoton excitation-involving nonlinear process. [12] In addition, upconversion nanostructures show advantages over conventional fluorophores, including high signal-to-noise ratio, superior photo-stability, and low toxicity. [36-39] In comparison, semiconductor quantum dots require external excitation energies close to the ultraviolet range, which could result in profound effects leading to photic damage. [40] The upconversion materials are excited by lower frequency near-infrared radiation and emit higher energy radiation in the visible light spectrum. Lanthanide-doped upconversion nanostructures show enhanced emission in the visible region ( $400 \text{ nm} < \lambda_{\text{em}} < 700 \text{ nm}$ ) with the near-infrared excitation wavelengths ( $700 \text{ nm} < \lambda_{\text{ex}} < 1200 \text{ nm}$ ). [41-42] The upconversion nanostructures utilizing near-infrared radiation (760 nm to 1400 nm) are very ineffective in producing retinal injuries and therefore much safer for ocular applications. [43-44]

Figure 4.1 showed the designed LRET sensor incorporating contact lens for detecting tear glucose directly. Concanavalin A (Con A), an enzyme with specific affinity to glucose, [45] was conjugated with the donor, NaGdF<sub>4</sub>: Er, Yb upconversion nanoparticles (NPs), through two Schiff bases (C=N). The acceptor of the LRET sensor was dextran-binding malachite green (MG) which has an absorption at the same wavelength of the red emission of the NaGdF<sub>4</sub>: Er, Yb, upconversion NPs. The emitted fluorescence of the donor was quenched by malachite green (MG) through the LRET mechanism. Dextran is a saccharide with affinity for Concanalin A. [46] In the presence of glucose, the binding between Con A and dextran could compete over by the binding between Con A and glucose. The most

significant advantages of using upconversion nanostructures include: (1) the nanostructures acted as an analyte (tear glucose) collector to achieve high concentration of analyte reacting with the LRET enzyme sensor due to the large surface area to volume ratio; (2) the nanostructures exhibited stable optical signals as shown in figure 4.1; and (3) large surface-to-volume ratio of enzyme-immobilized nanostructures could lead to higher selectivity for glucose sensing. The fluorescence intensity ( $I$ ) of the LRET sensor as a function of the concentration of glucose has been investigated thoroughly *in vitro* and *in vivo*.

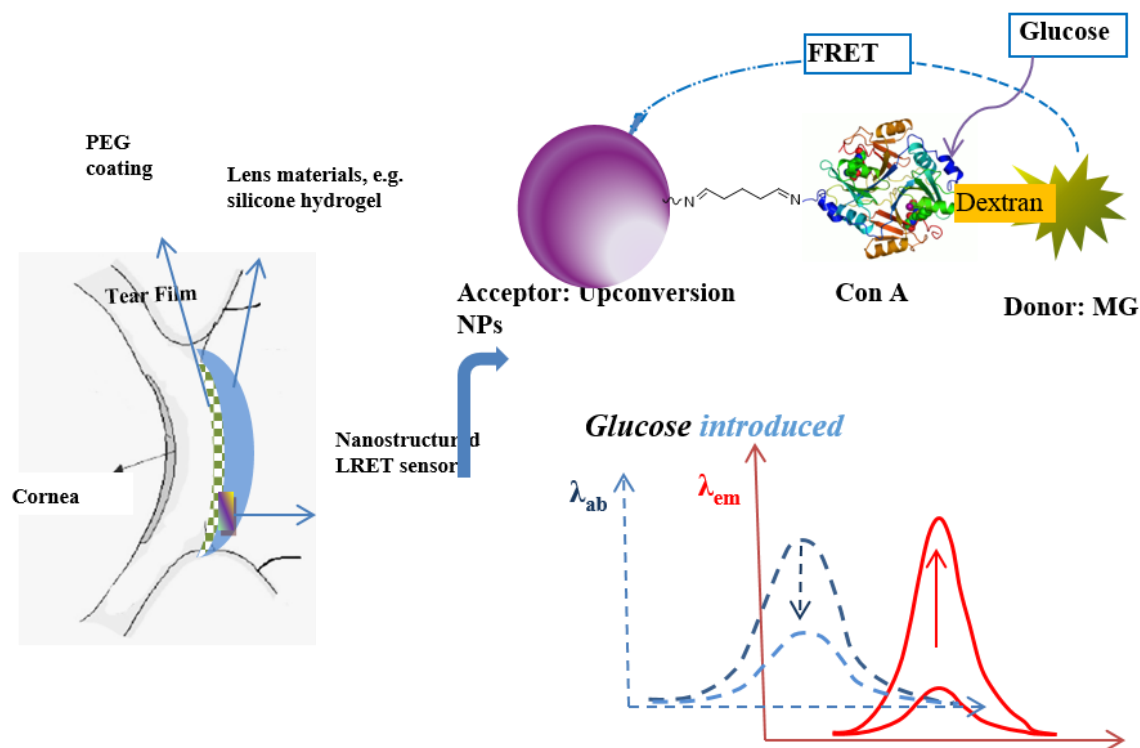


**Figure 4.1 Schematic of LRET sensor sensing mechanism.**

## 4.2 Experimental

### 4.2.1 Synthesis of Polyethylenimine (PEI) Modified Upconversion Nanostructures

$40 \pm 5$  nm paramagnetic upconversion NPs were synthesized by polyol method. [47] In a typical synthesise process, 1.6 mmol  $Gd(NO_3)_3 \cdot 6H_2O$ , 0.36 mmol  $Yb(NO_3)_3 \cdot 5H_2O$ , 0.38 mmol  $Er(NO_3)_3 \cdot 5H_2O$ , 0.7 g branched polyethylenimine (PEI), and 20 mL ethylene glycol

were added into a 100 mL three-neck round-bottom flask and dissolved by magnetic stirring. Then, 8 mmol NaF dissolved in 10 mL ethylene glycol were added dropwise into the 100 mL flask. Under reflux, the solution was heated to around 198 °C to keep ethylene glycol boiling for 6 hours under nitrogen gas protection. The as-synthesized upconversion nanocubes were centrifuged and purified with ethanol and water several times, then dried at 60 °C overnight.

#### 4.2.2 Synthesis of Malachite Green Dextran

Malachite green dextran was synthesized according to the method by McCartney et al. [35, 46] In short, malachite green (MG) isothiocyanate and 70,000 MW amino-dextran purchased from Life Technologies (Burlington, Ontario, Canada) were mixed in a sodium bicarbonate buffer (0.05 M, pH 9.6). Successful conjugation of the isothiocyanate and dextran to form MG-dextran was verified by thin layer chromatography. The isothiocyanate and MG-dextran had an  $R_f$  value of approximately 1.0 and less than 0.25, respectively (chapter 3 at section 3.2.2).

#### 4.2.3 Conjugation of Glucose Sensor Components

In short, the Con A solution 1 mg/mL, 2 mL was conjugated to upconverting nanoparticle 1 mg/mL, 2 mL with 200 µL 0.5 % glutaraldehyde solution at room temperature for 2 hours under mild ellipsoidal shaking. 10 mg malachite green-dextran was added and allowed to bind to Con A for an additional 2 hours. The biosensor was collected after thrice centrifugation for 5 minutes at 9000 rpm and resuspended in deionized water.

#### 4.2.4 Sensor Deposition onto Silicone Hydrogel

As a medium to contain the upconverting nanoparticle glucose biosensor, we deposited 200 µL of the glucose sensor suspended in water solution onto pieces of silicone hydrogels and put in 4 °C fridge to let dry. The hydrogel was sterilized by soaking in 75% ethanol.

#### 4.2.5 *In Vivo* Animal Model

This part was cooperated with Dr James Melling lab (Kinesiology, UWO). Six male Sprague-Dawley rats (Charles River Laboratories, St. Constant, QC, Canada) were housed

in a 12-hour light/dark cycle room with humidity (50%) and temperature (21.5 °C) kept constant. Intraperitoneal injections of STZ (20 mg/kg) dissolved in a citrate buffer (0.1M, pH 4.5) were given over five consecutive days were given to induce diabetes. Following the confirmation of diabetes (two blood glucose readings greater than 18mM) subcutaneous insulin pellets were implanted in the abdominal region of rats.

Ethics approval was obtained through the University of Western Ontario Research Ethics Board, in accordance with Canadian Council on Animal Care guidelines.

## 4.3 Results and Discussion

### 4.3.1 TEM and XRD

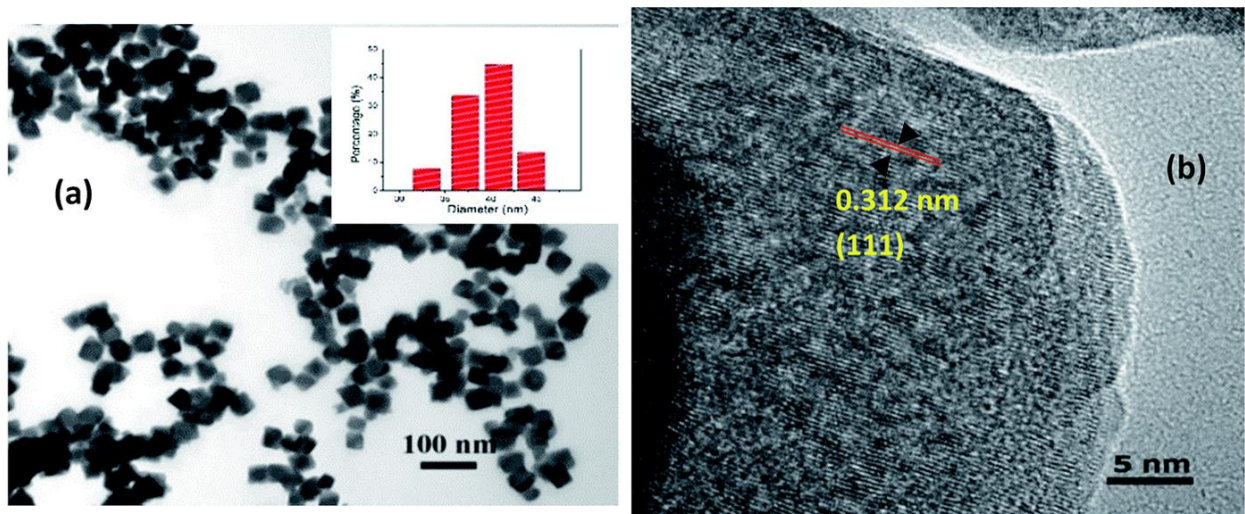


**Figure 4.2 (a) TEM micrograph of NaGdF<sub>4</sub>: Yb<sup>3+</sup>, Er<sup>3+</sup> UCNCs, the small inset is the size distribution histogram chart. (b) HRTEM image of as-synthesized NaGdF<sub>4</sub>: Yb<sup>3+</sup>, Er<sup>3+</sup> UCNCs.**

TEM and HRTEM were used to characterize the as-synthesized NaGdF<sub>4</sub>: Yb, Er UCNCs. Fig. 4.2 (a) showed the TEM micrograph of highly uniform nanocubes. The average length of the nanocubes was approximately 40±5 nm. Fig. 4.2 (b) showed the HRTEM image of as-synthesized upconversion nanocubes with highly crystalline structure. The measured inter-planar distance between two adjacent lattice planes was 0.312 nm, corresponding to the (1 1 1) plane of cubic phase NaGdF<sub>4</sub> (JCPDS 27-0697).



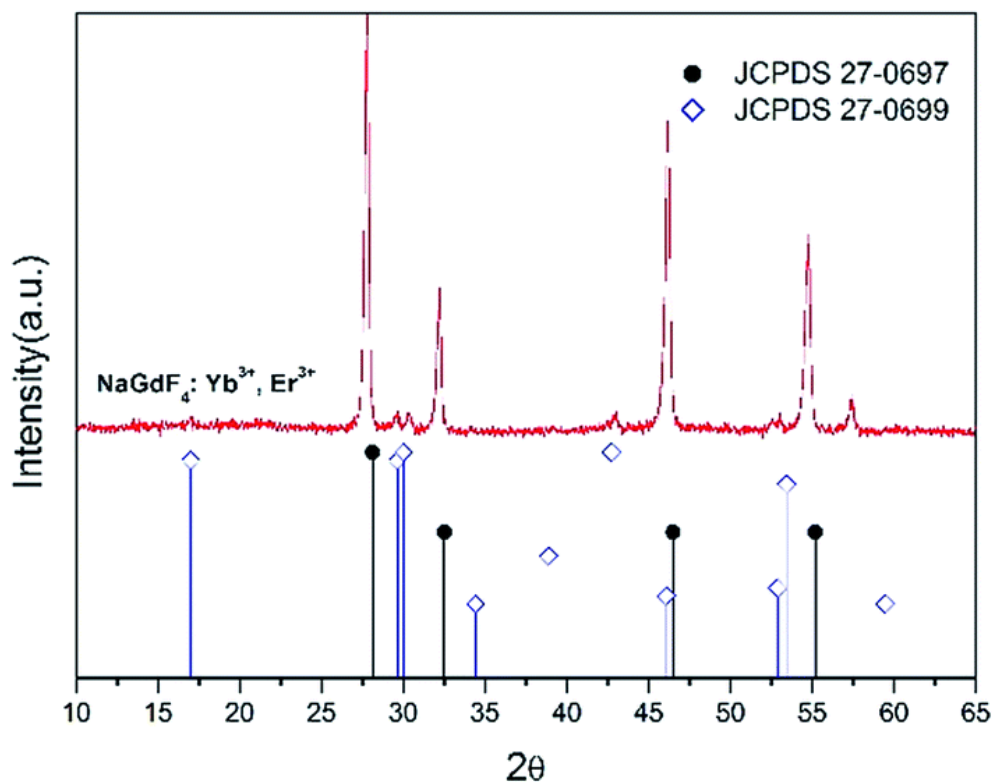


**Figure 4.3 XRD profile of NaGdF<sub>4</sub>: Yb<sup>3+</sup>, Er<sup>3+</sup> upconverting nanoparticles and the line pattern of standard cubic phase of NaGdF<sub>4</sub> (JCPDS 27-0697) and hexagonal phase of NaGdF<sub>4</sub> (JCPDS 27-0699).**

The XRD profile was shown in Fig. 4.3. The XRD profile indicated that standard cubic phase (JCPDS 27-0697) dominated in the crystal structures. [48] It was also noted that there were two small peaks around 2 theta at around 30, which could be caused by the other phase, hexagonal NaGdF<sub>4</sub> crystal (JCPDS 27-0699). Compared to the thermal decomposition for producing cubic UCNPs at high temperature over 300 °C, [8, 11] the one-pot method utilized ethylene glycol polyol solution at 198 °C to produce PEI modified upconverting nanoparticles. In addition, the dopants, i.e. Yb, and Er ions, normally would not change the crystal structures, but may slightly change the lattice strain of the crystals. Therefore, the characteristic peaks of cubic NaGdF<sub>4</sub> crystal acting as the host have a slight shift as compared to the standard cubic phase of NaGdF<sub>4</sub> (JCPDS 27-0697) crystal structure.

### 4.3.2 FTIR Spectrum of PEI Modified Upconverting Nanoparticles

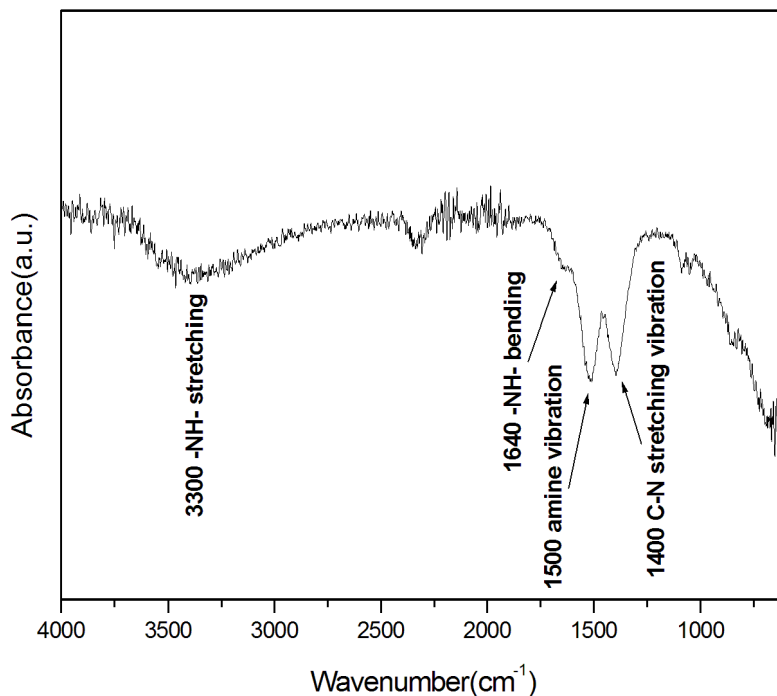


**Figure 4.4 FTIR spectrum of PEI capped NaGdF<sub>4</sub>: Yb, Er upconversion nanocubes.**

The successful capping of as-synthesized upconversion nanocubes with PEI to functionalize the surface with amine groups was confirmed by Fourier transform infrared (FTIR) spectroscopy. The obtained FTIR spectroscopy was similar to previous results. [49-51] As shown in figure 4.4, the broad peak at 3300 cm<sup>-1</sup> was attributed to the -NH- stretching. The small peak present at 1640 cm<sup>-1</sup> was due to the -NH- bending. The peak at 1500 cm<sup>-1</sup> was the vibration of the amine groups. And peak at 1400 cm<sup>-1</sup> was due to the stretching vibrations of C-N bonds. [24] These results confirmed the successful binding of PEI onto the nanocube surface.

### 4.3.3 Upconverting Fluorescence

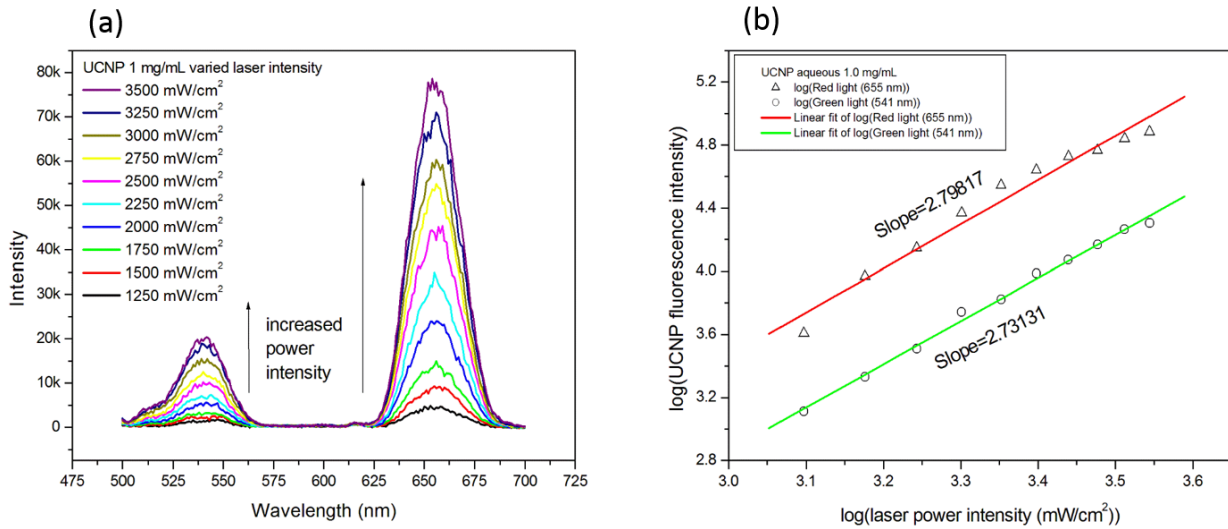


**Figure 4.5 Photoluminescent spectrum of NaGdF<sub>4</sub>: Er, Yb solution (1 mg/mL). (a) Photoluminescence as a function of laser light powered in the range of 0.5 W to 1.5 W. (b) Power dependence of red and green emissions.**

The fluorescence spectra of the upconverting nanoparticles were shown in Fig. 4.5. Under excitation at 980 nm, varied excitation density, two upconversion emission bands of green light at 541 nm and red light at 655 nm were observed. The green light emission ( $\lambda_{em}=541$  nm) was attributed to  $^4S_{3/2} \rightarrow ^4I_{15/2}$  electronic transition, while red light emission ( $\lambda_{em}=655$  nm) was attributed to  $^4F_{9/2} \rightarrow ^4I_{15/2}$  electronic transitions. Emission features of the synthesized upconversion nanoparticles were comparable to the reported results. [52-53] The two emission bands observed at 541 nm and 655 nm were attributed to a two-photon upconversion process.

### 4.3.4 Magnetic Properties Analysis

The magnetic properties of as-synthesized NaGdF<sub>4</sub>: Yb<sup>3+</sup>, Er<sup>3+</sup> upconversion nanocubes was measured with a Vibrating Sample Magnetometer (VSM). Fig. 4.6 (a) showed the hysteresis loop of NaGdF<sub>4</sub>: Yb<sup>3+</sup>, Er<sup>3+</sup> upconversion nanocubes under a magnetic field of  $\pm 10$  kOe under various temperatures, 85 K, 125 K, 150 K, 200 K, 250 K and 295 K. The UCNCs showed typical paramagnetic properties. [54-55]

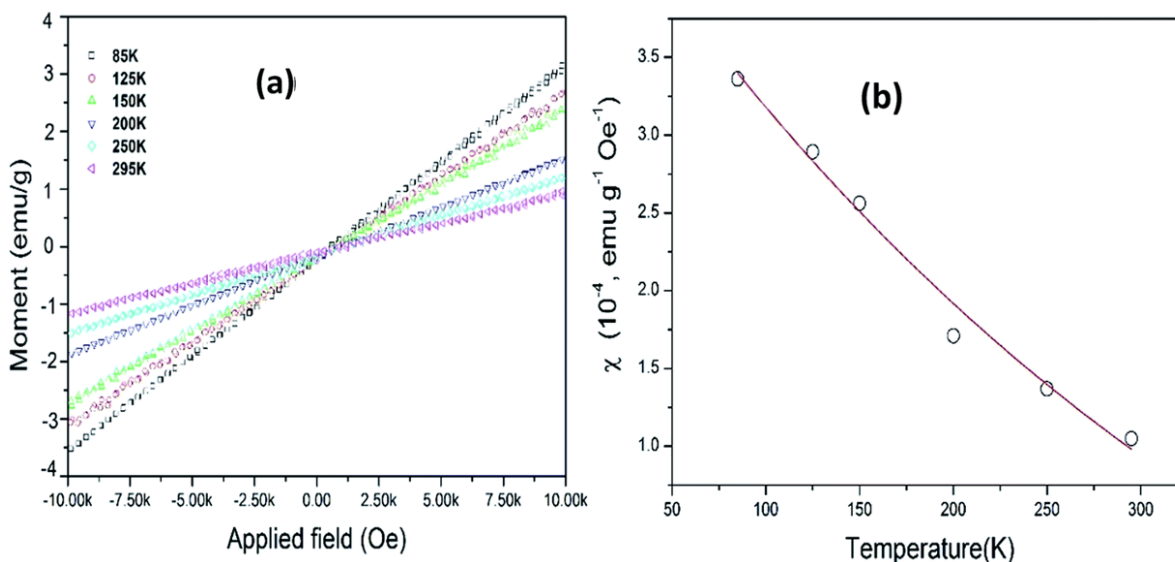


**Figure 4.6 (a) Magnetic hysteresis curves of PEI capped NaGdF<sub>4</sub>:Yb<sup>3+</sup>, Er<sup>3+</sup> nanocubes with temperatures. (b) Magnetic susceptibility of NaGdF<sub>4</sub>:Yb<sup>3+</sup>, Er<sup>3+</sup> nanocubes at various temperatures.**

The magnetic susceptibility ( $\chi$ ) of the UCNCs was calculated by using Curie law; [56]

$$\chi = \frac{M}{H}$$

Where M is the magnetization per weight, H is the magnetic field. Fig.4.6 (b) displayed the  $\chi$  value of the UCNCs as a function of temperature (T), which was a typical curve for paramagnetic materials. At room temperature (295 K),  $\chi$  value was  $1.049 \times 10^{-4} \text{ emu g}^{-1} \text{ Oe}^{-1}$ , which was 29% larger than the reported value of the NaGdF<sub>4</sub>: Yb<sup>3+</sup>, Er<sup>3+</sup> upconversion nanoparticles,  $\sim 0.813 \times 10^{-4} \text{ emu g}^{-1} \text{ Oe}^{-1}$ . [56-57] It increased with decreasing temperature, when temperature was 85 K,  $\chi$  value of the UCNCs was  $3.361 \times 10^{-4} \text{ emu g}^{-1} \text{ Oe}^{-1}$ , due to thermal fluctuation reduction at low temperatures. [58-59] Our produced UCNCs exhibited paramagnetic properties. Therefore, the magnetization (M) normally increased with reducing particle size as reduced particles size normally led to single domain, or low internal energy barrier. [60] In addition, the cubic structure could allow the nanoparticles to have easy magnetization along certain orientation, leading to the reduced magnetic field for saturating UCNCs. Reports have demonstrated that suitable surface modification could result in desired nanostructured in term of uniform particle size, and

shape. [61] Thus, the stronger magnetic susceptibility of the produced UCNCs could be related to their cubic structures, the small particle size, and surface modification.

#### 4.3.5 Cytotoxicity Study

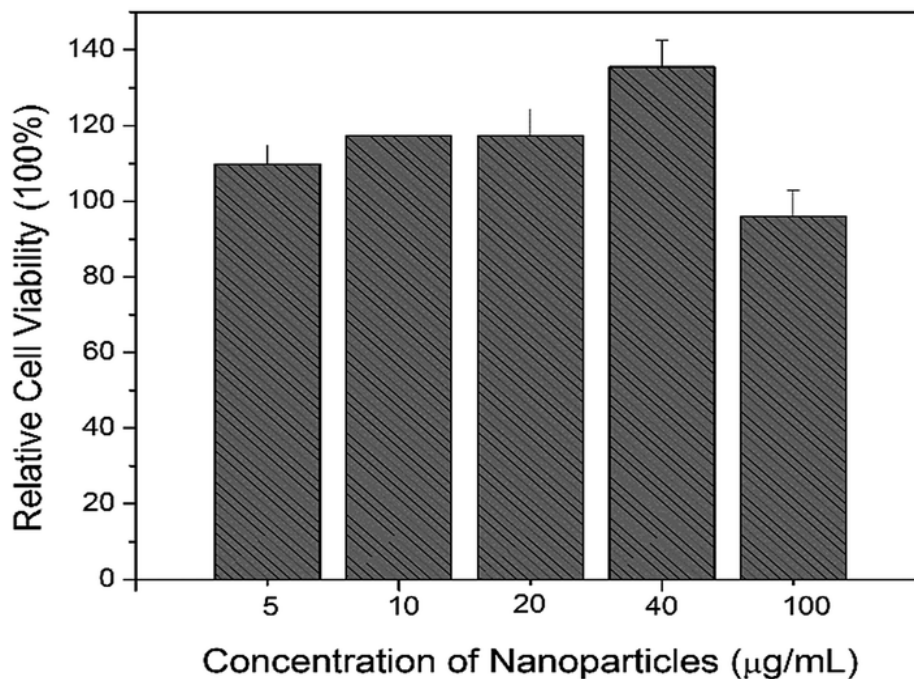


**Figure 4.7 Relative cell viability as a function of the concentration of UCNCs with surface modification.**

NIH/3T3 mouse fibroblast cells were used for the cytotoxicity test. The cells without the treatment of UCNCs was used as a control. The relative cell viability of UCNCs with PEI modification were over 110% when the concentration of UCNCs increased from 5 to 40  $\mu\text{g mL}^{-1}$ , it decreased to 97.3% when the concentration of UCNCs increased to 100  $\mu\text{g mL}^{-1}$  as shown in Fig. 4.7. The relative cell viability for materials with good biocompatibility was normally beyond 85%. [62] Therefore, the as-made UCNCs modified with amine functional group did not impose toxic effect on NIH/3T3 mouse fibroblast cells.

#### 4.3.6 Sensitivity of Sensor Construct to Detect Glucose in Solution

In order to monitor a broad range of glucose levels (0.01 mM to 10 mM) quickly, with a high signal response, two different synergistic materials were used to avoid high external

energy excitation of the LRET sensor; (1) NIR/IR excitable donor consisting of upconversion nanomaterials, and (2) an acceptor molecule competitively binding with a lectin protein with a high glucose affinity. NaGdF<sub>4</sub>: Er, Yb upconversion NPs modified with Polyethylenimine (PEI) was conjugated to Concanavalin A (Con A) protein using glutaraldehyde to covalently link the primary amino groups of the PEI and Con A. The nanobiosensors were then loaded with malachite green-dextran.

The premise of our biosensor construct utilizes Luminescence Resonance Energy Transfer (LRET) [30, 63] to monitor glucose levels as shown in figure 4.1. The donor molecule, upconversion NPs, once excited by NIR/IR radiation would emit energy at a higher energy than the initial excitation energy. In the absence of glucose, the malachite green-dextran acceptor absorbs this energy to decrease the detected fluorescence. In the presence of glucose, the malachite green dextran is competitively displaced from the Con A thus increasing the fluorescence as a function of glucose concentration.

#### 4.3.7 *In Vivo* Sensing of Glucose in Murine Tears

Four male Sprague-Dawley rats (Charles River Laboratories, St. Constant, QC, Canada) were treated with streptozotocin (STZ; Sigma-Aldrich, Oakville, ON, Canada) to induce diabetes. Rats were anesthetized with isoflurane for ease of application of the sensors to their eyes. Tear fluid was also collected from the ocular surface with a 1  $\mu$ L glass capillary tube for reference. A blood sample was taken from the saphenous vein concurrently with the application of the sensor for blood glucose concentration (Freestyle Lite Blood Glucose Monitoring System, Abbott Diabetes Care Inc., Mississauga, Ontario).

The glucose sensor deposited on silicone was gently applied PEG side towards the murine subject's eye for 15 seconds and removed. Samples were measured by the fluorospectrometry with excitation at 980 nm. Dynamic sensing are possible by developing or incorporating products like Google Lens.

#### 4.3.8 Contact Lens-like Material Incorporation of Glucose Sensor

Silicone hydrogel are more suitable as contact lens material in comparison to commercial lens materials as they contain enhanced features. In addition to great biocompatibility,

transparency, and stable chemical structures ideal for contact lens, the presence of siloxane groups increases oxygen transmissibility. [64-66]

The upconversion glucose nanobiosensors were deposited onto the surface of silicone hydrogels as a concentrated material droplet and allowed to dry. A uniform thin layer of polyethylene glycol (PEG) was coated over the silicone surface with a method similar to pulsed laser deposition to prevent dissociation of the sensor. [67-69]

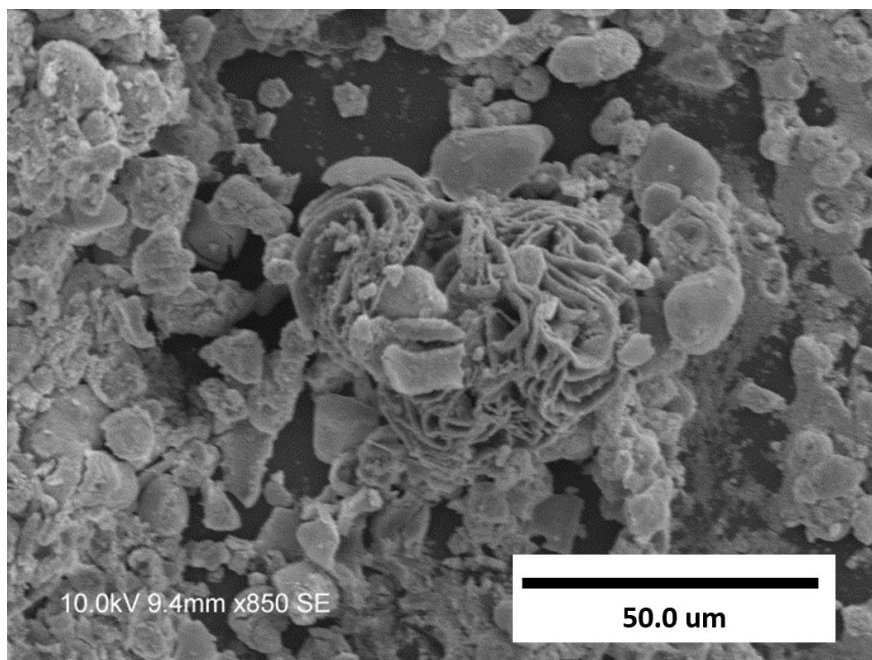


**Figure 4.8 SEM image of contact lens nanostructured glucose biosensor surface.**

The as-synthesized PEI capped upconversion nanoparticles were surface functionalized with amine group ( $-NH_2$ ). As a result, the polyethylenimine (PEI) capped upconversion nanoparticles were well dispersed in water. The successful surface modification by PEI was confirmed by Fourier transform infrared (FTIR) spectroscopy (figure 4.4). The amine group provides suitable opportunity to covalently adhere proteins through the use of chemical functional groups such as hydroxyl and amine groups. These groups were conjugated with Con A. In the tear, the present proteins could be avoided by applying the PEGylation of sensor surface. Figure 4.8 presented the SEM image of nanostructured glucose sensor chip surface. Some protein aggregates are present in the figure.

As shown in Figure 4.9, the sensor deposited onto silicone showed a linear response to plasma glucose with a  $R^2=0.97$  in the range of about 5 mM to 13 mM. Because the figure has not yet been published, we will keep the error bars etc. data before published.

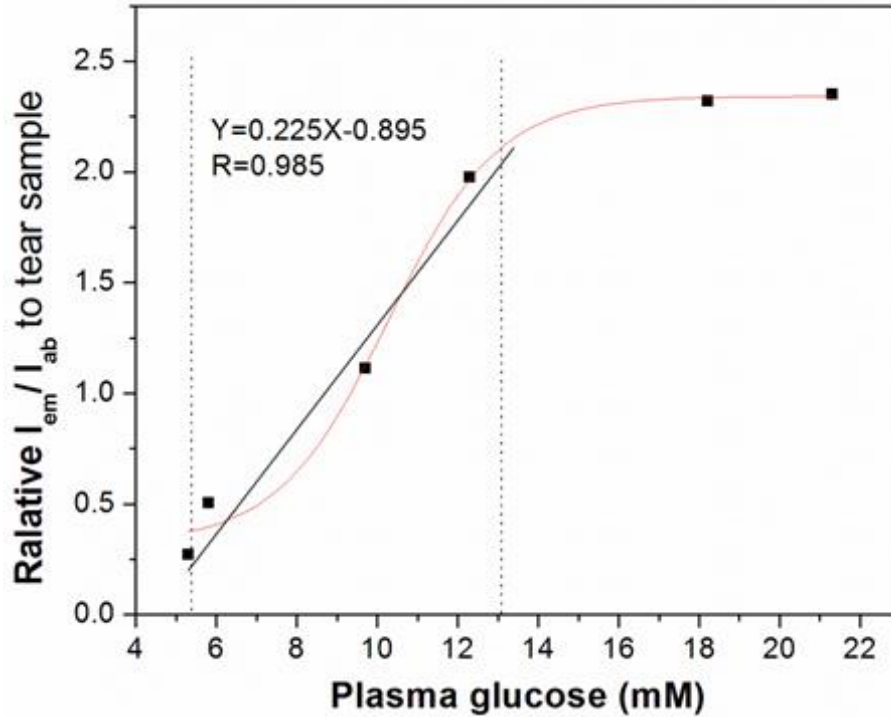


**Figure 4.9 Nanostructured upconverting glucose biosensor response to plasma glucose.**

#### 4.4 Conclusion

Our findings indicated upconversion nanomaterials are attractive as donor for noninvasive glucose sensing in contact lens. Its ability to be excited at the NIR range not only improves emission efficiency but ensures the safety of the retina. [43] The Con A protein demonstrated a high affinity for glucose resulting in an immediate change in fluorescent intensity with a linear response in a laboratory setting. Testing of the contact lens sensor on murine patients under normal and diabetic glucose conditions demonstrated a similar linear response.



## 4.5 References

- [1] François Auzel, Upconversion and Anti-Stokes Processes with f and d Ions in Solids. *Chemical Reviews* **2003**, *104* (1), 139-174.
- [2] Markus Haase; Helmut Schäfer, Upconverting Nanoparticles. *Angewandte Chemie International Edition* **2011**, *50* (26), 5808-5829.
- [3] S. Heer; K. Kömpe; H. U. Güdel; M. Haase, Highly Efficient Multicolour Upconversion Emission in Transparent Colloids of Lanthanide-Doped NaYF<sub>4</sub> Nanocrystals. *Advanced Materials* **2004**, *16* (23-24), 2102-2105.
- [4] Tae-Hyun Shin; Youngseon Choi; Soojin Kim; Jinwoo Cheon, Recent advances in magnetic nanoparticle-based multi-modal imaging. *Chemical Society Reviews* **2015**, *44* (14), 4501-4516.
- [5] Zhengquan Li; Yong Zhang; Shan Jiang, Multicolor Core/Shell-Structured Upconversion Fluorescent Nanoparticles. *Advanced Materials* **2008**, *20* (24), 4765-4769.
- [6] Oh Seok Kwon; Hyun Seok Song; João Conde; Hyung-il Kim; Natalie Artzi; Jae-Hong Kim, Dual-Color Emissive Upconversion Nanocapsules for Differential Cancer Bioimaging *In Vivo*. *ACS Nano* **2016**, *10* (1), 1512-1521.
- [7] Gangtao Dai; Zhiqiang Zhong; Xiaofeng Wu; Shiping Zhan; Shigang Hu; Pan Hu; Junshan Hu; Shaobing Wu; Junbo Han; Yunxin Liu, Magnetic tuning of upconversion luminescence in Au/NaGdF<sub>4</sub>:Yb<sup>3+</sup>/Er<sup>3+</sup> nanocomposite. *Nanotechnology* **2017**, *28* (15), 155702.
- [8] Yunxin Liu; Dingsheng Wang; Jianxin Shi; Qing Peng; Yadong Li, Magnetic Tuning of Upconversion Luminescence in Lanthanide-Doped Bifunctional Nanocrystals. *Angewandte Chemie International Edition* **2013**, *52* (16), 4366-4369.
- [9] Parthiban Ramasamy; Prakash Chandra; Seog Woo Rhee; Jinkwon Kim, Enhanced upconversion luminescence in NaGdF<sub>4</sub>:Yb,Er nanocrystals by Fe<sup>3+</sup> doping and their application in bioimaging. *Nanoscale* **2013**, *5* (18), 8711-8717.
- [10] Meng He; Peng Huang; Chunlei Zhang; Feng Chen; Can Wang; Jiebing Ma; Rong He; Daxiang Cui, A general strategy for the synthesis of upconversion rare earth fluoride nanocrystals via a novel OA/ionic liquid two-phase system. *Chemical Communications* **2011**, *47* (33), 9510-9512.
- [11] Wenbin Niu; Suli Wu; Shufen Zhang; Liap Tat Su; Alfred Iing Yoong Tok, Multicolor tunability and upconversion enhancement of fluoride nanoparticles by oxygen dopant. *Nanoscale* **2013**, *5* (17), 8164-8171.
- [12] Guanying Chen; Hailong Qiu; Paras N. Prasad; Xiaoyuan Chen, Upconversion Nanoparticles: Design, Nanochemistry, and Applications in Theranostics. *Chemical Reviews* **2014**, *114* (10), 5161-5214.

- [13] Niagara Muhammad Idris; Muthu Kumara Gnanasammandhan Jayakumar; Akshaya Bansal; Yong Zhang, Upconversion nanoparticles as versatile light nanotransducers for photoactivation applications. *Chemical Society Reviews* **2015**, *44* (6), 1449-1478.
- [14] Guofeng Wang; Qing Peng; Yadong Li, Lanthanide-Doped Nanocrystals: Synthesis, Optical-Magnetic Properties, and Applications. *Accounts of Chemical Research* **2011**, *44* (5), 322-332.
- [15] Wei Feng; Chunmiao Han; Fuyou Li, Upconversion-Nanophosphor-Based Functional Nanocomposites. *Advanced Materials* **2013**, *25* (37), 5287-5303.
- [16] Mei Chee Tan; Lara Al-Baroudi; Richard E. Riman, Surfactant Effects on Efficiency Enhancement of Infrared-to-Visible Upconversion Emissions of NaYF<sub>4</sub>:Yb-Er. *ACS Applied Materials & Interfaces* **2011**, *3* (10), 3910-3915.
- [17] Hangjun Wu; Zhengwen Yang; Jiayan Liao; Shenfeng Lai; Jianbei Qiu; Zhiguo Song; Yong Yang; Dacheng Zhou; Zhaoyi Yin, Upconversion luminescence properties of three-dimensional ordered macroporous CeO<sub>2</sub>: Er<sup>3+</sup>, Yb<sup>3+</sup>. *Journal of Alloys and Compounds* **2014**, *586* (Supplement C), 485-487.
- [18] Dan Li; Biao Dong; Xue Bai; Yu Wang; Hongwei Song, Influence of the TGA Modification on Upconversion Luminescence of Hexagonal-Phase NaYF<sub>4</sub>:Yb<sup>3+</sup>,Er<sup>3+</sup> Nanoparticles. *The Journal of Physical Chemistry C* **2010**, *114* (18), 8219-8226.
- [19] Yoshiki Ohashi; Murat Dogru; Kazuo Tsubota, Laboratory findings in tear fluid analysis. *Clinica Chimica Acta* **2006**, *369* (1), 17-28.
- [20] W. Kenneth Ward; Michael D. Wood; Heather M. Casey; Matthew J. Quinn; Isaac F. Federiuk, An Implantable Subcutaneous Glucose Sensor Array in Ketosis-prone Rats: Closed Loop Glycemic Control. *Artificial Organs* **2005**, *29* (2), 131-143.
- [21] D K Sen; G S Sarin, Tear glucose levels in normal people and in diabetic patients. *British Journal of Ophthalmology* **1980**, *64* (9), 693-695.
- [22] RF Heitz; JM Enoch, Leonardo da Vinci: An assessment on his discourses on image formation in the eye. *Advances in Diagnostic Visual Optics* **1987**, 19-26.
- [23] Lokendrakumar C. Bengani; Kuan-Hui Hsu; Samuel Gause; Anuj Chauhan, Contact lenses as a platform for ocular drug delivery. *Expert Opinion on Drug Delivery* **2013**, *10* (11), 1483-1496.
- [24] Jin Zhang; Robert Bi; William Hodge; Pei Yin; Wai Hei Tse, A nanocomposite contact lens for the delivery of hydrophilic protein drugs. *Journal of Materials Chemistry B* **2013**, *1* (35), 4388-4395.

- [25] Nicholas M. Farandos; Ali K. Yetisen; Michael J. Monteiro; Christopher R. Lowe; Seok Hyun Yun, Contact Lens Sensors in Ocular Diagnostics. *Advanced Healthcare Materials* **2015**, 4 (6), 792-810.
- [26] Jin Zhang; William Hodge; Cindy Hutnick; Xianbin Wang, Noninvasive Diagnostic Devices for Diabetes through Measuring Tear Glucose. *Journal of Diabetes Science and Technology* **2011**, 5 (1), 166-172.
- [27] Carl Zeiss Eye Examination With the Slit Lamp. <http://www.frankshospitalworkshop.com/equipment/documents/ophthalmology/equipment/Eye%20Examination%20with%20the%20Slit%20Lamp%20-%20Carl%20Zeiss.pdf> (accessed November 2<sup>nd</sup> 2017).
- [28] J. G. Lewis; P. J. Stephens, Tear Glucose in Diabetics. *British Journal of Ophthalmology* **1958**, 42 (12), 754-758.
- [29] Jennifer D. Lane; David M. Krumholz; Robert A. Sack; Carol Morris, Tear Glucose Dynamics in Diabetes Mellitus. *Current Eye Research* **2006**, 31 (11), 895-901.
- [30] L. Stryer; R. P. Haugland, Energy transfer: a spectroscopic ruler. *Proceedings of the National Academy of Sciences of the United States of America* **1967**, 58 (2), 719-726.
- [31] Sanjay Tyagi; Salvatore A. E. Marras; Fred Russell Kramer, Wavelength-shifting molecular beacons. *Nature Biotechnology* **2000**, 18 (11), 1191-1196.
- [32] Tomasz Heyduk, Measuring protein conformational changes by FRET/LRET. *Current Opinion in Biotechnology* **2002**, 13 (4), 292-296.
- [33] Ben N. G. Giepmans; Stephen R. Adams; Mark H. Ellisman; Roger Y. Tsien, The Fluorescent Toolbox for Assessing Protein Location and Function. *Science* **2006**, 312 (5771), 217-224.
- [34] Longyan Chen; Yige Bao; John Denstedt; Jin Zhang, Nanostructured bioluminescent sensor for rapidly detecting thrombin. *Biosensors and Bioelectronics* **2016**, 77, 83-89.
- [35] Longyi Chen; Wai Hei Tse; Yi Chen; Matthew W. McDonald; James Melling; Jin Zhang, Nanostructured biosensor for detecting glucose in tear by applying fluorescence resonance energy transfer quenching mechanism. *Biosensors and Bioelectronics* **2017**, 91, 393-399.
- [36] Peng Huang; Zhiming Li; Jing Lin; Dapeng Yang; Guo Gao; Cheng Xu; Le Bao; Chunlei Zhang; Kan Wang; Hua Song; Hengyao Hu; Daxiang Cui, Photosensitizer-conjugated magnetic nanoparticles for *in vivo* simultaneous magnetofluorescent imaging and targeting therapy. *Biomaterials* **2011**, 32 (13), 3447-3458.

- [37] Xingjun Zhu; Jing Zhou; Min Chen; Mei Shi; Wei Feng; Fuyou Li, Core-shell  $\text{Fe}_3\text{O}_4@ \text{NaLuF}_4$ : Yb, Er/Tm nanostructure for MRI, CT and upconversion luminescence tri-modality imaging. *Biomaterials* **2012**, 33 (18), 4618-4627.
- [38] Hon-Tung Wong; Ming-Kiu Tsang; Chi-Fai Chan; Ka-Leung Wong; Bin Fei; Jianhua Hao, *In vitro* cell imaging using multifunctional small sized  $\text{KGdF}_4$ :  $\text{Yb}^{3+}$ ,  $\text{Er}^{3+}$  upconverting nanoparticles synthesized by a one-pot solvothermal process. *Nanoscale* **2013**, 5 (8), 3465-3473.
- [39] Zuwu Wei; Lining Sun; Jinliang Liu; Jin Z. Zhang; Huiran Yang; Yang Yang; Liyi Shi, Cysteine modified rare-earth up-converting nanoparticles for *in vitro* and *in vivo* bioimaging. *Biomaterials* **2014**, 35 (1), 387-392.
- [40] William T. Ham; Harold A. Mueller; David H. Sliney, Retinal sensitivity to damage from short wavelength light. *Nature* **1976**, 260 (5547), 153-155.
- [41] Xiaomin Li; Fan Zhang; Dongyuan Zhao, Highly efficient lanthanide upconverting nanomaterials: Progresses and challenges. *Nano Today* **2013**, 8 (6), 643-676.
- [42] Yongsheng Liu; Datao Tu; Haomiao Zhu; Xueyuan Chen, Lanthanide-doped luminescent nanoprobes: controlled synthesis, optical spectroscopy, and bioapplications. *Chemical Society Reviews* **2013**, 42 (16), 6924-6958.
- [43] Nikolaos Kourkouvelis; Margaret Tzaphlidou, Eye Safety Related to Near Infrared Radiation Exposure to Biometric Devices. *The Scientific World Journal* **2011**, 11, 520-528.
- [44] P Hawse, Blocking the blue. *British Journal of Ophthalmology* **2006**, 90 (8), 939-940.
- [45] Ralph Ballerstadt; Colton Evans; Roger McNichols; Ashok Gowda, Concanavalin A for *in vivo* glucose sensing: A biotoxicity review. *Biosensors and Bioelectronics* **2006**, 22 (2), 275-284.
- [46] Lydia J. McCartney; John C. Pickup; Olaf J. Rolinski; David J. S. Birch, Near-Infrared Fluorescence Lifetime Assay for Serum Glucose Based on Allophycocyanin-Labeled Concanavalin A. *Analytical Biochemistry* **2001**, 292 (2), 216-221.
- [47] Longyi Chen; Wai Hei Tse; Alex Siemiarczuk; Jin Zhang, Special properties of luminescent magnetic  $\text{NaGdF}_4$ : $\text{Yb}^{3+}$ ,  $\text{Er}^{3+}$  upconversion nanocubes with surface modifications. *RSC Advances* **2017**, 7 (43), 26770-26775.
- [48] Chunyan Cao; Hyun Kyoung Yang; Jong Won Chung; Byung Kee Moon; Byung Chun Choi; Jung Hyun Jeong; Kwang Ho Kim, Hydrothermal synthesis and enhanced photoluminescence of  $\text{Tb}^{3+}$  in  $\text{Ce}^{3+}/\text{Tb}^{3+}$  doped  $\text{KGdF}_4$  nanocrystals. *Journal of Materials Chemistry* **2011**, 21 (28), 10342-10347.
- [49] Jing Chen; Changrun Guo; Meng Wang; Lei Huang; Liping Wang; Congcong Mi; Jing Li; Xuexun Fang; Chuanbin Mao; Shukun Xu, Controllable synthesis of  $\text{NaYF}_4$

:Yb,Er upconversion nanophosphors and their application to *in vivo* imaging of *Caenorhabditis elegans*. *Journal of Materials Chemistry* **2011**, *21* (8), 2632-2638.

[50] Qiang Ju; Datao Tu; Yongsheng Liu; Renfu Li; Haomiao Zhu; Jincan Chen; Zhuo Chen; Mingdong Huang; Xueyuan Chen, Amine-Functionalized Lanthanide-Doped KGdF<sub>4</sub> Nanocrystals as Potential Optical/Magnetic Multimodal Bioprobes. *Journal of the American Chemical Society* **2012**, *134* (2), 1323-1330.

[51] Chi-Fai Chan; Ming-Kiu Tsang; Hongguang Li; Rongfeng Lan; Frances L. Chadbourne; Wai-Lun Chan; Ga-Lai Law; Steven L. Cobb; Jianhua Hao; Wing-Tak Wong; Ka-Leung Wong, Bifunctional up-converting lanthanide nanoparticles for selective *in vitro* imaging and inhibition of cyclin D as anti-cancer agents. *Journal of Materials Chemistry B* **2014**, *2* (1), 84-91.

[52] Annina Aebischer; Stephan Heer; Daniel Biner; Karl Krämer; Markus Haase; Hans U. Güdel, Visible light emission upon near-infrared excitation in a transparent solution of nanocrystalline  $\beta$ -NaGdF<sub>4</sub>: Yb<sup>3+</sup>, Er<sup>3+</sup>. *Chemical Physics Letters* **2005**, *407* (1), 124-128.

[53] Feifei Li; Chunguang Li; Xiaomin Liu; Ying Chen; Tianyu Bai; Long Wang; Zhan Shi; Shouhua Feng, Hydrophilic, Upconverting, Multicolor, Lanthanide-Doped NaGdF<sub>4</sub> Nanocrystals as Potential Multifunctional Bioprobes. *Chemistry – A European Journal* **2012**, *18* (37), 11641-11646.

[54] Ronald A. J. Litjens; Terence I. Quickenden; Colin G. Freeman, Visible and near-ultraviolet absorption spectrum of liquid water. *Applied Optics* **1999**, *38* (7), 1216-1223.

[55] Wenjia Liu; Guixia Liu; Jinxian Wang; Xiangting Dong; Wensheng Yu, A new strategy to directly construct hybrid luminescence-photothermal-magnetism multifunctional nanocomposites for cancer up-conversion imaging and photothermal therapy. *RSC Advances* **2016**, *6* (4), 3250-3258.

[56] Ming-Kiu Tsang; Songjun Zeng; Helen L. W. Chan; Jianhua Hao, Surface ligand-mediated phase and upconversion luminescence tuning of multifunctional NaGdF<sub>4</sub>:Yb/Er materials with paramagnetic and cathodoluminescent characteristics. *Optical Materials* **2013**, *35* (12), 2691-2697.

[57] Qian Cheng; Jiehe Sui; Yu Li; Ziqiao Zhou; Wei Cai, Facile Synthesis of Multifunctional  $\beta$ -NaGdF<sub>4</sub>:Yb<sup>3+</sup>/Er<sup>3+</sup> Nanoparticles in Oleylamine. *Journal of Nanoscience and Nanotechnology* **2013**, *13* (1), 529-532.

[58] Rebecca J. Holmberg; Tomoko Aharen; Muralee Murugesu, Paramagnetic Nanocrystals: Remarkable Lanthanide-Doped Nanoparticles with Varied Shape, Size, and Composition. *The Journal of Physical Chemistry Letters* **2012**, *3* (24), 3721-3733.

[59] Guo Gao; Chunlei Zhang; Zhijun Zhou; Xin Zhang; Jiebing Ma; Chao Li; Weilin Jin; Daxiang Cui, One-pot hydrothermal synthesis of lanthanide ions doped one-dimensional upconversion submicrocrystals and their potential application *in vivo* CT imaging. *Nanoscale* **2013**, *5* (1), 351-362.

- [60] C. Ma; J.-Q. Yan; K. W. Dennis; R. W. McCallum; X. Tan, Size-dependent magnetic properties of high oxygen content  $\text{YMn}_2\text{O}_{5\pm\delta}$  multiferroic nanoparticles. *Journal of Applied Physics* **2009**, *105* (3), 033908.
- [61] Lei Lei; Daqin Chen; Ping Huang; Ju Xu; Rui Zhang; Yuansheng Wang, Modifying the size and uniformity of upconversion  $\text{Yb/Er:NaGdF}_4$  nanocrystals through alkaline-earth doping. *Nanoscale* **2013**, *5* (22), 11298-11305.
- [62] R. Mihai; I. P. Florescu; V. Coroiu; A. Oancea; M. Lungu, *In vitro* biocompatibility testing of some synthetic polymers used for the achievement of nervous conduits. *Journal of Medicine and Life* **2011**, *4* (3), 250-255.
- [63] Maja Stanisavljevic; Sona Krizkova; Marketa Vaculovicova; Rene Kizek; Vojtech Adam, Quantum dots-fluorescence resonance energy transfer-based nanosensors and their application. *Biosensors and Bioelectronics* **2015**, *74*, 562-574.
- [64] Karen French; Lyndon Jones, A decade with silicone hydrogels: Part 1. *Optometry Today* **2008**, *48* (16), 42-46.
- [65] M. Lira; L. Santos; J. Azeredo; E. Yebra-Pimentel; M. Elisabete C. D. Real Oliveira, Comparative study of silicone-hydrogel contact lenses surfaces before and after wear using atomic force microscopy. *Journal of Biomedical Materials Research Part B: Applied Biomaterials* **2008**, *85B* (2), 361-367.
- [66] Javier Pozuelo; Vicente Compañ; J. M. González-Méjome; María González; Sergio Mollá Oxygen and ionic transport in hydrogel and silicone-hydrogel contact lens materials: An experimental and theoretical study. *Journal of Membrane Science* **2014**, *452*, 62-72.
- [67] D. M. Bubb; B. R. Ringeisen; J. H. Callahan; M. Galicia; A. Vertes; J. S. Horwitz; R. A. McGill; E. J. Houser; P. K. Wu; A. Piqué; D. B. Chrisey, Vapor deposition of intact polyethylene glycol thin films. *Applied Physics A* **2001**, *73* (1), 121-123.
- [68] Katarzyna Rodrigo; Pawel Czuba; Bo Toftmann; Jørgen Schou; Roman Pedrys, Surface morphology of polyethylene glycol films produced by matrix-assisted pulsed laser evaporation (MAPLE): Dependence on substrate temperature. *Applied Surface Science* **2006**, *252* (13), 4824-4828.
- [69] P. Yin; G. B. Huang; W. H. Tse; Y. G. Bao; J. Denstedt; J. Zhang, Nanocomposited silicone hydrogels with a laser-assisted surface modification for inhibiting the growth of bacterial biofilm. *Journal of Materials Chemistry B* **2015**, *3* (16), 3234-3241.

## Chapter 5

### 5 Development of Carbon Dots/Graphene Oxide Glucose Biosensor

#### 5.1 Introduction

In this chapter, a facile microwave-assisted polyol process was developed to prepare fluorescent carbon dots. Graphene oxide was synthesized by the typical Hummers' method. A Glucose nanobiosensor was developed based on the carbon dots and graphene oxide for demonstration of carbon dots application in biosensing area. Both carbon dots and graphene oxide are highly biocompatible. We found that the photoluminescence of carbon dots could be adjusted by simply varying the ratio of carbon source to ethylene glycol, which has not yet been reported before. Other methods for preparing different photoluminescent carbon dots often used oxidative/reductive and/or acid/alkaline chemicals. Our method is facile and environmental friendly. The tunable photoluminescence range could extend from 470 nm to 540 nm in this system (excitation of 400 nm).

Carbon dots are a new member of carbon nanomaterials, the other carbon nanomaterials include graphene nanomaterials, carbon nanotube, bucky ball etc. [1] Their attracted properties include good biocompatibility, inertness, facile surface modification and special photoluminescent properties. [2-3] Various synthetic approaches have been explored for preparing carbon dots from bottom-up and/or top-down paths. [4-6] Due to carbon dots favorable fluorescence and low cytotoxicity, they have been broadly applied in areas of biosensing and bioimaging etc. [7-12] However, the mechanisms of carbon dots special fluorescence properties are still under debate among investigators. [13-17]

Microwave-assisted synthesis and modification of carbon nanomaterials has been explored due to carbon materials' strong interaction with microwave radiation. [18] Microwave assisted approach represents energy-saving and time-saving strategy for carbon dots

synthesis. Other common methods for carbon dots like hydrothermal method would often require several hours or days, high temperature and high pressure procedures. Many research groups used microwave to fast synthesize carbon dots. [19-23] Different carbon dots could show excitation-dependent or excitation-independent fluorescence. For multicolour carbon dots preparation, the reaction parameters like reaction temperature, reaction additives, doping elements (N, S etc.), pH, reaction time etc. have been widely investigated. [24-27]

Herein, we developed a facile strategy of synthesizing photoluminescent adjustable carbon dots at a certain range (470 nm to 540 nm under excitation of 400 nm) by varying precursors' concentrations. Zhu et al. [28] has prepared varied precursor concentrations carbon dots, but the fluorescence change of the carbon dots was within 10 nm range. Our method could tune carbon dots emission shift up to 70 nm range (sample 1 at 470 nm and sample 4 at 540 nm under 400 nm excitation). Fluorescent nanomaterials are affected by various parameters like surface states, solution pH, temperature etc. These parameters are needed for delicate consideration for nanomaterials *in vivo* and *in vitro* applications. In our carbon dots synthesis, the difference of all samples was the precursor concentration which could cause different carbon dots surface states. The main reason causing this phenomenon could be the different ratio of carbon precursors to ethylene glycol. Ethylene glycol is a reductive agents in the polyol process [29] which acts both as reaction solution and reductive agents. Comparatively, the solution of ethylene glycol was kept at the same volume in all the microwave assisted synthesis. The higher carbon precursor concentration environment are less reductive compared to lower precursor concentrations. As a result, the higher precursor carbon dots would have a higher oxidative surface state, therefore they were red-shifted. This speculation was in consistent with other references. [30-31] A higher oxidative surface state of carbon dots could cause the red-shift phenomenon.

At the same time, even though different samples of carbon dots displayed different colours under 312 nm UV panel excitation, each sample also behaved the typical excitation-dependent fluorescence properties (figure 5.9). Although the mechanism for this photoluminescence change has not been fully explained. This facile synthesis of carbon source concentration-induced multicolour carbon dots provided a multicolour platform for



many applications like electronic display, printing inks, and biosensors. The synthesized carbon dots were further constructed as glucose nanobiosensor. We developed a nanostructured glucose biosensor by using fluorescence resonance energy transfer (FRET) technique. Fluorescence resonance energy transfer (FRET) is an inexpensive and very sensitive method and has been used in molecule imaging and glucose test. [32-34] FRET is a distance-dependent energy transfer process from a fluorophore donor (D) to a fluorophore acceptor (A) in a nonradioactive process. FRET technique has been utilized for sensing the competitive reactions of glucose and other polysaccharide, such as dextran, to Concanavalin A (Con A) (a lectin protein that can bind glucose). [35-37]

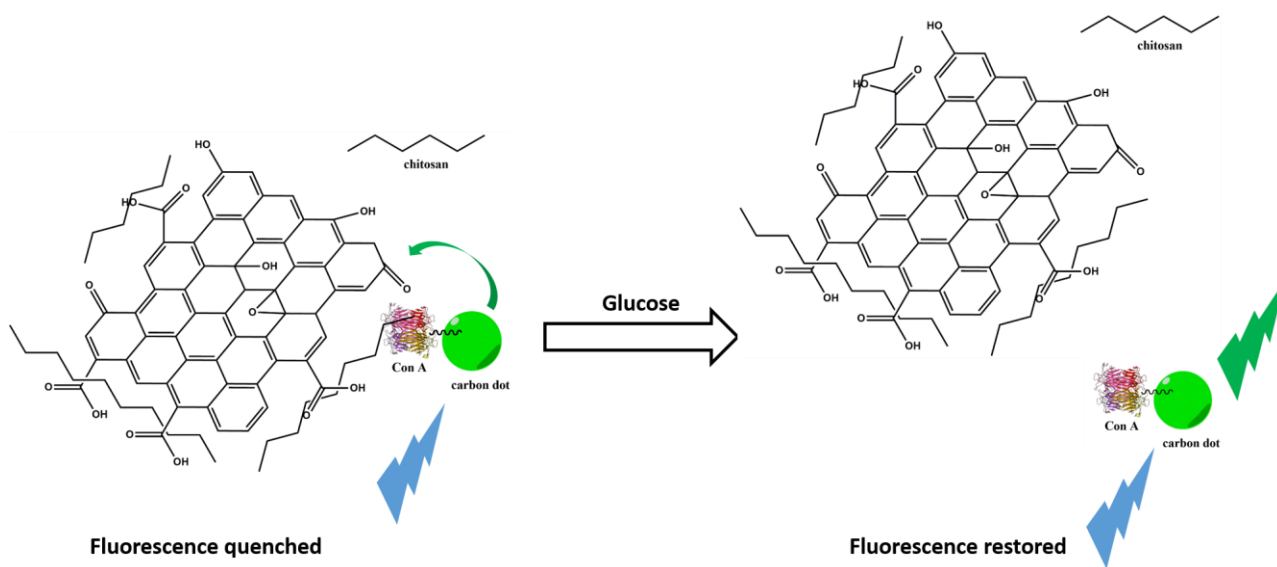


**Figure 5.1 Schematic mechanism of carbon dots/graphene oxide glucose nanobiosensor.**

In this study, we constructed a novel FRET glucose nanobiosensor using carbon dots (fluorescence donor) and graphene oxide (fluorescence acceptor, quencher). Both carbon dots and graphene oxide are highly biocompatible. [38-40] Various studies showed the biocompatibility of carbon dots and graphene oxide. Also the compositions of them are mostly carbon elements and hydrogen elements. As shown in figure 5.1, Concanavalin A (Con A) was bioconjugated onto carbon dots surface, the graphene oxide was modified with chitosan as the fluorescence quenching component. Carbon dots-Con A (CD-CA) were binding to the graphene oxide-chitosan (GO-CS) and the fluorescence was quenched

by the graphene oxide. The chitosan we used here are small molecule weight chitosan which are not so sticky. After the glucose was introduced, the CD-CA were released from the GO-CS and as a result, the carbon dots fluorescence was recovered.

## 5.2 Experimental

### 5.2.1 Materials

Citric acid (251275), L-histidine (H8000,  $\geq 99\%$ ), dialysis tube (PRUG10020, MWCO 1 kDa), Concanavalin A from *Canavalia ensiformis* (Jack bean) (C2010), N-(3-Dimethylaminopropyl)-N'-ethylcarbodiimide hydrochloride (03450), N-Hydroxysuccinimide (130672), Chitosan (448877) were purchased from Sigma-Aldrich. Graphite flake, natural, -325 mesh, 99.8% (metals basis) (CAAA43209-18) was purchased from VWR. Ethylene glycol was purchased from Caledon laboratories Ltd. All chemicals were used as received. Graphite flakes (natural, -325 mesh, 99.8%) was purchased from VWR International. Paraffin oil was purchased from Caledon Laboratory Chemicals. Sulfuric acid ( $\text{H}_2\text{SO}_4$ , 95.0 % – 98.0 %), potassium persulfate ( $\text{K}_2\text{S}_2\text{O}_8$ ), phosphorus pentoxide ( $\text{P}_2\text{O}_5$ ), Potassium permanganate ( $\text{KMnO}_4$ ), hydrogen peroxide ( $\text{H}_2\text{O}_2$ , 30 wt. %), hydrochloric acid (37 %), hydrazine solution (35 wt. %), ammonium hydroxide solution (28.0–30.0 wt. %) were purchased from Sigma-Aldrich. The water used in experiments were of 18.2 M $\Omega$  resistivity provided by Barnstead Water Purification System.

### 5.2.2 Preparation of Carbon Dots

A polyol microwave assisted method was adopted in the preparation of carbon dots. [41-42] For synthesizing the carbon dots used for constructing the glucose nanobiosensor, a typical process was as following: in a 20 mL glass vial, 100 mmol ethylene glycol, 0.5 mmol L-histidine and 0.5 mmol citric acid were added into the vial and mixed well. Then the vial was put in a home microwave oven and heated for 20 minutes. The deep brown color indicated the formation of carbon dots. The solutions was dialyzed against water and freeze-dried to obtain carbon dots powder sample. The powder samples were stored in 4 °C. For synthesizing a series of photoluminescent carbon dots, the chemical quantity were showed in table 5.1. Five samples were prepared.

**Table 5.1 Summary of carbon source and ethylene glycol quantity.**

Sample	Ethylene glycol (EG) (mmol)	Histidine (mmol)	Citric acid (mmol)	Carbon source to EG ratio (%)	Particle size (nm)
1	100	0.1	0.1	0.2	25±1.52
2	100	0.3	0.3	0.6	40±2.13
3	100	0.5	0.5	1.	19±1.12
4	100	1	1	2	40±2.12
5	100	3	3	6	25±1.91

### 5.2.3 Preparation of CD-Con A Conjugates:

1 mg carbon dots were firstly dissolved in 10 mL PBS buffer (0.1 mg/mL). EDC (1 mg) and sulfo-NHS (3 mg) were added to the carbon dots solution. The mixture was shaken for 1.5 hour at room temperature. Then the mixture was put to dialysis to remove excess small molecules. Then 2 mg Con A (dissolved in 2 mL PBS) was added and shaken at 4 °C for 2 hours, the solution was dialyzed against water and stored in 4 °C for future usage.

### 5.2.4 Preparation of Graphite Oxide

The graphite flakes were first preoxidized according to reference. [43] The oxidizing solution was prepared by adding 10 g of potassium persulfate and 10 g of phosphorus pentoxide into 30 mL concentrated sulfuric acid. Then 20 g of graphite flakes was added into the oxidizing solution. The oxidization process was continued under stirring and at 80 °C for a period of 6 hours. The mixture was diluted with water, filtered and washed until pH became neutral. The preoxidized graphite flakes was dried in air at room temperature.

The graphite oxide was prepared according to Hummers' method. [44] The preoxidized graphite flakes (10 g) were added into 230 mL cold concentrated sulfuric acid in ice-water bath. Then 30 g  $\text{KMnO}_4$  was added gradually with stirring and cooling so to keep the temperature of the mixture below 20 °C. Then the mixture was stirred at 35 °C for 2 hours. Then the mixture was diluted by 1,500 mL water and the reaction was terminated by adding 25 mL  $\text{H}_2\text{O}_2$  (30 wt. %). The mixture color changed into bright yellow. The graphite oxide was filtered and washed by 2,500 mL diluted HCl (3.7%) to remove metal ions and then washed by plenty water. The product was dried in air at room temperature. To completely remove the metals ions and acid, the graphite oxide was suspended in water to prepare a viscous, brown 2 wt. % dispersion and put to dialysis. Purified graphite oxide suspension was diluted into a 0.05 wt. % dispersion and used for following experiments.

### 5.2.5 Preparation of Graphene Oxide Solution

Graphene oxide was obtained by ultrasonication exfoliation of the 0.05 wt. % graphite oxide dispersion for 30 minutes. The obtained dispersion was centrifuged at 3,000 rpm for 30 minutes to remove unexfoliated graphite oxide.

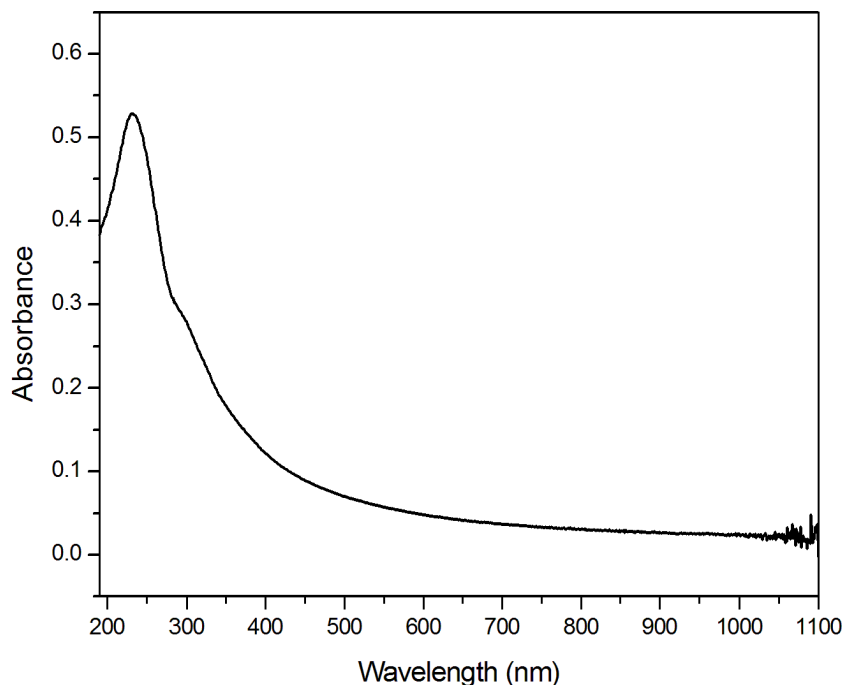


**Figure 5.2 UV-vis spectrum of graphene oxide solution.**

Figure 5.2 showed the UV-vis spectrum of graphene oxide solution, it has an absorbance peak of 231 nm. This result is consistent with previous reports, [45-46] confirming the successful preparation of graphene oxide.

### 5.2.6 Preparation of GO-CS Conjugates:

Graphene oxide solution (0.05 mg/mL) 10 mL was reacted with 2 mg EDC for 1 hour at room temperature. Then 2 mg chitosan was added and reacted overnight. Final product was dialyzed against water and stored in 4 °C for future usage.

### 5.2.7 GO-CS Titration

GO-CS concentrations were varied. Carbon dots 200  $\mu$ L (0.1 mg/mL) mixed with 200  $\mu$ L GO-CS solutions and incubated for 1 hour before fluorescence measurement.

### 5.2.8 Glucose Nanobiosensing

In a typical sensing process, 100  $\mu$ L CDs-Con A solution was mixed with 100  $\mu$ L (5  $\mu$ g/mL) GO-CS solution. Thereafter, varied concentration glucose (1  $\mu$ L) were added and incubated for 1.5 hour before fluorescence measurement. 1 mM–10 mM: Carbon dots-Con A 100  $\mu$ L, GO-CS 100  $\mu$ L, 5  $\mu$ g/mL; 0.2 mM–1 mM: Carbon dots-Con A 10  $\mu$ L + 90  $\mu$ L water, GO-CS 100  $\mu$ L, 1  $\mu$ g/mL; the mixture was put on a shaker for shaking 40 minutes at 120 RPM before measure their fluorescence. For the rat blood samples sensing, the aqueous glucose solution was replaced by rat blood samples.

### 5.2.9 Rat Blood Samples

This part was cooperated with Dr James Melling lab (Kinesiology, UWO). Four male Sprague-Dawley rats (Charles River Laboratories, St. Constant, QC, Canada) were housed in a 12-h light/dark cycle room with humidity (50%) and temperature (21.5 °C) kept constant. Rats were given water and chow ad libitum and made diabetic with streptozotocin (STZ; Sigma-Aldrich, Oakville, ON, Canada). Intraperitoneal injections of STZ (20 mg/kg) dissolved in a citrate buffer (0.1 M, pH 4.5) were given over five consecutive days. Following the confirmation of diabetes (two blood glucose readings greater than 18 mmol/L) subcutaneous insulin pellets were implanted in the abdominal region of rats. A

blood sample was taken from the saphenous vein and measured blood glucose concentration by a glucometer (Freestyle Lite Blood Glucose Monitoring System, Abbott Diabetes Care Inc., Mississauga, Ontario).

Ethics approval was obtained through the University of Western Ontario Research Ethics Board, in accordance with Canadian Council on Animal Care guidelines.

### 5.2.10 Characterizations

The fluorescent emission spectrum of carbon dots aqueous solutions were measured by fluorophotometry (QuantaMaster TM 30, PTI). The size and morphology of the carbon dots were measured by transmission electron microscope (TEM, Philips CM-10 transmission electron microscope operating at 80 kV). Fourier transform infrared (FTIR, Bruker Vector 22 in the range of  $400\text{ cm}^{-1}$ – $4000\text{ cm}^{-1}$ ) was used to obtain FTIR spectrum. UV-vis spectrum were obtained by Agilent Cary 60 UV-Vis.

## 5.3 Results and Discussion

### 5.3.1 Photoluminescent Tunable Carbon Dots

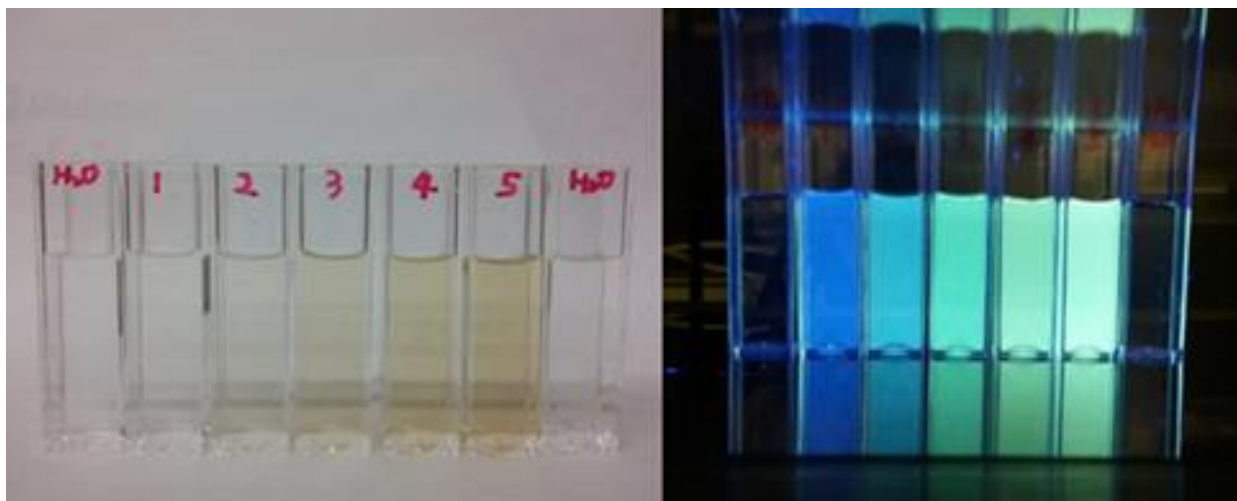


**Figure 5.3 Photo image of carbon dots under room light and under 312 nm excitation from UV panel.**

Varied carbon dots samples solution were prepared in the concentration of 0.1 mg/mL. Figure 5.3 showed the carbon dots solution under ambient light and under the UV panel of

312 nm excitation light. In the ambient environment, slightly yellow colour change were observed and the colour deepened from sample 1 to sample 5. Under the UV panel excitation (312 nm), varied colour emission were presented from blue emission to green emission to light yellow colour.

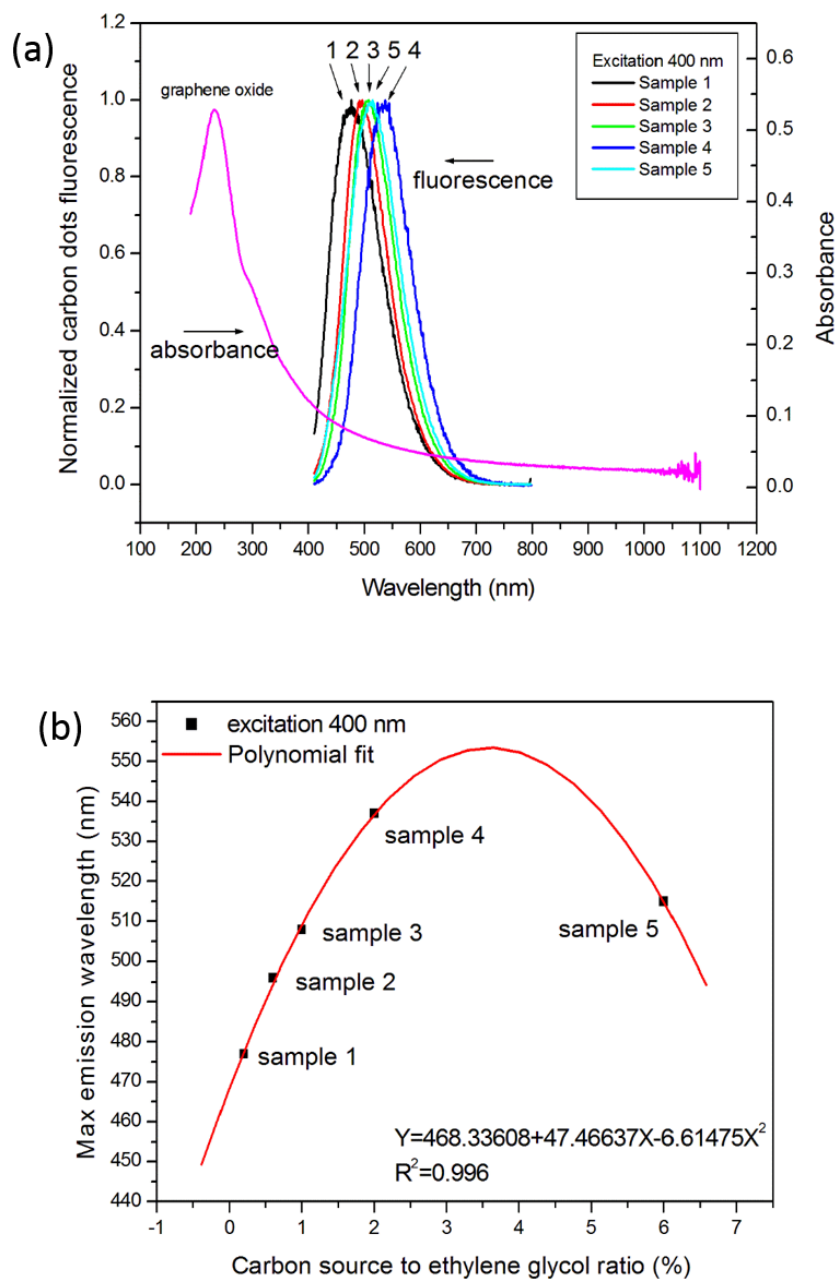


**Figure 5.4 (a) Photoluminescence spectrum of color tunable carbon dots excited by 400 nm and UV-vis absorbance spectrum of graphene oxide solution; (b) Emission peaks of carbon dots samples versus carbon source/ethylene glycol ratio (%).**

The fluorescence spectrum of the carbon dots (0.1 mg/mL) was recorded as shown in figure 5.4 (a). Excitation of 400 nm was used to obtain the photoluminescence spectra. Sample 1 to sample 5 has emission peaks at 477 nm, 496 nm, 508 nm, 537 nm and 515 nm, respectively. The emission peak of sample 5 went back to about the same emission peak position as sample 3. Figure 5.4 (b) showed the relationship of fluorescence emission peaks and the ratio of carbon source to ethylene glycol (under excitation of 400 nm). A polynomial fitting was applied with equation below, with  $R^2=0.996$ .

$$Y = 468.34 + 47.47X - 6.61X^2$$

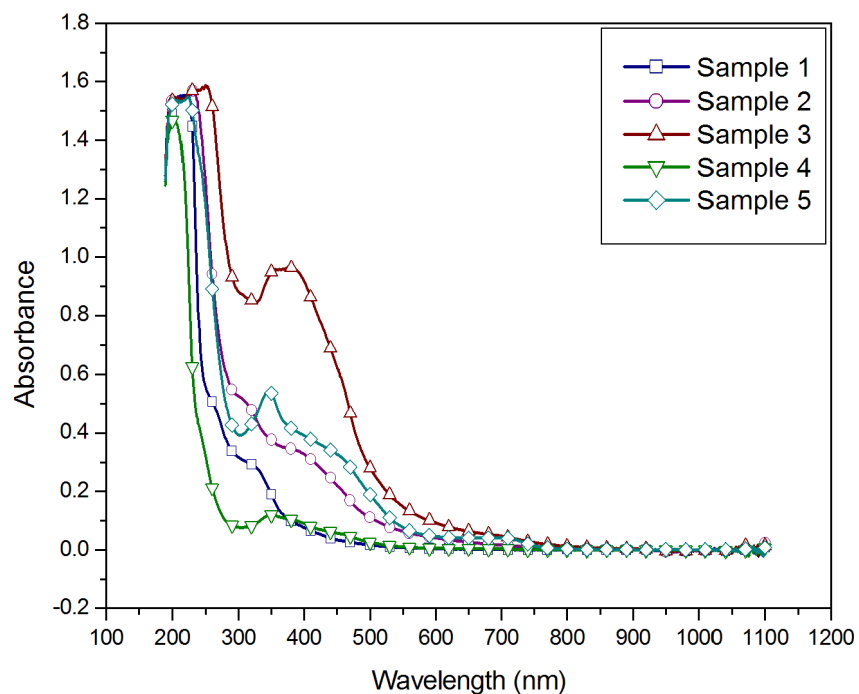


**Figure 5.5 UV-vis absorbance spectrum of carbon dots samples.**

The UV spectra of various carbon dots solution were measured and shown in figure 5.5. Typical absorbance curves of carbon dots were obtained similar to other research results. [47-50] Sample 3 and sample 5 has an obvious absorbance peak in 300 nm to 500 nm range. Sample 1, sample 2 and sample 4 showed comparatively weak absorbance peak in 300 nm to 500 nm range.



### 5.3.2 TEM Images of Carbon dots

TEM images of various carbon dots samples were measured (figure 5.6 and figure 5.7), but there was not a clearly relationship between the carbon dots particle size and their fluorescence. Although there was reports of nanoparticles size causing fluorescence changes, however, this was not the situation. Though the mechanism for precursor amount induced fluorescence change was not yet fully understood. This facile photoluminescent tunability provided an easy and environmental friendly method for producing certain colour emission of carbon dots. Due to the carbon composition of carbon dots, they normally possessed high biocompatibility and were very suitable for applications such as biosensing, bioimaging.

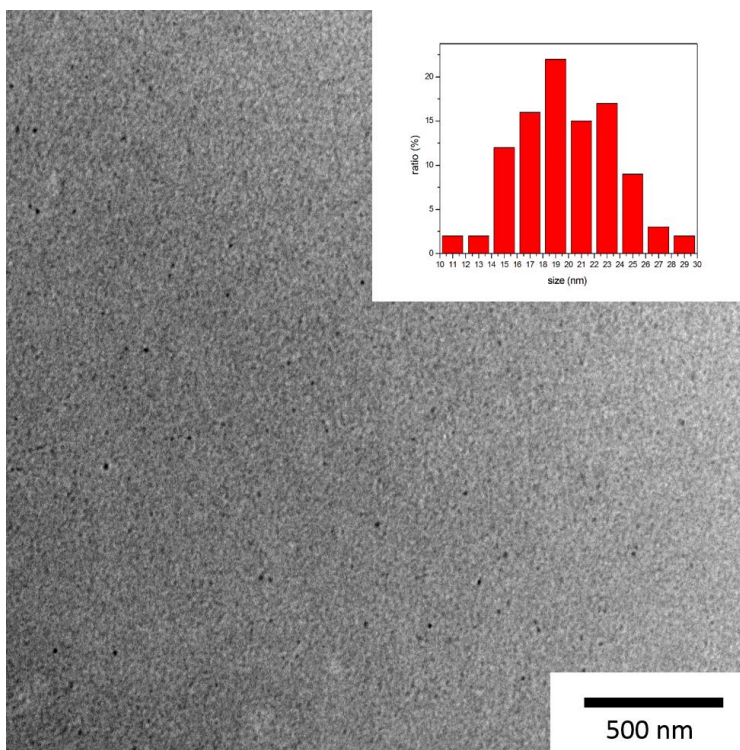


**Figure 5.6 TEM image of sample 3 carbon dots.**

The following parts were focused on constructing biocompatible glucose nanobiosensor based on sample 3 carbon dots. Figure 5.6 showed the TEM image of sample 3. It has an average particle size of about  $19 \pm 1.2$  nm. Figure 5.7 showed the TEM images of samples

1, 2, 4 and 5. Respectively, their average particle size were  $25\pm 1.52$  nm,  $40\pm 2.13$  nm,  $40\pm 2.12$  nm,  $25\pm 1.91$  nm.

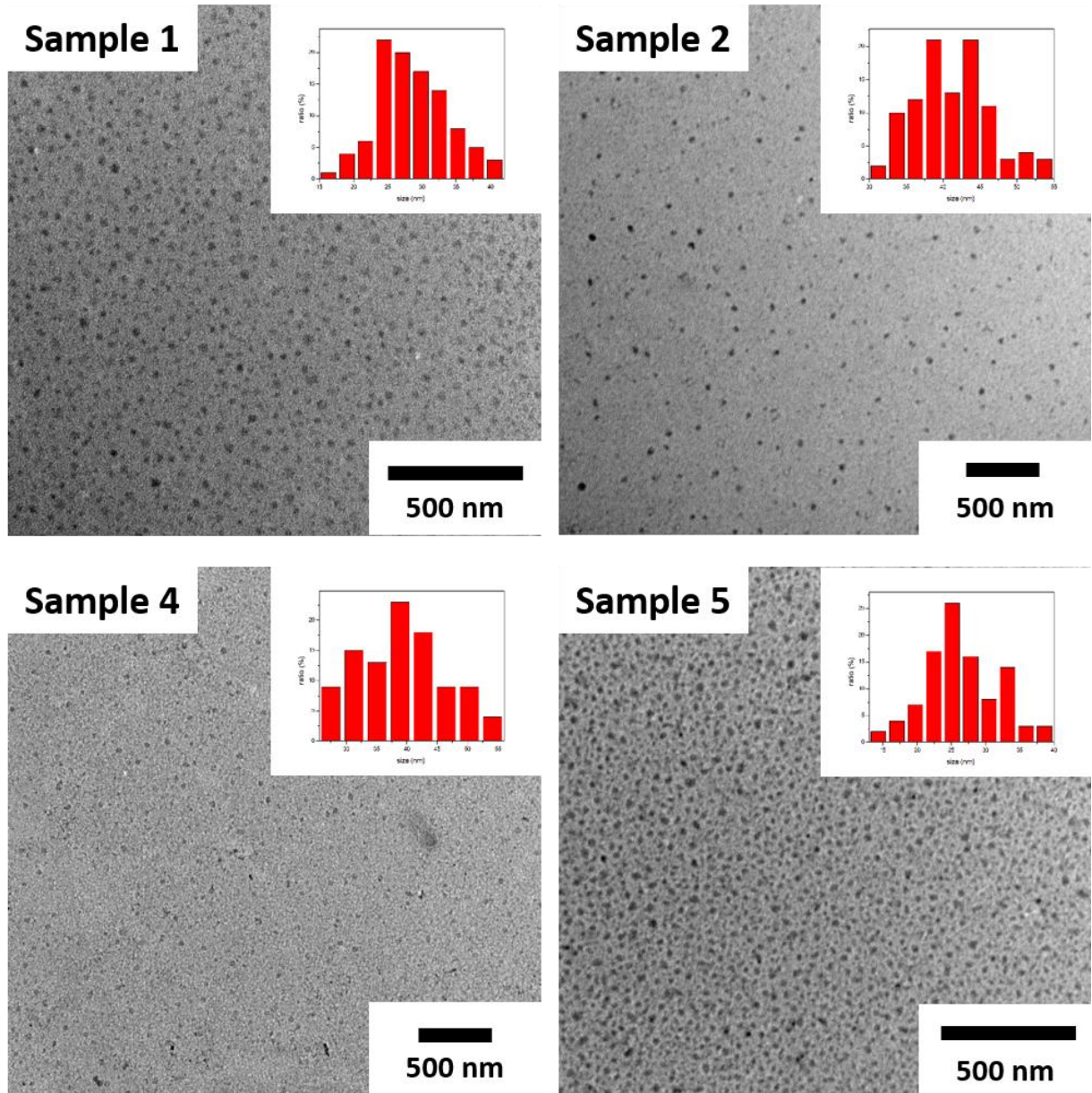


**Figure 5.7** TEM images of carbon dots sample 1, 2, 4 and 5.

### 5.3.3 Fluorescence of Carbon Dots and Carbon Dots-Con A Bioconjugate

Figure 5.8 showed the excitation-dependent fluorescence of carbon dots samples 1, 2, 4 and 5 (all 0.1 mg/mL). Figure 5.9 showed the carbon dots (sample 3 for the glucose nanobiosensor in the following text) fluorescence spectra. Typical excitation-dependent fluorescence was observed. The excitation wavelength changed from 340 nm to 500 nm with an increment of 20 nm. The strongest emission was located at about 500 nm by the excitation of 400 nm or 420 nm.

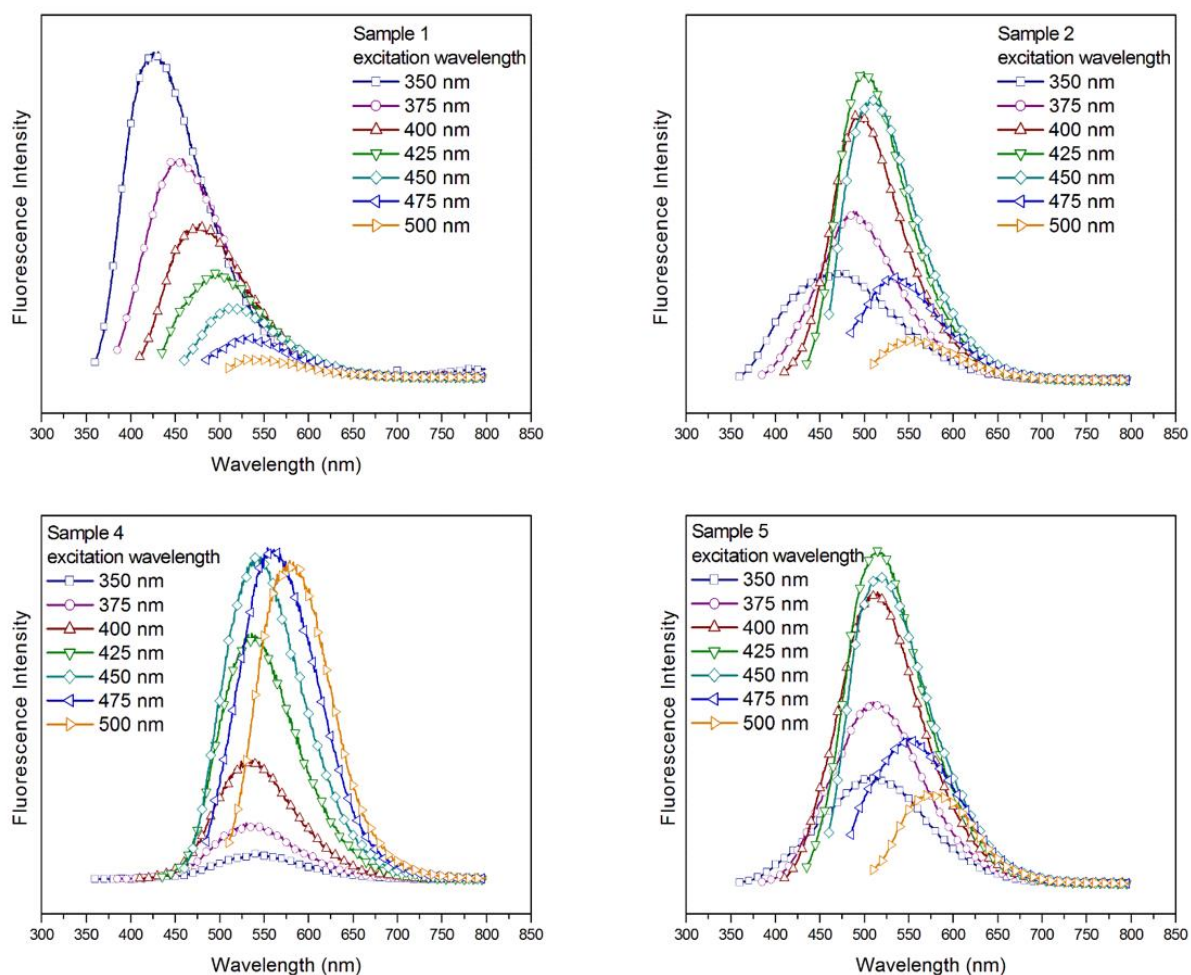


**Figure 5.8** Fluorescent spectrum of carbon dots sample of 1, 2, 4 and 5 (all 0.1 mg/mL).

The fluorescence of carbon dots-Con A bioconjugates were measured and shown in figure 5.10. Figure 5.10 showed similar pattern to figure 5.9 of unmodified carbon dots except

the twisted spectra were present. The spectrum curve twisted changes indicated the carbon dots fluorescence changed after the Con A bioconjugation. It reflected the Con A has been bioconjugated to the carbon dots. While the carbon dots-Con A bioconjugate remained the excitation-dependent fluorescence. The maxima emission peak was at 492 nm at the excitation of 400 nm.

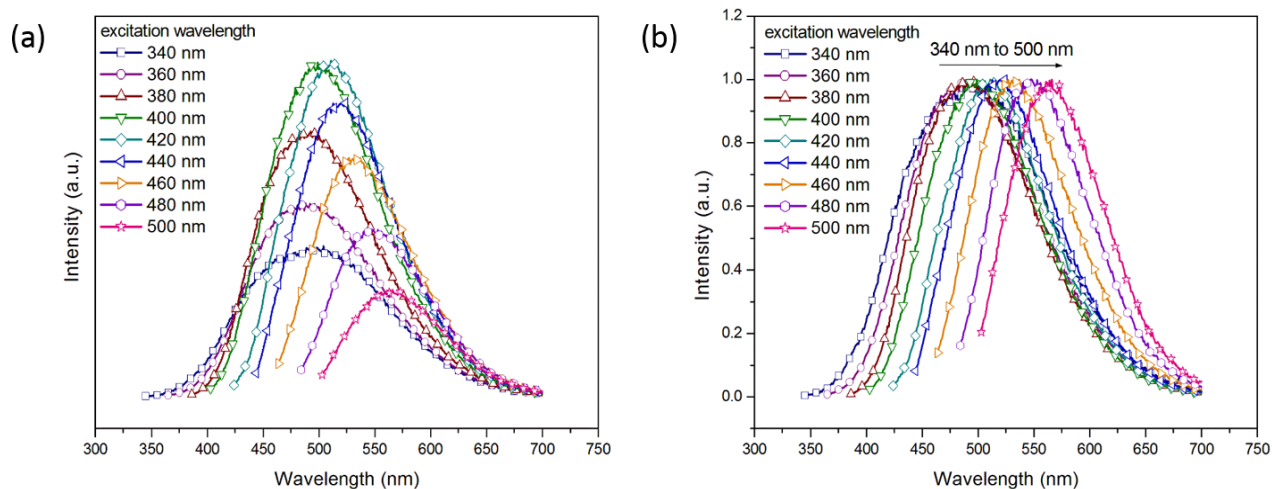


**Figure 5.9** Fluorescence spectrum of sample 3 carbon dots, (a) Measured spectrum and (b) Normalized fluorescence intensity spectrum.

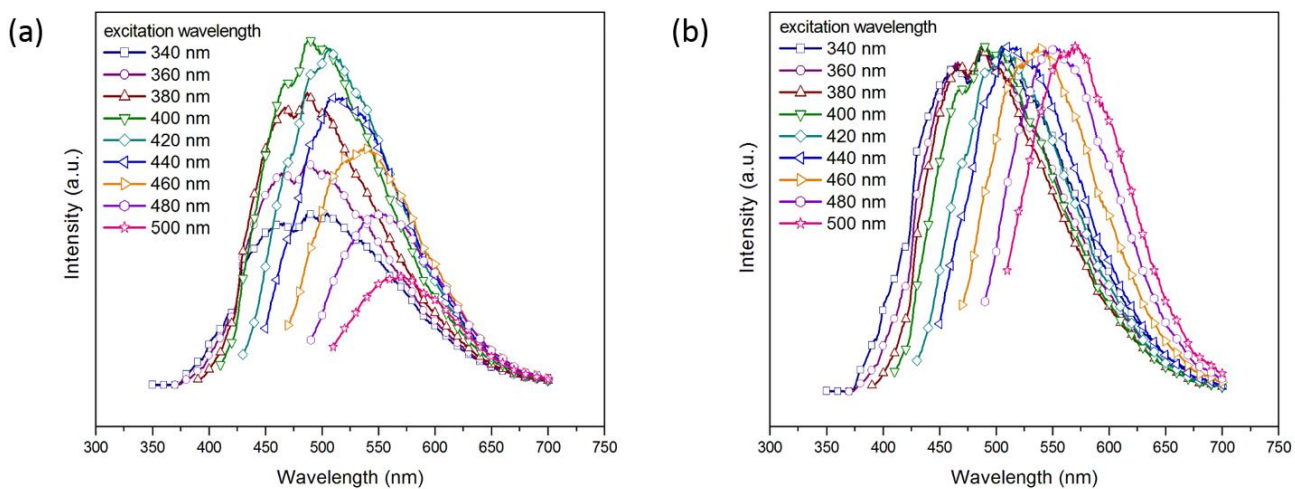


**Figure 5.10** Fluorescence spectrum of bioconjugate Con A-carbon dots (sample 3), (a) Measured spectrum and (b) Normalized spectrum.

### 5.3.4 UV-vis Spectrum

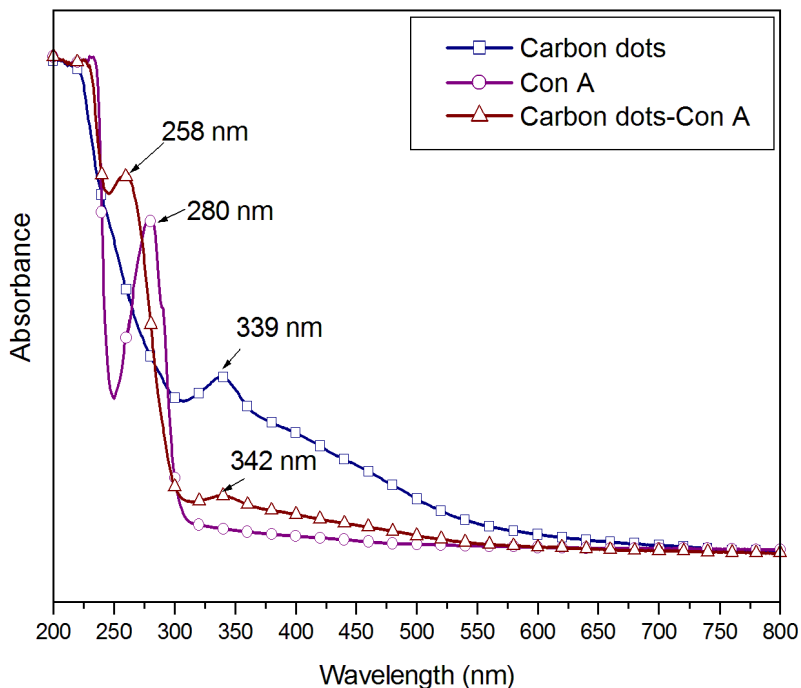


**Figure 5.11 UV-Vis absorbance spectrum of carbon dots, Con A and carbon dots-Con A bioconjugate.**

Con A and carbon dots-Con A bioconjugate were measured to confirm the successful bioconjugation. Figure 5.11 showed the UV-Vis spectra of carbon dots, Con A and Con A-carbon dots bioconjugate. Carbon dots have an absorbance peak at 339 nm, Con A has an absorbance peak at 280 nm. The bioconjugate of carbon dots-Con A has two peaks and the two peaks position were slightly shifted from single component peak. The two peaks position were at 258 nm (shifted from Con A absorbance peak at 280 nm) and 342 nm (shifted from carbon dots peak at 339 nm). The bioconjugate has two shifted peaks compared to their single components. This indicated the successful bioconjugation of Con A to carbon dots. [51-52]

### 5.3.5 FTIR Spectrum

Figure 5.12 showed the FTIR spectrum of graphene oxide, graphene oxide-chitosan conjugate and chitosan. The FTIR spectra indicated successful conjugation of chitosan onto graphene oxide. The peaks of graphene oxide-chitosan conjugate in the  $2981\text{ cm}^{-1}$  and  $2884$

$\text{cm}^{-1}$  indicated the  $-\text{CH}_2-$  groups from chitosan. The graphene oxide peak at  $1714 \text{ cm}^{-1}$  disappeared in the GO-CS conjugate showed the EDC conjugation of chitosan to the carboxylic groups on graphene oxide. The amine group peaks of  $1621 \text{ cm}^{-1}$  and  $1542 \text{ cm}^{-1}$  of chitosan shifted to  $1631 \text{ cm}^{-1}$  and  $1567 \text{ cm}^{-1}$  in the GO-CS chitosan also indicated the bond status changed after conjugation. [53]

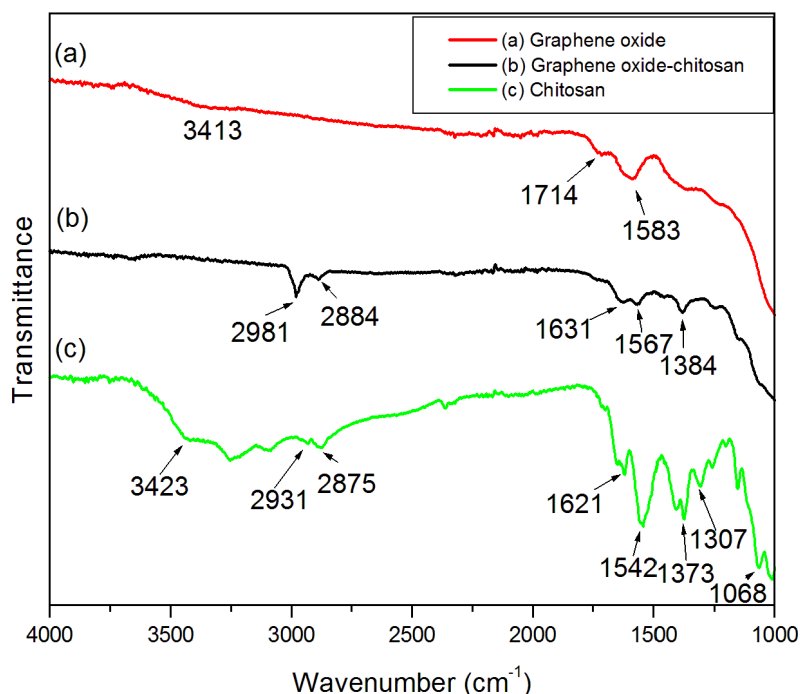


**Figure 5.12** FTIR spectrum of (a) graphene oxide, (b) graphene oxide-chitosan and (c) chitosan.

### 5.3.6 GO-CS Titration of Con A-Carbon Dots

Varied GO-CS concentration solution were mixed and incubated with certain carbon dots-Con A bioconjugate solutions. The fluorescence results were measured as shown in figure 5.13. The quenching effects of GO-CS were clearly presented and a linear quenching effects was observed. As the GO-CS concentration increased from  $0 \mu\text{g/mL}$  to  $10 \mu\text{g/mL}$ , the fluorescence of carbon dots were heavily quenched. The curve data were collected from the intensity at  $492 \text{ nm}$ .

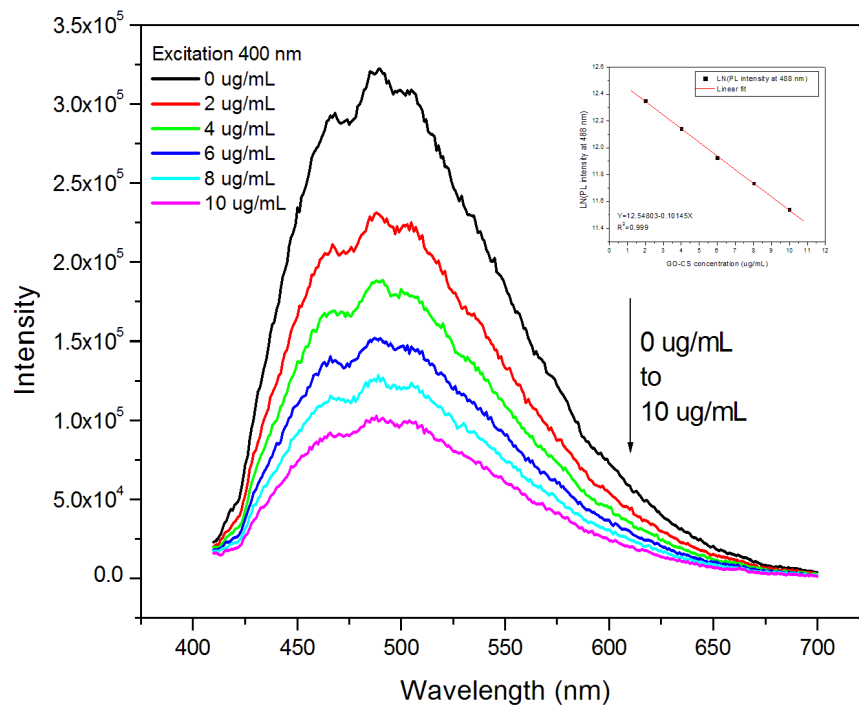


**Figure 5.13 Fluorescence spectra of GO-CS titration of Con A-carbon dots.**

### 5.3.7 Glucose Nanobiosensing

The glucose biosensing of two range of glucose levels were performed as data shown in figure 5.14, one glucose range was in the blood glucose level of 1 mM to 10 mM. Another glucose range was in the tear glucose range of 0.2 mM to 1 mM. Both results suggested good linear data. Except the lower glucose level biosensing showed less linearity. The reason may be due to the higher signal to noise ratio. In the 1 mM to 10 mM range, a higher concentration of graphene oxide-chitosan and carbon dots-Con A were used. In the lower glucose concentration of 0.2 mM to 1.0 mM, a lower concentration of carbon dots nanobiosensor were used in order to enlarge the signal-to-noise ratio.

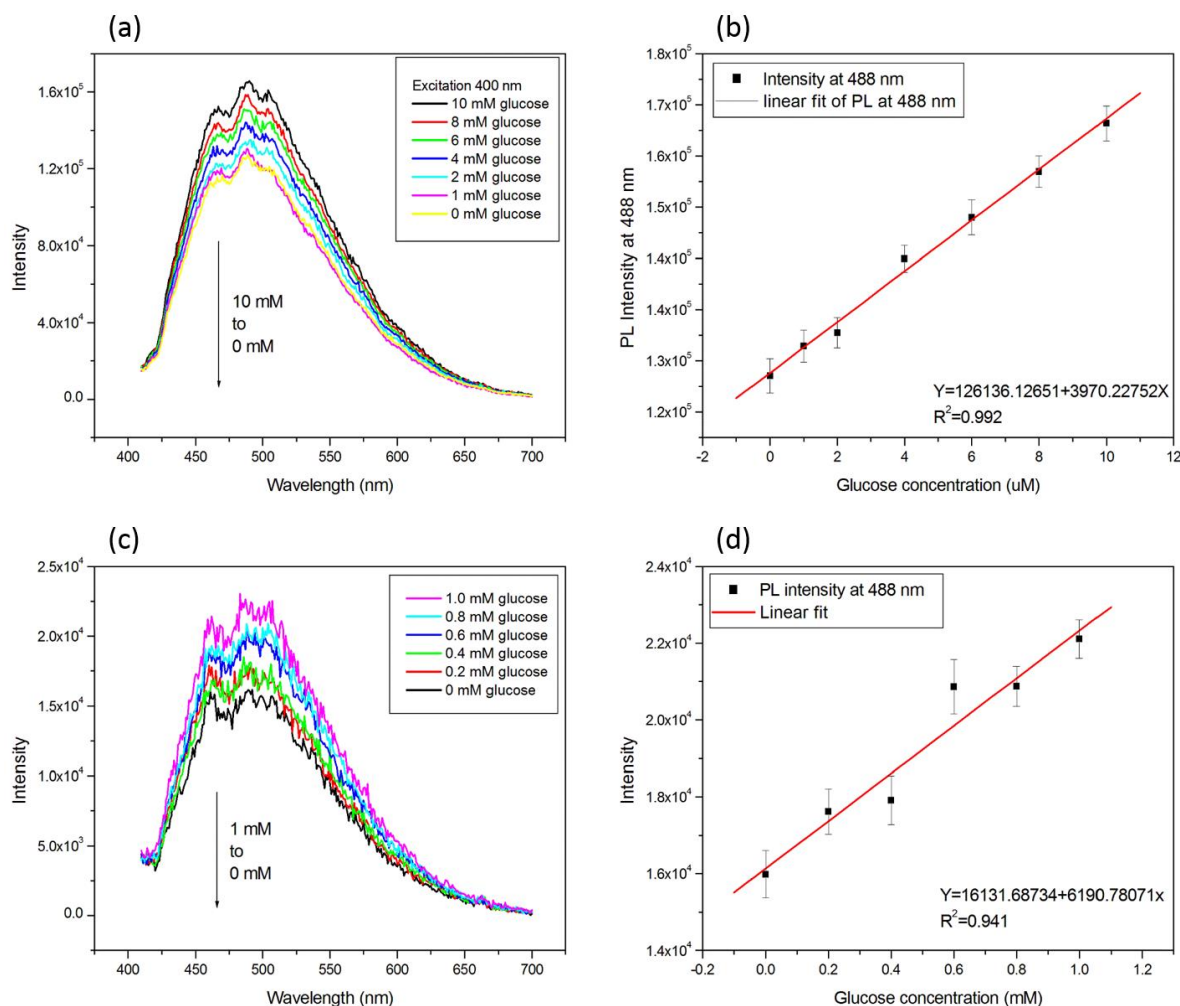


**Figure 5.14** Glucose biosensing of two ranges of glucose level. (a) and (b) shows the sensing results of glucose level in 1 mM to 10 mM; (c) and (d) shows the sensing results of glucose in 0.2 mM to 1 mM.

Various diluted rat blood samples of glucose concentration of 3 mM, 4.5 mM, 6 mM, 7.5 mM, 9 mM and 10.5 mM were prepared by dilution of rat blood and measured by the carbon dots/graphene oxide nanobiosensor. The result was shown in figure 5.15, a good linearity was obtained. Compared to aqueous glucose solution (figure 5.14 (a) and (b)), the blood samples has a lower fluorescent intensity. This might be caused by the other interferents presented in the blood compositions, like red blood cell, blood platelet etc. These interferents could cause autofluorescence and attenuate the excitation light and



carbon dots fluorescence. Nonspecific binding of proteins onto carbon dots may also cause the decrease of fluorescent signal.

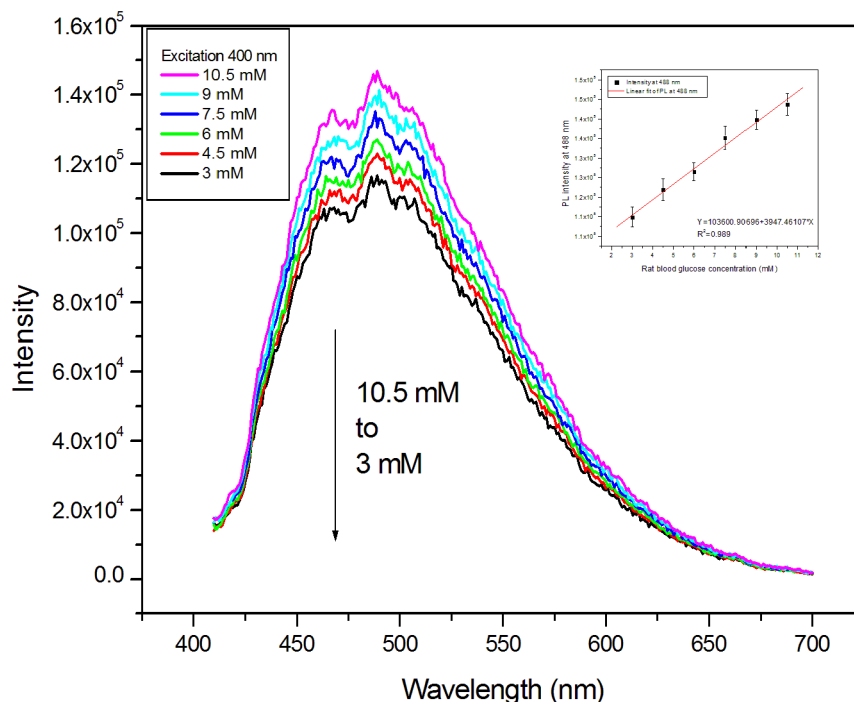


**Figure 5.15 Biosensing of diluted rat blood samples with glucose concentrations of 3 mM, 4.5 mM, 6 mM, 7.5 mM, 9 mM and 10.5 mM.**

## 5.4 Conclusion

A facile microwave assisted polyol synthesis of carbon dots method was developed. The photoluminescence of carbon dots could be adjusted at a certain range (470 nm to 540 nm under 400 nm excitation) by facile control of carbon source concentrations. Although the mechanism is not fully revealed, but this fluorescence control approach is facile and environmental friendly. Furthermore, a glucose nanobiosensor based on the carbon dots/graphene oxide was constructed for biosensing of glucose. Two glucose range of blood glucose level of 1 mM to 10 mM and tear glucose level of 0.2 mM to 1 mM were measured and good sensing results were obtained. We also measured the glucose concentration of a series of diluted rat blood samples and good linearity were obtained. The flexibility and broad sensing range of the carbon dots/graphene oxide nanobiosensor could be promising in glucose sensing.

## 5.5 References

- [1] Vasilios Georgakilas; Jason A. Perman; Jiri Tucek; Radek Zboril, Broad Family of Carbon Nanoallotropes: Classification, Chemistry, and Applications of Fullerenes, Carbon Dots, Nanotubes, Graphene, Nanodiamonds, and Combined Superstructures. *Chemical Reviews* **2015**, *115* (11), 4744-4822.
- [2] Sheila N Baker; Gary A Baker, Luminescent Carbon Nanodots: Emergent Nanolights. *Angewandte Chemie International Edition* **2010**, *49* (38), 6726-6744.
- [3] Haitao Li; Zhenhui Kang; Yang Liu; Shuit-Tong Lee, Carbon nanodots: synthesis, properties and applications. *Journal of Materials Chemistry* **2012**, *22* (46), 24230-24253.
- [4] Katerina Hola; Yu Zhang; Yu Wang; Emmanuel P. Giannelis; Radek Zboril; Andrey L. Rogach, Carbon dots-Emerging light emitters for bioimaging, cancer therapy and optoelectronics. *Nano Today* **2014**, *9* (5), 590-603.
- [5] Youfu Wang; Aiguo Hu, Carbon quantum dots: synthesis, properties and applications. *Journal of Materials Chemistry C* **2014**, *2* (34), 6921-6939.
- [6] Ruquan Ye; Changsheng Xiang; Jian Lin; Zhiwei Peng; Kewei Huang; Zheng Yan; Nathan P. Cook; Errol L. G. Samuel; Chih-Chau Hwang; Gedeng Ruan; Gabriel Ceriotti; Abdul-Rahman O. Raji; Angel A. Martí; James M. Tour, Coal as an abundant source of graphene quantum dots. *Nature Communications* **2013**, *4*, 2943.
- [7] Youxing Fang; Shaojun Guo; Dan Li; Chengzhou Zhu; Wen Ren; Shaojun Dong; Erkang Wang, Easy Synthesis and Imaging Applications of Cross-Linked Green Fluorescent Hollow Carbon Nanoparticles. *ACS Nano* **2012**, *6* (1), 400-409.
- [8] Jing Tang; Biao Kong; Hao Wu; Ming Xu; Yongcheng Wang; Yanli Wang; Dongyuan Zhao; Gengfeng Zheng, Carbon Nanodots Featuring Efficient FRET for Real-Time Monitoring of Drug Delivery and Two-Photon Imaging. *Advanced Materials* **2013**, *25* (45), 6569-6574.
- [9] Chih-Wei Lai; Yi-Hsuan Hsiao; Yung-Kang Peng; Pi-Tai Chou, Facile synthesis of highly emissive carbon dots from pyrolysis of glycerol; gram scale production of carbon dots/mSiO<sub>2</sub> for cell imaging and drug release. *Journal of Materials Chemistry* **2012**, *22* (29), 14403-14409.
- [10] Jia Zhang; Shu-Hong Yu, Carbon dots: large-scale synthesis, sensing and bioimaging. *Materials Today* **2016**, *19* (7), 382-393.
- [11] Prathik Roy; Po-Cheng Chen; Arun Prakash Periasamy; Ya-Na Chen; Huan-Tsung Chang, Photoluminescent carbon nanodots: synthesis, physicochemical properties and analytical applications. *Materials Today* **2015**, *18* (8), 447-458.
- [12] Xiangcheng Sun; Yu Lei, Fluorescent carbon dots and their sensing applications. *TRAC Trends in Analytical Chemistry* **2017**, *89*, 163-180.

- [13] Shoujun Zhu; Yubin Song; Xiaohuan Zhao; Jieren Shao; Junhu Zhang; Bai Yang, The photoluminescence mechanism in carbon dots (graphene quantum dots, carbon nanodots, and polymer dots): current state and future perspective. *Nano Research* **2015**, *8* (2), 355-381.
- [14] Volker Strauss; Johannes T. Margraf; Christian Dolle; Benjamin Butz; Thomas J. Nacken; Johannes Walter; Walter Bauer; Wolfgang Peukert; Erdmann Spiecker; Timothy Clark; Dirk M. Guldi, Carbon Nanodots: Toward a Comprehensive Understanding of Their Photoluminescence. *Journal of the American Chemical Society* **2014**, *136* (49), 17308-17316.
- [15] Marta J. Krysmann; Antonios Kelarakis; Panagiotis Dallas; Emmanuel P. Giannelis, Formation Mechanism of Carbogenic Nanoparticles with Dual Photoluminescence Emission. *Journal of the American Chemical Society* **2012**, *134* (2), 747-750.
- [16] Bo Peng; Xin Lu; Shi Chen; Cheng Hon Alfred Huan; Qihua Xiong; Evren Mutlugun; Hilmi Volkan Demir; Siu Fung Yu, Exciton dynamics in luminescent carbon nanodots: Electron–hole exchange interaction. *Nano Research* **2016**, *9* (2), 549-559.
- [17] Lei Wang; Shou-Jun Zhu; Hai-Yu Wang; Song-Nan Qu; Yong-Lai Zhang; Jun-Hu Zhang; Qi-Dai Chen; Huai-Liang Xu; Wei Han; Bai Yang; Hong-Bo Sun, Common Origin of Green Luminescence in Carbon Nanodots and Graphene Quantum Dots. *ACS Nano* **2014**, *8* (3), 2541-2547.
- [18] Almut M. Schwenke; Stephanie Hoepfener; Ulrich S. Schubert, Synthesis and Modification of Carbon Nanomaterials utilizing Microwave Heating. *Advanced Materials* **2015**, *27* (28), 4113-4141.
- [19] Xinyun Zhai; Peng Zhang; Changjun Liu; Tao Bai; Wenchen Li; Liming Dai; Wenguang Liu, Highly luminescent carbon nanodots by microwave-assisted pyrolysis. *Chemical Communications* **2012**, *48* (64), 7955-7957.
- [20] Hui Zhu; Xiaolei Wang; Yali Li; Zhongjun Wang; Fan Yang; Xiurong Yang, Microwave synthesis of fluorescent carbon nanoparticles with electrochemiluminescence properties. *Chemical Communications* **2009**, (34), 5118-5120.
- [21] Yi Liu; Ning Xiao; Ningqiang Gong; Hao Wang; Xin Shi; Wei Gu; Ling Ye, One-step microwave-assisted polyol synthesis of green luminescent carbon dots as optical nanoprobes. *Carbon* **2014**, *68*, 258-264.
- [22] Xiaohui Wang; Konggang Qu; Bailu Xu; Jinsong Ren; Xiaogang Qu, Microwave assisted one-step green synthesis of cell-permeable multicolor photoluminescent carbon dots without surface passivation reagents. *Journal of Materials Chemistry* **2011**, *21* (8), 2445-2450.
- [23] Weili Wei; Can Xu; Li Wu; Jiasi Wang; Jinsong Ren; Xiaogang Qu, Non-Enzymatic-Browning-Reaction: A Versatile Route for Production of Nitrogen-Doped

Carbon Dots with Tunable Multicolor Luminescent Display. *Scientific Reports* **2014**, *4*, 3564.

[24] Hui Nie; Minjie Li; Quanshun Li; Shaojun Liang; Yingying Tan; Lan Sheng; Wei Shi; Sean Xiao-An Zhang, Carbon Dots with Continuously Tunable Full-Color Emission and Their Application in Ratiometric pH Sensing. *Chemistry of Materials* **2014**, *26* (10), 3104-3112.

[25] Hui Ding; Shang-Bo Yu; Ji-Shi Wei; Huan-Ming Xiong, Full-Color Light-Emitting Carbon Dots with a Surface-State-Controlled Luminescence Mechanism. *ACS Nano* **2016**, *10* (1), 484-491.

[26] Yongqiang Dong; Hongchang Pang; Hong Bin Yang; Chunxian Guo; Jingwei Shao; Yuwu Chi; Chang Ming Li; Ting Yu, Carbon-Based Dots Co-doped with Nitrogen and Sulfur for High Quantum Yield and Excitation-Independent Emission. *Angewandte Chemie International Edition* **2013**, *52* (30), 7800-7804.

[27] Kateřina Holá; Mária Sudolská; Sergii Kalytchuk; Dana Nachtigallová; Andrey L. Rogach; Michal Otyepka; Radek Zbořil, Graphitic Nitrogen Triggers Red Fluorescence in Carbon Dots. *ACS Nano* **2017**.

[28] Shoujun Zhu; Qingnan Meng; Lei Wang; Junhu Zhang; Yubin Song; Han Jin; Kai Zhang; Hongchen Sun; Haiyu Wang; Bai Yang, Highly Photoluminescent Carbon Dots for Multicolor Patterning, Sensors, and Bioimaging. *Angewandte Chemie International Edition* **2013**, *52* (14), 3953-3957.

[29] H. Dong; Y. C. Chen; C. Feldmann, Polyol synthesis of nanoparticles: status and options regarding metals, oxides, chalcogenides, and non-metal elements. *Green Chemistry* **2015**, *17* (8), 4107-4132.

[30] Lei Bao; Zhi-Ling Zhang; Zhi-Quan Tian; Li Zhang; Cui Liu; Yi Lin; Baoping Qi; Dai-Wen Pang, Electrochemical Tuning of Luminescent Carbon Nanodots: From Preparation to Luminescence Mechanism. *Advanced Materials* **2011**, *23* (48), 5801-5806.

[31] Shengliang Hu; Adrian Trinchì; Paul Atkin; Ivan Cole, Tunable Photoluminescence Across the Entire Visible Spectrum from Carbon Dots Excited by White Light. *Angewandte Chemie International Edition* **2015**, *54* (10), 2970-2974.

[32] Th Forster, 10th Spiers Memorial Lecture. Transfer mechanisms of electronic excitation. *Discussions of the Faraday Society* **1959**, *27* (0), 7-17.

[33] Sanjay Tyagi; Salvatore A. E. Marras; Fred Russell Kramer, Wavelength-shifting molecular beacons. *Nature Biotechnology* **2000**, *18* (11), 1191-1196.

[34] Elizabeth A. Moschou; Bethel V. Sharma; Sapna K. Deo; Sylvia Daunert, Fluorescence Glucose Detection: Advances Toward the Ideal *In Vivo* Biosensor. *Journal of Fluorescence* **2004**, *14* (5), 535-547.

- [35] Ralph Ballerstadt; Colton Evans; Roger McNichols; Ashok Gowda, Concanavalin A for *in vivo* glucose sensing: A biotoxicity review. *Biosensors and Bioelectronics* **2006**, 22 (2), 275-284.
- [36] Ryan J. Russell; Michael V. Pishko; Christopher C. Gefrides; Michael J. McShane; Gerard L. Coté, A Fluorescence-Based Glucose Biosensor Using Concanavalin A and Dextran Encapsulated in a Poly(ethylene glycol) Hydrogel. *Analytical Chemistry* **1999**, 71 (15), 3126-3132.
- [37] John C. Pickup; Faeiza Hussain; Nicholas D. Evans; Olaf J. Rolinski; David J. S. Birch, Fluorescence-based glucose sensors. *Biosensors and Bioelectronics* **2005**, 20 (12), 2555-2565.
- [38] Sheng-Tao Yang; Xin Wang; Haifang Wang; Fushen Lu; Pengju G. Luo; Li Cao; Mohammed J. Meziani; Jia-Hui Liu; Yuanfang Liu; Min Chen; Yipu Huang; Ya-Ping Sun, Carbon Dots as Nontoxic and High-Performance Fluorescence Imaging Agents. *The Journal of Physical Chemistry C* **2009**, 113 (42), 18110-18114.
- [39] Nastassja Lewinski; Vicki Colvin; Rebekah Drezek, Cytotoxicity of Nanoparticles. *Small* **2008**, 4 (1), 26-49.
- [40] Yong Liu; Dingshan Yu; Chao Zeng; Zongcheng Miao; Liming Dai, Biocompatible Graphene Oxide-Based Glucose Biosensors. *Langmuir* **2010**, 26 (9), 6158-6160.
- [41] Hailong Dong; Ana Kuzmanoski; Go; Radian Popescu; Dagmar Gerthsen; Claus Feldmann, Polyol-mediated C-dot formation showing efficient Tb<sup>3+</sup>/Eu<sup>3+</sup> emission. *Chemical Communications* **2014**, 50 (56), 7503-7506.
- [42] Ningqiang Gong; Hao Wang; Shuai Li; Yunlong Deng; Xiao'ai Chen; Ling Ye; Wei Gu, Microwave-Assisted Polyol Synthesis of Gadolinium-Doped Green Luminescent Carbon Dots as a Bimodal Nanoprobe. *Langmuir* **2014**, 30 (36), 10933-10939.
- [43] Nina I. Kovtyukhova; Patricia J. Ollivier; Benjamin R. Martin; Thomas E. Mallouk; Sergey A. Chizhik; Eugenia V. Buzaneva; Alexandr D. Gorchinskiy, Layer-by-Layer Assembly of Ultrathin Composite Films from Micron-Sized Graphite Oxide Sheets and Polycations. *Chemistry of Materials* **1999**, 11 (3), 771-778.
- [44] William S. Hummers; Richard E. Offeman, Preparation of Graphitic Oxide. *Journal of the American Chemical Society* **1958**, 80 (6), 1339-1339.
- [45] Zhuang-Jun Fan; Wang Kai; Jun Yan; Tong Wei; Lin-Jie Zhi; Jing Feng; Yue-ming Ren; Li-Ping Song; Fei Wei, Facile Synthesis of Graphene Nanosheets *via* Fe Reduction of Exfoliated Graphite Oxide. *ACS Nano* **2011**, 5 (1), 191-198.
- [46] Dan Li; Marc B. Muller; Scott Gilje; Richard B. Kaner; Gordon G. Wallace, Processable aqueous dispersions of graphene nanosheets. *Nature Nanotechnology* **2008**, 3 (2), 101-105.

- [47] Soumen Chandra; Dipranjan Laha; Arindam Pramanik; Angshuman Ray Chowdhuri; Parimal Karmakar; Sumanta Kumar Sahu, Synthesis of highly fluorescent nitrogen and phosphorus doped carbon dots for the detection of Fe<sup>3+</sup> ions in cancer cells. *Luminescence* **2016**, 31 (1), 81-87.
- [48] Guoliang Li; Huili Fu; Xuejie Chen; Peiwei Gong; Guang Chen; Lian Xia; Hua Wang; Jinmao You; Yongning Wu, Facile and Sensitive Fluorescence Sensing of Alkaline Phosphatase Activity with Photoluminescent Carbon Dots Based on Inner Filter Effect. *Analytical Chemistry* **2016**, 88 (5), 2720-2726.
- [49] Zhimin Luo; Guangqin Qi; Keyu Chen; Min Zou; Lihui Yuwen; Xinwen Zhang; Wei Huang; Lianhui Wang, Microwave-Assisted Preparation of White Fluorescent Graphene Quantum Dots as a Novel Phosphor for Enhanced White-Light-Emitting Diodes. *Advanced Functional Materials* **2016**, 26 (16), 2739-2744.
- [50] Yongqiang Zhang; Xingyuan Liu; Yi Fan; Xiaoyang Guo; Lei Zhou; Ying Lv; Jie Lin, One-step microwave synthesis of N-doped hydroxyl-functionalized carbon dots with ultra-high fluorescence quantum yields. *Nanoscale* **2016**, 8 (33), 15281-15287.
- [51] Shuguang Yan; Yurong Tang; Mengling Yu, Resonance Rayleigh scattering detection of heparin with concanavalin A. *RSC Advances* **2015**, 5 (73), 59603-59608.
- [52] Fang-Fang Cheng; Guo-Xi Liang; Yuan-Yuan Shen; Rohit Kumar Rana; Jun-Jie Zhu, N-Acetylglucosamine biofunctionalized CdSeTe quantum dots as fluorescence probe for specific protein recognition. *Analyst* **2013**, 138 (2), 666-670.
- [53] Xiaoming Yang; Yingfeng Tu; Liang Li; Songmin Shang; Xiao-ming Tao, Well-Dispersed Chitosan/Graphene Oxide Nanocomposites. *ACS Applied Materials & Interfaces* **2010**, 2 (6), 1707-1713.

## Chapter 6

### 6 Development of FeCo/graphene Magneto-resistive Nanostructured Glucose Biosensor

#### 6.1 Introduction

In this chapter, a facile polyol process, one-step redox reaction, was used to synthesize Fe<sub>50</sub>Co<sub>50</sub> magnetic nanocrystals and to fabricate magnetic graphene/Fe<sub>50</sub>Co<sub>50</sub> hybrid nanosheets (MGFCs). The as-synthesized Fe<sub>50</sub>Co<sub>50</sub> magnetic nanocrystals with diameter around 400 nm have high saturation magnetization of 203.3 emu/g under 1 Tesla. Different weight ratios of graphene sheets to FeCo nanocrystals were synthesized and optimized to construct a nanostructured glucose biosensor using magneto-resistive mechanism.

Magneto-resistive structures are promising materials for applications in magnetic sensors, spintronic devices and magnetic random access memory (MRAM) devices. Recently, graphene based carbon magneto-resistive materials have attracted great interest due to graphene's excellent physicochemical properties. [1-2] Graphene nanosheets have high Young's modulus ( $\sim 1$  TPa), large specific surface area ( $2630 \text{ m}^2 \text{ g}^{-1}$ ), high intrinsic mobility ( $200\,000 \text{ cm}^2 \text{ v}^{-1} \text{ s}^{-1}$ ) and high thermal conductivity ( $\sim 5000 \text{ W m}^{-1} \text{ K}^{-1}$ ), optical transmittance ( $\sim 97.7\%$ ) and good electrical conductivity. These outstanding properties of graphene make them suitable materials for field effect transistors, sensors, biomedical applications, transparent conductive films, graphene/crystal composites and memory devices etc. [3-9]

Specifically, graphene/nanomaterials hybrid nanocomposites are being developed as novel nanosheets for diverse applications. These graphene/nanocrystals hybrid nanostructures often display advantageous synergistic properties of graphene and crystals. [10-13] Magnetic graphene composites were prepared by decorating magnetic crystals like FeCo, Ni<sub>x</sub>Co<sub>100-x</sub>, CoFe<sub>2</sub>O<sub>4</sub>, Fe<sub>3</sub>O<sub>4</sub>, FeNi<sub>3</sub> etc. onto graphene nanosheets. These magnetic graphene composites have large surface area and were mostly utilized as nanocatalysts.

And these catalysts were easily separated and purified from solution by external magnetic field. [14-19] Besides, the magnetic graphene composites were also investigated for their magnetoresistance applications.

Other nanomaterials and nanostructures were also studied for their magnetoresistive properties, like electrodeposited single crystal bismuth thin film, [20] non-magnetic silver chalcogenides. [21] MgO tunnel barriers. [22] These materials and structures showed large MR values, while graphene have excellent properties and easy synthesis methods, functionalization and fabrication. More importantly, graphene materials are recognized as supreme materials for magnetoresistive devices. Both theory studies [23-24] and experimental studies [25-26] already revealed the suitability of graphene based structures for magnetoresistive devices. Although at the very stage, magnetoresistance researches exploited multilayer magnetic/non-magnetic sandwiched structures, granular-matrix structures were later found to exert magnetoresistive effects as well. Graphene is a very suitable non-magnetic material for magnetoresistive matrix. The ferromagnetic granular particles are decorated onto graphene nanosheets with strategy for novel structures and functions.

In this chapter, we synthesized magnetic graphene/Fe<sub>50</sub>Co<sub>50</sub> hybrid nanosheets (MGFCs) by decorating Fe<sub>50</sub>Co<sub>50</sub> crystals onto graphene nanosheets *via* a facile polyol process. The crystal structure, morphology, magnetic properties and magnetoresistance of FeCo, FeCo/graphene nanomaterials were studied. The Fe<sub>50</sub>Co<sub>50</sub> crystals and MGFCs showed excellent ferromagnetic properties with very high saturation magnetization. For convenience, FeCo was used for representing Fe<sub>50</sub>Co<sub>50</sub> in the thesis. We prepared a series of FeCo/graphene nanocomposites by changing the graphene quantity from 30 mg to 120 mg with 10 mg step size. The magnetoresistance of the FeCo/graphene samples were measured and analyzed. Then we selected a ratio (80 mg graphene/FeCo) of FeCo/graphene nanocomposites as magnetoresistive sensor chip to construct a nanostructured glucose biosensor. Fe<sub>3</sub>O<sub>4</sub>/silica core/shell nanoparticle was used as the magnetic label. The sensor is shown in the figure 6.1. The sensor chip surface were modified with Con A, and the magnetic label surface was modified with phenylboronic acid. The magnetic label thus binded with glucose and sandwiched onto the chip surface.



The presence of magnetic label changed the magnetoresistance, which would be the glucose signal.

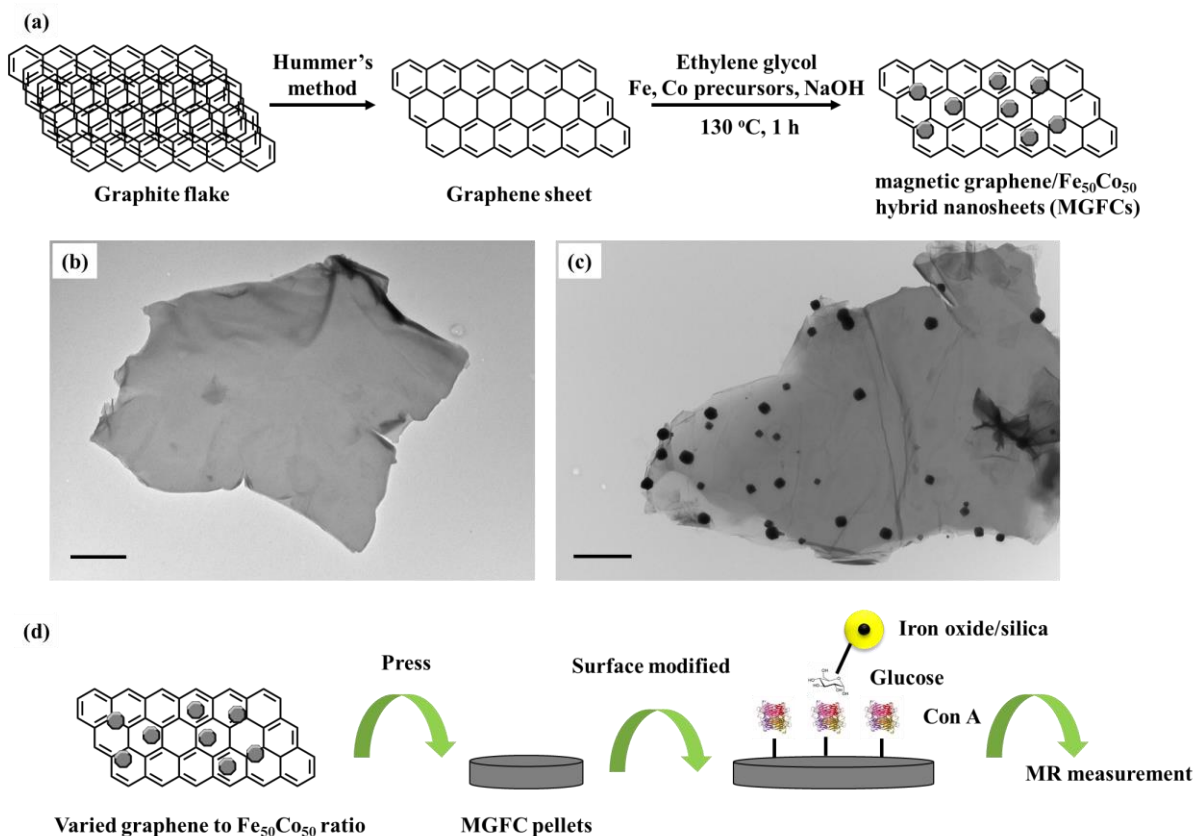


**Figure 6.1** Schematic of nanostructured magnetoresistive glucose biosensor. (a) Facile polyol process of production of magnetic graphene/Fe<sub>50</sub>Co<sub>50</sub> hybrid nanosheets. (b) TEM image graphene nanosheet, scale bar 1000 nm. (c) TEM image of magnetic graphene (120 mg) /Fe<sub>50</sub>Co<sub>50</sub> hybrid nanosheets, scale bar 1000 nm. (d) Hydraulic press for making magnetic graphene/Fe<sub>50</sub>Co<sub>50</sub> hybrid nanosheets and magnetoresistance measurements.

## 6.2 Experimental

### 6.2.1 Synthesis of Graphene Nanosheets

The graphene sheets used in this study was synthesized through a modified Hummers' method according to reference. [27] In the synthesis procedure, 1 g of graphite was mixed with 50 mL concentrated sulfuric acid, then 3 g of potassium permanganate was added

slowly into the mixture in ice-water bath to avoid overheating. This mixture was then stirred at room temperature for 20 minutes followed by 10 minutes of sonication. This stirring-sonication process was repeated for 12 times and then 200 mL water was added into the mixture. The solution was ultrasonicated for extra 2 hours and the pH was tuned to neutral by 1 M sodium hydroxide solution. This dispersion was treated with sonication for another 1 hour. The reduction of the graphene oxide to graphene sheets was carried out by adding 50 mL hydrazine hydrate into mixture after the mixture temperature reached 95 °C. The reduction process was lasted for 3 hours at 95 °C and then cooled to room temperature. The black graphene product was filtered and washed by 1 M hydrochloric acid and water to neutral pH. The black precipitate was freeze-dried store at room temperature.

### 6.2.2 Synthesis of Magnetic Fe<sub>50</sub>Co<sub>50</sub> Crystals

The magnetic Fe<sub>50</sub>Co<sub>50</sub> crystals were synthesized through a modified polyol process according to reference. [28] In a typical synthesis, 2.5 mmol FeCl<sub>2</sub> 4H<sub>2</sub>O and 2.5 mmol Co(CH<sub>3</sub>COO)<sub>2</sub> 4H<sub>2</sub>O metal salts precursors were mixed with 200 mmol sodium hydroxide in 100 mL ethylene glycol. The mixture was stirred under nitrogen gas protection and heated to 130 °C. After 1 hour reaction at 130 °C, the black FeCo nanocrystals were collected by magnet and washed by pure ethanol. The crystals were dried in vacuum under room temperature.

### 6.2.3 Synthesis of FeCo/graphene Magnetic Nanocomposites

The synthesis procedure was same as synthesis of FeCo. In a typical synthesis, varied mass of graphene powder (30 mg to 120 mg with increment of 10 mg), 2.5 mmol FeCl<sub>2</sub> 4H<sub>2</sub>O and 2.5 mmol Co(CH<sub>3</sub>COO)<sub>2</sub> 4H<sub>2</sub>O metal salts precursors were mixed with 200 mmol sodium hydroxide in 100 mL ethylene glycol. The mixture was stirred under nitrogen gas protection and heated to 130 °C. After 1 hour reaction at 130 °C, the black FeCo nanocrystals were collected by magnet and washed by pure ethanol. The crystals were dried in vacuum under room temperature. Graphene/FeCo composites were pressed and cut by hole punch into disk with diameter of 3.175 mm, thickness was about 100 μm. The

modification area (single side) is  $\pi \left( \frac{3.175 \text{ mm}}{2} \right)^2 = 7.92 \text{ mm}^2$

## 6.2.4 APTES Modification of GMR Sensor Surface

The graphene/FeCo surface was first cleaned by water and dried by nitrogen gas. APTES solution in DMSO (5%, w/v, 2  $\mu\text{L}$ ) was carefully applied to the graphene/FeCo surface area and kept for 4 hours at room temperature. Then the surface was carefully washed by water and dried by nitrogen gas. Glutaraldehyde solution (10%, 2  $\mu\text{L}$ ) was applied to the surface for 2 hours then the chip was washed and dried by nitrogen gas.

## 6.2.5 Con A Modification of GMR Sensor Surface

Con A solution (1 mg/mL) of 2  $\mu\text{L}$  was applied to the surface for 2 hours at 4  $^{\circ}\text{C}$  then the chip was washed, dried and stored in  $-20^{\circ}\text{C}$ . The wash solution was diluted to 100  $\mu\text{L}$  for BCA protein assay. The adsorbed Con A was measured as 0.162  $\mu\text{g}$  per film (figure 6.2). The chip surface was first modified with APTES to form the amine groups ( $-\text{NH}_2$ ). Then the Con A were bioconjugated to the amine groups using glutaraldehyde solution. BCA protein assay was used to measure the Con A quantity. The adsorbed Con A was measured as 0.162  $\mu\text{g}$  per film.

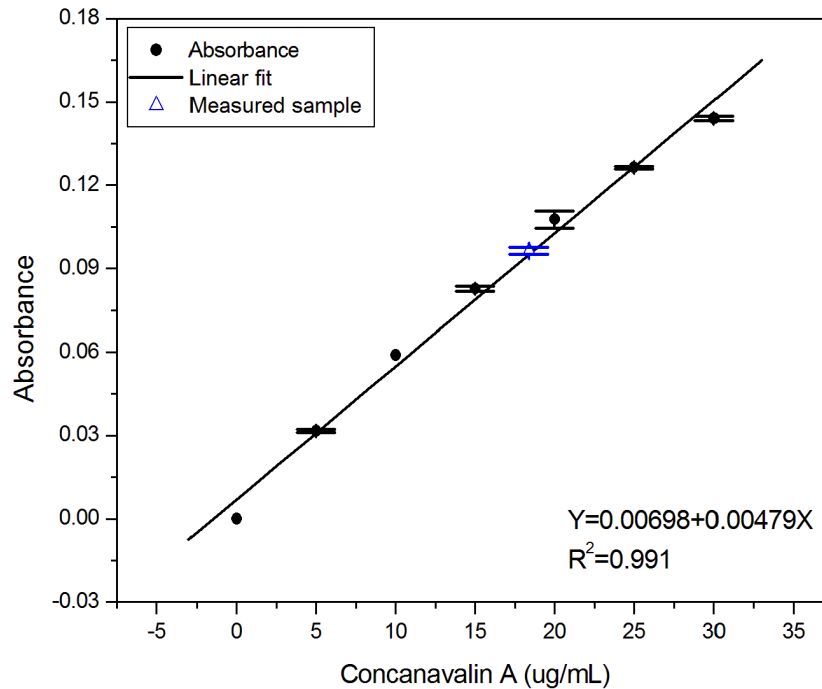


**Figure 6.2 Standard curve of Con A quantification by UV absorbance and quantity of Con A adsorbed on each MR film.**

## 6.2.6 Iron Oxide/Silica Surface Modification

Iron oxide (core 7 nm)/silica (shell 22 nm) (total about 50 nm) doped with FITC was prepared following reference. [29] GLYMO-APB (GA) was prepared following reference. [30] Glycidyloxypropyltrimethoxysilane (GLYMO) and 3-aminophenylboronic acid monohydrate (APB) were reacted to prepare boronic-acid bonded GLYMO. Typically, APB of 50 mg was dissolved in 20 mL of deionized water. The pH of solution was adjusted to 9.18 by 1 M aqueous NaOH. The, 40  $\mu$ L of GLYMO was slowly added into the APB solution with stirring while the solution was put at an ice-bath. The mixed solution was heated to 40  $^{\circ}$ C for reaction of 6 h with stirring. Subsequently the solution was placed into an ice-bath for 5 min, and 40  $\mu$ L of GLYMO was added and mixed again. Then the solution was raised to 60  $^{\circ}$ C for another 6 h with stirring. The prepared GA solution was stored in a refrigerator for usage. In a typical modification process, 5 mL GA solution, 20 mg iron oxide/silica was stirring at 75  $^{\circ}$ C for 2 hours and followed by centrifuge and wash. Then another 5 mL GA was added to the product for modification. Final product was washed and centrifuged.

## 6.2.7 Preparation of 3, 5-Dinitrosalicylic Acid (DNS) Solution

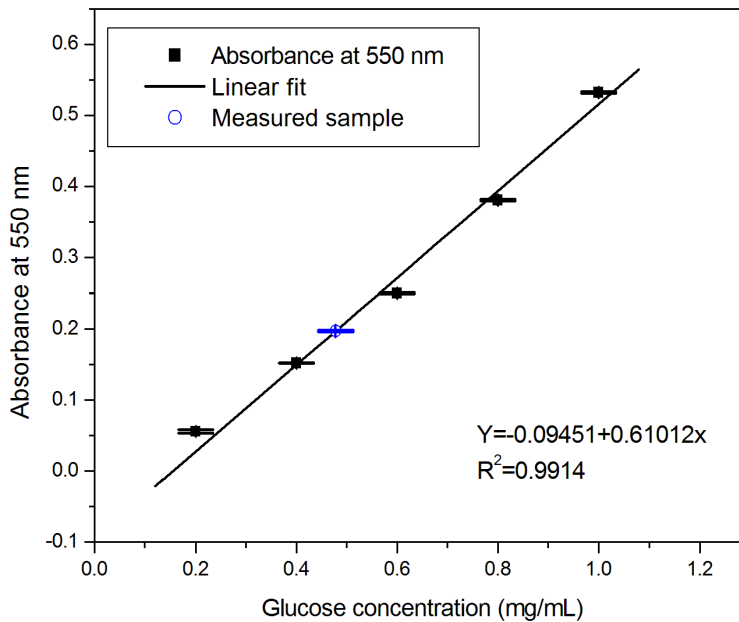


**Figure 6.3 Standard curve of glucose concentration by DNS assay and quantity of glucose adsorbed on each magnetic nanoparticle.**

The DNS solution [31-32] was prepared by the following step. 3, 5-dinitrosalicylic acid 2.5 g, phenol 0.5 g, sodium sulfite 0.075 g, sodium hydroxide 2.5 g, and potassium sodium tartrate 50 g were dissolved and mixed well in water and the final volume was 500 mL. After mixing well, the DNS solution was stored in 4 °C fridge. The colorimetric process was as following. Standard glucose solution 0.25 mL, DNS solution 0.75 mL, mixed and put in boiling water for 5 minutes. Then use tap water to cool down the solution to room temperature. Then add 2 mL water to each sample. And put in dark environment at room temperature for 20 minutes and then measure their UV-vis absorbance. The absorbance at 550 nm was used to draw the standard curve.

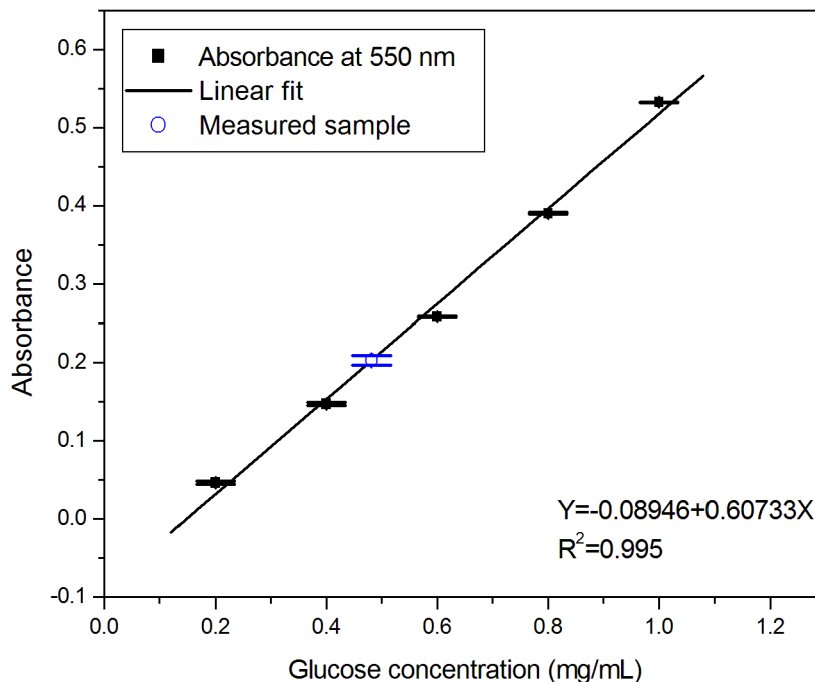


**Figure 6.4 Standard curve of glucose concentration by DNS assay and quantity of glucose adsorbed on each MR film.**

Glucose/Nanoparticle ratio was measured by DNS glucose colorimetric assay with range 0.2 mg/mL to 1 mg/mL, interval 0.2 mg/mL. 1 mg magnetic nanoparticle label adsorbed 0.220 mg glucose (figure 6.3); each magnetoresistive chip adsorbed 0.011 mg glucose using the DNS assay (figure 6.4).

Figure 6.3 showed the glucose standard curve analyzed by DNS colorimetric assay. After the glucose colorimetric reaction, the DNS solution was measured by UV-vis and the absorbance at 550 nm was used to quantify the glucose quantity. The calculation was that 1 mg magnetic nanoparticle label adsorbed 0.220 mg glucose.

Similarly, using DNS glucose assay, the glucose adsorbed on each MR sensor was calculated to be 0.011 mg glucose per film. The glucose contained in 3  $\mu\text{L}$  glucose solution of 10 mM was 0.0054 mg, which is smaller than the maxima glucose adsorbed on each film of 0.011 mg.

### 6.2.8 MR Measurement

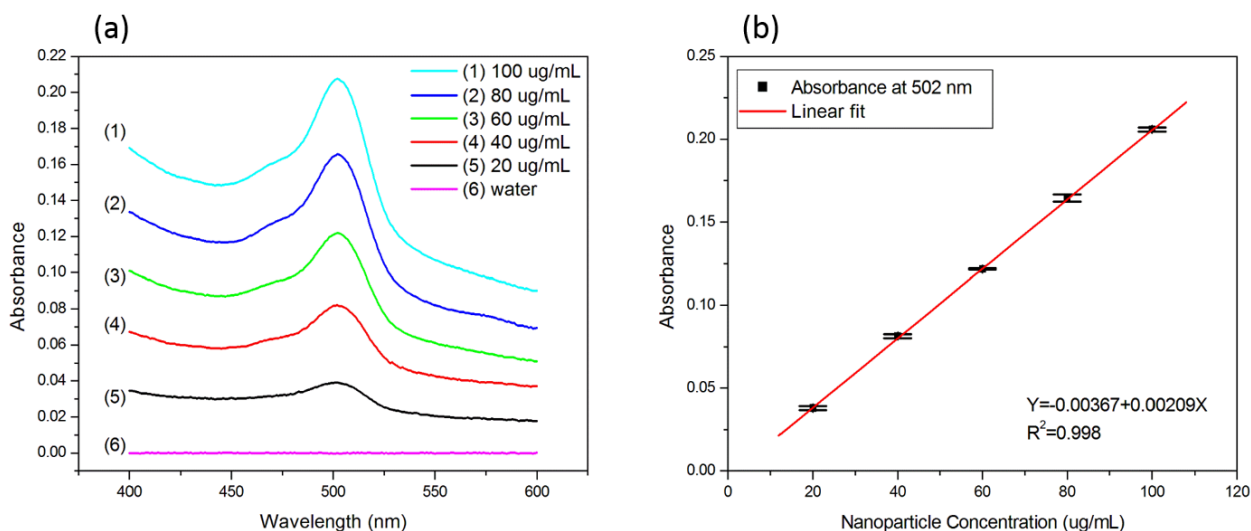


**Figure 6.5 Quantification of fluorescent magnetic label by doped dye (FITC) absorbance at 502 nm.**

In a typical MR measure, samples of known concentrations of glucose solutions (3  $\mu\text{L}$ , 0.2 mM to 10 mM) was applied and stayed for 1 hour. Then the chip was washed and dried by nitrogen gas. Then, 3  $\mu\text{L}$  magnetic nanoparticle solution (10 mg/mL) was added and stayed at room temperature for 1 hour. The magnetic label solution was washed and collected into 600  $\mu\text{L}$  volume ( $\sim 50 \mu\text{g/mL}$ ) for UV measurement. Standard curve was measured at range from 20  $\mu\text{g/mL}$  to 100  $\mu\text{g/mL}$ , interval 20  $\mu\text{g/mL}$  (figure 6.5).

The magnetic label was iron oxide/silica core/shell nanoparticle. The shell was doped with FITC dye, which has an UV-vis absorbance at 502 nm as shown in figure 6.5 (a). Using the magnetic label fluorescence standard curve (figure 6.5 (b)), we could measure the amount of magnetic label adsorbed on each MR sensor chip as shown in figure 6.6.

Using figure 6.5, the amount of magnetic label adsorbed on each MR sensor under different glucose concentrations could be measured as shown in figure 6.6. Because the MR sensor was first applied with a glucose solution. Then certain amounts of Con A was occupied by the glucose molecule. Then the magnetic label (saturated by excessive glucose) was applied, therefore, if the glucose solution has a higher glucose concentration, more Con A would be occupied. The less magnetic label could be bound onto the sensor.

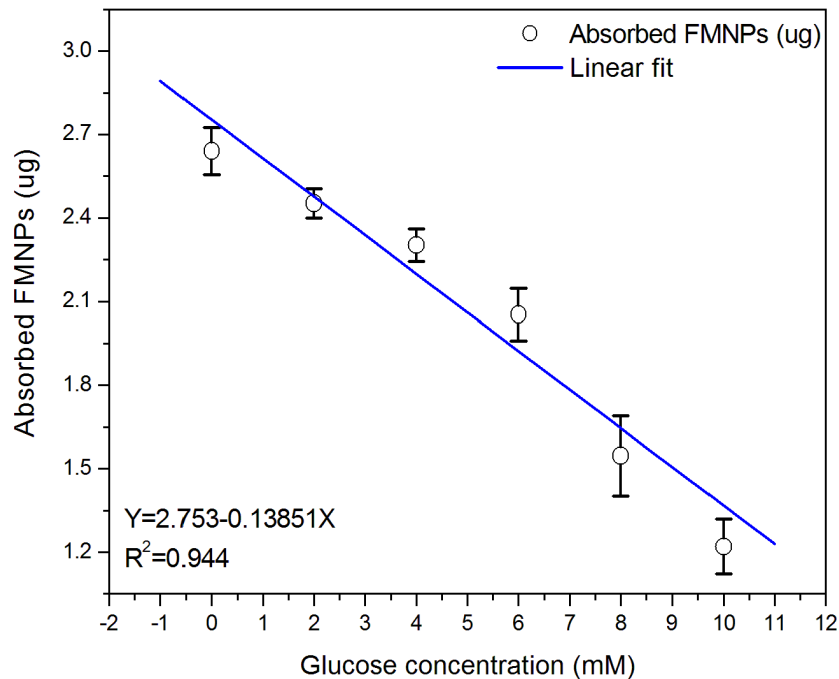


**Figure 6.6 Adsorbed fluorescent magnetic label on each MR sensor chip under different glucose concentrations.**

### 6.2.9 Rat Blood Samples Sensing

This part was cooperated with Dr James Melling lab (Kinesiology, UWO). In a typical MR measure. Samples of known concentrations of diluted blood samples (1  $\mu$ L, 0.2 mM to 10 mM) was applied to the sensor for 1 hour. Then the sensors were washed and dried by

nitrogen gas. Ethics approval was obtained through the University of Western Ontario Research Ethics Board, in accordance with Canadian Council on Animal Care guidelines.

## 6.3 Results and Discussion

### 6.3.1 Magnetic Nanoparticle Label Characterization

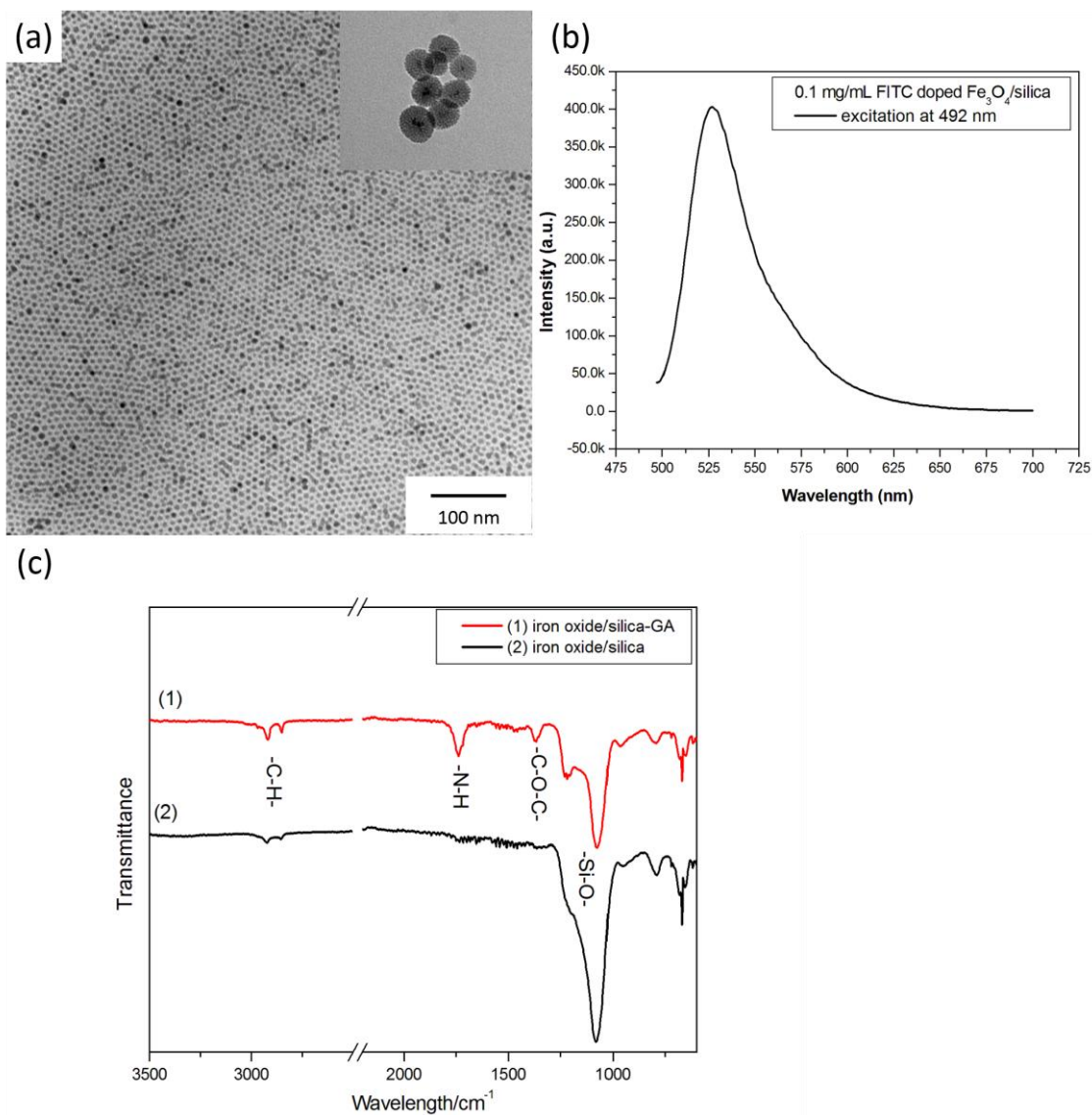


**Figure 6.7 (a) TEM image of iron oxide nanoparticle and inset of iron oxide/silica core/shell nanoparticle, scale bar 100 nm; (b) Fluorescence spectra of FITC doped iron oxide/silica core/shell nanoparticle; (c) FTIR spectrum of GA modified FITC-iron oxide/silica nanoparticle;**



The iron oxide nanoparticles were prepared by thermal decomposition approach. From the iron oxide nanoparticles TEM image, an average nanoparticle size of  $7 \text{ nm} \pm 0.21 \text{ nm}$  was measured by calculating over 100 nanoparticles. The size distribution was narrow. Furthermore, the iron oxide was surface coated with a silica layer doped with fluorescein isothiocyanate (FITC) dye. The dye has an excitation wavelength of 492 nm and an emission wavelength at 527 nm. The doping dye worked as fluorescence label to quantify the magnetic label using the fact that FITC has UV absorbance at 502 nm.

The silica shell thickness was average  $22 \text{ nm} \pm 3.42 \text{ nm}$ . The silica surface was modified with phenylboronic acid. The phenylboronic acid recognizes glucose and could bind glucose through a diol hydrogen bond. The FTIR spectrum of the core/shell nanoparticles confirmed the successful conjugation of phenylboronic acid on silica surface.

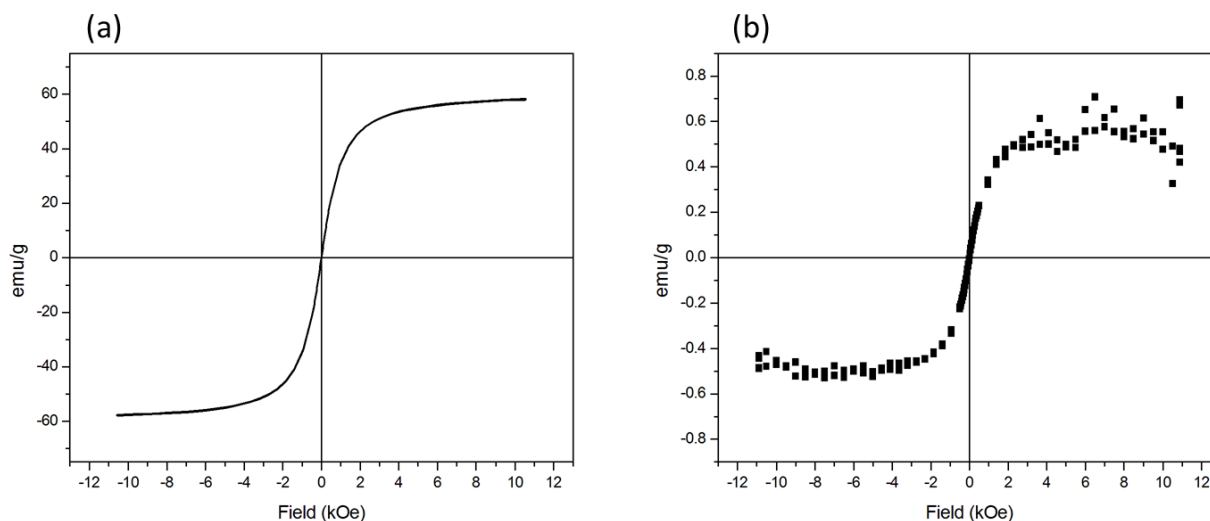


**Figure 6.8 (a) Magnetic hysteresis loop of Fe<sub>3</sub>O<sub>4</sub> nanoparticles; (b) Magnetic hysteresis loop of FITC-iron oxide/silica core/shell nanoparticle.**

The magnetic properties of iron oxide core and core/shell nanoparticle were characterized by the vibrating sample magnetometer (VSM). The iron oxide core was superparamagnetic with a magnetization of 58 emu/g at 1 T. After coated with a shell of silica the magnetization of the core/shell nanoparticle dropped down to about 0.5 emu/g at 1 T. The reason should be the silica coating. But from the hysteresis loop of the core/shell nanoparticle, the core/shell nanoparticles were still superparamagnetic.

### 6.3.2 Magnetoresistance Chip Characterization

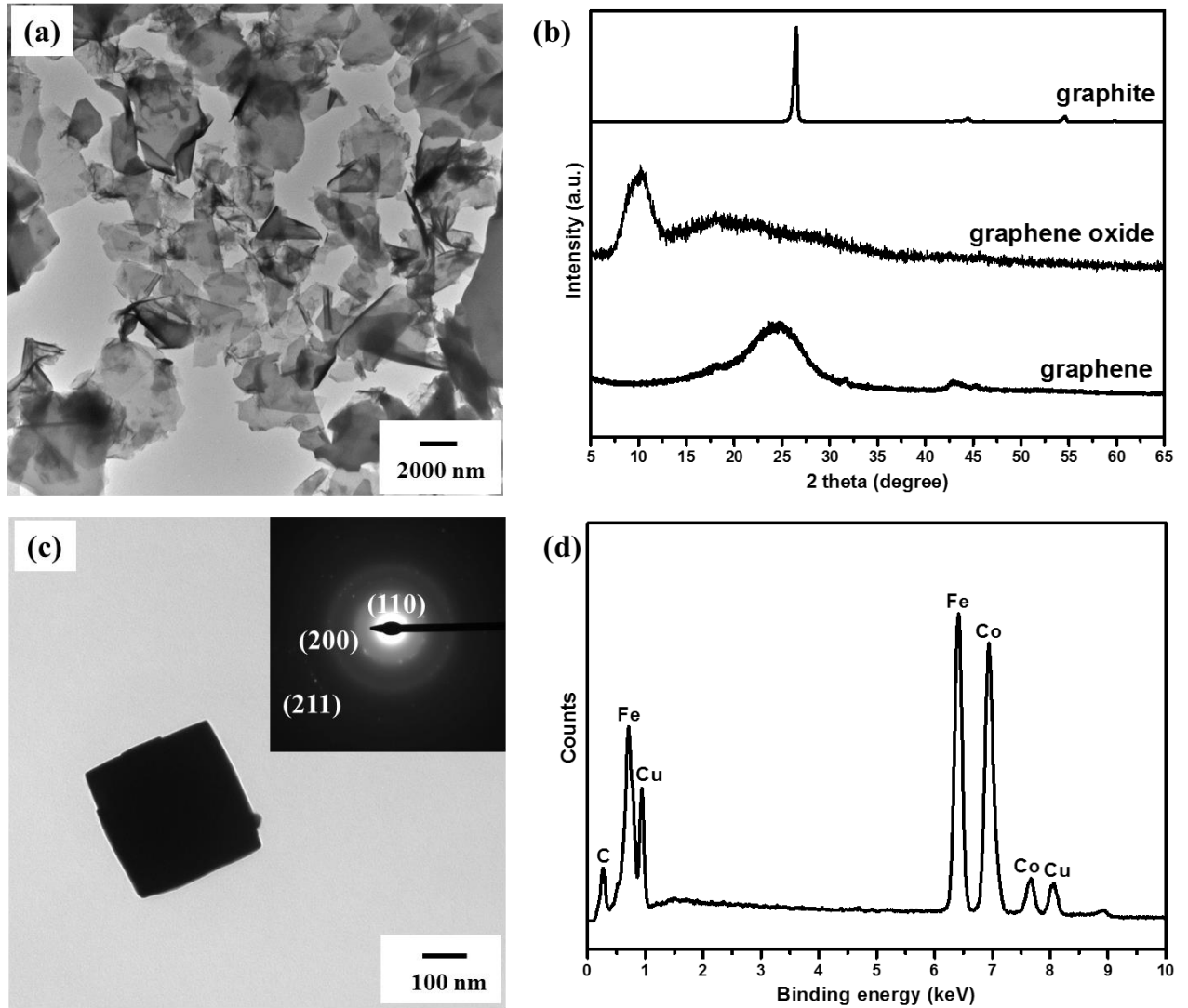


**Figure 6.9 (a) TEM image of graphene (scale bar 2000 nm), (b) XRD pattern of graphite and graphene, (c) TEM image (scale bar 100 nm) of single Fe<sub>50</sub>Co<sub>50</sub> crystal, inset image is corresponding electron diffraction pattern of Fe<sub>50</sub>Co<sub>50</sub> crystal, and (d) Energy-dispersive X-ray analysis of Fe<sub>50</sub>Co<sub>50</sub> crystals.**

Graphene nanosheets were prepared by the Hummers' method. The FeCo nanoparticle were prepared by a polyol process. Then varied graphene nanosheets were added into the FeCo polyol process to obtain the FeCo/graphene magnetic nanocomposites. The graphene nanosheets were characterized by TEM and XRD as shown in figure 6.9 (a) (b). From the characteristic XRD spectrum of graphite, graphene oxide and graphene, and compared

them with references. [33-35] Successful preparation of graphene nanosheets was confirmed. The FeCo nanoparticle was characterized by TEM and EDX in figure 6.9 (c) (d). The electron diffraction of FeCo nanoparticle confirmed the FeCo crystal structure. The EDX spectra showed the FeCo element. The C and Cu signal came from the carbon copper grid.

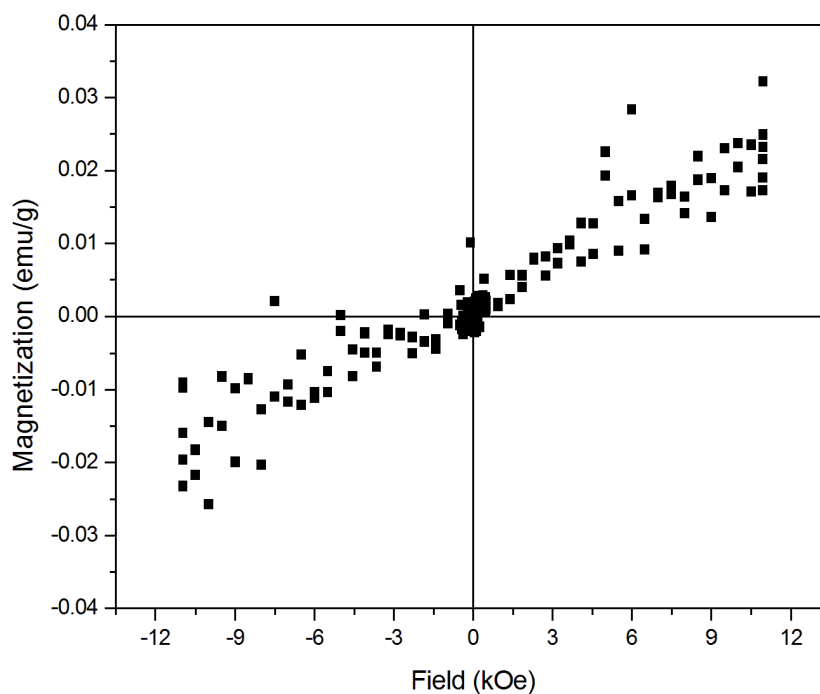


**Figure 6.10 Magnetic hysteresis loop of graphene nanosheets.**

The graphene nanosheets hysteresis loop was shown in figure 6.10, from the weak signal of the loop (0.02 emu/g at 1 T), we could neglect the graphene nanosheets magnetization here.

The FeCo nanoparticle size was calculated from figure 6.11 (a) at about average 500 nm. From the TEM image, the FeCo nanoparticle were severely connected and aggregated. This may be caused by the particles ferromagnetic property and ultra-strong magnetization of FeCo nanoparticle (202 emu/g at 1 T in figure 6.11 (b)). Figure 6.11 (c) showed one of the samples of graphene (30 mg)/FeCo magnetic nanocomposite. The FeCo nanoparticles size was about 440 nm, and they were dispersed around the graphene nanosheets. The magnetic hysteresis loops of 3 magnetic FeCo/graphene nanocomposites were presented in figure

6.11 (d), respectively samples of graphene (30 mg, 60 mg and 120 mg)/FeCo. They have a magnetization at 1 T of 97 emu/g, 78 emu/g and 40 emu/g for graphene 30 mg, 60 mg and 120 mg. The insets in figure 6.11 (b) (d) demonstrated the ferromagnetic property of FeCo nanoparticle and graphene/FeCo nanocomposites.

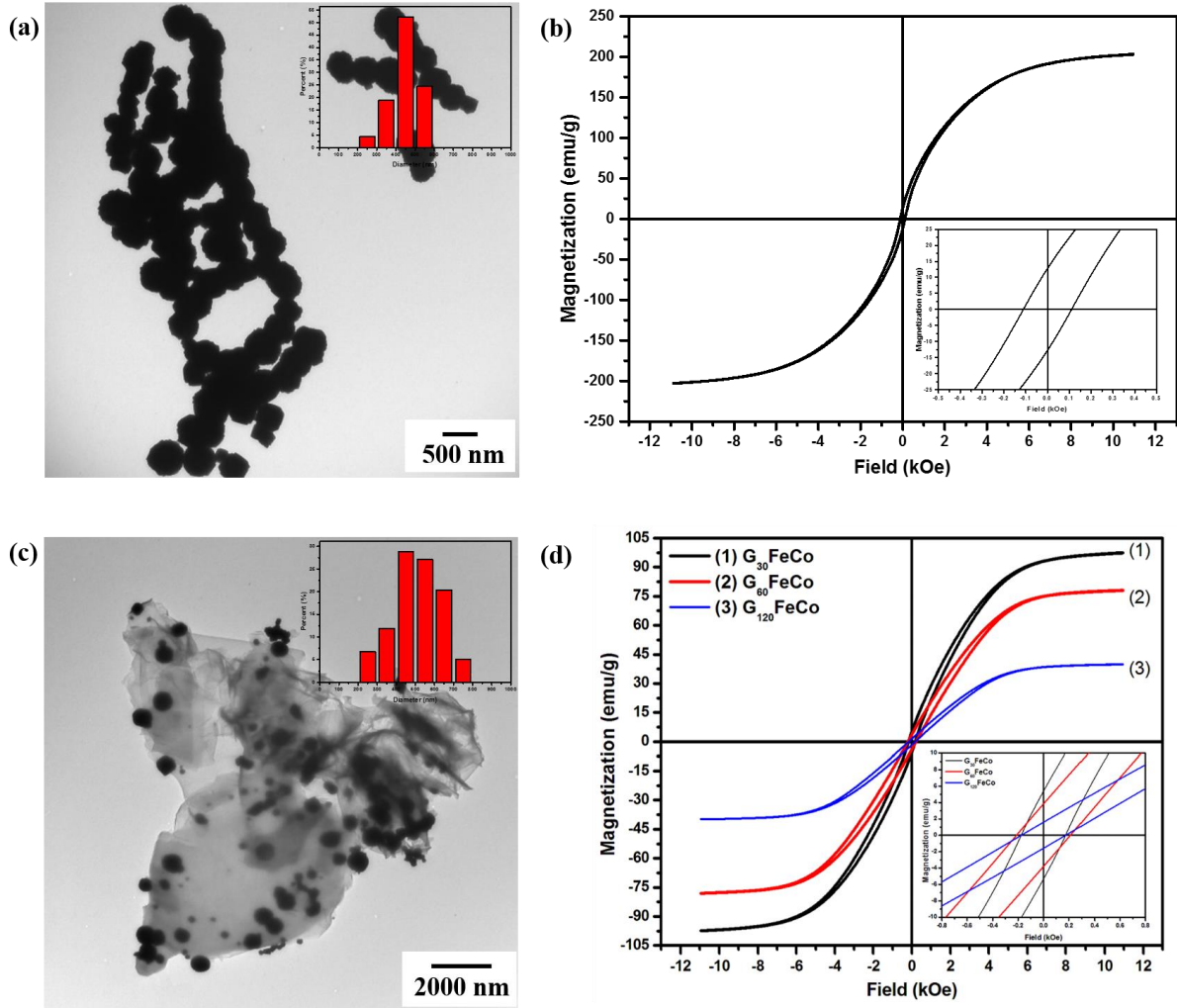


**Figure 6.11** Samples morphology and magnetic properties of  $\text{Fe}_{50}\text{Co}_{50}$  crystals and magnetic graphene/ $\text{Fe}_{50}\text{Co}_{50}$  hybrid nanosheets samples: (a)  $\text{Fe}_{50}\text{Co}_{50}$  crystal (scale bar 500 nm), (b) FeCo magnetic hysteresis loop, inset showing the enlarged area near  $\text{Field}=0$ , (c)  $\text{G}_{30}\text{FeCo}$  hybrids (graphene 30 mg) (scale bar 2000 nm), (d)  $\text{G}_{30}\text{FeCo}$ ,  $\text{G}_{60}\text{FeCo}$  and  $\text{G}_{120}\text{FeCo}$  magnetic nanocomposites magnetic hysteresis loop, inset showing the enlarged area near  $\text{Field}=0$ .

Table 6.1 summarized the magnetic FeCo/graphene nanocomposites samples.

**Table 6.1 Magnetic data of FeCo crystal and graphene/FeCo magnetic nanocomposites at room temperature.**

Samples	$M_s$ (emu/g)	$M_r$ (emu/g)	$M_r/M_s$	$H_c$ (Oe)
Fe <sub>50</sub> Co <sub>50</sub> crystal	203.3	12.81	0.063	110.9
G <sub>30</sub> FeCo	97.5	5.37	0.055	175.1
G <sub>60</sub> FeCo	78.0	3.83	0.049	212.1
G <sub>120</sub> FeCo	39.9	1.59	0.040	174.5

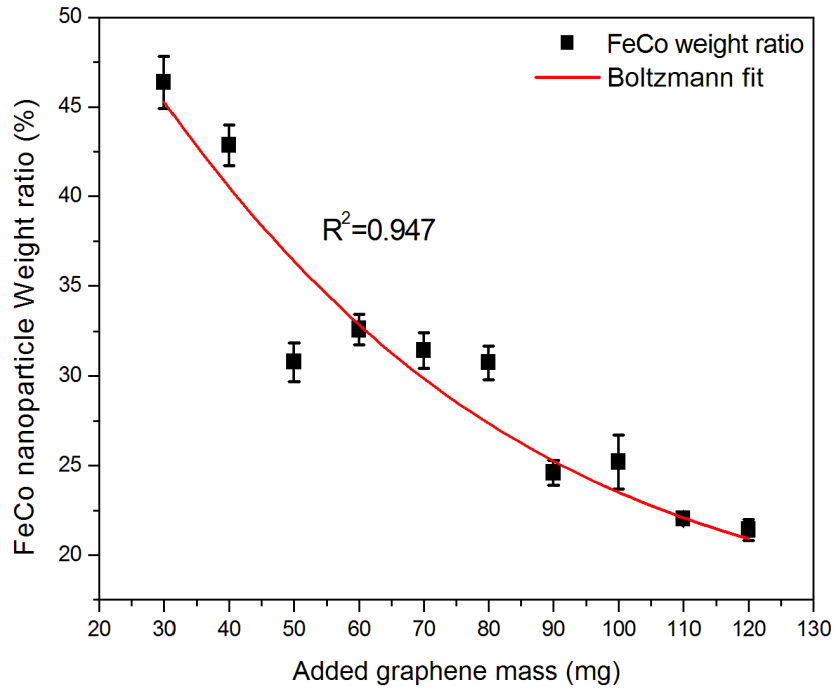


**Figure 6.12 Actual FeCo weight ratio data from SEM-EDX spectra of a series of magnetic graphene/FeCo samples.**

A series of varied quantity of graphene powder to FeCo ratio were prepared and their magnetoresistance were measured. The graphene quantity were 30 mg up to 120 mg with 10 mg increment. Together we have prepared 10 magnetic graphene/FeCo samples. These samples were analyzed by SEM-EDX and scanned several spots per sample to get the actual average FeCo nanoparticles weight percentage in each sample as shown in figure 6.12. The Y axis was the FeCo EDX average measured data, x axis was the added graphene mass. Figure 6.12 showed that by keeping the FeCo reaction condition unchanged, the increasing of graphene nanosheets decreased the FeCo nanoparticle weight ratio on the nanocomposites. A decline trend could be envisioned and fitted using Boltzmann function.

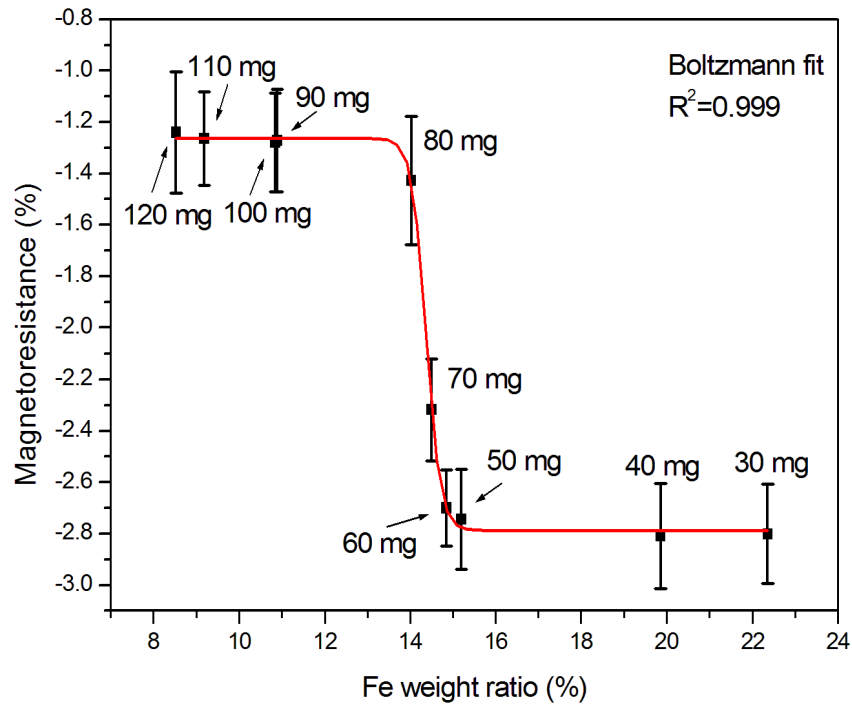


**Figure 6.13 Magnetoresistance of a series of varied graphene mass graphene/FeCo samples.**

These samples magnetoresistance were measured as shown in figure 6.13. Y axis was the magnetoresistance, x axis was the Fe weight ratio. The label in the graph indicated the added graphene quantity. As the magnetic label was Fe<sub>3</sub>O<sub>4</sub>/silica, therefore we made the X axis into Fe weight ratio. The binding of magnetic label increased the Fe content on the MR sensor chip. The sample of graphene (80 mg)/FeCo was at a sharp dropping point,

which showed that a minute increasing of magnetic label could decreased the MR in a sharp way. Therefore, the graphene (80 mg)/FeCo sample was chosen as the MR sensor chip.

### 6.3.3 Glucose Biosensing of Diluted Rats Blood Samples

Figure 6.14 showed the SEM image of FeCo/graphene nanopcomposite sensor chip surface. The rat blood glucose concentration were measured by marketed glucometer. Diluted rat blood samples of known glucose concentrations of 2 mM, 4 mM, 6 mM, 8 mM and 10 mM were measured by the MR sensor chip as showed in figure 6.15. In the sensing process, diluted blood was applied to the sensor chip surface. Then magnetic label (saturated by excessive glucose) was applied. Therefore, if the sample has a higher glucose concentration, the binding of magnetic label would be less. The MR signal was increasing as the glucose increased.

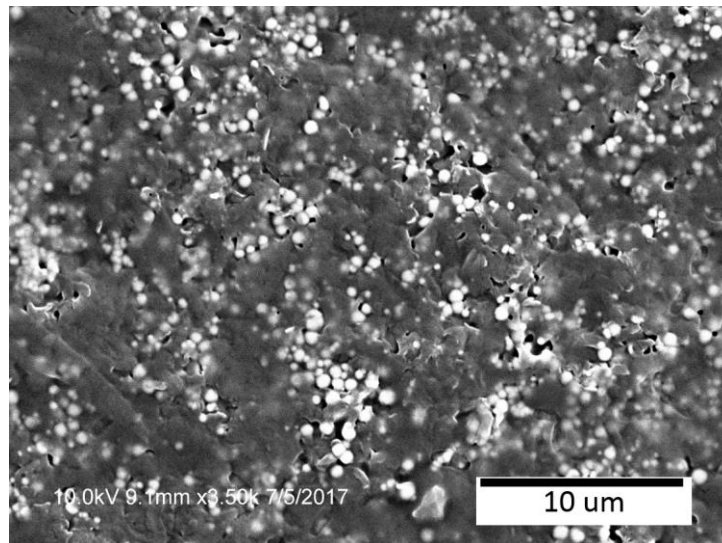


**Figure 6.14 SEM image of nanostructured magneto-resistive glucose biosensor chip surface.**

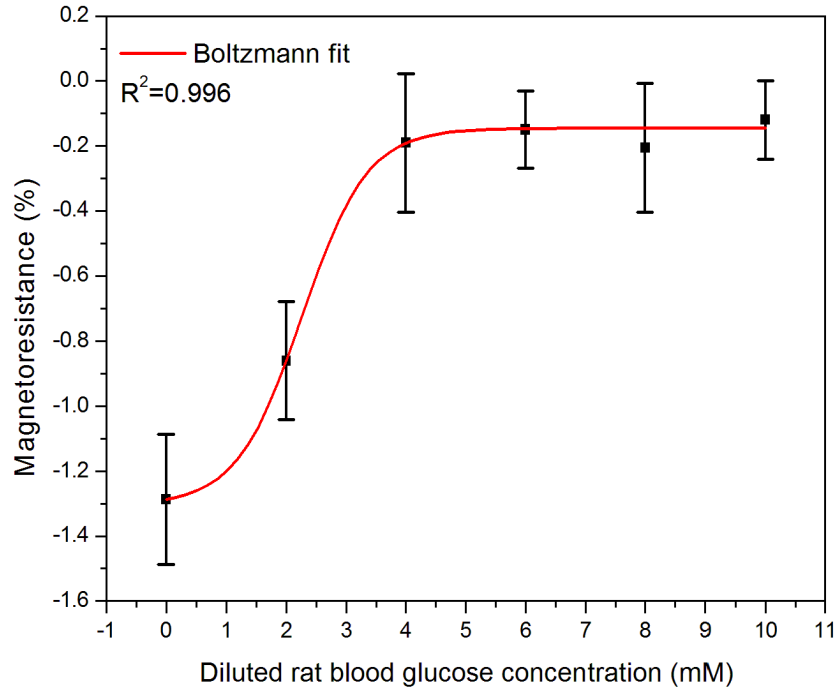


**Figure 6.15 Nanostructured magnetoresistive biosensor sensing diluted rat blood glucose concentration.**

## 6.4 Conclusion

In conclusion, we have developed a magnetoresistive nanostructured glucose biosensor. The MR chip detector was constructed by magnetic graphene/FeCo nanocomposite with surface bioconjugated with Con A. The magnetic label was iron oxide/silica core/shell nanoparticle with surface modified with phenylboronic acid. Diluted rat blood samples with certain glucose concentrations were measured with this MR biosensor with good results.

## 6.5 References

- [1] A. K. Geim; K. S. Novoselov, The rise of graphene. *Nature Materials* **2007**, 6 (3), 183-191.
- [2] Andre K. Geim, Random Walk to Graphene (Nobel Lecture). *Angewandte Chemie International Edition* **2011**, 50 (31), 6966-6985.



- [3] Yanwu Zhu; Shanthi Murali; Weiwei Cai; Xuesong Li; Ji Won Suk; Jeffrey R. Potts; Rodney S. Ruoff, Graphene and Graphene Oxide: Synthesis, Properties, and Applications. *Advanced Materials* **2010**, 22 (35), 3906-3924.
- [4] Xiao Huang; Zongyou Yin; Shixin Wu; Xiaoying Qi; Qiyuan He; Qichun Zhang; Qingyu Yan; Freddy Boey; Hua Zhang, Graphene-Based Materials: Synthesis, Characterization, Properties, and Applications. *Small* **2011**, 7 (14), 1876-1902.
- [5] Matthew J. Allen; Vincent C. Tung; Richard B. Kaner, Honeycomb Carbon: A Review of Graphene. *Chemical Reviews* **2010**, 110 (1), 132-145.
- [6] Sungjin Park; Rodney S. Ruoff, Chemical methods for the production of graphenes. *Nature Nanotechnology* **2009**, 4 (4), 217-224.
- [7] Robert F. Service, Beyond graphene. *Science* **2015**, 348 (6234), 490-492.
- [8] Jonathan K. Wassei; Richard B. Kaner, Oh, the Places You'll Go with Graphene. *Accounts of Chemical Research* **2013**, 46 (10), 2244-2253.
- [9] Kai Yang; Liangzhu Feng; Zhuang Liu, Stimuli responsive drug delivery systems based on nano-graphene for cancer therapy. *Advanced Drug Delivery Reviews* **2016**, 105 (Part B), 228-241.
- [10] Nan Gao; Xiaosheng Fang, Synthesis and Development of Graphene-Inorganic Semiconductor Nanocomposites. *Chemical Reviews* **2015**, 115 (16), 8294-8343.
- [11] Perry T. Yin; Shreyas Shah; Manish Chhowalla; Ki-Bum Lee, Design, Synthesis, and Characterization of Graphene-Nanoparticle Hybrid Materials for Bioapplications. *Chemical Reviews* **2015**, 115 (7), 2483-2531.
- [12] Nuria Alegret; Alejandro Criado; Maurizio Prato, Recent Advances of Graphene-based Hybrids with Magnetic Nanoparticles for Biomedical Applications. *Current Medicinal Chemistry* **2017**, 24 (5), 529-536.
- [13] Kim Truc Nguyen; Yanli Zhao, Integrated graphene/nanoparticle hybrids for biological and electronic applications. *Nanoscale* **2014**, 6 (12), 6245-6266.
- [14] Lianbo Ma; Xiaoping Shen; Guoxing Zhu; Zhenyuan Ji; Hu Zhou, FeCo nanocrystals encapsulated in N-doped carbon nanospheres/thermal reduced graphene oxide hybrids: Facile synthesis, magnetic and catalytic properties. *Carbon* **2014**, 77, 255-265.
- [15] Song Bai; Xiaoping Shen; Guoxing Zhu; Minzhi Li; Haitao Xi; Kangmin Chen, *In situ* Growth of Ni<sub>x</sub>Co<sub>100-x</sub> Nanoparticles on Reduced Graphene Oxide Nanosheets and Their Magnetic and Catalytic Properties. *ACS Applied Materials & Interfaces* **2012**, 4 (5), 2378-2386.

- [16] Kyle D. Gilroy; Aleksey Ruditskiy; Hsin-Chieh Peng; Dong Qin; Younan Xia, Bimetallic Nanocrystals: Syntheses, Properties, and Applications. *Chemical Reviews* **2016**, *116* (18), 10414-10472.
- [17] Wenjing Zhang; Xiaojian Li; Ruitao Zou; Huizi Wu; Haiyan Shi; Shanshan Yu; Yong Liu, Multifunctional glucose biosensors from Fe<sub>3</sub>O<sub>4</sub> nanoparticles modified chitosan/graphene nanocomposites. *Scientific Reports* **2015**, *5*, 11129.
- [18] Jiří Tuček; Zdeněk Sofer; Daniel Bouša; Martin Pumera; Kateřina Holá; Aneta Malá; Kateřina Poláková; Markéta Havrdová; Klára Čépe; Ondřej Tomanec; Radek Zbořil, Air-stable superparamagnetic metal nanoparticles entrapped in graphene oxide matrix. *Nature Communications* **2016**, *7*, 12879.
- [19] Xuejing Zheng; Qian Zhu; Huiqing Song; Xinrui Zhao; Tao Yi; Hongli Chen; Xingguo Chen, *In Situ* Synthesis of Self-Assembled Three-Dimensional Graphene–Magnetic Palladium Nanohybrids with Dual-Enzyme Activity through One-Pot Strategy and Its Application in Glucose Probe. *ACS Applied Materials & Interfaces* **2015**, *7* (6), 3480-3491.
- [20] F. Y. Yang; Kai Liu; Kimin Hong; D. H. Reich; P. C. Searson; C. L. Chien, Large Magnetoresistance of Electrodeposited Single-Crystal Bismuth Thin Films. *Science* **1999**, *284* (5418), 1335-1337.
- [21] R. Xu; A. Husmann; T. F. Rosenbaum; M. L. Saboungi; J. E. Enderby; P. B. Littlewood, Large magnetoresistance in non-magnetic silver chalcogenides. *Nature* **1997**, *390* (6655), 57-60.
- [22] Stuart S. P. Parkin; Christian Kaiser; Alex Panchula; Philip M. Rice; Brian Hughes; Mahesh Samant; See-Hun Yang, Giant tunnelling magnetoresistance at room temperature with MgO (100) tunnel barriers. *Nature Materials* **2004**, *3* (12), 862-867.
- [23] F. Muñoz-Rojas; J. Fernández-Rossier; J. J. Palacios, Giant Magnetoresistance in Ultrasmall Graphene Based Devices. *Physical Review Letters* **2009**, *102* (13), 136810.
- [24] Feng Zhai; Kai Chang, Theory of huge tunneling magnetoresistance in graphene. *Physical Review B* **2008**, *77* (11), 113409.
- [25] Jingwei Bai; Rui Cheng; Faxian Xiu; Lei Liao; Minsheng Wang; Alexandros Shailos; Kang L. Wang; Yu Huang; Xiangfeng Duan, Very large magnetoresistance in graphene nanoribbons. *Nature Nanotechnology* **2010**, *5* (9), 655-659.
- [26] Jianming Lu; Haijing Zhang; Wu Shi; Zhe Wang; Yuan Zheng; Ting Zhang; Ning Wang; Zikang Tang; Ping Sheng, Graphene Magnetoresistance Device in van der Pauw Geometry. *Nano Letters* **2011**, *11* (7), 2973-2977.
- [27] Sina Abdolhosseinzadeh; Hamed Asgharzadeh; Hyoung Seop Kim, Fast and fully-scalable synthesis of reduced graphene oxide. *Scientific Reports* **2015**, *5*, 10160.

- [28] D. Kodama; K. Shinoda; K. Sato; Y. Konno; R. J Joseyphus; K. Motomiya; H. Takahashi; T. Matsumoto; Y. Sato; K. Tohji; B. Jeyadevan, Chemical Synthesis of Sub-micrometer- to Nanometer-Sized Magnetic FeCo Dice. *Advanced Materials* **2006**, *18* (23), 3154-3159.
- [29] Jaeyun Kim; Hoe Suk Kim; Nohyun Lee; Taeho Kim; Hyoungsu Kim; Taekyung Yu; In Chan Song; Woo Kyung Moon; Taeghwan Hyeon, Multifunctional Uniform Nanoparticles Composed of a Magnetite Nanocrystal Core and a Mesoporous Silica Shell for Magnetic Resonance and Fluorescence Imaging and for Drug Delivery. *Angewandte Chemie International Edition* **2008**, *47* (44), 8438-8441.
- [30] Yawei Xu; Zhangxiong Wu; Lijuan Zhang; Haojie Lu; Pengyuan Yang; Paul A. Webley; Dongyuan Zhao, Highly Specific Enrichment of Glycopeptides Using Boronic Acid-Functionalized Mesoporous Silica. *Analytical Chemistry* **2009**, *81* (1), 503-508.
- [31] G. L. Miller, Use of Dinitrosalicylic Acid Reagent for Determination of Reducing Sugar. *Analytical Chemistry* **1959**, *31* (3), 426-428.
- [32] <https://eng.umd.edu/~nsw/ench485/lab4a.htm>. (accessed November 2<sup>nd</sup> 2017).
- [33] Zhuang-Jun Fan; Wang Kai; Jun Yan; Tong Wei; Lin-Jie Zhi; Jing Feng; Yue-ming Ren; Li-Ping Song; Fei Wei, Facile Synthesis of Graphene Nanosheets *via* Fe Reduction of Exfoliated Graphite Oxide. *ACS Nano* **2011**, *5* (1), 191-198.
- [34] Cheng Zhu; T. Yong-Jin Han; Eric B. Duoss; Alexandra M. Golobic; Joshua D. Kuntz; Christopher M. Spadaccini; Marcus A. Worsley, Highly compressible 3D periodic graphene aerogel microlattices. *Nature Communications* **2015**, *6*.
- [35] Xusheng Du; Hong-Yuan Liu; Yiu-Wing Mai, Ultrafast Synthesis of Multifunctional N-Doped Graphene Foam in an Ethanol Flame. *ACS Nano* **2016**, *10* (1), 453-462.

## Chapter 7

### 7 Summary and Recommendations

#### 7.1 Summary and Conclusion

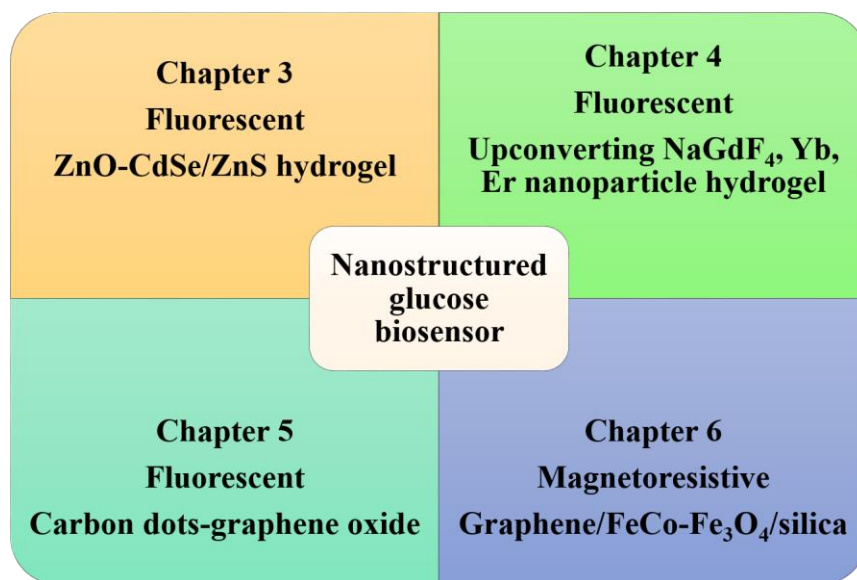


**Figure 7.1 Schematic of my work on four nanostructured glucose biosensors.**

The overall objective of my PhD work was to develop nanostructured glucose biosensor (figure 7.1), which utilizes nanomaterials and nanostructures to construct glucose biosensor with high selectivity and sensitivity. A variety of nanomaterials were prepared and integrated into several different glucose nanobiosensors. These nanostructured glucose biosensors were properly functionalized with suitable biomolecules and functional chemical groups. Rats tear and blood samples were analyzed by the designed nanobiosensors and good results were achieved. The sensing results demonstrated various fluorescent/magneto resistive nanomaterials and nanostructures could be exploited as glucose biosensors. Three glucose biosensors were based on fluorescence resonance energy transfer mechanism, respectively ZnO/QD biosensor, upconverting nanomaterials biosensor and carbon dots-graphene oxide biosensor. The last glucose biosensor was based

on magnetoresistance mechanism, this MR sensor was composed of FeCo/graphene magnetoresistive chip and magnetic label of Fe<sub>3</sub>O<sub>4</sub>/silica core/shell nanoparticles. The brief summary of each glucose biosensor are stated below.

### **Development of ZnO/QD Patterned Nanostructured Glucose Biosensor**

In chapter 3, a nanostructured glucose biosensor was developed to detect glucose in tear by using fluorescence resonance energy transfer (FRET) quenching mechanism. The designed FRET pair were CdSe/ZnS quantum dots (donor) and dextran-binding malachite green (MG-dextran) (quencher). Concanavalin A (Con A) is a lectin protein with specific affinity to glucose and Con A is bioconjugated onto quantum dots. Con A can also bind other saccharides like dextran with much lower affinity. The quantum dots-Con A-dextran-MG structure was formed. In the presence of glucose, the quenched emission of QDs through the FRET mechanism was restored by displacing the dextran-MG from Con A. To have a dual-modulation sensor for convenient and accurate detection, the nanostructured FRET sensors were assembled onto a patterned ZnO nanorod array deposited on the synthetic silicone hydrogel. Consequently, the concentration of glucose detected by the patterned sensor could be converted to fluorescence spectrum with high signal-to-noise ratio and calibrated image pixel values. The photoluminescence intensity of the patterned FRET sensor increased linearly with increasing glucose concentration from 0.03 mM to 3 mM, which covered the range of tear glucose levels for both diabetics and healthy people. Meanwhile, the calibrated values of pixel intensities of the fluorescence images captured by a handheld fluorescence microscope increased with increasing glucose concentration. Four male Sprague-Dawley rats with different blood glucose concentrations were utilized to demonstrate the quick response of the patterned FRET sensor to 2  $\mu$ L of diluted tear samples (2  $\mu$ L original tear mixed with 5  $\mu$ L PBS solution). The highlights are listed below:

1. This nanostructured biosensor was designed for dual detection of tear glucose.
2. Fluorescence intensity increased linearly with glucose level from 0.03 mM to 3 mM.
3. Image pixel intensity value of the sensor was corresponding to the glucose level.

4. Animal test indicated that the sensor could measure the glucose concentration in 2  $\mu\text{L}$  diluted rat tear within 30 seconds.

#### **Development of Upconversion NaGdF<sub>4</sub>: Yb, Er Glucose Biosensor**

In chapter 4, a nanostructured glucose biosensor was designed using upconverting nanomaterials to sense rat tear glucose *in vivo*. The fluorescence resonance energy transfer donor was upconverting nanomaterials with surface bioconjugated of Con A. The modified upconverting nanomaterials were excited by 980 nm near-infrared light and emitted visible light at 541 nm and 655 nm. The acceptor was the malachite green-dextran (MG-dextran), which could quench the fluorescence emission of 655 nm from upconversion nanomaterials. These upconverting nanomaterials glucose nanobiosensors were deposited onto hydrogel surface and applied as contact lens prototype sensor to sense rat tear glucose *in vivo*. In the presence of glucose, the quenched emission of upconverting nanomaterials was restored by displacing the dextran-MG from Con A. The highlights are listed below:

1. The nanostructures acted as an analyte (tear glucose) collector to achieve high concentration of analyte reacting with the FRET sensor.
2. The upconverting nanostructures exhibited stable fluorescence signals.
3. Large surface-to-volume ratio of the nanostructures could lead to higher selectivity for glucose sensing.
4. The fluorescence intensity (I) of the FRET sensor as a function of the glucose concentration have been investigated *in vitro* and *in vivo*.

#### **Development of Carbon Dots/Graphene Oxide Glucose Biosensor**

In chapter 5, a facile microwave assisted synthesis method of tunable photoluminescent carbon dots was developed. Glucose nanobiosensor based on this carbon dots and graphene oxide was constructed. Both carbon dots and graphene oxide are highly biocompatible. We found that the photoluminescence of carbon dots could be adjusted (within a certain range) by simply varying carbon source amount, which has not yet been reported before. Other methods for preparing different photoluminescent carbon dots often use oxidative and/or

reductive chemicals. While our method is facile and environmental friendly. The tunable photoluminescence range could extend from 470 nm to 540 nm in this system. The highlights are listed below:

1. Facile microwave assisted polyol process for preparation of carbon dots, and the carbon dots fluorescence was tunable by simply adjusting precursor quantity with a range from 470 nm to 540 nm.
2. This glucose nanobiosensor composed of biocompatible carbon dots (donor) and graphene oxide (acceptor or quencher) using fluorescence resonance energy transfer (FRET) quenching technique.
3. Glucose sensing range was adjustable by applying adequate quantity of donor and acceptor (quencher). Linearity of glucose level of 1 mM to 10 mM and glucose level of 0.2 mM to 1 mM was obtained.
4. Diluted rat blood samples were measured by carbon dots/graphene oxide based nanobiosensor with good linearity.

### **Development of FeCo/graphene Magneto-resistive Nanostructured Glucose Biosensor**

In chapter 6, a facile polyol synthesis process was developed to fabricate Magnetic Graphene/FeCo hybrid nanosheets (MGFCs). These MGFCs were then pressed into thin films and applied as nanostructured magneto-resistive chip for glucose biosensor. The magneto-resistive chip surface was modified with Con A, the magnetic nanoparticle label was Fe<sub>3</sub>O<sub>4</sub>/silica with surface modified with phenylboronic acid. The presence of glucose would connect the magnetic labels to the magneto-resistive chip surface, thus causing the magneto-resistance signal change. Diluted rat blood samples were measured by the magneto-resistive biosensor. The tear samples are collected from Dr James Melling's lab in Kinesiology, UWO. And the amounts of tear samples collected are very little. Therefore, in some measurement, we used diluted blood samples. Although diluted blood samples are not the same with tear samples, the sensing results are useful for future study when we have enough tear samples. The highlights are listed below:

1. Facile polyol preparation of FeCo/graphene nanocomposites, and the composition was tunable by adjusting the FeCo precursor's quantity and graphene quantity.
2. The MGFCs chip showed magnetoresistive properties and the magnetoresistance was tunable by using different ratio Fe, Co and graphene quantity.
3. Diluted rat blood samples were measured by this nanostructured magnetoresistive glucose biosensor with range of 0 mM to 4 mM.

## 7.2 Contributions of the Research to the Current State of Knowledge

Diabetes is a worldwide spread disease among populations. It is a chronic disease characterized by longtime high glucose level of patients. Many complications often accompany with diabetes disease, causing great suffering to diabetic patients. [1-5] The high glucose concentration is present in blood and other body fluid like tear, urine, saliva, sweat etc. [6-7] Therefore, glucose level in human body fluids is the direct biomarker for diabetes. Controlling blood glucose concentration is currently prevalent approach to manage diabetes. Measuring blood glucose is the prevalent method to monitor glucose level in human body. The widely used marketed glucometer is based on electrochemical sensing technique. But the glucometer requires a certain amount of blood, which is invasive and sometimes causing infection risk to people. The implanted electrochemical glucometer on the other hand may have problems like biocompatibility, biofouling of the sensing electrode and longevity, calibration etc. [8-9] Tear is a continuous body fluid and a good target for continuous glucose sensing. Certain relationship of tear glucose and blood glucose does exist and have been investigated since 1930s. Compared to blood glucose which is often in the level of 4 mM to 20 mM, tear glucose concentration is in the level of 0.1 mM to 0.5 mM. [10-15] Nanomaterials and nanostructures have novel chemical, physical and biological properties and nanostructured glucose biosensor could have higher sensitivity and selectivity, which could be integrated into other devices or chips. Contact lens based nanostructured glucose biosensor is one promising developing direction. Some limitations include the whether every person is suitable to wear contact lens and the tear glucose are affected by every person's eye status (eye disease etc.). These limitations may



be solved by setting up personal care systems and applied corresponding managements to individual situations.

All in all, nanostructured glucose biosensor are promising for better monitoring glucose level and my PhD work is focused on developing fluorescent and magnetoresistive nanostructured glucose biosensors. A variety of nanomaterials and nanostructures were prepared and integrated into several glucose nanobiosensors. Good glucose sensing results were obtained and rat tear samples and rat blood samples were analyzed by the designed glucose nanobiosensors.

To have a whole view on the nanomaterials and nanostructures studied in my work, let's look at the fluorescent nanomaterials chapters. In chapter 3, we used CdSe/ZnS quantum dots, the coating layer of ZnS greatly lowered the toxicity of the CdSe quantum dots and enhance its fluorescence. The coating could seal the Cd element inside. This quantum dots glucose nanobiosensor used UV light as fluorescent source. The emission could be tuned by tuning quantum dots size. Single UV excitation could excite different emission quantum dots, which was promising for multiplex sensing.

Comparatively, in chapter 4, we adopted upconverting nanomaterials which were excited by near-infrared light of 980 nm and emitted visible light at 541 nm and 655 nm. On the other hand, the use of 980 nm near-infrared excitation could avoid the auto-fluorescence effect. Therefore, the upconverting nanomaterials based glucose biosensor was a step forward to enhance the sensor's signal-to-noise ratio. Moreover, upconverting nanomaterials have better biocompatibility than the semiconductor quantum dots.

In chapter 5, we used carbon dots, a new nanocarbon materials discovered in 2006, to develop the fluorescent glucose nanobiosensor. Carbon dots are commonly synthesized by carbonization of biomolecules or molecules. The composition has carbon, hydrogen, oxygen elements, sometimes doped with other elements like sulfur, nitrogen etc. Carbon dots has good biocompatibility and has no toxic elements compared to quantum dots. Carbon dots has strong fluorescence and excitation-dependent fluorescence properties. Some carbon dots are reported to have even upconverting properties. Therefore, carbon dots are promising for biosensor development.

**Table 7.1 Summary of investigated fluorescent nanomaterials.**

Fluorescent nanomaterial	Pros	Cons
CdSe/ZnS quantum dots	Stable and strong fluorescence	Toxic elements like Cd
	Multiplex sensing	UV excitation tissue auto-fluorescence
Upconverting nanomaterial	980 nm excitation low background noise	Fluorescence difficult to tune
	Biocompatible	
	Stable fluorescence	
Carbon dots (carbon nanomaterial)	Highly biocompatible	Fluorescence mechanisms not fully understood
	Facile preparation by various methods	
	Fluorescence strong/stable enough for biosensing	
Carbon dots (carbon nanomaterial)	Excitation-dependent emission, tunable by doping nitrogen etc. elements	Reproducibility
	Possible upconverting fluorescence	

Last chapter was focused on carbon nanomaterials based magnetoresistive nanostructured glucose biosensor. FeCo/graphene nanocomposites were used as magnetoresistive chip and iron oxide/silica was used as magnetic label.

### **Development of ZnO/QD Patterned Nanostructured Glucose Biosensor**

Quantum dots have stable and strong fluorescent properties, which favor their usage in various applications. One application of quantum dots is used as fluorescent sensor transducer. The quantum dots are prepared and the surface modification protocols have been developed and accumulated. [16-21] The main stream quantum dots contains toxic semiconductor elements like Cd element, which limit their biomedical applications and disposal. And the traditional synthesis method would use high boiling point organic solutions, which are unfriendly to human and environment. Coating of quantum dots is one method to make them biocompatible, but coating could affect the photoluminescence properties. In recent years, more and more research has focused on aqueous synthesis of quantum dots and non-toxic elements containing quantum dots. [22-24] In the ZnO/QD nanostructured glucose biosensor, we assembled the quantum dots nanobiosensor onto ZnO nanorod arrays chip. The chip was then patterned using photolithography to show contrast between sensing parts and non-sensing parts. The large surface area of ZnO nanorod arrays could enlarge the fluorescent signal. Thus the sensor has high sensitivity. The chip was deposited on biocompatible hydrogel, making it promising to integrate into contact lens glucose biosensor. Rat tear samples were measured with good results.

### **Development of Upconversion NaGdF<sub>4</sub>: Yb, Er Glucose Biosensor**

Upconversion is an anti-Stokes luminescence phenomenon. The excitation source of upconverting nanomaterials is near-infrared light (normally 980 nm). [25-28] Therefore, upconverting nanomaterials are very suitable for biosensing applications. Similarly, the prepared upconverting nanomaterials are surface modified with biocompatible layers like inorganic or polymer coatings. In the upconverting nanomaterials glucose biosensor. We developed a method to prepare upconverting nanomaterials with as-synthesized surface modified by amine group ( $-NH_2$ ). Then Con A was bioconjugated to upconverting nanomaterials surface. The modified upconverting nanomaterials were integrated into

hydrogel materials and applied to sense rat tear *in vivo* and rat blood sample *in vitro* with good results. This nanostructured glucose biosensor demonstrated a contact lens prototype model for tear glucose sensing.

### **Development of Carbon Dots/Graphene Oxide Glucose Biosensor**

Carbon dots are novel nanocarbon materials. It has good biocompatibility and intriguing fluorescence properties. Although the exact mechanisms of their fluorescence properties are not fully uncovered. Their facile synthesis and strong fluorescence properties has attracted intense research and applied in glucose biosensors area. [29-32] In the carbon dots glucose nanobiosensor study, we developed a facile microwave assisted polyol preparation method for synthesizing carbon dots. We found that the carbon dots fluorescence was tunable from 470 nm to 540 nm by adjusting precursor's quantity. The precursors were histidine and citric acid. The polyol process was adopted with solution of ethylene glycol. Further, we constructed a glucose nanobiosensor using this carbon dots (fluorescence donor) and graphene oxide (fluorescence quencher). Both the fluorescence donor and quencher are highly biocompatible and their quantity are adjustable to accommodate different sensing environment. Rat blood samples were measured by the carbon dots nanobiosensor with good results.

### **Development of FeCo/graphene Magneto-resistive Nanostructured Glucose Biosensor**

Because most biocomponents do not contain magnetic elements, the magnetic sensing has zero background noise and high sensitivity. Magneto-resistive biosensors have been developed and used in sensing other biomolecules, proteins, cells etc. [33-37] In this magneto-resistive glucose biosensor, we endeavored to develop a magneto-resistive glucose biosensor. FeCo/graphene nanocomposites were prepared by a polyol process. The composition of Fe, Co and graphene are tunable by adjusting the precursor ratio. We used Fe<sub>50</sub>Co<sub>50</sub> nanoparticle formula and change the graphene quantity to study the magneto-resistance. Then we found a sharp dipping position (graphene (80 mg)/FeCo) of the magneto-resistance versus graphene quantity curve. We then used the graphene/FeCo nanocomposites at that dipping point to develop magneto-resistive chip sensor. The magnetic label of iron oxide/silica core/shell nanoparticles were prepared by thermal

decomposition and then surface coating with dye-doped silica. Con A was modified onto chip surface, while the magnetic label were surface modified with phenylboronic groups. Rat blood samples were measured by this magnetoresistive biosensor with good results.

### 7.3 Future Studies

My PhD work focused on synthesizing and fabricating different nanomaterials and nanostructures for glucose biosensor application. Therefore, I would be discussing the nanomaterials and nanostructures synthesis, surface modification, fabrication and chemophysical properties in the following paragraphs. These aspects would greatly affect biosensors' biocompatibility, selectivity, sensitivity.

#### **Development of ZnO/QD Patterned Nanostructured Glucose Biosensor**

First the toxicity of quantum dots is a general concern for its practical application. However this problem is intrinsic for Cd quantum dots. A layer of ZnS coating was applied to the CdSe quantum dots to improve the biocompatibility. A reliable surface modification could sufficiently lower the quantum dots' toxicity while retaining the fluorescence. [38-40] Second the assembling of quantum dots nanobiosensor onto ZnO nanorod could be difficult to control. Therefore the reproducibility is a concern. The current conjugation method was using glutaraldehyde. Better conjugation method is required to be able to control the conjugation process. Third the sensor longevity needs to be considered as well.

#### **Development of Upconversion NaGdF<sub>4</sub>: Yb, Er Glucose Biosensor**

The upconversion nanomaterials used was the NaGdF<sub>4</sub>, Yb, Er. First the synthesis method was polyol process at 200 °C at round bottom flask. At this condition, the crystal structures of the upconverting nanoparticle was difficult to control. XRD results indicated mixed hexagonal and cubic crystal structures both present in the nanoparticles. The crystal structure affected greatly the upconverting fluorescence. Hexagonal structure shows superior fluorescence intensity compared to the cubic. [41-43] So other methods of high reaction temperatures or using autoclave could better control the crystal structures. Second consideration was the controlled deposition of upconverting nanomaterials on hydrogel and

immobilization approach. We used drop casting method and then covered the sensors with polyethylene glycol. This might need further improvements.

### **Development of Carbon Dots/Graphene Oxide Glucose Biosensor**

This glucose nanobiosensor used carbon nanomaterials, carbon dots (fluorescence donor) and graphene oxide (fluorescence quencher). Firstly, the graphene oxide reproducibility was a concern. Graphene oxide is a mixture of different size nanosheets. [44-47] Different batches of graphene oxide might need calibration to obtain signal reproducibility. Secondly, the excitation light was 400 nm, which could cause tissue auto-fluorescence problem. Some research reported the upconverting fluorescence from carbon dots, which could be excited by 980 nm. [48-50] Therefore, developing upconverting carbon dots or graphene quantum dots would be advantageous for carbon dots application in biosensors.

### **Development of FeCo/graphene Magneto-resistive Nanostructured Glucose Biosensor**

This study involved also carbon nanomaterials. Graphene nanosheets were decorated with FeCo nanoparticles through polyol process and iron oxide/silica core/shell magnetic nanoparticles were used as magnetic label. Firstly, different size of graphene nanosheets would be a concern. Secondly, other ratios of FeCo nanoparticle to graphene are also needed to be studied. The FeCo nanoparticle used throughout the experiment was Fe<sub>50</sub>Co<sub>50</sub>. Other FeCo ratios like Fe<sub>25</sub>Co<sub>75</sub> or Fe<sub>75</sub>Co<sub>25</sub> etc. could have different magneto-resistive effects. Thirdly, the chip surface nanostructures would need more controllable fabrication process.

## **7.4 References**

- [1] Brooke E. Harcourt; Sally A. Penfold; Josephine M. Forbes, Coming full circle in diabetes mellitus: from complications to initiation. *Nature Reviews Endocrinology* **2013**, 9 (2), 113-123.
- [2] Richard I. G. Holt; Alex J. Mitchell, Diabetes mellitus and severe mental illness: mechanisms and clinical implications. *Nature Reviews Endocrinology* **2015**, 11 (2), 79-89.

- [3] Lei Chen; Dianna J. Magliano; Paul Z. Zimmet, The worldwide epidemiology of type 2 diabetes mellitus—present and future perspectives. *Nature Reviews Endocrinology* **2012**, 8 (4), 228-236.
- [4] Jason Flannick; Stefan Johansson; Pal R. Njolstad, Common and rare forms of diabetes mellitus: towards a continuum of diabetes subtypes. *Nature Reviews Endocrinology* **2016**, 12 (7), 394-406.
- [5] Matthew C. Riddle, Controlling glucose levels in elderly people—benefits versus risks. *Nature Reviews Endocrinology* **2015**, 11, 257.
- [6] Joseph Wang, Electrochemical Glucose Biosensors. *Chemical Reviews* **2008**, 108 (2), 814-825.
- [7] Qian Wu; Li Wang; Haojie Yu; Jianjun Wang; Zhefu Chen, Organization of Glucose-Responsive Systems and Their Properties. *Chemical Reviews* **2011**, 111 (12), 7855-7875.
- [8] Scott P. Nichols; Ahyeon Koh; Wesley L. Storm; Jae Ho Shin; Mark H. Schoenfisch, Biocompatible Materials for Continuous Glucose Monitoring Devices. *Chemical Reviews* **2013**, 113 (4), 2528-2549.
- [9] Joseph Wang, Glucose Biosensors: 40 Years of Advances and Challenges. *Electroanalysis* **2001**, 13 (12), 983-988.
- [10] Frederick Ridley, The Intraocular Pressure and Drainage of the Aqueous Humour. *British Journal of Experimental Pathology* **1930**, 11 (4), 217-240.
- [11] D Michail; P Vancea; N Zolog, Sur l'élimination lacrymale du glucose chez les diabétiques. *CR Soc. Biol., Paris* **1937**, 125, 1095.
- [12] J. G. Lewis; P. J. Stephens, Tear Glucose in Diabetics. *British Journal of Ophthalmology* **1958**, 42 (12), 754-758.
- [13] Antonio R. Gasset; Lewis E. Braverman; Marie C. Fleming; Ronald A. Arky; Barry R. Alter, Tear Glucose Detection of Hyperglycemia. *American Journal of Ophthalmology* **1968**, 65 (3), 414-420.
- [14] K Motoji, The glucose content of tear fluid in normal and diabetic subjects. *Japanese Journal of Clinical Ophthalmology* **1971**, 25, 1945-50.
- [15] D K Sen; G S Sarin, Tear glucose levels in normal people and in diabetic patients. *British Journal of Ophthalmology* **1980**, 64 (9), 693-695.
- [16] W. Russ Algar; Kimihiro Susumu; James B. Delehanty; Igor L. Medintz, Semiconductor Quantum Dots in Bioanalysis: Crossing the Valley of Death. *Analytical Chemistry* **2011**, 83 (23), 8826-8837.

- [17] Jipei Yuan; Weiwei Guo; Erkang Wang, Utilizing a CdTe Quantum Dots–Enzyme Hybrid System for the Determination of Both Phenolic Compounds and Hydrogen Peroxide. *Analytical Chemistry* **2008**, *80* (4), 1141-1145.
- [18] Ute Resch-Genger; Markus Grabolle; Sara Cavaliere-Jaricot; Roland Nitschke; Thomas Nann, Quantum dots versus organic dyes as fluorescent labels. *Nature Methods* **2008**, *5* (9), 763-775.
- [19] Isabel Costas-Mora; Vanesa Romero; Isela Lavilla; Carlos Bendicho, An overview of recent advances in the application of quantum dots as luminescent probes to inorganic-trace analysis. *TRAC Trends in Analytical Chemistry* **2014**, *57*, 64-72.
- [20] K. David Wegner; Niko Hildebrandt, Quantum dots: bright and versatile *in vitro* and *in vivo* fluorescence imaging biosensors. *Chemical Society Reviews* **2015**, *44* (14), 4792-4834.
- [21] X. Michalet; F. F. Pinaud; L. A. Bentolila; J. M. Tsay; S. Doose; J. J. Li; G. Sundaresan; A. M. Wu; S. S. Gambhir; S. Weiss, Quantum Dots for Live Cells, *in Vivo* Imaging, and Diagnostics. *Science* **2005**, *307* (5709), 538.
- [22] Peter Reiss; Marie Carrière; Christophe Lincheneau; Louis Vaure; Sudarsan Tamang, Synthesis of Semiconductor Nanocrystals, Focusing on Nontoxic and Earth-Abundant Materials. *Chemical Reviews* **2016**, *116* (18), 10731-10819.
- [23] Lihong Jing; Stephen V. Kershaw; Yilin Li; Xiaodan Huang; Yingying Li; Andrey L. Rogach; Mingyuan Gao, Aqueous Based Semiconductor Nanocrystals. *Chemical Reviews* **2016**, *116* (18), 10623-10730.
- [24] Vladimir Lesnyak; Nikolai Gaponik; Alexander Eychmuller, Colloidal semiconductor nanocrystals: the aqueous approach. *Chemical Society Reviews* **2013**, *42* (7), 2905-2929.
- [25] Guofeng Wang; Qing Peng; Yadong Li, Lanthanide-Doped Nanocrystals: Synthesis, Optical-Magnetic Properties, and Applications. *Accounts of Chemical Research* **2011**, *44* (5), 322-332.
- [26] Markus Haase; Helmut Schäfer, Upconverting Nanoparticles. *Angewandte Chemie International Edition* **2011**, *50* (26), 5808-5829.
- [27] Guanying Chen; Hailong Qiu; Paras N. Prasad; Xiaoyuan Chen, Upconversion Nanoparticles: Design, Nanochemistry, and Applications in Theranostics. *Chemical Reviews* **2014**, *114* (10), 5161-5214.
- [28] Niagara Muhammad Idris; Muthu Kumara Gnanasammandhan Jayakumar; Akshaya Bansal; Yong Zhang, Upconversion nanoparticles as versatile light nanotransducers for photoactivation applications. *Chemical Society Reviews* **2015**, *44* (6), 1449-1478.



- [29] Guosong Hong; Shuo Diao; Alexander L. Antaris; Hongjie Dai, Carbon Nanomaterials for Biological Imaging and Nanomedicinal Therapy. *Chemical Reviews* **2015**, *115* (19), 10816-10906.
- [30] Youfu Wang; Aiguo Hu, Carbon quantum dots: synthesis, properties and applications. *Journal of Materials Chemistry C* **2014**, *2* (34), 6921-6939.
- [31] Shoujun Zhu; Yubin Song; Xiaohuan Zhao; Jieren Shao; Junhu Zhang; Bai Yang, The photoluminescence mechanism in carbon dots (graphene quantum dots, carbon nanodots, and polymer dots): current state and future perspective. *Nano Research* **2015**, *8* (2), 355-381.
- [32] Katerina Hola; Yu Zhang; Yu Wang; Emmanuel P. Giannelis; Radek Zboril; Andrey L. Rogach, Carbon dots-Emerging light emitters for bioimaging, cancer therapy and optoelectronics. *Nano Today* **2014**, *9* (5), 590-603.
- [33] S. X. Wang; G. Li, Advances in Giant Magnetoresistance Biosensors With Magnetic Nanoparticle Tags: Review and Outlook. *IEEE Transactions on Magnetics* **2008**, *44* (7), 1687-1702.
- [34] Yi Wang; Wei Wang; Lina Yu; Liang Tu; Yinglong Feng; Todd Klein; Jian-Ping Wang, Giant magnetoresistive-based biosensing probe station system for multiplex protein assays. *Biosensors and Bioelectronics* **2015**, *70*, 61-68.
- [35] Li Kirsten Li; 李丽. Development of biodetection platform with magnetoresistive sensors and magnetic nanoparticles. The University of Hong Kong (Pokfulam, Hong Kong), 2013.
- [36] X. Sun; D. Ho; L. M. Lacroix; J. Q. Xiao; S. Sun, Magnetic Nanoparticles for Magnetoresistance-Based Biodetection. *IEEE Transactions on NanoBioscience* **2012**, *11* (1), 46-53.
- [37] Gungun Lin; Denys Makarov; Oliver G. Schmidt, Magnetic sensing platform technologies for biomedical applications. *Lab on a Chip* **2017**, *17* (11), 1884-1912.
- [38] Robert Wilson; David G. Spiller; Alison Beckett; Ian A. Prior; Violaine S é, Highly Stable Dextran-Coated Quantum Dots for Biomolecular Detection and Cellular Imaging. *Chemistry of Materials* **2010**, *22* (23), 6361-6369.
- [39] Juan B. Blanco-Canosa; Miao Wu; Kimihiro Susumu; Eleonora Petryayeva; Travis L. Jennings; Philip E. Dawson; W. Russ Algar; Igor L. Medintz, Recent progress in the bioconjugation of quantum dots. *Coordination Chemistry Reviews* **2014**, *263-264*, 101-137.
- [40] Andrew M. Smith; Hongwei Duan; Aaron M. Mohs; Shuming Nie, Bioconjugated quantum dots for *in vivo* molecular and cellular imaging. *Advanced Drug Delivery Reviews* **2008**, *60* (11), 1226-1240.

- [41] Feng Wang; Yu Han; Chin Seong Lim; Yunhao Lu; Juan Wang; Jun Xu; Hongyu Chen; Chun Zhang; Minghui Hong; Xiaogang Liu, Simultaneous phase and size control of upconversion nanocrystals through lanthanide doping. *Nature* **2010**, 463 (7284), 1061-1065.
- [42] Karl W. Krämer; Daniel Biner; Gabriela Frei; Hans U. Güdel; Markus P. Hehlen; Stefan R. Lüthi, Hexagonal Sodium Yttrium Fluoride Based Green and Blue Emitting Upconversion Phosphors. *Chemistry of Materials* **2004**, 16 (7), 1244-1251.
- [43] Chenghui Liu; Hui Wang; Xinrong Zhang; Depu Chen, Morphology- and phase-controlled synthesis of monodisperse lanthanide-doped NaGdF<sub>4</sub> nanocrystals with multicolor photoluminescence. *Journal of Materials Chemistry* **2009**, 19 (4), 489-496.
- [44] Chun Kiang Chua; Martin Pumera, Chemical reduction of graphene oxide: a synthetic chemistry viewpoint. *Chemical Society Reviews* **2014**, 43 (1), 291-312.
- [45] Dan Li; Marc B. Muller; Scott Gilje; Richard B. Kaner; Gordon G. Wallace, Processable aqueous dispersions of graphene nanosheets. *Nature Nanotechnology* **2008**, 3 (2), 101-105.
- [46] Owen C. Compton; SonBinh T. Nguyen, Graphene Oxide, Highly Reduced Graphene Oxide, and Graphene: Versatile Building Blocks for Carbon-Based Materials. *Small* **2010**, 6 (6), 711-723.
- [47] A. K. Geim, Graphene: Status and Prospects. *Science* **2009**, 324 (5934), 1530-1534.
- [48] Xiaofang Jia; Jing Li; Erkang Wang, One-pot green synthesis of optically pH-sensitive carbon dots with upconversion luminescence. *Nanoscale* **2012**, 4 (18), 5572-5575.
- [49] Alfonso Salinas-Castillo; Maria Ariza-Avidad; Christian Pritz; Maria Camprubi-Robles; Belen Fernandez; Maria J. Ruedas-Rama; Alicia Megia-Fernandez; Alejandro Lapresta-Fernandez; Francisco Santoyo-Gonzalez; Annelies Schrott-Fischer; Luis F. Capitan-Vallvey, Carbon dots for copper detection with down and upconversion fluorescent properties as excitation sources. *Chemical Communications* **2013**, 49 (11), 1103-1105.
- [50] Shujuan Zhuo; Mingwang Shao; Shuit-Tong Lee, Upconversion and Downconversion Fluorescent Graphene Quantum Dots: Ultrasonic Preparation and Photocatalysis. *ACS Nano* **2012**, 6 (2), 1059-1064.

# Appendices

## Appendix 1

Permission for reuse of figure 2.1 in the thesis.



The screenshot shows the RightsLink interface. At the top left is the Copyright Clearance Center logo. To its right is the RightsLink logo. Further right are navigation buttons for Home, Account Info, and Help, along with a chat icon. Below the Copyright Clearance Center logo is the ACS Publications logo with the tagline "Most Trusted. Most Cited. Most Read." The main content area displays publication details: Title: Functional and Multifunctional Nanoparticles for Bioimaging and Biosensing; Author: Subramanian Tamil Selvan, Timothy Thatt Yang Tan, Dong Kee Yi, et al; Publication: Langmuir; Publisher: American Chemical Society; Date: Jul 1, 2010; Copyright © 2010, American Chemical Society. On the right side, it shows the user is logged in as Longyi Chen with account number 3000964476 and a LOGOUT button.

### PERMISSION/LICENSE IS GRANTED FOR YOUR ORDER AT NO CHARGE

This type of permission/license, instead of the standard Terms & Conditions, is sent to you because no fee is being charged for your order. Please note the following:

- Permission is granted for your request in both print and electronic formats, and translations.
- If figures and/or tables were requested, they may be adapted or used in part.
- Please print this page for your records and send a copy of it to your publisher/graduate school.
- Appropriate credit for the requested material should be given as follows: "Reprinted (adapted) with permission from (COMPLETE REFERENCE CITATION). Copyright (YEAR) American Chemical Society." Insert appropriate information in place of the capitalized words.
- One-time permission is granted only for the use specified in your request. No additional uses are granted (such as derivative works or other editions). For any other uses, please submit a new request.

If credit is given to another source for the material you requested, permission must be obtained from that source.

BACK

CLOSE WINDOW

Copyright © 2017 Copyright Clearance Center, Inc. All Rights Reserved. [Privacy statement](#). [Terms and Conditions](#).

Comments? We would like to hear from you. E-mail us at [customercare@copyright.com](mailto:customercare@copyright.com)

## Appendix 2

Permission for reuse of figure 2.2 in the thesis.

### ROYAL SOCIETY OF CHEMISTRY LICENSE TERMS AND CONDITIONS

Dec 14, 2017

This Agreement between Longyi Chen ("You") and Royal Society of Chemistry ("Royal Society of Chemistry") consists of your license details and the terms and conditions provided by Royal Society of Chemistry and Copyright Clearance Center.

License Number	4247920224339
License date	Dec 14, 2017
Licensed Content Publisher	Royal Society of Chemistry
Licensed Content Publication	Chemical Society Reviews
Licensed Content Title	Chemical modifications and bioconjugate reactions of nanomaterials for sensing, imaging, drug delivery and therapy
Licensed Content Author	Vasudevanpillai Biju
Licensed Content Date	Nov 13, 2013
Licensed Content Volume	43
Licensed Content Issue	3
Type of Use	Thesis/Dissertation
Requestor type	academic/educational
Portion	figures/tables/images
Number of figures/tables/images	1
Format	electronic
Distribution quantity	1
Will you be translating?	no
Order reference number	
Title of the thesis/dissertation	Development of Nanostructured Glucose Biosensor
Expected completion date	Jan 2018
Estimated size	180
Requestor Location	Longyi Chen 1151 Richmond Street  London, ON N6A 3K7 Canada Attn: Longyi Chen
Billing Type	Invoice
Billing Address	Longyi Chen 1151 Richmond Street  London, ON N6A 3K7 Canada Attn: Longyi Chen
Total	0.00 USD

## Appendix 3

Permission for reuse of figure 2.3 in the thesis.

### JOHN WILEY AND SONS LICENSE TERMS AND CONDITIONS

Dec 14, 2017

---

This Agreement between Longyi Chen ("You") and John Wiley and Sons ("John Wiley and Sons") consists of your license details and the terms and conditions provided by John Wiley and Sons and Copyright Clearance Center.

License Number	4247920797871
License date	Dec 14, 2017
Licensed Content Publisher	John Wiley and Sons
Licensed Content Publication	Chemistry - A European Journal
Licensed Content Title	A New Nanobiosensor for Glucose with High Sensitivity and Selectivity in Serum Based on Fluorescence Resonance Energy Transfer (FRET) between CdTe Quantum Dots and Au Nanoparticles
Licensed Content Author	Bo Tang,Lihua Cao,Kehua Xu,Linhai Zhuo,Jiechao Ge,Qingling Li,Lijuan Yu
Licensed Content Date	Mar 3, 2008
Licensed Content Pages	8
Type of use	Dissertation/Thesis
Requestor type	University/Academic
Format	Electronic
Portion	Figure/table
Number of figures/tables	1
Original Wiley figure/table number(s)	figure 1
Will you be translating?	No
Title of your thesis / dissertation	Development of Nanostructured Glucose Biosensor
Expected completion date	Jan 2018
Expected size (number of pages)	180
Requestor Location	Longyi Chen 1151 Richmond Street  London, ON N6A 3K7 Canada Attn: Longyi Chen
Publisher Tax ID	EU826007151
Billing Type	Invoice
Billing Address	Longyi Chen 1151 Richmond Street  London, ON N6A 3K7 Canada Attn: Longyi Chen

## Appendix 4

Permission for reuse of figure 2.4 in the thesis.

### JOHN WILEY AND SONS LICENSE TERMS AND CONDITIONS

Dec 14, 2017








---

This Agreement between Longyi Chen ("You") and John Wiley and Sons ("John Wiley and Sons") consists of your license details and the terms and conditions provided by John Wiley and Sons and Copyright Clearance Center.

License Number	4247921088350
License date	Dec 14, 2017
Licensed Content Publisher	John Wiley and Sons
Licensed Content Publication	Small
Licensed Content Title	Optical Detection of Glucose by Means of Metal Nanoparticles or Semiconductor Quantum Dots
Licensed Content Author	Lily Bahshi,Ronit Freeman,Ron Gill,Itamar Willner
Licensed Content Date	Feb 18, 2009
Licensed Content Pages	5
Type of use	Dissertation/Thesis
Requestor type	University/Academic
Format	Electronic
Portion	Figure/table
Number of figures/tables	1
Original Wiley figure/table number(s)	abstract figure
Will you be translating?	No
Title of your thesis / dissertation	Development of Nanostructured Glucose Biosensor
Expected completion date	Jan 2018
Expected size (number of pages)	180
Requestor Location	Longyi Chen 1151 Richmond Street  London, ON N6A 3K7 Canada Attn: Longyi Chen
Publisher Tax ID	EU826007151
Billing Type	Invoice
Billing Address	Longyi Chen 1151 Richmond Street  London, ON N6A 3K7 Canada Attn: Longyi Chen
Total	0.00 USD
Terms and Conditions	

## Appendix 5

Permission for reuse of figure 2.5 in the thesis.

**Title:** Glucose Biosensor Based on Nanocomposite Films of CdTe Quantum Dots and Glucose Oxidase

**Author:** Xinyu Li, Yunlong Zhou, Zhaozhu Zheng, et al

**Publication:** Langmuir

**Publisher:** American Chemical Society

**Date:** Jun 1, 2009

Copyright © 2009, American Chemical Society

Logged in as:  
Longyi Chen  
Account #:  
3000964476

[LOGOUT](#)

### PERMISSION/LICENSE IS GRANTED FOR YOUR ORDER AT NO CHARGE

This type of permission/license, instead of the standard Terms & Conditions, is sent to you because no fee is being charged for your order. Please note the following:

- Permission is granted for your request in both print and electronic formats, and translations.
- If figures and/or tables were requested, they may be adapted or used in part.
- Please print this page for your records and send a copy of it to your publisher/graduate school.
- Appropriate credit for the requested material should be given as follows: "Reprinted (adapted) with permission from (COMPLETE REFERENCE CITATION). Copyright (YEAR) American Chemical Society." Insert appropriate information in place of the capitalized words.
- One-time permission is granted only for the use specified in your request. No additional uses are granted (such as derivative works or other editions). For any other uses, please submit a new request.

If credit is given to another source for the material you requested, permission must be obtained from that source.

[BACK](#)

[CLOSE WINDOW](#)

Copyright © 2017 [Copyright Clearance Center, Inc.](#) All Rights Reserved. [Privacy statement](#). [Terms and Conditions](#).

Comments? We would like to hear from you. E-mail us at [customercare@copyright.com](mailto:customercare@copyright.com)

## Appendix 6

Permission for reuse of figure 2.6 in the thesis.

Encapsulation of FRET-based glucose and maltose biosensors to develop functionalized silica nanoparticles

G. Faccio, M. B. Bannwarth, C. Schulenburg, V. Steffen, D. Jankowska, M. Pohl, R. M. Rossi, K. Maniura-Weber, L. F. Boesel and M. Richter, *Analyst*, 2016, 141, 3982

DOI: [10.1039/C5AN02573G](https://doi.org/10.1039/C5AN02573G)

This article is licensed under a Creative Commons Attribution 3.0 Unported Licence. Material from this article can be used in other publications provided that the correct acknowledgement is given with the reproduced material.



## Appendix 7

Permission for reuse of figure 2.7 in the thesis.

### ROYAL SOCIETY OF CHEMISTRY LICENSE TERMS AND CONDITIONS

Dec 14, 2017

This Agreement between Longyi Chen ("You") and Royal Society of Chemistry ("Royal Society of Chemistry") consists of your license details and the terms and conditions provided by Royal Society of Chemistry and Copyright Clearance Center.

License Number	4247930028682
License date	Dec 14, 2017
Licensed Content Publisher	Royal Society of Chemistry
Licensed Content Publication	Chemical Communications (Cambridge)
Licensed Content Title	Glucose-triggered release using enzyme-gated mesoporous silica nanoparticles
Licensed Content Author	Elena Aznar,Reynaldo Villalonga,Cristina Giménez,Félix Sancenón,M. Dolores Marcos,Ramón Martínez-Máñez,Paula Díez,José M. Pingarrón,Pedro Amorós
Licensed Content Date	May 15, 2013
Licensed Content Volume	49
Licensed Content Issue	57
Type of Use	Thesis/Dissertation
Requestor type	academic/educational
Portion	figures/tables/images
Number of figures/tables/images	1
Format	electronic
Distribution quantity	1
Will you be translating?	no
Order reference number	
Title of the thesis/dissertation	Development of Nanostructured Glucose Biosensor
Expected completion date	Jan 2018
Estimated size	180
Requestor Location	Longyi Chen 1151 Richmond Street  London, ON N6A 3K7 Canada Attn: Longyi Chen
Billing Type	Invoice
Billing Address	Longyi Chen 1151 Richmond Street  London, ON N6A 3K7 Canada Attn: Longyi Chen

## Appendix 8

Permission for reuse of figure 2.8 in the thesis.

### ELSEVIER LICENSE TERMS AND CONDITIONS




Dec 14, 2017


This Agreement between Longyi Chen ("You") and Elsevier ("Elsevier") consists of your license details and the terms and conditions provided by Elsevier and Copyright Clearance Center.

License Number	4247930178442
License date	Dec 14, 2017
Licensed Content Publisher	Elsevier
Licensed Content Publication	Biosensors and Bioelectronics
Licensed Content Title	Simultaneous detection of hydrogen peroxide and glucose in human serum with upconversion luminescence
Licensed Content Author	Jiali Liu,Lili Lu,Aiqin Li,Juan Tang,Shiguo Wang,Suying Xu,Leyu Wang
Licensed Content Date	Jun 15, 2015
Licensed Content Volume	68
Licensed Content Issue	n/a
Licensed Content Pages	6
Start Page	204
End Page	209
Type of Use	reuse in a thesis/dissertation
Intended publisher of new work	other
Portion	figures/tables/illustrations
Number of figures/tables/illustrations	1
Format	electronic
Are you the author of this Elsevier article?	No
Will you be translating?	No
Original figure numbers	scheme 1
Title of your thesis/dissertation	Development of Nanostructured Glucose Biosensor
Expected completion date	Jan 2018
Estimated size (number of pages)	180
Requestor Location	Longyi Chen 1151 Richmond Street  London, ON N6A 3K7 Canada Attn: Longyi Chen
Total	0.00 USD
Terms and Conditions	

## Appendix 9

Permission for reuse of figure 2.9 in the thesis.

HomeAccount InfoHelp



**Title:**

**Author:**

**Publication:**

**Publisher:**

**Date:**

Copyright © 2015, American Chemical Society

MnO<sub>2</sub>-Nanosheet-Modified Upconversion Nanosystem for Sensitive Turn-On Fluorescence Detection of H<sub>2</sub>O<sub>2</sub> and Glucose in Blood

Jing Yuan, Yao Cen, Xiang-Juan Kong, et al

Applied Materials

American Chemical Society

May 1, 2015

Logged in as:  
Longyi Chen  
Account #:  
3000964476

LOGOUT

### PERMISSION/LICENSE IS GRANTED FOR YOUR ORDER AT NO CHARGE

This type of permission/license, instead of the standard Terms & Conditions, is sent to you because no fee is being charged for your order. Please note the following:

- Permission is granted for your request in both print and electronic formats, and translations.
- If figures and/or tables were requested, they may be adapted or used in part.
- Please print this page for your records and send a copy of it to your publisher/graduate school.
- Appropriate credit for the requested material should be given as follows: "Reprinted (adapted) with permission from (COMPLETE REFERENCE CITATION). Copyright (YEAR) American Chemical Society." Insert appropriate information in place of the capitalized words.
- One-time permission is granted only for the use specified in your request. No additional uses are granted (such as derivative works or other editions). For any other uses, please submit a new request.

If credit is given to another source for the material you requested, permission must be obtained from that source.

BACK

CLOSE WINDOW

Copyright © 2017 [Copyright Clearance Center, Inc.](#) All Rights Reserved. [Privacy statement](#). [Terms and Conditions](#).

Comments? We would like to hear from you. E-mail us at [customercare@copyright.com](mailto:customercare@copyright.com)

## Appendix 10

Permission for reuse of figure 2.10 in the thesis.



RightsLink®

**SPRINGER NATURE**

**Title:** The pH-switchable agglomeration and dispersion behavior of fluorescent Ag nanoclusters and its applications in urea and glucose biosensing  
**Author:** Jang Xue Dong, Zhong Feng Gao, Ying Zhang, Bang Lin Li, Wei Zhang et al.  
**Publication:** NPG Asia Materials  
**Publisher:** Springer Nature  
**Date:** Dec 9, 2016  
Copyright © 2016, Springer Nature

### **Creative Commons**

This is an open access article distributed under the terms of the [Creative Commons CC BY](#) license, which permits unrestricted use, distribution, and reproduction in any medium, provided the original work is properly cited.

You are not required to obtain permission to reuse this article.

Are you the [author](#) of this Springer Nature article?

To order reprints of this content, please contact Springer Nature by e-mail at [reprintswarehouse@springernature.com](mailto:reprintswarehouse@springernature.com), and you will be contacted very shortly with a quote.

# Appendix 11

Permission for reuse of figure 2.11 in the thesis.

## JOHN WILEY AND SONS LICENSE TERMS AND CONDITIONS

Dec 14, 2017

This Agreement between Longyi Chen ("You") and John Wiley and Sons ("John Wiley and Sons") consists of your license details and the terms and conditions provided by John Wiley and Sons and Copyright Clearance Center.

License Number	4247930429755
License date	Dec 14, 2017
Licensed Content Publisher	John Wiley and Sons
Licensed Content Publication	Angewandte Chemie International Edition
Licensed Content Title	Periplasmic Binding Proteins as Optical Modulators of Single-Walled Carbon Nanotube Fluorescence: Amplifying a Nanoscale Actuator
Licensed Content Author	Hyeonseok Yoon, Jin-Ho Ahn, Paul W. Barone, Kyungsuk Yum, Richa Sharma, Ardemis A. Boghossian, Jae-Hee Han, Michael S. Strano
Licensed Content Date	Jan 18, 2011
Licensed Content Pages	4
Type of use	Dissertation/Thesis
Requestor type	University/Academic
Format	Electronic
Portion	Figure/table
Number of figures/tables	1
Original Wiley figure/table number(s)	abstract figure
Will you be translating?	No
Title of your thesis / dissertation	Development of Nanostructured Glucose Biosensor
Expected completion date	Jan 2018
Expected size (number of pages)	180
Requestor Location	Longyi Chen 1151 Richmond Street  London, ON N6A 3K7 Canada Attn: Longyi Chen
Publisher Tax ID	EU826007151
Billing Type	Invoice
Billing Address	Longyi Chen 1151 Richmond Street  London, ON N6A 3K7 Canada Attn: Longyi Chen
Total	0.00 USD

## Appendix 12

Permission for reuse of figure 2.12 in the thesis.



**Title:** Simple and Cost-Effective Glucose Detection Based on Carbon Nanodots Supported on Silver Nanoparticles

**Author:** Jin-Liang Ma, Bin-Cheng Yin, Xin Wu, et al

**Publication:** Analytical Chemistry

**Publisher:** American Chemical Society

**Date:** Jan 1, 2017

Copyright © 2017, American Chemical Society

Logged in as:  
Longyi Chen  
Account #: 3000964476

[LOGOUT](#)

### PERMISSION/LICENSE IS GRANTED FOR YOUR ORDER AT NO CHARGE

This type of permission/license, instead of the standard Terms & Conditions, is sent to you because no fee is being charged for your order. Please note the following:

- Permission is granted for your request in both print and electronic formats, and translations.
- If figures and/or tables were requested, they may be adapted or used in part.
- Please print this page for your records and send a copy of it to your publisher/graduate school.
- Appropriate credit for the requested material should be given as follows: "Reprinted (adapted) with permission from (COMPLETE REFERENCE CITATION). Copyright (YEAR) American Chemical Society." Insert appropriate information in place of the capitalized words.
- One-time permission is granted only for the use specified in your request. No additional uses are granted (such as derivative works or other editions). For any other uses, please submit a new request.

If credit is given to another source for the material you requested, permission must be obtained from that source.

[BACK](#)

[CLOSE WINDOW](#)

Copyright © 2017 [Copyright Clearance Center, Inc.](#) All Rights Reserved. [Privacy statement](#). [Terms and Conditions](#).

Comments? We would like to hear from you. E-mail us at [customercare@copyright.com](mailto:customercare@copyright.com)

## Appendix 13

Permission for reuse of published journal paper (Biosensors and Bioelectronics 2017, 91, 393-399.) in the thesis (chapter 3).

 **Copyright Clearance Center**  **RightsLink®**

[Home](#) [Account Info](#) [Help](#) 



**Title:** Nanostructured biosensor for detecting glucose in tear by applying fluorescence resonance energy transfer quenching mechanism

**Author:** Longyi Chen, Wai Hei Tse, Yi Chen, Matthew W. McDonald, James Melling, Jin Zhang

**Publication:** Biosensors and Bioelectronics

**Publisher:** Elsevier

**Date:** 15 May 2017

© 2016 Elsevier B.V. All rights reserved.

**Logged in as:** Longyi Chen  
**Account #:** 3000964476

[LOGOUT](#)

Please note that, as the author of this Elsevier article, you retain the right to include it in a thesis or dissertation, provided it is not published commercially. Permission is not required, but please ensure that you reference the journal as the original source. For more information on this and on your other retained rights, please visit: <https://www.elsevier.com/about/our-business/policies/copyright#Author-rights>

[BACK](#)

[CLOSE WINDOW](#)

Copyright © 2017 [Copyright Clearance Center, Inc.](#) All Rights Reserved. [Privacy statement](#). [Terms and Conditions](#).

Comments? We would like to hear from you. E-mail us at [customercare@copyright.com](mailto:customercare@copyright.com)

## Appendix 14

Permission for reuse of published journal paper (RSC Advances 2017, 7 (43), 26770-26775.) in the thesis (part of chapter 4).

Special properties of luminescent magnetic NaGdF<sub>4</sub>: Yb<sup>3+</sup>, Er<sup>3+</sup> upconversion nanocubes with surface modifications

L. Chen, W. H. Tse, A. Siemiarzuk and J. Zhang, RSC Adv., 2017, 7, 26770

DOI: 10.1039/C7RA03380J

This article is licensed under a Creative Commons Attribution 3.0 Unported Licence. Material from this article can be used in other publications provided that the correct acknowledgement is given with the reproduced material.



## Curriculum Vitae

Name: Longyi Chen

Post-secondary Education and Degrees: Sun Yat-sen University  
Guangzhou, Guangdong, China  
Bachelor in Chemical Engineering and Technics, 2007–2011

Sun Yat-sen University  
Guangzhou, Guangdong, China  
Master in Chemical Technology, 2011–2013

University of Western Ontario  
London, Ontario, Canada  
PhD in Chemical and Biochemical Engineering, 2014–2018

Related Work Experience: Graduate Teaching Assistant  
The University of Western Ontario  
2014–2018

### Publications:

- [1] Longyi Chen, Michelle Dotzert, James Melling and Jin Zhang. Graphene/FeCo nanocomposites for magnetoresistive glucose biosensing. In preparation.
- [2] Longyi Chen, Michelle Dotzert, James Melling and Jin Zhang. Tunable Photoluminescent Carbon Dots as Glucose Biosensor. Submitted.
- [3] Wai Hei Tse, Longyi Chen, Yi Chen, Matthew W. McDonald, James Melling and Jin Zhang. Harnessing Protein-conjugated Upconversion Nanostructures to Build a Hydrogel-based Biosensor for Tear Glucose Measurement. Submitted. (Longyi Chen and Wai Hei Tse contributed equally)
- [4] Longyan Chen; Longyi Chen; Michelle Dotzert; James Melling; Jin Zhang, Nanostructured biosensor using bioluminescence quenching technique for glucose detection. *Journal of Nanobiotechnology* 2017, 15 (1), 59.

- [5] Longyi Chen; Wai Hei Tse; Alex Siemiarzuk; Jin Zhang, Special properties of luminescent magnetic NaGdF<sub>4</sub>: Yb<sup>3+</sup>, Er<sup>3+</sup> upconversion nanocubes with surface modifications. RSC Advances 2017, 7 (43), 26770-26775.
- [6] Longyi Chen; Wai Hei Tse; Yi Chen; Matthew McDonald; James Melling; Jin Zhang, Nanostructured biosensor for detecting glucose in tear by applying fluorescence resonance energy transfer quenching mechanism. Biosensors and Bioelectronics 2017, 91, 393-399. (Longyi Chen and Wai Hei Tse contributed equally)
- [7] Yi Chen; Longyi Chen; Longyan Chen; Jin Zhang, Deposition of ZnO Nanocrystals on Fe<sub>3</sub>O<sub>4</sub> Nanocubes and Their Special Luminescent and Magnetic Properties. Particle & Particle Systems Characterization 2015, 32 (9), 893-898.

Conferences:

- [1] Longyi Chen, Wai Hei Tse and Jin Zhang. 100<sup>th</sup> Canadian Chemistry Conference and Exhibition. Poster, May 28-June 1, 2017, Toronto, Ontario, Canada.
- [2] Longyi Chen, Wai Hei Tse and Jin Zhang. 33<sup>rd</sup> Annual Meeting of the Canadian Biomaterials Society. Oral presentation. May 24-27, 2017, Winnipeg, Manitoba, Canada.